THE EVALUATION OF NOVEL CONJUGATED UNSATURATED KETONES AS CANDIDATE ANTINEOPLASTIC AGENTS

A Thesis Submitted to the
College of Graduate and Postdoctoral Studies
In Partial Fulfillment of the Requirements
For the Degree of Doctor of Philosophy
In the College of Pharmacy and Nutrition
University of Saskatchewan
Saskatoon

By

Praveen Kumar Goud Roayapalley

PERMISSION TO USE

In presenting this thesis/dissertation in partial fulfillment of the requirements for a Postgraduate degree from the University of Saskatchewan, I agree that the Libraries of this University may make it freely available for inspection. I further agree that permission for copying of this thesis/dissertation in any manner, in whole or in part, for scholarly purposes may be granted by the professor or professors (Drs. J. R. Dimmock and R. K. Sharma) who supervised my thesis/dissertation work or, in their absence, by the Head of the Department or the Dean of the College in which my thesis work was done. It is understood that any copying or publication or use of this thesis/dissertation or parts thereof for financial gain shall not be allowed without my written permission. It is also understood that due recognition shall be given to me and to the University of Saskatchewan in any scholarly use which may be made of any material in my thesis/dissertation.

Requests for permission to copy or to make other uses of materials in this thesis/dissertation in whole or part should be addressed to:

Dean of the College of Pharmacy and Nutrition
University of Saskatchewan
Saskatoon, Saskatchewan S7N 5E5
Canada

OR

Dean
College of Graduate and Postdoctoral Studies
University of Saskatchewan
116 Thorvaldson Building, 110 Science Place
Saskatoon, Saskatchewan S7N 5C9 Canada

ABSTRACT

Cancer is a huge medical problem. One of the ways of treating this complaint is by the use of anticancer drugs. However this therapy suffers from two major drawbacks namely undue toxicity to non-malignant cells and the development of drug resistance. The compounds which comprise the basis of this thesis are conjugated unsaturated ketones which differ structurally from contemporary anticancer medication and some of these compounds have noteworthy antineoplastic properties. These unsaturated ketones have a greater affinity for thiols than hydroxyl and amino groups. Hence the toxicity to nucleic acids may be absent or much lower than that of many contemporary anticancer agents. This thesis describes the development of three series of cytotoxic compounds.

Series **15** are a cluster of 3,5-bis(benzylidene)-4-piperidones which in general are far more toxic to various tumor cells than to non-malignant ones. Some physicochemical constants of the aryl substituents correlated with potencies. In addition, attempts to condense various aldehydes with 2,2,6,6-tetramethyl-4-piperidone led to the isolation of some acyclic 1,5-diaryl-1,4-dien-3-ones.

Series **33** were created by placing a *N*-acyl group on some of the enones in series **15**. The biodata was very encouraging with very high potencies to tumor cells while significantly lower toxicity to normal cells was noted. Representative compounds caused apoptosis in some malignant cells.

Series **71** are quaternary ammonium salts which were prepared to preferentially react with tumor mitochondria rather than this organelle of normal cells. These molecules too demonstrated higher toxicity to neoplasms than non-malignant cells and representative compounds have drug-like properties.

This study has revealed the encouraging antineoplastic properties of several different clusters of compounds and provided direction for future studies.

ACKNOWLEDGMENTS

I would like to express how grateful I am to everyone who has made my PhD journey possible and supported me in my hardships.

First and foremost, I would like to thank my supervisor Dr. Jonathan R Dimmock for his patience, guidance, motivation, and support during my PhD program. I would like to express my gratitude towards my co-supervisor Dr. Rajendra K Sharma for his inputs and advice during my graduate studies.

I would like to thank my advisory committee members Dr. Ed Krol, Dr. Anas El-Aneed, Dr. Michel Gravel and Dr. David Palmer for their valuable suggestions during the committee meetings.

I would like to express my special thanks to Drs. Jane Alcorn and David Blackburn for their tremendous support and motivation during my program.

I would also like to express my gratitude to Dr. Mohammed Abdul Rasheed, for his immense support and the motivation which made me come to Canada for my PhD studies.

I am thankful to all the College of Pharmacy and Nutrition staff; particularly to Claire Sutton, Merry Beazely, Sandy Knowles, Jenn Pippin, Erin Smith-Windsor, Christine Ruys for administrative assistance. I thank my lab mates Dr. Swagatika Das, Dr. Alireza Daroudi and Dr. Umashankar Das for their support.

I express my gratitude to Drs. Marcelo Sales and Alexandra Bartole-Scott, for providing me with teaching assistantships in the Chemistry Department. Also, I express my sincere thanks to Tina Leckie and Duane Turner for providing me with a job in University Library.

I would like to extend my deepest and sincere thanks to Drs. Mahesh Gangishetty, Asish Kumar Reddy Somidi, Venkata Krishna Garapati, Ravi Siripurapu and Krishna Reddy Annadi for their immense support during my program.

I thank my wonderful parents Roayapalley Krishna and Kalavathi for their unconditional love, support and encouragement. I am grateful to my brother Roayapalley Naveen Kumar and sister-in-law Roayapalley Vinoda Vani, who have supported me from a distance. I am grateful to my wonderful wife Rekha (Sinchu), who supported me, believed in me and gave me all the time when I need moral support. My special heartly thanks to my beloved better half Rekha. This journey would have never been possible without their immeasurable love, support, care, guidance, and prayers. I will be always thankful for their devotion. I am blessed to have them as my family.

I extend my deepest thanks to my in-laws Narayan and Shanthamma, sister Siddagoni Kavitha, brother-in-law Siddagoni Venkatesh, sister-in-law Roopa Ravi Kumar, brother Ravi Kumar, my nephews Siddagoni Jagadish and Chethan Gowda, and my sweet nieces Roayapalley Niharika, Roayapalley Shanvitha, Siddagoni Rohitha, and Tanusha Gowda for their affection, support and prayers.

DEDICATION

OM SAI RAM

This thesis is written in dedication to **Shree Sadhguru Sainath Maharaj** of Shiridi

TABLE OF CONTENTS

ABSTRACT ..... **ii**

ACKNOWLEDGMENTS ..... **iv**

DEDICATION ..... **vi**

LIST OF TABLES ..... **xi**

LIST OF FIGURES ..... **xii**

LIST OF SCHEMES ..... **xv**

LIST OF ABBREVATIONS ..... **xvii**

LIST OF PLOTS ..... **xxiii**

Chapter 1 ..... **1**

1.1 Introduction *1*

1.2 Distribution of cancer *2*

1.3 Cancer treatment *4*

1.4 Challenges of cancer treatment *8*

1.5 α,β-Unsaturated ketones as anticancer and cytotoxic agents *14*

1.5.1 The development of 1,5-diaryl-3-oxo-1,4-pentadienes as cytotoxic agents. 24

1.6 Cancer drug targets *34*

1.6.1 Traditional therapies vs targeted therapies in cancer 34
1.6.2 Monoclonal antibodies: One of the major classes of targeted therapies in cancer 37
1.6.3 Angiogenesis (AG) inhibitors 40
1.6.4 Microtubule inhibitors 41
1.6.5 DNA intercalators and groove binding agents 42
1.6.6 The role of thiols in regulating cancer development and growth 43
1.7 Mannich bases *47*
1.8 Mitochondria *55*
1.8.1 Mitochondrial membrane potential (MMP) Ψ 58
1.8.2 More hyperpolarised mitochondrial membrane potential in cancer cells 58
1.8.3 Approaches to targeting compounds to mitochondria 60
1.8.4 Accumulation of lipophilic cations in the mitochondria of intact cells 63
1.9 Conclusions *66*
Hypotheses and Objectives: 68
Chapter 2 70
2.1 Introduction *70*
2.2 Synthesis of 3,5-bis(arylidene)-4-piperidones *70*
2.2.1 General procedure for the synthesis of 3,5-bis(arylidene)-4-piperidones (15) 71
2.3 Analytical data *72*
2.4 Biological results *81*

2.4.1 Methodology 85

2.5 Discussion 87

2.6 Unusual reactions observed in the 2,2,6,6-tetramethyl-4-piperidone (TMP) project. 95

2.7 Plausible Reaction Mechanism: 98

2.7.1 General procedure for the synthesis of 1,5-bis(aryl)-1,4-pentadien-3-ones 99

2.8 Analytical data 101

Chapter 3 103

3.1 Introduction 103

3.2 Syntheses of N-aroyl analogs of 3,5-bis(arylidene)-4-piperidones 104

3.2.1 General procedure for the synthesis of 3,5-bis(arylidene)-4-piperidones (15a-n) 104

3.2.2 General procedure for the synthesis of *N*-aroyl analogs of 3,5-bis(arylidene)-4-piperidones (33a-n) 105

3.3 Analytical data 106

3.4 Biological results 115

3.4.1 Methodology 117

3.5 Discussion 119

Chapter 4 129

4.1 Introduction 129

4.2 Synthesis of 4-piperidone-oxime 129

4.2.1 General procedure for the synthesis of 4-piperidone-oxime 130

4.3 Synthesis of oximes and quaternary salts 131

4.3.1 Synthesis of compounds 32a-i 132

4.3.2 Synthesis of compounds 70a-i 132

4.4 Analytical data 133

4.5 Synthesis of compound 72 139

4.6 Synthesis of compounds 71a-h, and 73 140

4.7 Analytical data 141

4.8 Biological results 148

4.8.1 Methodology 154

4.9 Discussion 157

Conclusions and future work 165

References 172

LIST OF TABLES

Table 1.1. Antineoplastic agents and their primary toxicities 11

Table 1.2. Classification of conjugated monoclonal antibodies and their targets 38

Table 2.1. Evaluation of **15**, **15a-t** against Ca9-22, HSC-2, and HSC-4 human oral squamous cell carcinoma cell lines..... 81

Table 2.2. Evaluation of **15**, **15a-t** against HGF, HPLF, and HPC human non-malignant cells. 83

Table 2.3. Evaluation of **15, 15a-t** towards Colo205, HT-29, CEM and Hs27 cells. 84

Table 2.4. Identification of lead molecules based on the data in Tables 2.1 and 2.2. 85

Table 2.5. Reaction conditions and % yields of unusual reactions 100

Table 3.1. Evaluation of **33, 33a-n** against four human tumour cell lines 115

Table 3.2. Evaluation of **33**, **33a-n** against HGF, HPLF, and HPC human normal cell lines ... 116

Table 4.1. Evaluation of **70a-h**, **71a-h**, **71** and **72** against Ca9-22, HSC-2 and HSC-4 neoplastic cells 148

Table 4.2. Evaluation of **70a-i**, **71a-h**, **71** and **72** against HGF, HPLF and HPC non-malignant cells 150

Table 4.3. Evaluation of **70a-i**, **71a-h**, **72** and **73** against human CEM cells 151

Table 4.4. Evaluation of **70a-h** and **72** against a panel of human tumor cells 152

Table 4.5. Evaluation of **70a-h** and **72** against some human colon cancer cells. 152

Table 4.6. Evaluation of **70c**, **d**, **71c-e** for some drug-like properties and oral bioavailability 153

LIST OF FIGURES

Figure 1.1. Chemical structures of some anticancer drugs used in chemotherapy. 6

Figure 1.2. Chemical structures of tyrosine kinase inhibitors..... 10

Figure 1.3. Drug efflux by P-glycoprotein..... 13

Figure 1.4. Inhibition of P-glycoprotein to prevent drug efflux. 13

Figure 1.5. Tautomers of curcumin..... 15

Figure 1.6. Michael acceptor reaction with a nucleophile (Nu) attacking at the β-position thereby generating an α,β-functionalized ketone. 20

Figure 1.7. Hypothetical tautomeric isomers of curcumin-GSH adducts. 20

Figure 1.8. Unsaturated monoketones and 2,6-bis(arylidene) cyclohexanone cytotoxins..... 21

Figure 1.9. Development of the 1,5-diaryl-3-oxo-1,4-pentadienyl pharmacophore. 23

Figure 1.10. Sequential Michael reaction of protein thiols with an arylidene dienone electrophile. 24

Figure 1.11. 1,5-Diaryl-3-oxo-1,4-pentadienyl compounds as lead cytotoxic agents. 25

Figure 1.12. 1-[4-(2-Alkylaminoethoxy)phenylcarbonyl]-3,5-bis(arylidene)-4-piperidone hydrochlorides..... 26

Figure 1.13. Heterocyclic α,β -unsaturated carbonyl compounds with the 1,5-diaryl-3-oxo-1,4-pentadienyl pharmacophore. 28

Figure 1.14. Quaternary ammonium salts of α,β -unsaturated carbonyl compounds with the 1,5-diaryl-3-oxo-1,4-pentadienyl pharmacophore as cytotoxic agents. 30

Figure 1.15. Diethyl[(4-oxopiperidin-1-yl)(aryl)methyl]phosphonates..... 32

Figure 1.16. Buthionine sulfoximine **46** and oxothiazolidine carboxylic acid ester **47**..... 45

Figure 1.17. Glutathione (GSH)..... 46

Figure 1.18. 1-*p*-Chlorophenyl-4,4-dimethyl-5-diethylamino-1-penten-3-one hydrobromide. .. 47

Figure 1.19. General structures of double, bis and tris Mannich bases. 48

Figure 1.20. General structures of the Mannich bases with anticancer and cytotoxic activity.... 51

Figure 1.21. 3,5-bis(arylidene)-4-piperidone related Mannich bases. 52

Figure 1. 22. Structure of a mitochondrion. 56

Figure 1.23. The electrochemical proton gradient and ATP synthase. 57

Figure 1.24. Anatomy of a typical molecule with a different functional group conjugated to the TPP+ cation through a space linker. 61

Figure 1.25. Some examples of TPP^+ conjugated compounds for delivering in to mitochondria. 62

Figure 1.26. Cellular uptake of TPP+-linked compounds driven by plasma membrane and mitochondrial membrane potentials..... 64

Figure 1.27. Schematic representation of the transport of an MTC from the mitochondrial IMS to the matrix through the mitochondrial inner membrane 65

Figure 2.1. 3,5-Bis(benzylidene)-4-piperidone showing interaction between equatorial hydrogen atom at position 2 of the 4-piperidone with the *ortho* proton of the aryl ring. 96

Figure 3.1. Apoptosis by **33g** in HL-60 cells. 117

Figure 4.1. Disruption of MMP in the cells with **71b** and **71c.** 151

LIST OF SCHEMES

Scheme 1.1. Modifications of conjugated α,β-unsaturated ketone compounds to increase bioavailability. 18

Scheme 1.2. Synthesis of *N*-acryloyl derivatives of 3,5-bis(arylidene)-4-piperidone. 22

Scheme 1.3. Synthetic sequence for the preparation of α-aminophosphonates of 3,5-bis(arylidene)-4-piperidone derivatives..... 33

Scheme 1.4. Synthesis of Mannich bases of 6-hydroxyaurones. 53

Scheme 1.5. Sequential thiol alkylation. 54

Scheme 2.1. Synthesis of 3,5-bis(arylidene)-4-piperidones. 70

Scheme 2.2. Attempted synthesis of 3,5-dibenzylidene-2,2,6,6-tetramethylpiperidin-4-one. 96

Scheme 2.3. Plausible reaction mechanism for the formation of unusual acyclic compounds….98

Scheme 2.4. Proposed synthetic route for 3,5-dibenzylidene-2,2,6,6-tetramethylpiperidin-4-ones. 99

Scheme 2.5. Synthesis of 1,5-bis(aryl)-1,4-pentadien-3-one compounds. 99

Scheme 3.1. Syntheses of *N*-aroyl analogs of 3,5-bis(arylidene)-4-piperidones. 104

Scheme 4.1. Synthesis of 4-piperidone-oxime. 129

Scheme 4.2. Syntheses of oximes and their corresponding quaternary salts including the dimeric compounds **72** and **73**. 131

Scheme 5.1. General structure of the proposed series of compounds. 168

Scheme 5.2. Syntheses of the proposed series **75**. 170

Scheme 5.3. Reaction of **71** analogs with cysteine to form mono adducts **76** and bis adducts **77**. 171

LIST OF ABBREVATIONS

ABC	ATP-binding cassette
AcOH	Acetic acid
ADME	Absorption, distribution, metabolism, and excretion
ADP	Adenosine diphosphate
AG	Angiogenesis
AIDS	Acquired immunodeficiency syndrome
ALCL	Anaplastic large cell lymphoma
ASIR	Age-standardized incidence rates
ATP	Adenosine triphosphate
BBO	Broadband Observe
BCRP	Breast cancer resistance protein
br	Broad (spectral)
BSO	Buthionine sulfoximine
BV	Brentuximab Vedotin
°C	Degrees Celsius
CCNU	Lomustine
CC_{50}	Concentrations of the compounds required to kill 50% of the cells
CD	Cluster of differentiation
CDDP	Cis-diamminedichloroplatinum(II)
CEM	Lymphoblastic cells
COX-2	Cyclooxygenase 2

CRL-1790	Human fetal colon epithelial cell line
Cys	Cysteine
δ	Chemical shift (in parts per million)
d	Doublet(spectral)
dec	Decomposed
DLCO	Diffusing capacity for carbon monoxide
DMEM	Dulbecco's modified eagle medium
DMSO	Dimethylsulfoxide
DNA	Deoxyribonucleic acid
DTIC	Dacarbazine
EGF	Epidermal growth factor
EGFR	Epidermal growth factor receptor
Et_3N	Triethylamine
FAR	Fluorescence activity ratio
FBS	Fetal bovine serum
FDA	Food and Drug Administration
FGF	fibroblast growth factor
5-FU	5-Fluorouracil
GCL	γ-glutamylcysteine ligase
GCLC	Glutamate-cysteine ligase catalytic subunit
GGT	γ-glutamyl-transpeptidase
GSH	Glutathione

GSSG	Glutathione oxidized form
GST	Glutathione S-transferase
^{1}H	Proton(spectral)
HBA	Hydrogen bond acceptor atoms
HBD	Hydrogen bond donor atoms
HCT-116	Human colorectal carcinoma cell line
HE	Hydroethidine
HEK	Human embryonic kidney
HER2	Human epidermal growth factor receptor type 2
HGF	Human gingival fibroblasts
HL	Hodgkin lymphoma
HMBC	Heteronuclear multiple bond correlation
HPC	Human pulp cells
HPC	Hematopoietic precursor cells
HPLF	Human periodontal ligament fibroblasts
HSC	Human squamous cell carcinoma
HUVEC	Human umbilical vein endothelial cell line
IC_{50}	Concentrations of the compounds required to inhibit 50% of the biochemical function
IMS	Intermembrane space
J	Coupling constant (spectral)
lit.	Literature
Ψ	Mitochondrial membrane potential

m	Multiplet (spectral)
$[M]^+$	Parent molecular ion
MDR	Multi drug resistance
MHz	Mega hertz (spectral)
min	Minute(s)
MMAE	Monomethyl auristatin-E
mp	Melting point
MR	Molecular refractivity
MRP	Multidrug resistance protein
MS	Mass spectrometry
MTCs	Mitochondria-targeted cations
MTT	3-(4,5-dimethylthiazol-2-yl)-2,5-diphenyltetrazolium bromide
MW	Molecular weight
m/*z*	Mass-to-charge ratio
N	Normality
NCI	National Cancer Institute
NMR	Nuclear magnetic resonance
Nu	Nucleophile
PARP	Poly ADP-ribose polymerase
PBS	Phosphate buffered saline
P-gp	P-glycoprotein
PI	Propidium iodide
ppm	Parts per million

PSA	Polar surface area
PSE	Potency-selectivity expression
*i*Pr	Isopropyl
q	Quartet (spectral)
QAS	Quaternary ammonium salts
QSAR	Quantitative structure activity relationship
RB	Rotatable bonds
RD	Rhabdomyosarcoma
RNA	Ribonucleic acid
ROS	Reactive oxygen species
RPMI	Roswell Park Memorial Institute
s	Singlet (spectral)
SAR	Structure activity relationship
SI	Selectivity index
SOD	Superoxide dismutase
t	Triplet (spectral)
TLC	Thin layer chromatography
TMP	2,2,6,6-tetramethyl-4-piperidone
TNF-α	Tumor necrosis factor-alpha gene
TPP^+	Triphenyl phosphonium cation
v	Volume
VEGF	Vascular endothelial growth factor
WHO	World Health Organization

w	Weight
w/v	Weight per volume

LIST OF PLOTS

Plot 2.1. Linear plot between the average CC_{50} values of series **15** towards the six neoplastic cell lines and the sigma/sigma star (σ/σ*) values 94

Plot 2.2. Semilogarithmic plot between the average CC_{50} values of series **15** towards the six neoplastic cell lines and the sigma/sigma star (σ/σ*) values 95

Plot 3.1. Linear plot between the average CC_{50} values of series **33** towards the four neoplastic cell lines and the sigma/sigma star (σ/σ*) values 125

Plot 3.2. Semilogarithmic plot between the average CC_{50} values of series **33** towards the four neoplastic cell lines and the sigma/sigma star (σ/σ*) values 125

Plot 3.3. Linear plot between the average CC_{50} values and the average SI values of series **33** towards the four neoplastic cell lines. 127

Plot 3.4. Semilogarithmic plot between the average CC_{50} values and the average SI values of series **33** towards the four neoplastic cell lines. 127

Chapter 1

1.1 Introduction

Cancer is one of the leading causes of death in Canada and in fact 30% of all deaths are caused by cancer. In 2019, it is estimated that in Canada 220,400 new cases of cancer will be diagnosed and 82,100 deaths from cancer will occur.[1] Lung, breast, colorectal and prostate cancers are predicted to be the most common among the diagnosed cancers. These four cancers account for 48% of all the cancer diagnoses in 2019.[2] Cancer is a disease which is characterized by uncontrolled cell proliferation which leads to complex abnormalities in the normal functions of organs which are affected by this disease. Tumours are a group of abnormal cells. Tumours grow and behave differently, depending on whether they are malignant (cancerous), precancerous or benign (non-cancerous).[3] Precancerous conditions have the potential for the cells to develop into cancer. Benign tumours rarely cause serious problems which are life-threatening unless they occur in a vital organ and grow to a large size exerting an impact on the neighbouring tissues. In general, these tumours tend to grow slowly and stay in one place, not spreading to other parts of the body. These growths can be easily removed by surgery and once removed they usually do not come back. Benign tumours usually stay non-cancerous, except in very rare cases.[3]

Precancerous (premalignant) cells are also abnormal cells that may develop into cancer unless they are treated properly. Some cells may develop mild changes that will disappear without any treatment. But other cells pass on genetic changes and thereby the number of new cells gradually

increases and become more abnormal until they turn into cancer. It may take a long time for this to happen.[4] Malignant tumours are cancerous and can start in any one of the millions of cells in our bodies. Cancer cells have a larger nucleus that looks different from the nuclei in normal cells. Cancer cells behave, grow and function quite differently from normal cells.[5] Cancerous tumours vary in their size, shape and grow in an uncontrolled, abnormal way invading the nearby tissues, blood vessels or lymphatic vessels in the body by metastasis.[5] They can interfere with the normal body functions and become life threatening. Malignant tumours can also come back (reoccur) after they have been treated or removed completely.[5]

1.2 Distribution of cancer

Worldwide, one in seven deaths is due to cancer; cancer causes more deaths than AIDS, tuberculosis, and malaria combined. When countries are grouped according to income, cancer is the second leading cause of death in high-income countries (following cardiovascular diseases) and the third leading cause of death in low- and middle-income countries (following cardiovascular diseases and infectious and parasitic diseases).[6]

By 2030, the global cancer burden is expected the rise to 21.7 million new cases and 13 million cancer deaths simply due to the growth and ageing of the population. However, the estimated future cancer burden will be considerably larger due to the adoption of lifestyles that are known to increase cancer risks such as smoking, poor diet and physical inactivity in economically developing countries. Cancers related to these factors, such as lung, breast, and colorectal cancers are already on the rise in economically transitioning countries. In economically developed countries, the three most commonly diagnosed cancers are prostate, lung, and colorectal among males and breast, colorectal, and lung among females.[7]

The most common types of cancer also vary by geographical areas. Although there is no increase in age-standardized incidence rates (ASIR), every year there is an increase in the number of Canadians diagnosed with cancer. In 2030, the estimated projection of the number of cancers diagnosed will be almost 80% greater than the number diagnosed in 2005.[1]

Colorectal, lung, breast and prostate cancers are the four most commonly diagnosed cancers in Canada. According to Canadian Cancer Society's statistics, in 2017, these four cancers accounted for about half of all the cancer diagnoses and cancer deaths in Canada.[8.] These four types of cancers, along with cervical cancer, represent cancers for which screening or early detection likely have had (or will have) a big impact on the stage at which they are diagnosed.

Colorectal cancer is the second most common type of cancers diagnosed in Canada, accounting for a projected 26,800 new cases in 2017 (13% of all cancers). Most of the colorectal cancers develop in the colon, though around 30% develop in the rectum.[9] Colon and rectal cancers have very similar causes and risk factors, but rectal cancer is more strongly associated with red meat intake than colon cancer and colon cancer is more strongly linked to alcohol use.[9] Survival rates for the diagnoses of early stage rectum cancer are lower than for colon cancer. From 1988 to 2010 the age-standardized incidence rate for colorectal cancer disease dropped 11.3% among males and 14.5% among females. The decline in colorectal cancer incidence rates appears confined to older adults as rates are increasing among adults younger than 50 years of age in Canada and in the United States. [10, 11]

1.3 Cancer treatment

Cancer therapy is a process of treating cancer through various methods. The location of treatment of cancer depends on the type of a tumour. There are many treatment options such as chemotherapy, surgery, hormone therapy, gene therapy, radiation therapy, targeted therapy and immunotherapy available to treat cancer. In most cases, the physicians opt for one method of treating cancer or a combination of two methods at the same time depending on the type and stage of the disease if it has spread and the location where it is, and if the cancer patient has any health problems. For some people, chemotherapy may be the only treatment one receives. Chemotherapy is used to treat many types of cancer and has a huge impact in combatting various types of cancers due to its high rate of success and selectivity.[12]

Anticancer drugs used in chemotherapy are classified into several groups based on their chemical structures, mechanisms of action and their relationships to other drugs. The major classes include alkylating agents (e.g. ifosfamide, cyclophosphamide, melphalan, chlorambucil, busulfan), antimetabolites (e.g. floxuridine, cytarabine, 5-fluorouracil, methotrexate), antibiotics (e.g. doxorubicin, epirubicin, bleomycin, dactinomycin), topoisomerase inhibitors (e.g. mitoxantrone, irinotecan), mitotic/microtubule inhibitors (e.g. paclitaxel, vincristine, docetaxel, vinblastine), corticosteroids (e.g. dexamethasone, tamoxifen, flutamide and prednisone), monoclonal antibodies (e,g. bevacizumab, cetuximab, rituximab) and antibody drug conjugates ADC (e.g., inotuzumab, ozogamicin, gemtuzumab, ozogamicin, trastuzumab, emtansine). The chemical structures of some anticancer drugs used in chemotherapy are shown in **Figure 1.1**.

Alkylating agents:

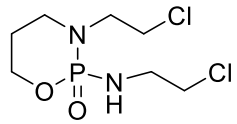

1

Ifosfamide (Isophosphamide)

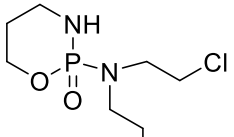

2

Cyclophosphamide

Antimetabolites:

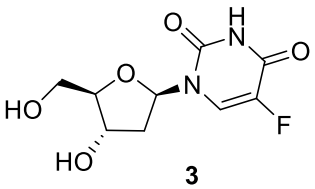

3

Floxuridine

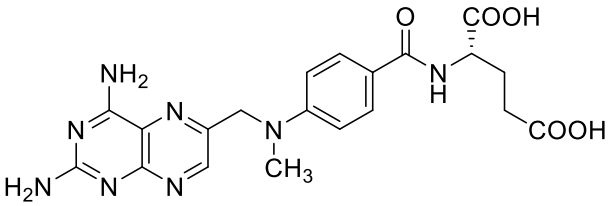

4

Methotrexate

Antibiotics:

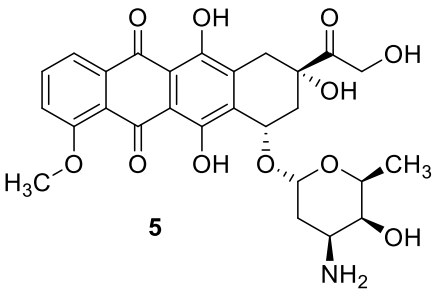

5

Doxorubicin

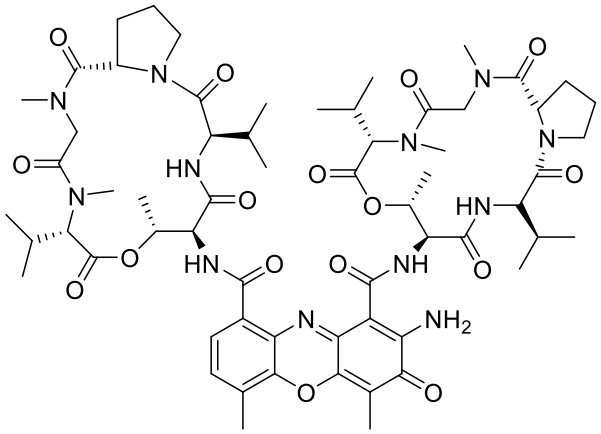

6

Dactinomycin

Microtubule inhibitors:

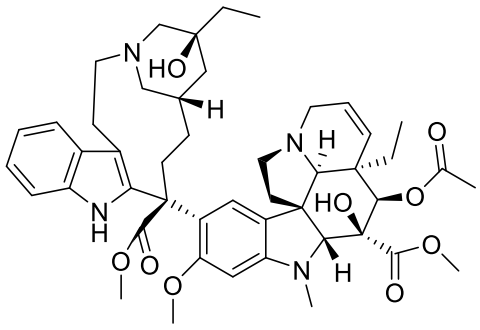

7

Vinblastine

Corticosteroids:

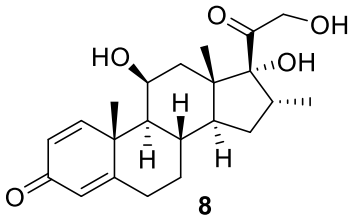

8

Prednisolone

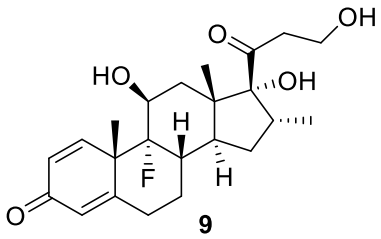

9

Dexamethasone

Figure 1.1. Chemical structures of some anticancer drugs used in chemotherapy.

The mono-therapy approach is a very common treatment method for many different forms of cancers. This conventional medication is generally less effective than multiple treatments. In the traditional treatment of cancer, to increase the efficacy of the cancer-treating drugs, combination therapy is a widely used treatment option whereby the combination of two or more therapeutic treatment methods is used to specifically target the cancer-inducing or cell sustaining pathways.[13] In this therapy, the combination of two or more anticancer drugs whose function are different from the each other, boosts the efficiency of the overall treatment compared to the monotherapy. This

is because the combination therapy targets the cancer cells in a synergistic or an additive manner.[14] The mono-therapeutic techniques non-selectively target the proliferating cells, which ultimately leads to the destruction of both normal and cancerous cells.[15] Chemotherapy can be toxic to the cancer patients with multiple side effects, and can also reduce their immune system by affecting the bone marrow cells and increasing the susceptibility to host diseases[16]. Even though combination therapy can be toxic, if the modes of action of the drugs differ, then the usual doses of the drugs used in monotherapy can be reduced.[17] In other words, combination therapy may be able to prevent the toxic effects on normal cells while simultaneously producing cytotoxic effects on cancer cells.[18]

Furthermore, mono-therapy treatment is more likely to lead to drug resistance because the constant treatment with a single chemotherapeutic agent induces cancer cells to recruit alternative rescue pathways.[19] The major drawback of all the drugs that act on a specific molecular target is the ease with which multidrug resistance can develop. For example, when the cells in an adenocarcinoma were treated with the doxorubicin, there was an upregulation of an ATP-dependent cassette pump to eliminate the drug leading to a state of drug resistance.[20] In this study, the combination of paclitaxel and sorafenib in low concentration was evaluated to target cancer stem cells. The combination therapy can produce a more effective treatment response to cancerous cells in fewer cycles, and therefore this treatment method reduces the incidence of multidrug resistance.[21]

1.4 Challenges of cancer treatment

Cancer chemotherapy including combination therapy, while a common method of treating cancer, is associated with a lack of selectivity that causes multiple adverse effects in the patients. The other challenge with drug therapy of cancer is multidrug resistance (MDR). MDR is involved in the failure of several cancer treatments. MDR has been receiving a great attention in the recent years due to a large number of mechanisms discovered and involved in the process of drug resistance in cancer treatment which hampers the effectiveness of many anti-cancer drugs in use. The participation of ATP-binding cassette (ABC) transporters is one of the mechanisms involved in the multidrug resistance. The ABC transporters can be defined as a group of plasma membrane and intracellular organelle proteins that are involved in the process of elimination of the substrates from the cancer cells. These ABC transporters are involved in the clearance of intracellular constituents such as ions, hormones, lipids and other small molecules from the cell and thereby effecting both directly and indirectly drug absorption, distribution, metabolism and excretion (ADME) of the anticancer drugs.[22] The most common side effects caused by chemotherapy in cancer patients include anemia, appetite loss, bleeding and bruising (thrombocytopenia), constipation, diarrhea, hair loss (alopecia), lymphedema, memory or concentration problems, nausea and vomiting, and nerve problems (peripheral neuropathy).[23] Recently approved anticancer agents for the treatment of solid tumours include antibody-based or synthetic kinase inhibitor-based signal transduction agents that are designed to "target" particular messenger proteins whose overexpression can result in abnormal cellular proliferation.[24, 25] Some of the side effects associated with different types of anticancer drugs are discussed below.

Alkylating agents react with the proteins that bond together to form a double helix structure of a DNA molecule, adding an alkyl group to some or all of them and prevents the proteins from normal linking up and causing breakage of the DNA strands thereby eventually causing the death of the cell. These are active in treating different types of solid and hematologic tumours that include leukemias and lymphomas, sarcomas and lung, breast, and gynecologic cancers. The anticancer agent that is primarily associated with cardiotoxicity in this class is cyclophosphamide.[26]

Antimicrotubule agents including paclitaxel and docetaxel may cause atrial or ventricular arrhythmias and atrioventricular block.[26] Pyrimidine-based agents including 5- fluorouracil or its analogues such as capecitabine, have been reported as inducing coronary artery spasm.[26, 27] Targeted agents including the Her2/Neu inhibitors, trastuzumab and lapatinib have been shown to cause a significant decrease in left ventricular function which can cause heart failure.[28] Anti-angiogenic agents including bevacizumab have potential cardio-toxicities that include hypertension, myocardial infarction, left ventricular dysfunction, venous thrombosis, stroke, and endovascular damage.[28]

Neurologic toxicity is one of the concerns caused by the chemotherapeutic agents that include the vinca alkaloids (vincristine and vinblastine), and the platinum agents. The most common neuro toxicity is a sensory peripheral neuropathy, which varies from mild to very severe. The vital neurotoxic expressions include hyponatremia, seizures, and encephalopathy.[29]

Platinum anticancer agents are alkylating-like agents, which bind to DNA and causes intra-strand cross-linking that interferes with DNA transcription and induces apoptosis in cancer cells. This class of drugs include cisplatin and its derivatives carboplatin and oxaliplatin. Cisplatin is the most

nephrotoxic anticancer agent among these three drugs.[30] Platinum agents also form the origin for renal electrolyte wasting, particularly of potassium and magnesium ions.[29]

Recent targeted anticancer agents with anti-angiogenic activity include monoclonal antibodies and tyrosine kinase inhibitors.[30, 31, 32] These anti-angiogenic active agents include bevacizumab and the tyrosine kinase inhibitors sorafenib, sunitinib, and pazopanib.[32] The mechanism of action of these agents is believed to be by inhibiting the formation of vascular channels that are essential for the tumors survival and growth. This blood vessel growth is blocked through the inhibition of vascular endothelial growth factor (VEGF) receptors.[32, 33] Primary perioperative toxicities associated with some of the antineoplastic agents is given in Table 1.1.

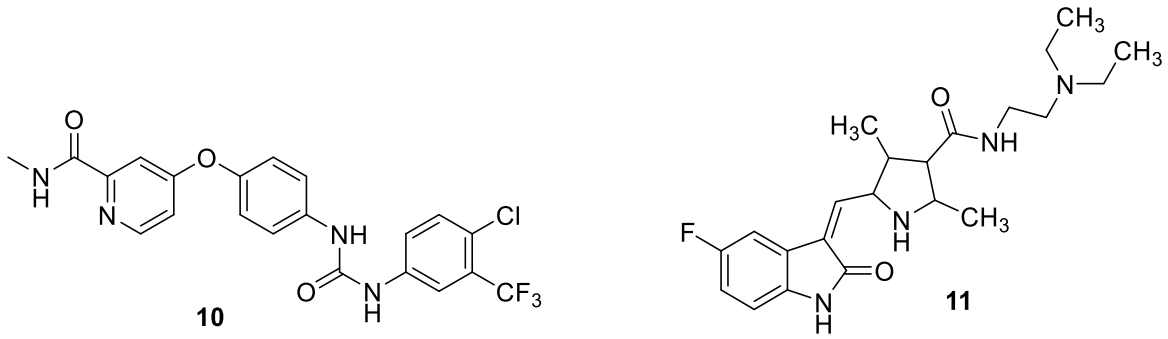

Sorafenib Sunitinib

Figure 1.2. Chemical structures of tyrosine kinase inhibitors.

Table 1.1. Antineoplastic agents and their primary toxicities [29]

Primary antineoplastic agent (class)	**Primary perioperative toxicity of concern**
Cytotoxic chemotherapy (except vincristine, bleomycin, others)	Myelosuppression
Anthracyclines	Cardiotoxicity
Platinum agents	Nephrotoxicity, electrolyte wasting, peripheral neuropathy
Antitumor antibiotics	Pulmonary toxicity (decreased DLCO, fibrosis)
Alkylating agents	Cardiotoxicity, pulmonary toxicity, hemorrhagic cystitis
Vinca alkaloids	Neurotoxicity, occasionally seizures, encephalopathy
Antimetabolites	Possible cardiotoxicity
Taxanes	Neuropathy
Corticosteroids	Adrenal suppression
Signal transduction inhibitors	Thrombosis, bleeding, diathesis, delayed wound healing

This situation makes the currently available drugs a challenge in treating cancers. The emergence of multidrug resistance is also a serious problem for the successful treatment of cancers.[34, 35] Several biochemical pathways are responsible for drug resistance.[34, 35] The most extensively studied ones are the membrane transporter proteins[36] that act as efflux pumps. Overexpression of a number of these transporter proteins enhances the efflux of chemotherapeutic drugs, resulting in a decrease in the drug concentrations in the cancer cells. **Figure 1.3** shows the efflux of a drug by P-glycoprotein (P-gp). The inhibition of efflux pumps is mainly done to improve the delivery of therapeutic agents. P-gp can be inhibited by blocking the drug binding site either competitively,

non-competitively **(Figure 1.4)** or allosterically.[37] The goal is to achieve improved drug bioavailability, uptake of the drug into the targeted organ or cells, and more efficacious cancer chemotherapy through the ability to selectively block the action of P-gp.[37] The best-known efflux pumps are the ABC superfamily of transporters such as P-glycoprotein (P-gp), the multidrug resistance protein (MRP) and the breast cancer resistance protein (BCRP)[38] families that use ATP as their energy source. The human P-gp is encoded by the mdr1 gene. Inhibition of the functions of P-gp to reverse MDR has been extensively studied and reported in the literature.[39, 40]

Various classes of P-gp modulators are reported which include calcium channel blockers, calmodulin antagonists, steroidal agents, protein kinase C inhibitors, immunosuppressive drugs, antibiotics, and surfactants. The co-administration of a non-toxic MDR-modulator with a cytotoxic drug may enhance the outcome of cancer treatment. Also, a cytotoxic agent displaying MDR-modulating properties can be effective in treating drug-resistant tumours. No precise conclusions on the molecular features characterizing MDR revertants have yet been confirmed; however, the general features of MDR modulators include the amphiphilic nature of the molecule, the presence of aromatic rings and a basic nitrogen bearing a positive charge at neutral pH.[41] This knowledge may be very useful for the design and/or the selection of novel MDR modulators for clinical testing.[2]

The compounds in series **29** demonstrate potent multidrug resistance (MDR) revertant properties having fluorescence activity ratio (FAR) values in the range of 49-179 while a reference drug verapamil has a FAR figure of 4.2 at a concentration of 4 µg/ml in murine L-5178 lymphoma cells.[42] A FAR value of greater than 1 shows a reversal of MDR. A representative compound **30** in series **29** displayed a FAR value of 10.8 towards MDR Colo 320 colon cancer cells at a

concentration of 4 μg/mL.[42] These results show that the compounds in series **29** can reverse MDR in drug-resistant cancer cells mediated by P-glycoprotein.

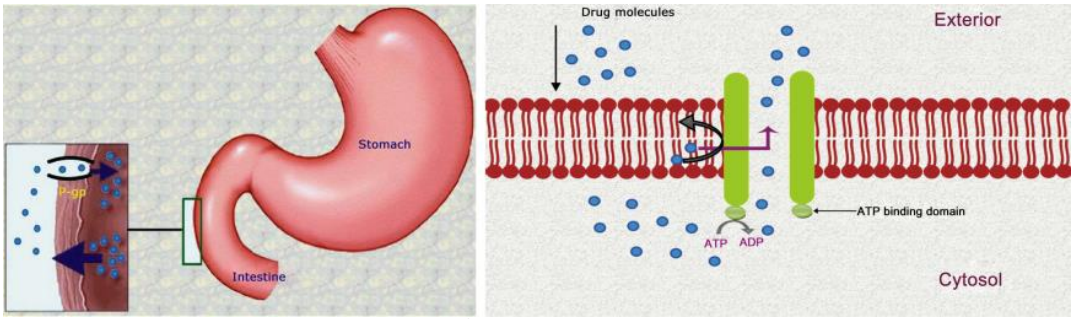

Source: Amin, M. L. P-glycoprotein Inhibition for Optimal Drug Delivery. *Drug Target Insights*, **2013**, *7*, 27–34

Figure 1.3. Drug efflux by P-glycoprotein.[37]

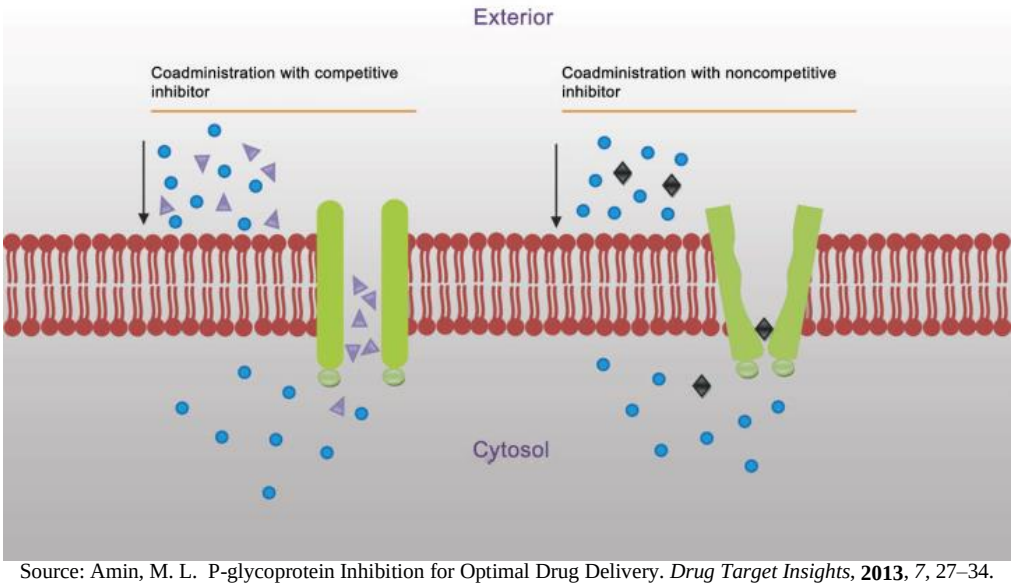

Source: Amin, M. L. P-glycoprotein Inhibition for Optimal Drug Delivery. *Drug Target Insights*, **2013**, *7*, 27–34.

Figure 1.4. Inhibition of P-glycoprotein to prevent drug efflux.[37]

1.5 α,β-Unsaturated ketones as anticancer and cytotoxic agents

In treating cancer, although a variety of drugs are available, compounds containing the α,β-unsaturated keto group are significant because of their high cytotoxic potencies and selectivity towards malignant cells rather than harming normal cells.[43] Many natural compounds which possess these functionalities are well known for their antifungal, antibacterial, antiviral, antimalarial and cytotoxic properties.[44] Chalcones are potent cytotoxic agents which have aroused significant interest, and several reports deal with the discovery of antineoplastic chalcone derivatives.[45] It is believed that the cytotoxic potencies of these derivatives are mainly due to the presence of the α,β-unsaturated carbonyl functionality in their moieties which acts as a Michael acceptor for cellular thiols and other nucleophiles.

The natural product curcumin is well known for its anticancer and chemopreventive properties. Curcumin can react with multiple molecular targets and hence has many differing pharmacological properties that includes anticarcinogenic, antioxidant, antimicrobial, anti-inflammatory, cardiovascular-protective, hepatoprotective, Alzheimer-easing, and antiarthritic properties properties which have been attributed to an α,β-unsaturated carbonyl group attached to an aryl ring in curcumin.[46] Despite the promising bioactivities associated with curcumin in *in vitro* assays, its clinical development has been hampered by its poor aqueous solubility, low *in vivo* efficacy and unfavourable and highly variable pharmacokinetics.

The presence of the active methylene group which undergoes keto-enol tautomerism in the curcumin molecule contributes to its adverse fate in clinical developments, as only the keto tautomer contributes to the overall bioactivity of curcumin. Apart from this problem, there are bioavailability issues arising due to the presence of phenolic and diketo groups and aromatic rings

with hydroxyl groups. The molecular structure of curcumin can be modified at three sectors in the molecule, to produce an "improved curcumin" that can address the issues of poor aqueous solubility and bioavailability. These sectors include the aromatic rings, the β-diketone moiety, and the two double bonds conjugated to the aromatic rings (**Figure 1.5**).

Successful structural modifications of curcumin produced analogues that resulted in potential anticancer drug candidates that target various stages/processes in cancer cell growth. Successful anticancer agents that are developed based on curcuminoid structures normally retain the conjugated α,β-unsaturated ketone functionality in their structures.[47] The β-diketone curcumin analogues have shown potent cytotoxicity to breast and prostate cancer cell lines. The SAR analysis of such analogues showed that the ortho-substituted α,β-unsaturated ketones are the most potent antioxidants which is an important finding for chemoprevention.[48]

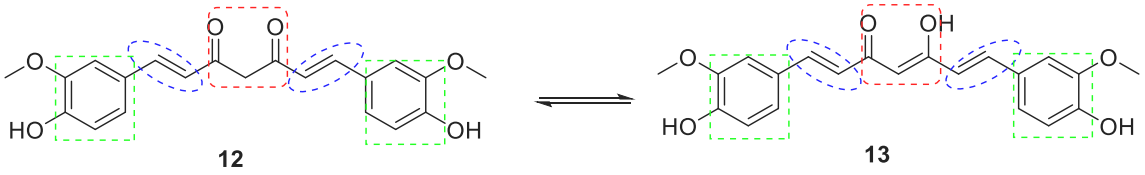

Figure 1.5. Tautomers of curcumin.

The lipophilic nature of curcumin limited its use for cancer treatment (logP=3.1) and as a result large quantity needed to be administered. It has a high first-pass effect, and some degree of intestinal metabolism takes place, particularly glucuronidation and sulfation and therefore it has low bioavailability. As discussed earlier, P-glycoprotein is a transporter protein that enhances the efflux of chemotherapeutic drugs, resulting in a decrease in the drug concentrations in the cancer cells and curcumin faces challenges of P-glycoprotein mediated drug resistance when administered

orally. Hence it is of interest to synthesize analogs of curcumin that have a better physicochemical profile than curcumin but with improved pharmacokinetic behaviour. It is well understood that proinflammatory states are linked to tumour promotion,[49, 50] and subsequently phytochemicals like curcumin that exhibit strong anti-inflammatory properties are anticipated to have some degree of chemopreventive activity.

Preclinical cancer research using curcumin has shown that it inhibits carcinogenesis in various types of cancers, including colorectal, pancreatic, gastric, prostate, hepatic, breast, and oral cancers, and leukemia, and at various stages of carcinogenesis.[51] Anti-inflammatory mechanisms implicated in the anticarcinogenic potential of curcumin include (1) inhibition of the enzymes NF-κB and COX-2 (increased levels of COX-2 are associated with many cancer types)[52, 53, 54] (2) inhibition of arachidonic acid metabolism via lipoxygenase and scavenging of free radicals that are generated in this pathway[54] (3) lowered expression of inflammatory cytokines IL-1b, IL-6, and TNF-α, resulting in growth inhibition of cancer cell lines[50] and (4) the down-regulation of enzymes, such as protein kinase C, that mediates inflammation and tumor-cell proliferation.[55]

Although the modes of action of curcumin on cellular pathways continue to be studied, there has been much research devoted to developing and understanding the structure-activity relationships (SARs) that are responsible for the drug's anticancer properties. By synthesizing a large number of analogues and subjecting them to biological screening, researchers hope to achieve an improvement in curcumin's anti-cancer and pharmacological profile while retaining its low toxicity. These structural modifications of curcumin (C-7) were made by replacing its central β-diketone moiety by a mono-carbonyl group to produce a new (C-5) 1,5-diaryl-3-oxo-1,4-pentadienyl mono carbonyl analogues (MCA).

The successful synthesis of such analogues (**Figure 1.8)** has resulted in the development of a number of potential anticancer candidates that target various stages and/or processes in cancer cell growth. Although there are a few exceptions, successful anticancer compounds based on curcuminoid structures, ordinarily retain the conjugated α,β-unsaturated ketone moieties. Advances in SARs suggest that a variety of structural types are tolerated with retention of potency.[47] Other experiments using diketone curcumin analogues are cytotoxic to prostate and breast cancer cell lines.[47] Treatment of these cancers has traditionally involved hormonal therapy. The α,β-unsaturated β-diketone moiety of curcumin has received much attention regarding its mechanistic role in promoting cytotoxicity. A very recent report outlined the synthesis of MCA's and their cytotoxic evaluations against Molt4/C8, CEM and L1210 cells in which the average IC_{50} values of **15b**, **16a**, and **17** were 38.3, 0.78 and >500 μM respectively.[56]

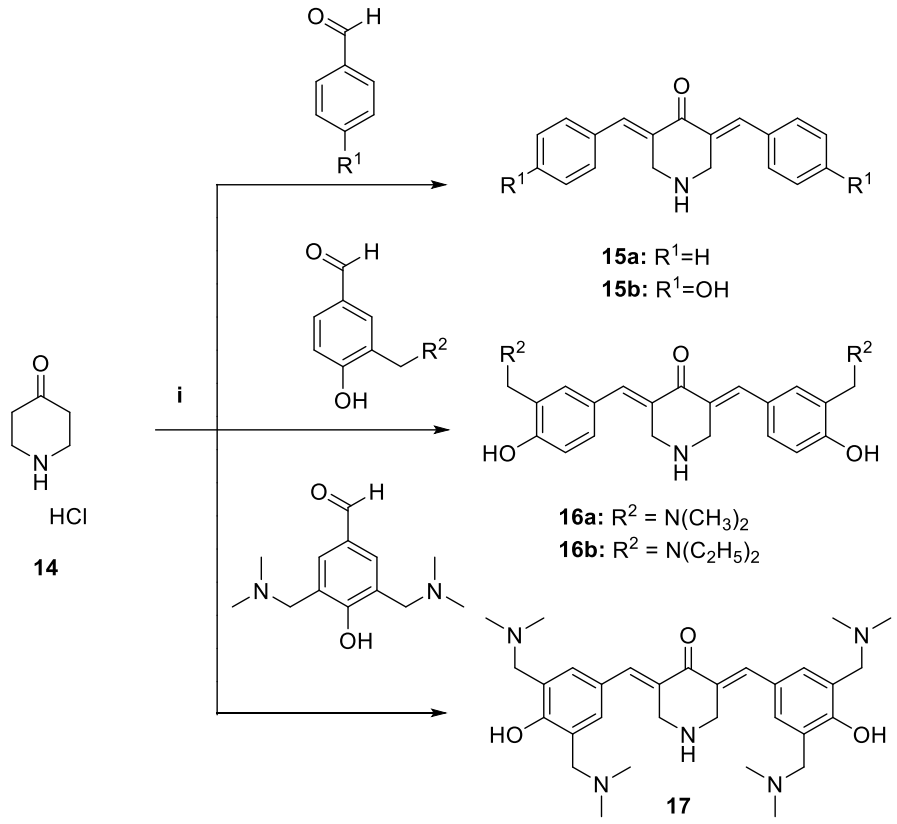

Reagents: (i) HCl/CH_3COOH, followed by K_2CO_3

Scheme 1.1. Modifications of conjugated α,β-unsaturated ketone compounds to increase bioavailability.

Compound **15a** showed promising cytotoxic properties against murine P388 cells whereas the in vivo results demonstrated only a marginal increase in efficacy.[57] The decrease in cytotoxic potencies in-vivo may be due to a variety of factors e.g., facile metabolism, excretion, plasma-protein binding, and a low plasma half-life. On the other hand, the lipophilicity of **15a** may be responsible for its lack of potency. In order to reduce the hydrophobicity of **15a**, the authors introduced hydroxyl groups in the aryl rings and also incorporated alkylaminoalkyl groups into the aryl rings of **15a** in this study with the consideration that the rate and extent of reaction of these

molecules with cellular thiols will be influenced by the magnitude of the atomic charges on the olefinic carbon atoms.

The pH in some tumours is lower than the non-malignant cells,[58] and in the case of compounds such as amines in such circumstances, the percentage of charged ions in the neoplastic tissues will be higher which will lower the electron density on the olefinic carbon atoms and greater toxicity will occur in tumours. The authors hypothesized that in addition to the reaction of cellular thiols with the olefinic carbon atoms, the alkylaminoalkyl groups present in these molecules could react at contiguous binding sites and thereby enhancing the cytotoxic potencies. For example, the methylene and methyl groups are available to form van der Waals bonds with different cellular constituents, whereas the nitrogen atoms of the dialkylaminoalkyl group can form hydrogen bonds. Hence the presence of the alkylaminoalkyl group may influence the IC_{50} values significantly. These considerations led to the development of compounds **15b-17**. In another article, the authors reported that some of these compounds **15b-17** induced glutathione oxidation and mitochondria-mediated cell death in HCT-116 colon cancer cells.[59] The compounds **15a** and **16a** were four times more potent than curcumin. Also, these compounds were tested against human non-malignant CRL-1790 colon cells which demonstrated that GI_{50} values of all these compounds were greater towards CRL-1790, indicating more tumour-selective toxicity.[59] In general, conjugated enones act as Michael acceptors with thiols preferred over amino or hydroxyl nucleophiles.[60]

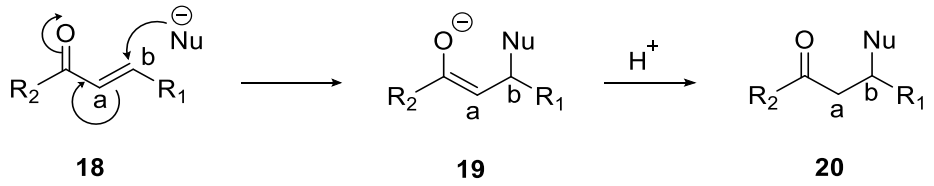

Figure 1.6. Michael acceptor reaction with a nucleophile (Nu) attacking at the β-position thereby generating an α,β-functionalized ketone.

Studies to exploit curcumin's potential as a Michael acceptor includes the interaction between curcumin and glutathione (GSH), but the products from the reactions are complex and ill-defined.[61, 62]

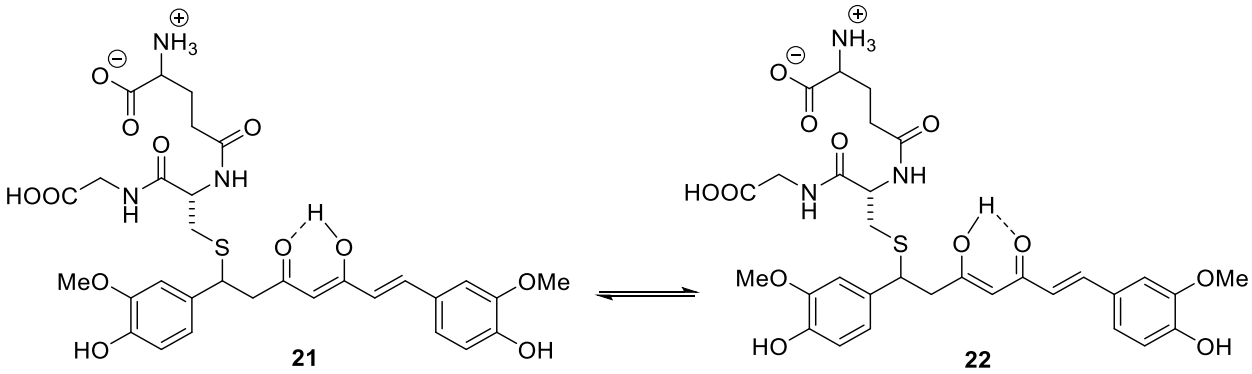

Figure 1.7. Hypothetical tautomeric isomers of curcumin-GSH adducts.

The synthesis, cytotoxicity, and SAR of α,β-unsaturated monoketo systems have been examined. For example, a variety of 2,6-bis(arylidene)cyclohexanones (series **24**) are three to five times more potent than 5-fluorouracil (5-FU) as cytotoxins against L1210, Molt 4/C8, and CEM cells.[63, 64]

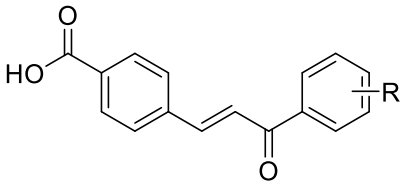

23

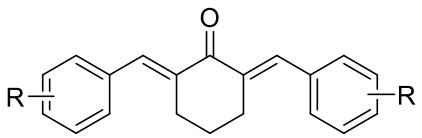

24

Figure 1.8. Unsaturated monoketones and 2,6-bis(arylidene) cyclohexanone cytotoxins.

However, compounds with more than one conjugated carbonyl group are generally more active than those with only a single α,β-unsaturated keto group. This observation supports the "sequential cytotoxicity" hypothesis, which suggest that some cancer cells are more susceptible to multiple chemical insults (in this case, two sites for thiol alkylation as opposed to one) than normal cells. For instance, the *N*-acryloyl derivatives (**27a-f**) have been reported to exhibit[65] up to 25-fold higher cytotoxic potencies against P388, L1210, Molt 4/C8, and CEM neoplasms compared to the analogs without the acryloyl group.

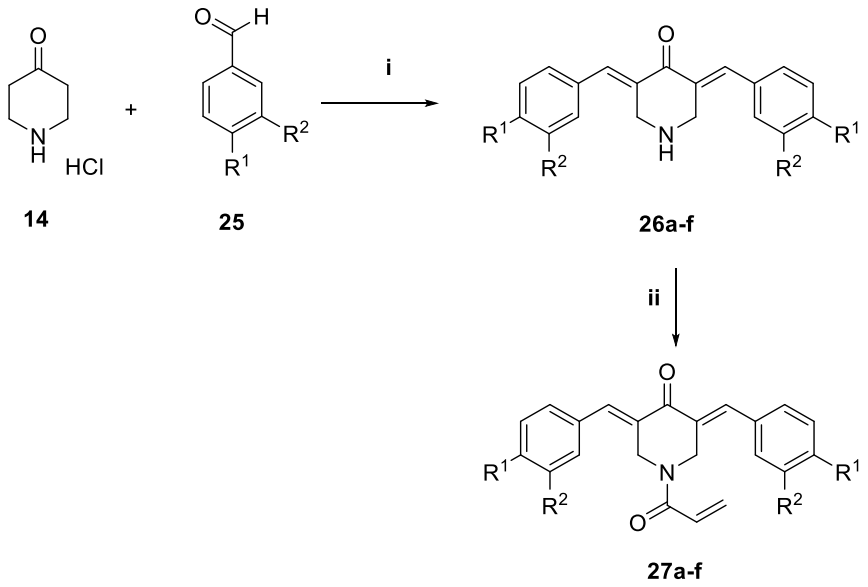

Reagents: (i) HCl/CH_3COOH, followed by K_2CO_3; (ii) $CH_2=CHCOCl/K_2CO_3$ **a:** $R^1= R^2= H$; **b:** $R^1= Cl$, $R^2= H$; **c:** $R^1= R^2= Cl$; **d:** $R^1= F$, $R^2= H$; **e:** $R^1= NO_2$, $R^2 = H$; **f:** $R^1 = OCH_3$, $R^2 = H$

Scheme 1.2. Synthesis of *N*-acryloyl derivatives of 3,5-bis(arylidene)-4-piperidone.

Dr. Dimmock *et al*. have investigated several series of α,β-unsaturated ketone derivatives as cytotoxic thiol-alkylating agents based on the following considerations. (1) These compounds have a specific or preferential affinity for thiols rather than amino or hydroxyl groups;[66, 67] hence the genotoxic side effects caused by the interactions of a number of contemporary anticancer drugs with nucleic acids can be avoided. (2) Thiol concentrations are elevated in many tumours,[68, 69] and the lowering of thiol concentrations (and hence interfering with the redox system in cells) may be more damaging to tumours than normal tissues. Also, high concentrations of such thiols (e.g. GSH) contribute to MDR due to their ability to detoxify electrophilic anticancer agents and their metabolites. (3) Some cellular thiols play an important role in cell division whereby the concentrations of thiols increase just before and during mitosis.[70] Those tumours possessing a higher mitotic index than the corresponding normal cells are more likely to be damaged by thiol

alkylators. (4) Conjugated unsaturated ketones are structurally and mechanistically divergent from the anticancer drugs used today.[71] Thus tumours are unlikely to be resistant to them.

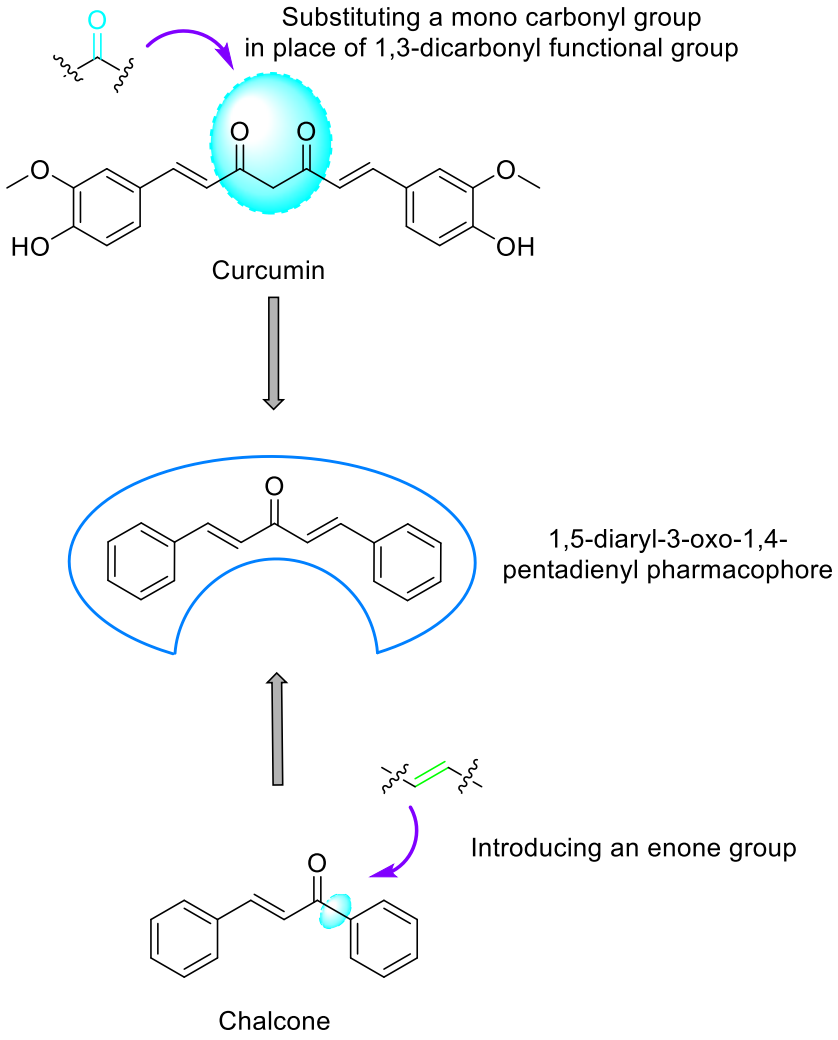

Figure 1.9. Development of the 1,5-diaryl-3-oxo-1,4-pentadienyl pharmacophore.[72]

These structural modifications of curcumin were made by replacing its central β-diketone moiety by a mono-carbonyl group to produce a new promising 1,5-diaryl-3-oxo-1,4-pentadienyl pharmacophore (**Figure 1.9**) that retains the cytotoxic potencies of curcumin and chalcones with the desired selectivity and drug-like properties.

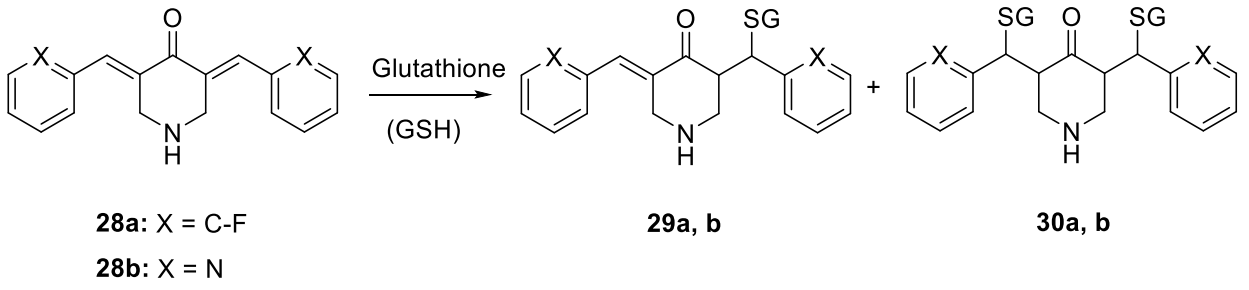

Figure 1.10. Sequential Michael reaction of protein thiols with an arylidene dienone electrophile.[72]

Dimmock's research lab has made significant contributions in developing potent antineoplastic agents which possess the 1,5-diaryl-3-oxo-1,4-pentadienyl pharmacophore.[73] An important aspect of developing these antineoplastics is in regards to the hypothesis of sequential cytotoxicity which states that "a chemical insult prior to a subsequent chemical attack on cellular thiol constituents may produce greater toxicity to cancers than normal cells." In other words, an initial reaction with a cellular thiol by cytotoxic agents will sensitize the malignant cells preferentially and a second interaction with another thiol will cause more damage to malignant cells than normal cells. Some of the evidence in support of this hypothesis is that on several occasions, the lowering of the concentrations of cellular thiols prior to the administration of various anticancer agents enhances the toxicity of the drug to the tumours rather than normal cells. For instance, the α,β-unsaturated ketone ethacrynic acid enhances the cytotoxicity of various alkylating agents.[74, 75] Probably this effect is due to a tumour having a greater requirement for thiols for their growth compared to normal cells.[76]

1.5.1 The development of 1,5-diaryl-3-oxo-1,4-pentadienes as cytotoxic agents.

The 1,5-diaryl-3-oxo-1,4-pentadienyl pharmacophoric group was placed on cycloalkyl and heterocyclic scaffolds such as cyclohexane,[64, 77, 63] 2-tetralone[78] or piperidines that revealed a

number of lead cytotoxic molecules with encouraging cytotoxic potencies.[43] The cytotoxic potencies of these scaffolds show the substituted piperidines to be the most promising cytotoxic agents (**Figure 1.11**).

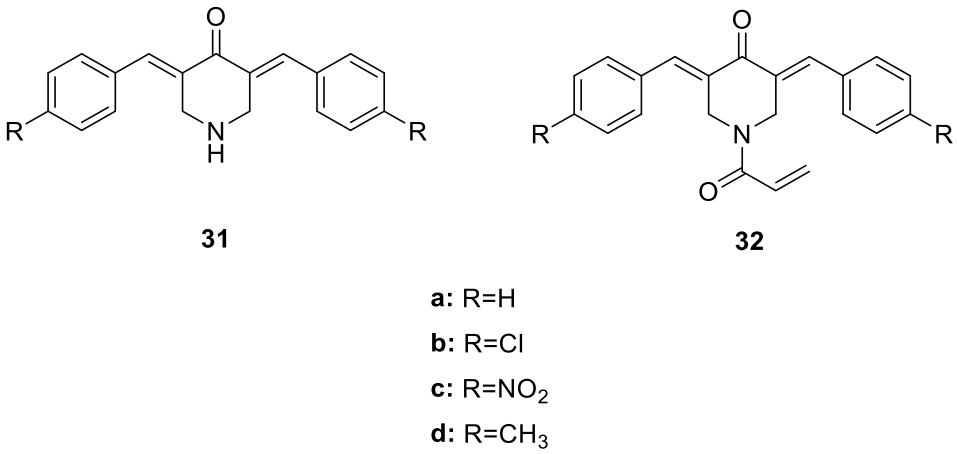

Figure 1.11. 1,5-Diaryl-3-oxo-1,4-pentadienyl compounds as lead cytotoxic agents.

A novel series **31** have IC_{50} values towards human Molt4/C8 and CEM T-lymphocytes in the low micromolar range (2-13 μM) while the IC_{50} figures against murine P388 leukemic cells (0.2-0.8 μM) were more favorable than the data towards murine L1210 neoplasms (8-42 μM).[65] Various series of these compounds show greater cytotoxicity towards neoplasms (human HSC-2 and HSC-4 squamous cell carcinomas and human HL-60 promyelocytic leukemic cells) than non-malignant cells (normal human HGF gingival fibroblasts, HPC pulp cells and HPLF periodontal ligament fibroblasts). The average selective index values (SI, the ratio of the average CC_{50} values of the compound towards several normal cells/CC_{50} figures towards a neoplastic cell line) of **31a-d** are 10, 4.3, 13 and 29 revealing that the compounds are tumour-selective cytotoxins and can be considered for further development.[79] The high SI figure of **31d** of 29 is noteworthy and establishes it as a lead cytotoxic agent. With the aim of developing potent cytotoxic agents,

additional thiol alkylating sites were introduced into the arylidene dienone **31** which led to the development of the *N*-acryloyl-3,5-bis(benzylidene)-4-piperidones **32**.[80]

A hypothesis is that the 1,5-diaryl-3-oxo-1,4-pentadienyl group in **32** aligns at a primary binding site and the *N*-acryloyl group will interact at the auxiliary binding site which may lead to a greater cytotoxic potency of **32** compared to **31**. The *N*-acyl derivatives **32** were designed and developed based on the following fact. Series **31** is predicted to have a significant percentage of the molecules in the ionized form which may hamper their passage into the neoplastic cells, and *N*-acylation will overcome this problem. The conversion of series **31** compounds into the corresponding *N*-acryloyl analogs **32** increased both the capacity for thiol alkylation and cytotoxicity in the case of Molt 4/C8 cells while similar trends were noted in the CEM, P388 and L1210 screens.[65] The modes of action of **31c** and **32c** revealed that both molecules inhibit the biosynthesis of DNA, RNA and proteins in murine L1210 cells.[65]

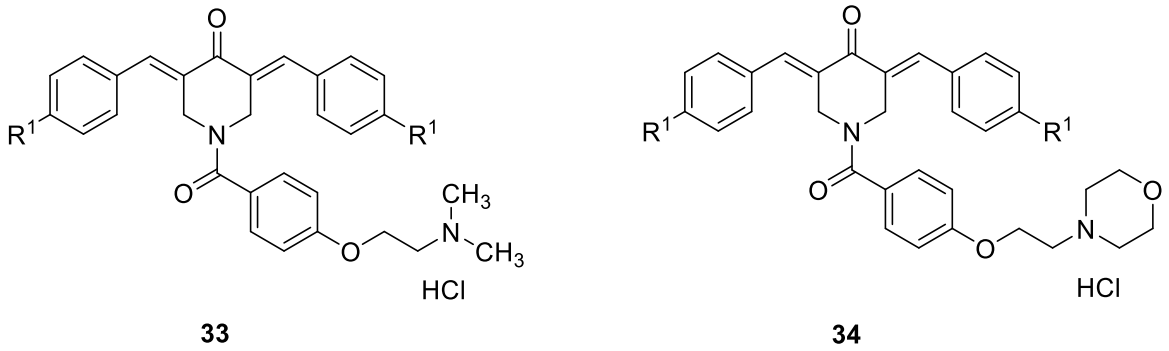

Figure 1.12. 1-[4-(2-Alkylaminoethoxy)phenylcarbonyl]-3,5-bis(arylidene)-4-piperidone hydrochlorides.

The *N*-acyl derivatives 1-[4-(2-alkylaminoethoxy)phenylcarbonyl]-3,5-bis(arylidene)-4-piperidone hydrochlorides **33** were developed,[81] and the substituents on the piperidyl nitrogen

atom were chosen using certain groups and atoms that are capable of forming van der Waals, hydrogen and ionic bonds at receptor sites (**Figure 1.12**). The IC_{50} values of the compounds in series **33** were compared with the data for the analogs **31** in which the aryl substituents are identical using human Molt 4/C8 and CEM T-lymphocytes and L1210 cell lines. The potencies of the dienones **33** are either increased, are equipotent or decreased by 48%, 35% and 17%, respectively, of the comparisons made.[81] Some compounds in series **33** showed IC_{50} values in the submicromolar to nanomolar range against a panel of human colon cancer cells, and the average IC_{50} values are lower than 5-fluorouracil (5-FU) which is used extensively in treating colon cancers. The compounds in series **33** display greater toxicity to the neoplastic HL-60, HSC-2 and HSC-4 tumour cells than non-malignant HGF, HPC and HPLF normal cells.[82] Two-thirds of the SI figures are over 5.

A mode of action study using a representative compound **34** disclosed that it causes internucleosomal DNA fragmentation in HL-60 cells and activated caspase-3 in HL-60 and HSC-2 cells.[82] This compound caused apoptosis and to a lesser extent autophagy (the degradation of subcellular constituents by creating acidic organelles in response to stress factors).

A number of heterocyclic α,β-unsaturated carbonyl compounds with a 1,5-diaryl-3-oxo-1,4-pentadienyl pharmacophore were shown to possess remarkable activity against various human cancer cell lines,[83] and most of these compounds displayed preferential toxicity toward cancer cells. Moreover, the study conducted by Sun *et al*. evaluating the multidrug resistance reversal properties confirmed that all the compounds reverse MDR, particularly, the tertiary amines **35a**, **36a**, **37a**, **38a**, and **39a** (**Figure 1.13**) which are more potent.[84] The data presented in this work can

encourage the synthesis and bioevaluations of the dual effect of compounds possessing both MDR reversal and antiproliferative properties in the future.[84]

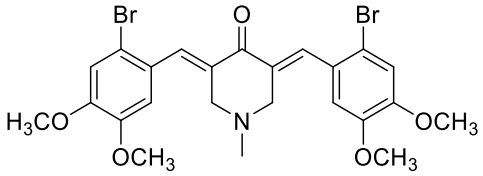

35a

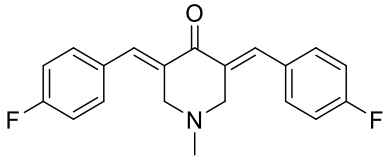

36a

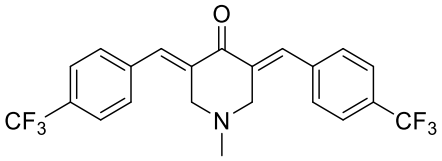

37a

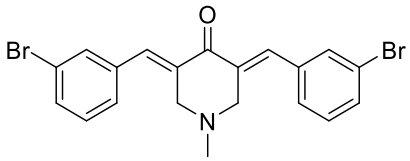

38a

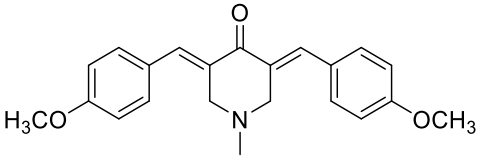

39a

Figure 1.13. Heterocyclic α,β -unsaturated carbonyl compounds with the 1,5-diaryl-3-oxo-1,4-pentadienyl pharmacophore.

Nine human tumor cell lines, including A549, U937 (respiratory system), Hela(reproductive system), HT- 29(digestive system), K562(circulatory system), MCF-7(breast cancer) , U87 and U251(nervous system), HepG2(immune system), and a human umbilical vein endothelial cell line (HUVEC) were used to evaluate compounds (**Figure 1.13** and **Figure 1.14**) **35a-35d, 36a-36d, 37a-37d, 38a-38d**, and **39a-d** in order to confirm whether they demonstrate antiproliferative activities toward a variety of neoplasms.[84]

The biological evaluation revealed that the compounds synthesized demonstrate potent antiproliferative activity toward Hela, HT-29, K562, U937, U87, U251 and HepG2 cell lines, and Hela, K562 and U87 are the most sensitive to these compounds. Overall, these compounds are substantially more potent than a reference anticancer drug cisplatin (CDDP) against almost all tumour cells used.[84] In particular, compounds **37a-d** bearing a strong electron-withdrawing 4-trifluoromethyl group in the arylidene benzene rings displayed the greatest antiproliferative activity, and 64% of the IC_{50} values are submicromolar.[84] The possible reason is that electron-withdrawing groups are helpful to diminish the electron density on the adjacent olefinic carbon atoms, which may result in the nucleophilic attack more easily by cellular components, for instance, thiols.[85]

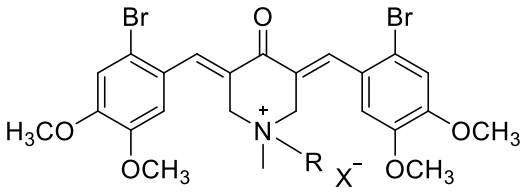

35b-35d

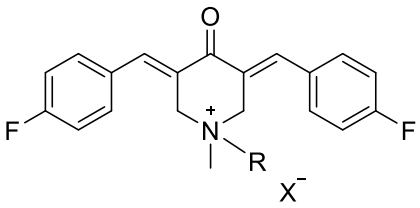

36b-36d

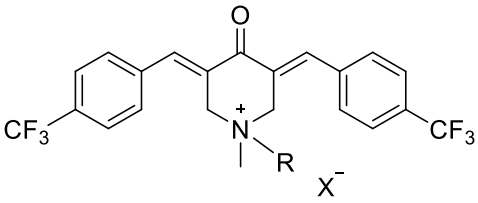

37b-37d

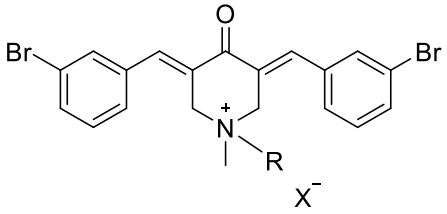

38b-38d

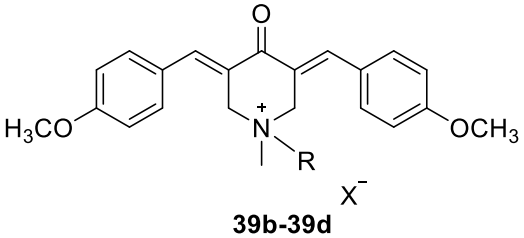

39b-39d

R=

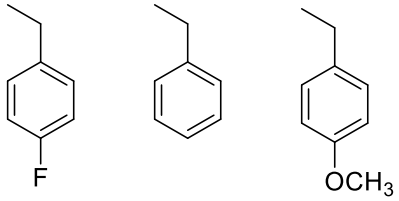

b **c** **d**

X= Br or Cl

Figure 1.14. Quaternary ammonium salts of α,β -unsaturated carbonyl compounds with the 1,5-diaryl-3-oxo-1,4-pentadienyl pharmacophore as cytotoxic agents.

It has been reported that a number of quaternary ammonium salts (QAS) have displayed significant antiproliferative ability.[86, 87, 88] Here the compounds synthesized by Sun *et al.* were designed to form *N*-methyl-*N*-substituted benzyl QAS on the piperidone nitrogen, however, there were no remarkable changes in the activity against all tumor cell lines used.[84]

Another purpose of preparing these quaternary ammonium salt derivatives is to improve the water solubility of the compounds, as it has been found that the solubility of this type of non-quaternary derivatives is poor according to the authors' previous studies[89, 88] thus resulting certain difficulties during the biological evaluation. Attaching various groups to the piperidone nitrogen atom in these α,β -unsaturated carbonyl compounds with the 1,5-diaryl-3-oxo-1,4-pentadienyl pharmacophore may possess inherent biological activity, improve pharmacological properties of the dienone pharmacophore or facilitate interaction with a receptor binding site.[43]

Organophosphorus groups, such as phosphonate, bisphosphonate and phosphates are used as structural modifiers of 3,5-bis(arylidene)-4-piperidones. It was reported that the direct phosphorylation on the free nitrogen of 3,5-bis(arylidene)-4-piperidones with diethyl chlorophosphate provided the corresponding amides (**Figure 1.15**). Some of the phosphonates showed higher anticancer activity than non-phosphorylated analogues.[90] Moreover, these amides exhibited higher cytotoxicity toward cancer cells as compared to normal cells.[91] Singh et al. reported that the *N*-phosphorylated 3,5-bis(arylidene)-4-piperidones possess good membrane permeability.[92] High cytotoxicity toward malignant cells was also demonstrated by 3,5-bis(arylidene)-4-piperidones bearing a diethyl phosphonate and tetraethyl (methylene)bisphosphonate groups attached to the piperidone nitrogen atom through short alkylene chains.[93, 94]

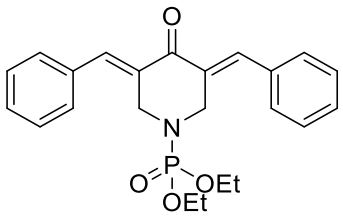

40

Figure 1.15. Diethyl[(4-oxopiperidin-1-yl)(aryl)methyl]phosphonates.

Makarov et al developed a synthetic approach to the novel 1,5-diaryl-3-oxo-1,4-pentadiene-4-piperidones modified with a diethyl phosphonate group connected to the nitrogen atom of the piperidone motif through a short linker group.[95] The preparative procedure for the synthesis of diethyl α-amino (aryl)methyl phosphonates **42** containing a 4- piperidone ring as an amine unit was shown in the scheme 1.3 The diethyl[(4-oxopiperidin-1-yl)(aryl) methyl] phosphonates were used as starting compounds to prepare the corresponding α-aminophosphonates of 3,5-bis (arylidene)-4-piperidones ; these compounds were screened in vitro for inhibitory activity toward various cancer cells.[95]

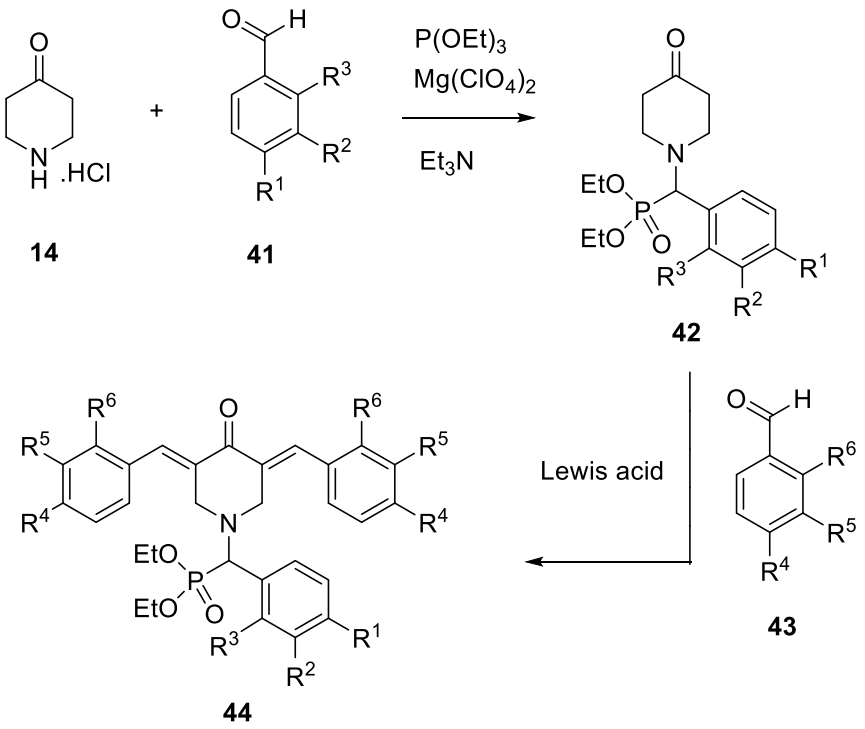

42a: $R^1 = R^2 = R^3 = H$
42b: $R^1 = F,\ R^2 = R3 = H$
42c: $R^1 = OCH_3,\ R^2 = R3 = H$
42d: $R^1 = R^2 = R^3 = OCH_3$
42e: $R^1 = R^3 = OCH_3,\ R^2 = H$

Scheme 1.3. Synthetic sequence for the preparation of α-aminophosphonates of 3,5-bis(arylidene)-4-piperidone derivatives.[96]

The cytotoxic activity of the compounds **44a-n** (Scheme 1.3) was tested in vitro against human malignant cell lines, such as RD (rhabdomyosarcoma), PC3 (prostate cancer), HCT116 (colon cancer), MCF7 (breast cancer), and normal human embryonic kidney (HEK293) cell line. The results obtained in this study showed that majority of the phosphonates **44a-n** showed IC_{50} values in the range of 2.5-8.5 μM, except the compound **44g** with dimethylamino groups in the para position of bis(arylidene)piperidone motif with low cytotoxicity.[96] Such a low cytotoxicity of other

3,5-bis(4-dimethylaminobenzylidene)-4-piperidones is also known from other studies as reported by Makarov *et al*.[93] stated that this low cytotoxicity may be due to the presence of the strong electron-releasing character of dimethylamino substituents present at the para position of aryl rings.

The compounds **44c, 44f, 44k, 44m** having methoxy substituents in the aromatic rings also showed lower activity toward MCF7 cells in contrast to the other active compounds. The nitro-derivative **44d**, showed the highest cytotoxic activity towards the studied cell lines, with all the inhibitory concentrations lower than 3.0 μM. The nitro-compound **44i** and the cyano analogue **44j** have strong electron-withdrawing substituents in benzylidene moieties and displayed good cytotoxicity toward cancer cells having IC_{50} values in the range of 3.0-4.3 μM.[96]

1.6 Cancer drug targets

1.6.1 Traditional therapies vs targeted therapies in cancer

For the past half century, non-surgical cancer treatment has been dominated by two main types of traditional therapies: chemotherapy and radiation therapy. Chemotherapy refers to treatment with drugs that have the potential to kill cancer cells. Radiation therapy refers to the use of high-energy radiation from X-rays, gamma rays, neutrons, protons, and other sources to kill cancer cells and shrink tumours. Targeted therapies are often described regarding how they differ from traditional therapies such as chemotherapy and radiation therapy.[97]

Like normal cells, cancer cells replicate themselves and proliferate by copying their DNA.[98] Several important classes of cancer chemotherapies along with their mechanisms of action and the way they act to treat cancer are discussed at the beginning of the literature survey. Although the different classes of chemotherapies may act at different stages of the DNA replication process, the important thing to note is that these drugs interfere with DNA replication. However, because DNA replication is a common process that all cells use when they want to make more copies of themselves, chemotherapies cannot distinguish between cancerous cells that are being replicated and normal cells that are being replicated. Thus, classic chemotherapy leads to many side effects because it also tends to kill normal cells that are undergoing replication (discussed in the section of challenges of cancer treatment).

If chemotherapies are not specific for cancerous cells, why don't they kill all the cells in our bodies? The answer is that most of our cell populations do not continuously replicate themselves as cancer cells do. For the most part, our organs such as the brain, heart, kidneys, and liver are already formed. Certain cells in these organs can and do replicate, but they do not replicate out of control like cancer cells. Because these cell types are not undergoing repeated, rapid cell division, they are generally not bothered by chemotherapies. Additionally, normal tissues can repair themselves and continue to grow; thus, even if they are injured by chemotherapy, the effects are rarely permanent.

However, not all of our cells escape the effects of chemotherapies. The fast-growing normal cells most often affected by chemotherapy are blood cells in the bone marrow, cells lining the digestive tract (such as the mouth, esophagus, and stomach), and cells in hair follicles. Chemotherapy can also cause side effects such as nausea and vomiting interfering with processes other than cell

replication. The effects of chemotherapy on these cells types lead to some of the most common side effects (as discussed in the section on challenges of cancer treatment).

Ideally, we would have treatments for cancer that effectively kill only the diseased cells without harming healthy cells, even those that replicate quickly. Basic science research has led to a greater understanding of how cells work and what goes awry in cancer. As a result of this work, investigators have developed a growing list of drugs that are better able to "target" specific features of cancer cells while minimizing effects on healthy cells. These treatments have come to be known as targeted therapies.

Targeted cancer therapies involve drugs or other substances that block the growth and spread of cancer by interfering with molecules that are more specifically involved in cancer cell growth and progression than in normal cell activity. These drugs act on cell markers and/or biochemical pathways to prevent the cancer cells from replicating or proliferating. The goal of these targeted therapies is to kill the cancerous cells while leaving the normal cells unharmed. By focusing on changes in the cell that are specific to cancer, targeted cancer therapies may be more effective than chemotherapy and radiotherapy.

Drug targets in cancer research are very often highlighted with mutated genes. Overexpression of some specific genes such as epidermal growth factor (EGF), HER-2, insulin growth factor receptors, cyclins, have been correlated with cancer-causing factors in some cancers.[99] The targeted drugs that are being used in cancer treatment follow different modes of action. The strategy for chemotherapy includes targeting of drugs at specific genes, proteins/enzymes that are found in malignant cells or targeting the internal tissue environment that contributes to the development and survival of cancer cells. Targeted therapy is often used along with chemotherapy

to restrict the growth and invasion of the cancer cells. Targeted therapy has emerged as a promising method for developing selective anticancer agents.[100] Some of the drug targets are discussed below.

1.6.2 Monoclonal antibodies: One of the major classes of targeted therapies in cancer

Monoclonal antibodies are proteins made in the laboratory that can bind to the substances in the body, including the components of cancer cells. Each type of monoclonal antibody is designed in a way that it binds to one substance. Monoclonal antibodies attach themselves to the substance (often a protein) on cancer cells, thereby blocking the signals for cell growth and cell proliferation. In some cases, the attachment of monoclonal antibodies to cancer cells leads to the death of the cells. As large proteins, these monoclonal antibodies cannot typically enter inside the cells. For this reason, they usually bind to substances or parts of substances that are located on the surface of the cell(s) or in the areas outside the cells such as plasma.

Monoclonal antibodies are of two types: namely naked and conjugated monoclonal antibodies. Naked monoclonal antibodies can attach to antigens on cancer cells and thereby interfering with cell growth and proliferation or cause cell death. These are the most common types of monoclonal antibodies in use today. However, it is possible to attach the monoclonal antibody to a cytotoxic substance/drug that potently kills cancerous cells. In this way, the monoclonal antibody acts as the arrow that targets the cancerous cells, while the substance attached to this arrow (monoclonal antibody) acts as a cell poison. Conjugated antibodies can be classified into several groups depending on the type of substance attached on to them. Primarily there are three main classes of conjugated antibodies, which are radiolabeled (attached to radioactive particles), chemolabeled (attached to chemotherapy drugs), and immunotoxins (attached to cell toxins).

In cancer therapy, the monoclonal antibodies in use have different approaches of mediating tumour cell death, which are well linked with the natural function of the target antigen. Monoclonal antibodies can directly act on the cancer cells by the blocking of growth factor receptors that are required for the cancer cell growth. Cetuximab is one of the first monoclonal antibodies to target the epidermal growth factor receptor (EGFR) and has been approved in the treatment of colorectal cancer. Cetuximab binds on the cell surface of EGFR and prevents the ligand binding site of EGFR which in turn inhibits the intracellular receptor signalling. This results in the cell-cycle arrest, induction of apoptosis and thus the downregulation of cell surface expression of EGFR takes place. Another example of a monoclonal antibodies is Trastuzumab and it has been used to target effectively the human epidermal growth factor receptor type 2 (HER2).[101]

Table 1.2. Classification of conjugated monoclonal antibodies and their targets

Class of Conjugated Monoclonal Antibody	**Description**	**Examples**	**Target**
Chemolabeled	Monoclonal antibody attached to the chemotherapy drug	Brentuximab vedotin (Adcetris®)	CD30 antigen on white blood cells attached to the drug known as Monomethyl Auristatin E (MMAE)
Radiolabeled	Monoclonal antibody attached to small radioactive particles	Ibritumomab tiuxetan (Zevalin®), Tositumomab (Bexxar®)	CD20 antigen on certain white blood cells
Immunotoxin	Monoclonal antibody attached to a cellular toxin	NA	NA

****NA**: No products approved yet

Brentuximab Vedotin (BV) is an antibody-drug conjugate that specifically delivers the potent cytotoxic drug monomethyl auristatin E (MMAE) to CD30-positive cells. BV is FDA-approved for treatment of relapsed/refractory Hodgkin lymphoma (HL) and anaplastic large cell lymphoma (ALCL); however, many patients do not achieve complete remission and develop BV resistant disease.[102]

Although no immunotoxins are currently available for the treatment of cancer, many are under study. A related drug that consists of an immune system protein that is not an antibody is attached to a toxin made by the organism that causes diphtheria. This drug is known as denileukin diftitox (Ontak®) and is used to treat some types of cancers.[103]

At least nine different monoclonal antibodies are approved by the United States Food and Drug Administration (FDA) for the treatment of cancer. Examples: Avastin®, Bexxar®, Campath®, Erbitux®, Rituxan®, Vectibix®, Yervoy®, and Zevalin®. [104]

Alemtuzumab (Campath®)

Alemtuzumab is a humanized, unconjugated monoclonal antibody used to treat chronic lymphocytic leukemia.[105] Alemtuzumab binds to a protein called the CD52 antigen, a protein located on certain white blood cells known as B cells and T cells. After the attachment of the drug to the CD52 antigen, alemtuzumab initiates the destruction of the cell by the immune system. The abbreviation CD stands for “cluster of differentiation” and refers to a group of antigens on the surfaces of white blood cells that react with different antibodies. Each type of white blood cell expresses a pattern of CD antigens that can be used to help distinguish it from other types of white blood cells that are at different stages of maturity or perform different functions.[106] The antigens

themselves have a variety of different functions such as allowing cells to adhere to one another, acting as receptors, and regulating immune responses.[107]

Bevacizumab (Avastin®)

Bevacizumab is also a humanized and unconjugated monoclonal antibody which is directed against vascular endothelial growth factor (VEGF).[108] VEGF is a growth factor that helps vascular endothelial cells to grow, and these vascular endothelial cells make up the inside of blood vessels.[109] Cancers need a constant blood supply to bring them oxygen and nutrients so that they can grow and proliferate.[110] VEGF is a growth factor that stimulates new blood vessel formation, which helps tumors to grow and proliferate.[110] Bevacizumab binds to VEGF to form a complex that prevents VEGF from binding to its receptors on the surface of cells.[110] VEGF is the signal that initiates the growth pathway in vascular endothelial cells. Without the VEGF signal, the growth pathway is not activated and results in no growth of these cells and no new blood vessels. And without new blood vessels, cancers cannot grow.[111] That is, all tumours need a blood supply and VEGF is a key factor needed for generating this blood supply. For this reason, it seems that all tumours would be sensitive to antibodies against VEGF.

1.6.3 Angiogenesis (AG) inhibitors

Angiogenesis (AG) is a process whereby a tumour develops new blood vessels for cell growth and metastasis. Small tumours can obtain oxygen and nutrients by diffusion, but as they grow into large tumours, they need new blood vessels for obtaining the required nutrients for growth, invasion and metastasis. Anti-angiogenic and pro-angiogenic factors are involved in the process of development of new blood vessels.[112] Vascular endothelial growth factor (VEGF), fibroblast

growth factor (FGF), and angiogenin are a few pro-angiogenic factors that are produced in tumor-associated angiogenesis which in turn induces the proliferation, migration and invasion of endothelial cells in new vascular structures.[112] A clinical trial in the year 2003 resulted in the prolonged survival of cancer patients with metastatic colorectal cancer. In this clinical trial, the chemotherapy was administrated successfully in combination with humanized neutralizing antibodies that targets the anti-vascular endothelial growth factor (VEGF). This resulted in an FDA approval for the therapy and provided a proof-of-concept that anti-angiogenic therapy can be used effectively in treating cancer. Several antibodies and tyrosine kinase inhibitors are designed to target the pro-angiogenic signaling pathways and have been approved as cancer therapies. In spite of a having large number of FDA-approved drugs, the success of anti-angiogenic treatment has been limited, providing only a short-term relief from tumor growth before resistance occurs. This limitation has several explanations that includes, tumors making use of alternative modes of angiogenesis and advancement of resistance mechanisms, and the tumors can find access to blood supply through vascular co-option, thus bypassing the need of tumor angiogenesis.[113] Some of the angiogenesis inhibitors with their modes of action are (a) Angiostatin K13: Inhibitor of endothelial cell growth and angiogenesis, (b) Fumagillin: Inhibitor of endothelial cell proliferation and angiogenesis, and (c) Genistein: Downregulates the transcription of genes involved in controlling angiogenesis.

1.6.4 Microtubule inhibitors

Microtubules are heterodimers composed of α and β tubulins. These are involved in many biological process e.g., cell signalling, intracellular transport and maintenance of cell shape.[114] Microtubules are important targets for anticancer drug development due to their significant role in

mitosis. During the cell division, the mitotic spindle is responsible for the movement of chromosomes to the opposite sides of the cell. These spindles are composed of microtubules that have tubulin as a monomer.[115, 116] Microtubule inhibiting agents are compounds/drugs that interfere with the microtubule assembly. Currently, these agents are being used in clinical therapy as they are able to suppress microtubule dynamics in fast dividing tumour cells by misdirecting the formation of a functional mitotic spindle. These microtubule inhibitors can be classified as stabilizing and destabilizing agents. Microtubule stabilizing agents act by promoting the polymerization in cancer cells. Taxanes (paclitaxel and docetaxel) and epothilones are examples of these stabilizing agents.[100] Some examples of microtubule inhibitors used as anticancer agents are (a) paclitaxel which binds to β tubulin and promotes the formation of highly stable microtubules that resist depolymerization thereby preventing cell division,[117] and (b) dolastatin 15 which is reported to interact with tubulin and induce apoptosis.[118] Recent studies reveal plinabulin a synthetic analog derived from the marine natural product "diketopiperazine phenylahistin" is a micro-tubulin inhibitor. Plinabulin has been moved into phase III clinical trials in combination with docetaxel as a combination agent for treating non-small cell lung cancer and for the inhibition of chemotherapy-induced neutropenia.[119] This cancer therapy could block the cancer cells in the G2/M phase of the cell cycle and thereby induces apoptosis through caspase-3, caspase-8, caspase-9, and PARP (poly ADP-ribose polymerase) cleavage. Plinabulin was also known to inhibit the cell proliferation by disrupting the tumor vascular endothelial cells.[119]

1.6.5 DNA intercalators and groove binding agents

The major mechanisms that are involved in drug-DNA interactions are intercalation and groove bindings. (I) Intercalation is a process in which a planar molecule is inserted between DNA base

pairs resulting in the distortion of DNA whereby there is a reduction in the lengthening and helical twist.[120] DNA intercalating agents are classified into monofunctional (e.g. ellipticine, actinomycins and fused quinoline compounds) and bi or poly (e.g. ditercalinium and echinomycin) functional intercalating molecules. DNA intercalating agents disturb the process of recognition and function of DNA associated proteins (polymerases, topoisomerases, transcription factors and DNA repair systems).[121] These intercalators can be toxic or non-toxic, depending on the presence or absence of different functional groups (e.g. basic, cationic, and electrophilic) that are required for the genotoxicity.[122] (II) Groove binding agents, unlike intercalators, bind to the minor groove of DNA as a standard lock and key model. These groove-binding agents do not induce large conformational changes in the DNA. Groove binding molecules are more sequence selective and do not show a G-C region preference. On the other hand, DNA intercalators show a preference for G-C regions being less sequence selective. Intercalators and groove binders are often both anticancer and antibacterial agents. Mitomycin and anthracyclines are DNA crosslinkers as well as groove-binding agents.[123] Some examples of DNA intercalators used as anticancer agents are (a) chlorambucil which alkylates DNA and in leukemia cells, it induces apoptosis by a p53 dependent mechanism,[124] and (b) cyclophosphamide (a nitrogen mustard) which crosslinks DNA and causes strand breakage.[125]

1.6.6 The role of thiols in regulating cancer development and growth

In the maintenance of an intracellular redox balance, many enzymatic systems are involved. Glutathione (GSH) is one of the key molecules[126] (**Figure 1.17**) that plays an important role in regulating the antioxidant defense systems.[127] GSH is a tripeptide molecule and is involved in the synthesis of proteins and nucleic acids. It protects cells by cellular detoxification of electrophiles,

xenobiotics and oxygen-related toxic species like free radicals and peroxides. Glutathione S-transferase (GST) is a detoxification enzyme and it catalyzes the reaction between GSH and cytotoxic agents containing electrophilic centers to produce a glutathione conjugate that is chemically less reactive, less toxic, water-soluble and can be easily excreted from the body. Therefore glutathione S-transferase can inactivate various electrophile-producing anticancer agents by conjugation to GSH, making the anticancer agents less affective. Electrophilic centers if present in anticancer agents, react with GSH and form conjugates through GST mediation, which are then excreted from the body. GST's therefore utilizes its detoxification mechanisms in the biotransformation of the anticancer agents into less toxic metabolites making them less effective or leading to the failure of chemotherapy.[128] Cellular processes, including cell differentiation, proliferation, apoptosis, and disturbances in GSH homeostasis are involved in the causes and progression of many human diseases including cancer. While GSH deficiency, or a decrease in the GSH/glutathione disulfide ratio, leads to an increased susceptibility towards oxidative stress implicated in the progression of cancer, elevated GSH levels increase the antioxidant capacity and the resistance to oxidative stress is observed in many cancer cells. Elevated levels of GSH are known to be observed in many types of tumors which makes the neoplastic tissues more resistant to chemotherapy[129, 130]. Moreover, the content of GSH in some tumor cells is typically associated with higher levels of GSH-related enzymes, such as γ-glutamylcysteine ligase (GCL), γ-glutamyl-transpeptidase (GGT) activities, and GSH-transporting export pumps.[130, 131] Therefore it is not surprising that the GSH system has attracted the attention of a number of scientists as a possible target for medical intervention with a view to combat cancer progression and chemoresistance.

The importance of GSH in altering cellular responses to certain chemotherapy drugs has been demonstrated by virtue of the development of agents that either inhibit[132] or stimulate,[133] intracellular GSH synthesis. The main research in this field has been directed towards depleting GSH by a specific inhibition of γ-glutamylcysteine ligase (GCL) which is a key enzyme of GSH biosynthesis. In this context, buthionine sulfoximine (BSO) (**46** in **Figure 1.16**) is the most popular GSH-depleting agent studied in both preclinical and early clinical trials, and studies in various cell types have shown BSO to markedly enhance the cytotoxicity of many chemotherapy drugs[134, 135] and hypoxic cell radiosensitizers.[136] Contrarily, increasing the GSH levels prior to drug treatment by oxothiazolidine carboxylate has shown a significant protection against chemotherapy drug-mediated cytotoxicity.[137, 138]

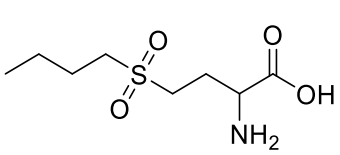

46

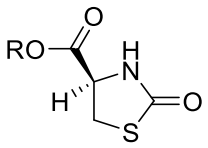

47

Figure 1.16. Buthionine sulfoximine **46** and oxothiazolidine carboxylic acid ester **47**.

It is also evident that many antioxidant enzymes are induced by GSH depletion at the transcriptional level. The broad distribution of GSH among all living organisms reflects its important biological roles. As mentioned earlier the major function of GSH is the detoxification of xenobiotics and some endogenous compounds. These substances are electrophiles and form conjugates with GSH, either spontaneously or enzymatically, in reactions catalyzed by GSH-S-transferases (GST).[139]

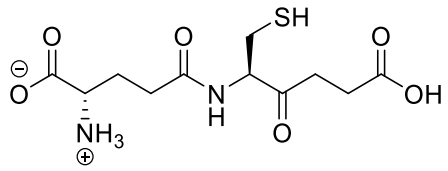

48

Figure 1.17. Glutathione (GSH).

In many normal and malignant cells, increased GSH levels are associated with cellular proliferation and are essential for cell cycle progression.[140, 141] The increase in GSH is a major contributing factor in drug resistance by binding to, or reacting with, drugs, interacting with ROS, preventing damage to proteins or DNA, or by participating in DNA repair processes. In melanoma cells, GSH depletion and γ-glutamyl-transpeptidase (GGT) inhibition significantly increased cytotoxicity via oxidative stress.[142] Moreover, it has been found that the human multidrug resistance protein (MRP), which is a member of the superfamily of ATP-binding cassette membrane transporters, can lead to resistance to multiple classes of chemotherapeutic agents.[143, 144] Several studies have shown coordinated overexpression of GCLC (glutamate-cysteine ligase catalytic subunit is an enzyme in humans and it is encoded by the GCLC gene) and MRP(multidrug resistance protein) in drug-resistant tumor cell lines, in human colorectal tumors and in human lung cancer specimens.[143, 144]

Since the thiol concentrations are elevated in many types of tumours,[68, 145] the lowering of thiol concentrations may be selectively more damaging to tumours than normal cells. Therefore thiol alkylators, which will lower intracellular thiol concentrations, may sensitize malignant cells to anticancer drugs. As discussed earlier, a number of cellular thiols play an important role in cell division whereby the concentrations of thiols increase just before and during mitosis.[146, 147] These

conjugated unsaturated ketones are therefore potential candidates in treating drug resistant tumours. For example 1-*p*-chlorophenyl-4,4-dimethyl-5-diethylamino-1-penten-3-one hydrobromide **(Figure 1.18)**, which is a Mannich base derivative of an α,β-unsaturated styryl ketones, is an antineoplastic agent[67] and had been reported to react with protein thiols.[66] Cyclophosphamide, melphalan, chlorambucil, carmustine, lomustine (CCNU), dacarbazine (DTIC), and busulfan are some examples of antineoplastic agents which can alkylate electron rich nucleophilic groups such as sulfhydryl, hydroxyl, amino, and phosphate groups present in intracellular macromolecules. The importance of cytotoxic thiol alkylators has been reviewed.[71]

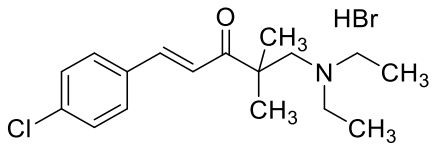

49

Figure 1.18. 1-*p*-Chlorophenyl-4,4-dimethyl-5-diethylamino-1-penten-3-one hydrobromide.

1.7 Mannich bases

A Mannich reaction is a three-component condensation reaction between a substrate containing at least one active hydrogen atom, an aldehyde component and an amine reagent producing a class of compounds known as Mannich bases. Mannich reactions are also known as aminoalkylation reactions as they are the derivatives of a substrate obtained through substitution by an aminoalkyl moiety. Although primary amines (including ammonia) may be employed as amine reagents in aminoalkylations, secondary aliphatic amines (R_2NH) are the most commonly used amine reagents in the Mannich reactions. Regardless of the structural diversity, all the substrates should have an activating functional group that renders the substrate active in the Mannich reaction. The carbonyl

group in ketones, phenolic hydroxyl substituent in phenols, terminal carbon-carbon triple bond in alkynes, and the heteroatom in heterocycles are common examples of activating groups.

Substitution of a substrate with a single aminomethyl function results in mono-Mannich bases, but two aminomethyl groups can also form with substrates having more than one active hydrogen atom producing bis Mannich bases such as **50**-**53** derived from dialkyl ketones, alkyl aryl ketones, 4-substituted phenols and pyrrole, respectively. Also, the aminomethylation of a substrate having a reactive hydrogen(X-H) with amine reagents other than secondary amines (such as ammonia, having three reactive hydrogen atoms on the nitrogen atom, or primary amines R-NH2, having two reactive hydrogen atoms on the nitrogen atom) may lead to tris-Mannich bases **54** and bis-Mannich bases **55**, respectively (**Figure 1.19**). An important application of the Mannich reaction is in the field of medicinal chemistry[148] since a number of Mannich bases possess biological activities.

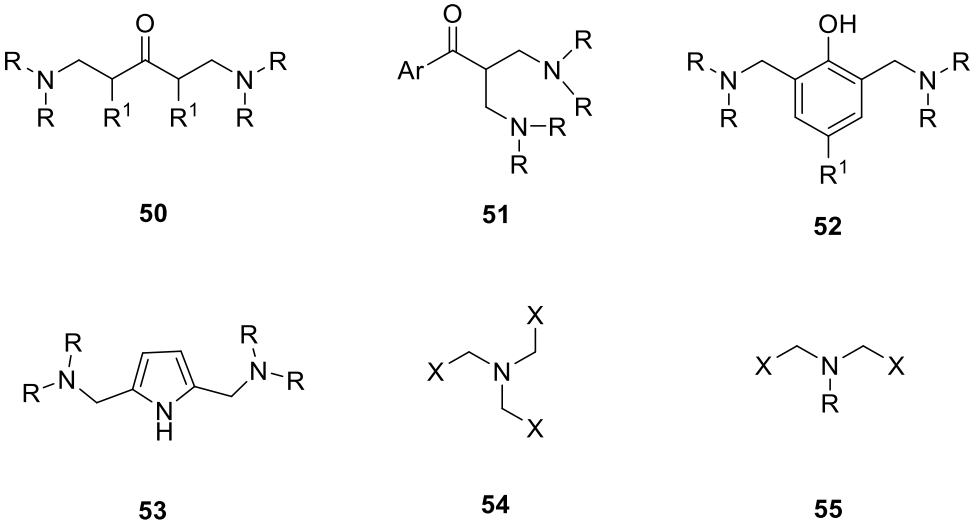

Figure 1.19. General structures of double, bis and tris Mannich bases.

Aminomethylation of drugs could be used as a tool to improve drug delivery properties of a drug into the human body or a target receptor. Aminomethylation is one way to increase the hydrophilic

properties of drugs by introducing a polar functional group into the drug moeity, the well-known rolicycline being one of the most common examples.[149] Water solubility of the drug can be further enhanced by the quaternization of the nitrogen atom of the aminomethyl derivative thereby making an ammonium salt. Alternatively the lipophilic properties of a drug can be altered through a Mannich reaction by choosing the appropriate amine reagent.[150] Further, the aminomethylated drugs could act as prodrugs, releasing the active drug ingredient under controlled hydrolytic conditions via deaminomethylation or deamination.[151]

Lawsone (2-hydroxy-1,4-naphthoquinone) is a naturally occurring naphthoquinone which is extracted from dry powdered leaves of the henna plant (Lawsonia inermis) and showed weak toxicity towards both human hepatocytes and various triple-negative MDA-MB-231 breast cancer, the BxPC-3 pancreas cancer, and the PC-3(AR-) prostate cancer cell lines.[152] Introducing a nitrogen atom into lawsone or naphthoquinone molecule enhances their anticancer activities.[153] Quinonoid compounds derived from lawsone are known to have cytotoxic evolution against cancer cells HCT-116 (human colon carcinoma cells), PC3 (human prostate cancer cells), HL-60 (human promyelocytic leukemia cells), SF295 (human glioblastoma cells) and NCI-H460 (human lung cancer cells) shown antitumor activity with IC_{50} values <2 mM.[154] One of the strategies for introducing a nitrogen atom in lawsone is the formation of its Mannich base via the Mannich reaction. Lawsone Mannich bases derived from salicylaldehyde or nitro furfural are shown to have antiparasitic activity.[155] Cytotoxicity of Mannich bases has been attributed partially to the α,β-unsaturated ketones liberated by deamination.[156] These α,β-unsaturated ketones have a markedly greater affinity for thiols over amino and hydroxy nucleophiles. This preferential affinity may

result in a lack of mutagenicity and carcinogenicity which are associated with certain alkylating agents due to presumed interaction with nucleic acids.[157]

The anticancer and cytotoxic activities of certain ketone Mannich bases, structurally related to α,β-unsaturated ketones[158] were reviewed. These two groups of compounds were shown to exert their cytotoxic action through the alkylation of cellular thiols such as glutathione (GSH) or cysteine, and may be useful in sensitizing tumor cells to antineoplastic agents, and even reverse drug resistance.[71] Compounds possessing both a Mannich base moiety and an activated unsaturated carbon-carbon double bond in their structure (for example, Mannich bases of chalcones such as **59**) have been considered as representative compounds for the evaluation of the sequential cytotoxicity theory.[159] In addition, Mannich bases **58** of enones, which can be easily synthesized from alkyl aryl ketones in one synthetic step, showed marked cytotoxicity towards numerous cancer cell lines.[160] Furthermore, ortho-phenolic Mannich bases may undergo deamination to yield ortho-quinone methides. Mannich bases of chalcones derived from either phenolic aldehydes or ketones are a class of compounds for which structure **59** is prototypical, have been examined also as cytotoxic agents.[161] From the last decade, research on more potent anticancer agents having these four types of cytotoxic Mannich bases in their structures e.g., **56-59** (**Figure 1.20)** has steadily continued.[160]

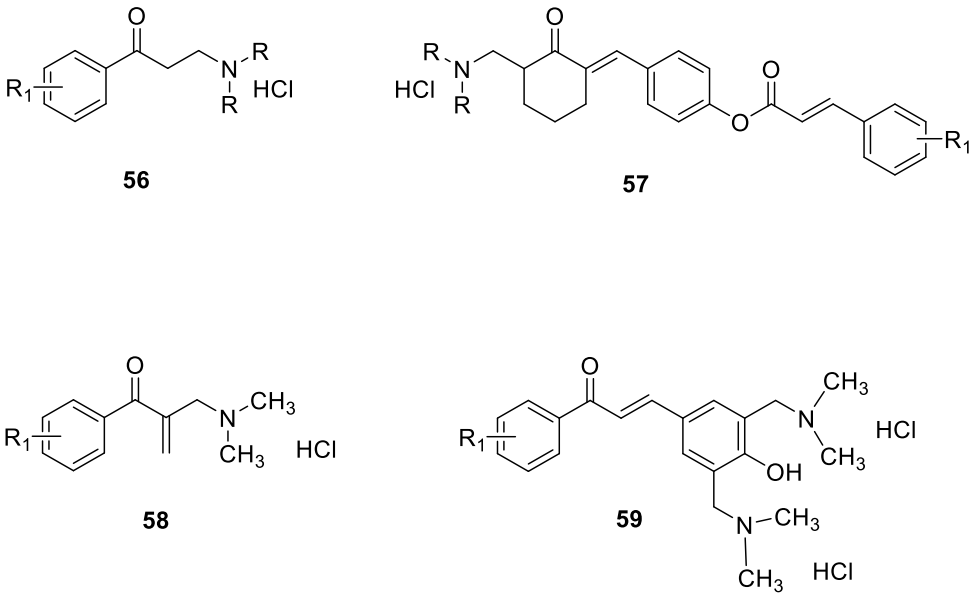

Figure 1.20. General structures of the Mannich bases with anticancer and cytotoxic activity.

The conformational arrangement of these Mannich bases can influence the interaction of these compounds with the cellular constituents. Restricted conformational mobility of the Mannich bases can be attained by forming cyclic Mannich bases. Dimmock *et al* developed a series of 3,5-bis(arylidene)-4-piperidone related Mannich bases **60** which have a ring nitrogen atom at the β-position to the two enone functional groups (**Figure 1.21**). These compounds exhibited cytotoxic activity against P388 cells. The substituents on the aryl rings were chosen to vary the electronic properties, which can influence the cytotoxicity of the compounds towards malignant cells.[162]

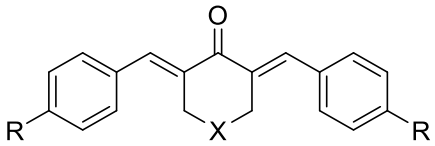

60

a: R= H; X= NH. HCl

b: R= $N(CH_3)_2$; X= NH. HCl

c: R= H; X= NCH_3. HCl

d: R= $N(CH_3)_2$; X= NCH_3. HCl

e: R= H; X= $\overset{\oplus}{N}(CH_3)_2$ $Br^{\ominus}$

f: R= $N(CH_3)_2$; X=$\overset{\oplus}{N}(CH_3)_2$ $I^{\ominus}$

g: R= H; X= CH_2

Figure 1.21. 3,5-bis(arylidene)-4-piperidone related Mannich bases.

2-Benzylidenebenzofuran-3(2H)-ones, commonly known as aurones, represent a subclass of flavonoids with pharmacological potential.[163, 164] Recent studies by Popova *et al*, revealed that the Mannich base derivatives of these aurones exhibited inhibition of the proliferation of PC-3 prostate cancer cells (antiproliferative activity) with IC_{50} values in the 7-84 μM range.[165]

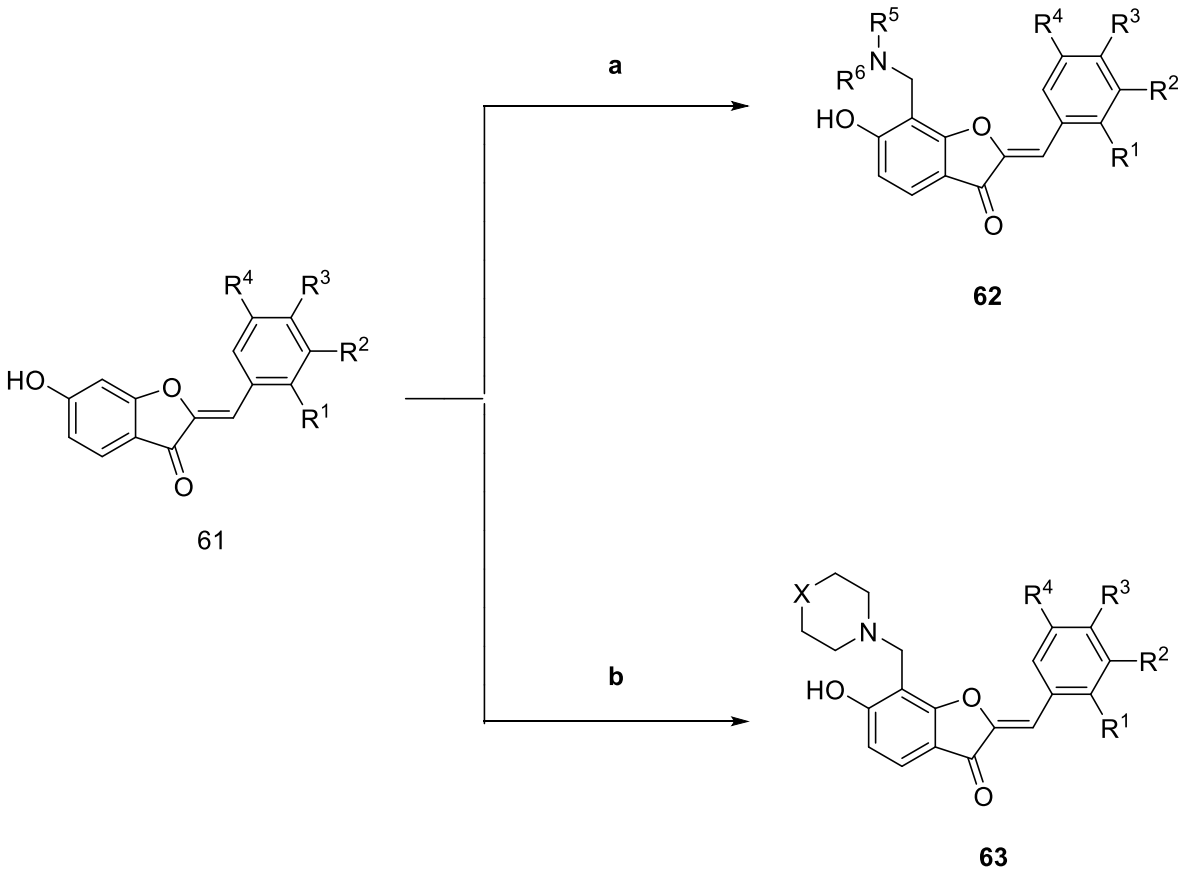

Reagents: a) $CH_2(NR^5R^6)_2$, *i*PrOH, 80 °C; b) $CH_2(NC_4H_8X)_2$, *i*PrOH, 80 °C

Scheme 1.4. Synthesis of Mannich bases of 6-hydroxyaurones.

Another recent article by Tugrak *et al* reports that under suitable reaction conditions, Mannich bases can undergo deamination processes to generate α,β-unsaturated ketones, which is the most likely site of action for their cytotoxic activities.[166] The α,β-unsaturated ketones thus produced by the deamination process of Mannich bases generally react with nucleophiles, especially with thiols, which are converted to increased cytotoxic compounds.[166]

The Mannich base **(64)** containing an α,β-unsaturated ketone motif, may be able to undergo a deamination process and produced compound **(65)**, which is a quinone methide. Compound **65**

now has two alkylation centers in its chemical structure as shown in the Scheme 1.5. First thiol alkylation can take place at the side chain of the molecule generating a thiol-alkylated compound. Then the second or consecutive thiol alkylation occurs at the aryl ring of the quinone methide formed to produce the bis thiol alkylated compound **67**. This is in accordance with the sequential cytotoxicity hypothesis, as proposed by Dimmock et al.[167]

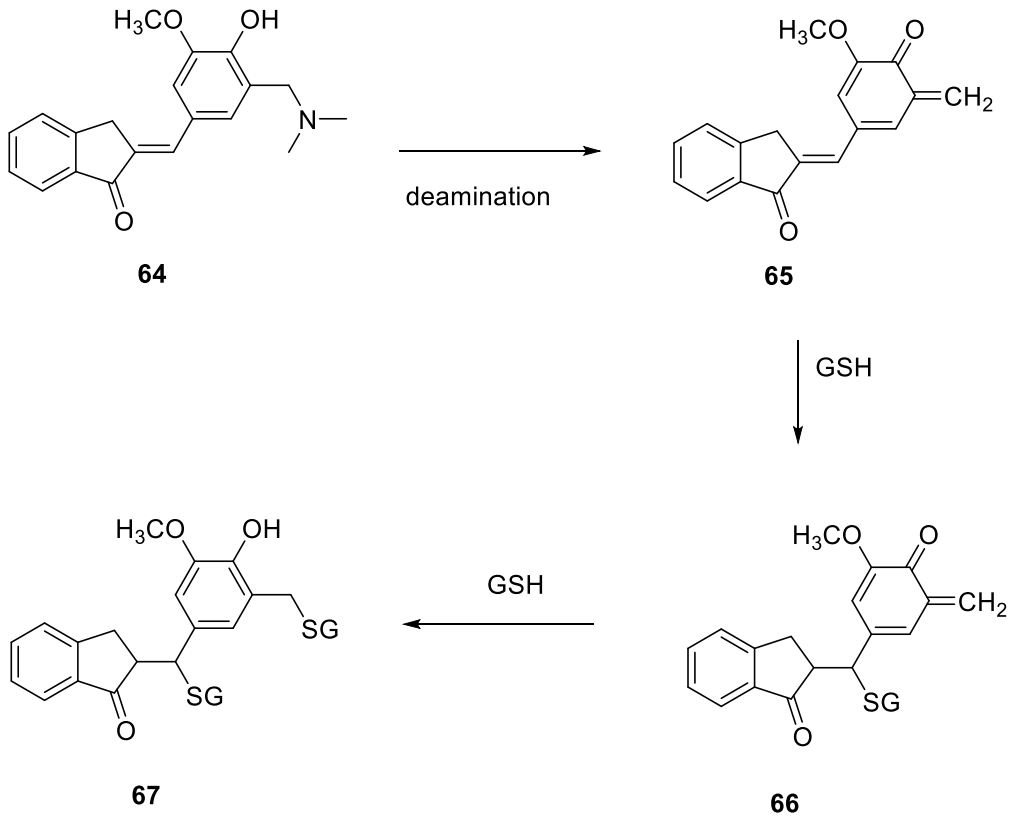

Scheme 1.5. Sequential thiol alkylation.

Most of the compounds showed CC_{50} values in the low micromolar range (5.4 -18 μM) towards Ca9-22, HSC-2, HSC-3, and HSC-4 cell lines. Human normal oral cells gingival fibroblasts (HGF), periodontal ligament fibroblasts (HPLF), and pulp cells (HPC) are also used in the

experiment. The selectivity index (SI) values of greater than 1 were obtained for all compounds against all tumor cell lines.[166]

1.8 Mitochondria

Mitochondria are membrane-bound organelles present in the cytoplasm of eukaryotic cells. They can be considered as the power generators of the cell which converts oxygen and nutrients into adenosine triphosphate (ATP) (**Figure 1.22**). ATP is the primary chemical energy of the cells that powers all metabolic activities in the cell.[168] Higher animals would not exist without mitochondria because their cells would be able to get energy only from anaerobic respiration (in the absence of oxygen), a process which is much less efficient than aerobic respiration. In fact, mitochondria enable cells to produce 15 times more ATP than they produce in the absence of oxygen, and complex animals like humans need large amounts of energy in order to survive. [169]

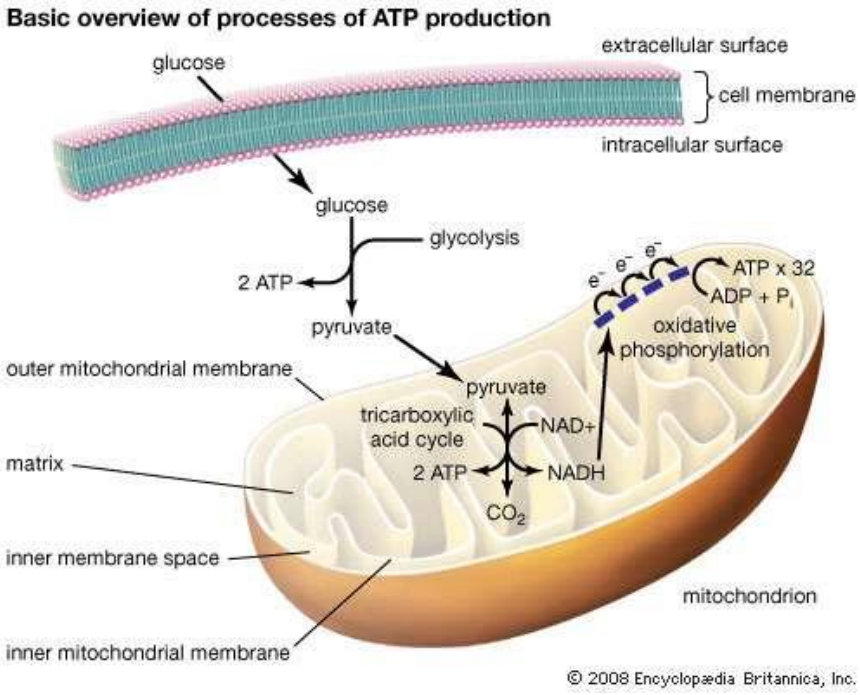

source: (https://www.britannica.com/science/mitochondrion) [170]

Figure 1.22. Structure of a mitochondrion.

The structure of a mitochondrion is very important in the functioning of the organelle. A mitochondrion consists of two membranes, an outer and inner membrane composed of phospholipid bilayers and proteins.[98] The outer mitochondrial membrane completely surrounds the inner membrane leaving a small intermembrane space between the two membranes. The outer mitochondrial membrane possesses many protein-based pores which are large enough to allow the passage of ions and molecules. In contrast, the inner mitochondrial membrane is associated with restricted permeability.[171]

The inner mitochondrial membrane also consists of some proteins which are involved in electron transport and ATP synthesis. Inside this inner membrane is the mitochondrial matrix, where the citric acid cycle produces electrons which travel from one protein complex to the next within the

inner mitochondrial membrane. At the end of this process of the electron transport chain, oxygen is the final electron acceptor which produces water (H_2O). At the same time, ATP is produced during this electron transport chain and this process is called oxidative phosphorylation.

During the electron transport process, the participating proteins will push the protons out from the matrix into the intermembrane space and this creates a concentration gradient of protons that another protein called ATP synthase uses to power the synthesis of the energy carrier molecule ATP (**Figure 1.23**).

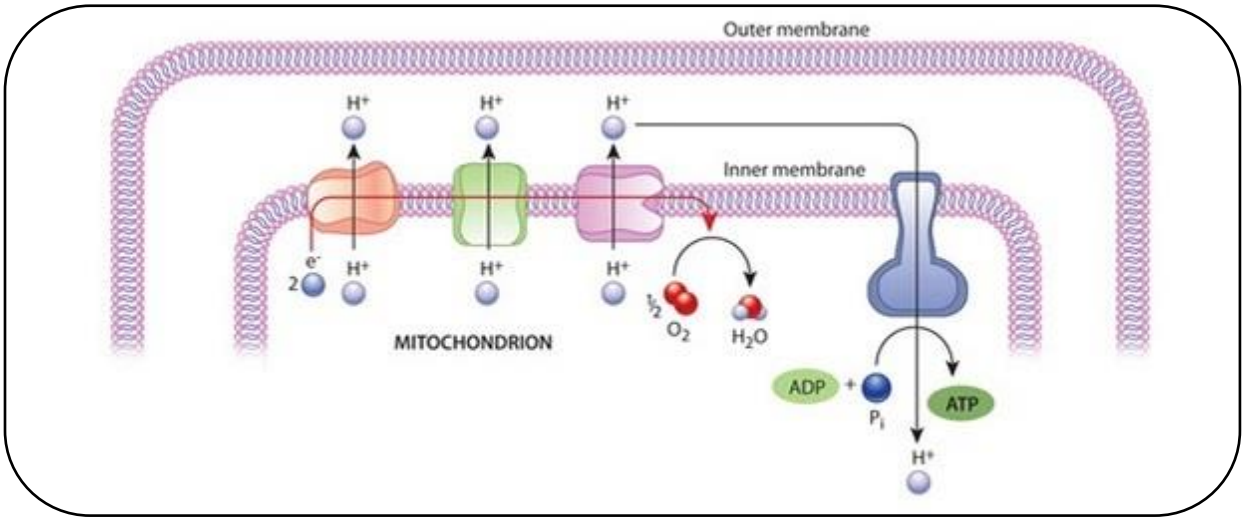

Figure 1.23. The electrochemical proton gradient and ATP synthase.[171]

In the inner mitochondrial membrane, a high energy electron is passed along an electron transport chain. The energy released pumps the hydrogen out of the matrix space. The gradient created by this process drives hydrogen back into the membrane through the protein ATP synthase and the enzymatic activity of ATP synthase will synthesize ATP from ADP.[171]

Source: **2014 Nature Education** (https://www.nature.com/scitable/topicpage/mitochondria-14053590) Accessed on Feb 26, 2018.

1.8.1 Mitochondrial membrane potential (MMP) Ψ

Mitochondria are commonly referred as the power houses of the cells and play a vital role in cellular physiology. The majority of the cellular energy (ATP) in eukaryotic cells is generated in the mitochondria through the process of oxidative phosphorylation where the electrons are transferred from electron donors to the electron acceptors such as oxygen.[172] This electron transport chain creates an electrochemical gradient which drives the synthesis of ATP[173, 168] and produces the mitochondrial membrane potential (MMP). The mitochondrial membrane potential is frequently used for assessing the functioning of mitochondria in the context of the fate of the cells in biological and biomedical research.[174] Mitochondrial dysfunctions are associated with various biological disorders such as cancer, cardiovascular problems, diabetes, and neurodegenerative diseases.[175] Xenobiotic compounds show their toxicity either by a direct or a secondary effect on mitochondrial function. Many of these compounds reduce the MMP by interacting with a variety of macromolecules in the mitochondria, and thereby affecting different functions of mitochondria. A decrease in the MMP may also be linked to apoptosis.[176, 177]

1.8.2 More hyperpolarised mitochondrial membrane potential in cancer cells

Many cancer cells are more hyperpolarised MMP(Ψ) than the normal cells.[178, 179] The mitochondrial membrane potential in normal cells is between -108 and -159 mV, with an average value of -139 mV.[180, 181] The optimum MMP for the maximum production of ATP is between -130 to -140 mV, for all living organisms.[181] If the cancer is more invasive and dangerous, then a

more hyperpolarised MMP is observed.[182, 183] The hyperpolarisation of the mitochondrial membrane potential can be >50% greater in cancer cells than normal cells.[184] e.g. MMP(Ψ) ≈ -210 mV in mouse Neu4145 mammary gland tumor cells.[185] Sometimes the hyperpolarisation of MMP in cancer cells can be double that of normal cells.[186] In general the MMP of cancer cells is extremely sub-optimal (less than optimal) for ATP production.

Lipophilic cations can cross the membranes and by their positive charge they are attracted and accumulate in the mitochondrial matrix which is negative inside because of the MMP. Cancer cells have a more hyperpolarised MMP and therefore the delocalized lipophilic cations are more attracted to their mitochondria and than this organelle in non-malignant cells.[179] According to some authors, based on Nernst's law, cations which are capable of permeating biological membranes can accumulate in the mitochondrial matrix at a 10 fold higher level with each 60 mV of transmembrane voltage.[184] For example if the MMP of a cancer cell is 60 mV more hyperpolarised than that of a normal cell, then a single charged lipophilic cation will accumulate 10 times more in the mitochondrial matrix of cancer cells than normal cells (T=300 K)[184] and a lipophilic cation with a double charge will accumulate 100 times more than a normal cell.[187] So, the delocalized lipophilic cationic poisons are selectively targeted more to cancer cells than normal cells. Different delocalised lipophilic cations have been shown to accumulate in the matrix of mitochondria and selectively kill cancer cells in vitro and in vivo.[178, 188, 189] This confirms that the cancer cells have more hyperpolarised MMP.[189]

1.8.3 Approaches to targeting compounds to mitochondria

Mitochondria are one of the important targets for new drug designs in cancer, cardiovascular, and neurological diseases.[190] An effective way to deliver the drugs selectively to mitochondria is by covalent linking it to a delocalized lipophilic cation such as an alkyltriphenylphosphonium ion to a pharmacophore of interest. Other delocalized lipophilic cations, such as rhodamine, natural and synthetic mitochondria-targeting peptides, and nanoparticle vehicles, have been used for the effective delivery of small molecules into mitochondria. Targeting the mitochondria has been developed to investigate mitochondrial physiology, dysfunction, the interaction between mitochondria and other subcellular organelles and for the treatment of neurological, and cardiovascular and cancer diseases.[191, 192] Over the last two decades, research on cancer therapy is mainly focused on developing selective targeting and accumulation of mitochondria-targeted cations (MTCs) and their capability to modify ROS-mediated redox signaling and antiproliferative pathways in cancer cells.[193, 194, 195]

In a recent article, the authors discussed the strategies and physicochemical foundations for targeting and transporting the compounds to mitochondria.[190] The development and applications of mitochondria-targeted bioactive molecules are compounds for the development of new therapeutics in the fields of cancer and neurodegenerative diseases.[190] Due to the negative mitochondrial membrane potential of the inner membrane, the positively charged compounds accumulate in the mitochondrial matrix against their concentration gradient.[190]

Alkylated triphenylphosphonium cations were initially used as probes to study the mechanism of coupling of the mitochondrial membrane potential with oxidative phosphorylation and

consequently used to determine the mitochondrial membrane potential in a cell.[196, 195] As shown in **Figure 1.24** the "blue end" of the molecule is a parent molecule containing a nitroxide group (−N−O•) that exhibits a superoxide dismutase (SOD) mimetic activity, a phenolic hydroxyl group (−OH) with a chain-breaking radical scavenging ability, a radiolabeled technetium group for use in metabolic imaging, or a hydroethidine (HE) moiety that can form a specific marker product upon reaction with a superoxide radical anion ($O_2^{\bullet -}$). The "blue colored part of the molecule" is bound to a delocalized lipophilic cation (shown in red) through an alkyl chain space linker (shown in green). Depending on the length of the space linker (typically n = 2-10 carbon atoms chain) the lipophilicity, may modulate the cellular uptake.

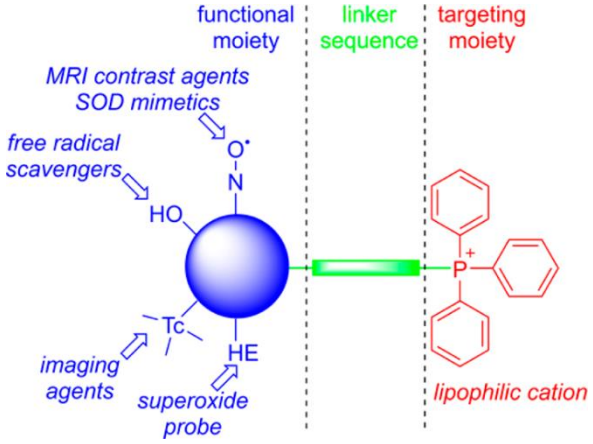

Source: *Chem. Rev.* 2017, 117, 10043-10120.[190]

Figure 1.24. Anatomy of a typical molecule with a different functional group conjugated to the TPP+ cation through a space linker.[190]

Some examples of the TPP+-conjugated compounds for their mitochondrial targeted delivery are shown in **Figure 1.25**. The color-coding represents the three parts of the mitochondria-targeted

molecules (1) functional moiety in blue, (2) space linker in green, and (3) the targeting moiety in red.

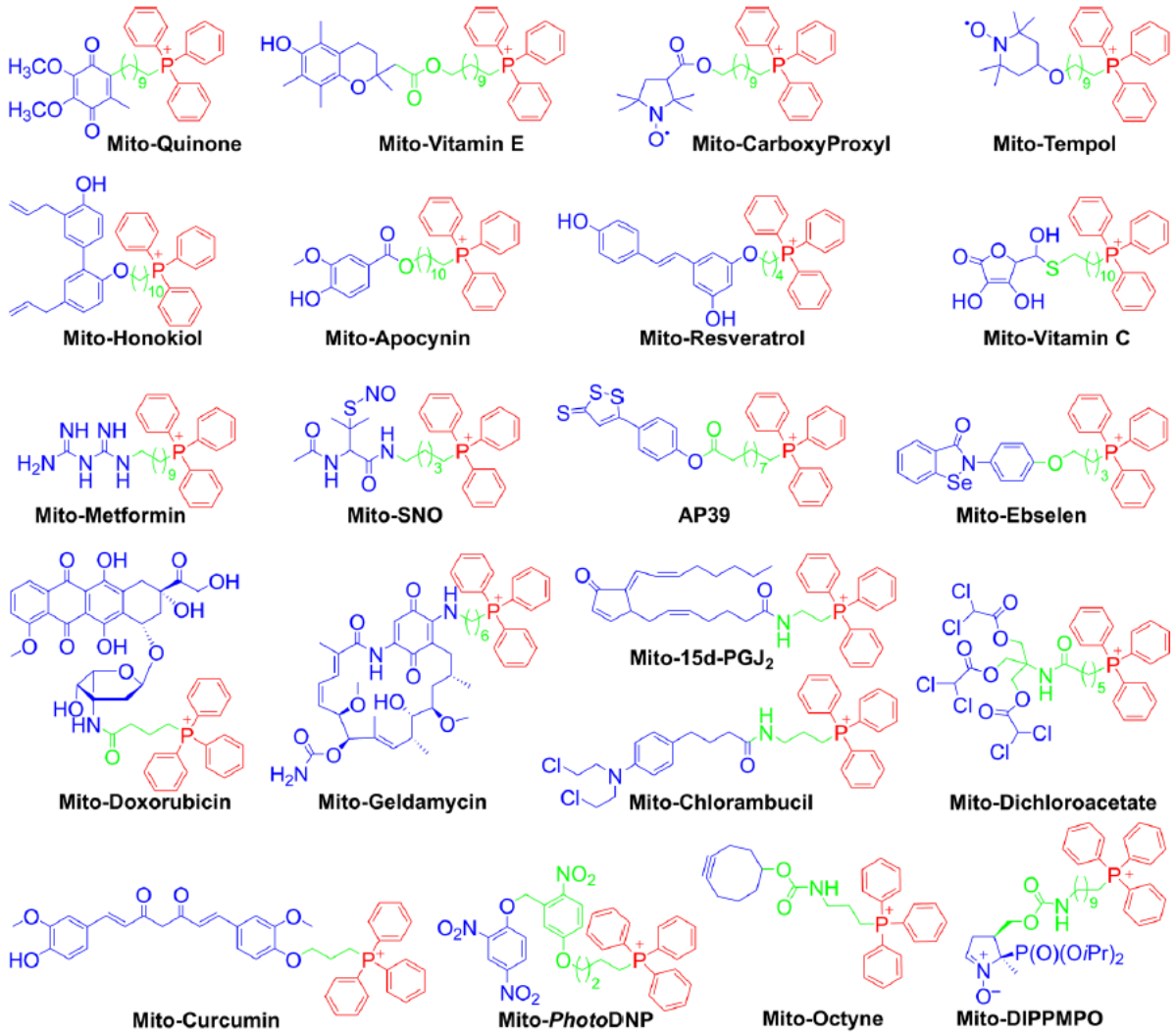

Figure 1.25. Some examples of TPP^+ conjugated compounds for delivering into mitochondria.[190]

Source: *Chem. Rev*. **2017**, 117, 10043-10120.

1.8.4 Accumulation of lipophilic cations in the mitochondria of intact cells

The selective intake of delocalized lipophilic cations through mitochondria in cells is based on the mitochondrial membrane potential-driven accumulation of the positively charged ion(s). The degree of accumulation of any delocalized charged ions/species across the mitochondrial membrane occurs against the concentration gradient of the mitochondrial membrane potential. At any equilibrium, the concentrations of the ion on either side of the charged membrane can be obtained by using the Nernst equation:

$$\Delta\Psi = \frac{RT}{nF} \ln \frac{c_{in}}{c_{out}}$$

where R is the universal gas constant, T is the temperature (K), n is the valency of the charged species, F is Faraday's constant, and c_{out} and c_{in} are the concentrations of the ions/species on either side of the charged membrane with the potential ΔΨ. For a single-charged cationic species accumulating in a space surrounded by a membrane with a potential ΔΨ which is negative inside and the temperature is 37 °C, the Nernst equation can be simplified as follows:

$$\Delta\Psi\ (\mathrm{mV}) = 61.5 \times \log_{10} \frac{c_{in}}{c_{out}}$$

To enter the mitochondria of the cells, the compound must cross both the plasma and the mitochondrial membrane of the cell. Fortunately, in both cases, the membrane potential is negative inside. A stepwise accumulation of the cationic compounds takes place initially in the cell cytosol, then afterwards inside the mitochondria. As shown in **Figure 1.26**, the plasma membrane potential is between 30-60 mV which makes a 3-5-fold increase in the cytosolic concentration of cations in

comparison to the extracellular medium. The mitochondrial membrane potential is in the range of 120-180 mV which increases the concentration of the cation in the mitochondrial matrix by a 100-1000-fold. For example, an alkyltriphenylphosphonium cation added extracellularly at the concentration of 1 μM could reach an intra-mitochondrial concentration in the range of 0.1-1.0 mM or higher concentrations.[190]

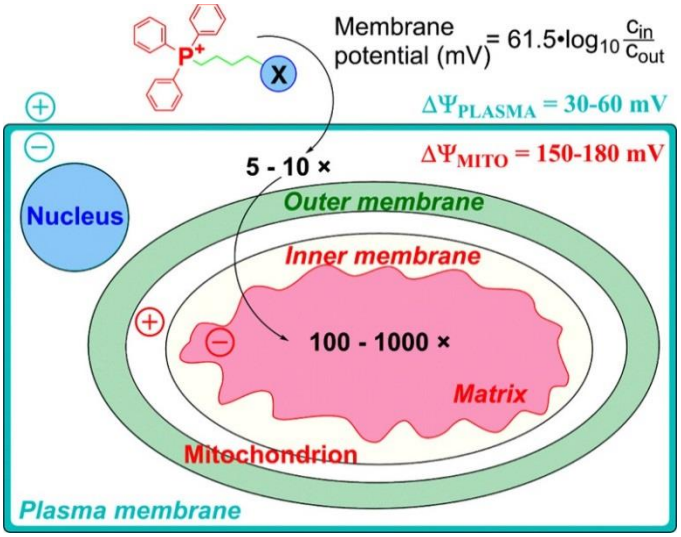

Figure 1.26. Cellular uptake of TPP+-linked compounds driven by plasma membrane and mitochondrial membrane potentials.[190]

Source: *Chem. Rev*. **2017**, 117, 10043-10120.

The passage of a delocalized lipophilic cation through the mitochondrial inner membrane takes place in a multistep process. Initially, the cation binds to the intermembrane space (IMS) at the side of the mitochondrial membrane. Being within the phospholipid layer of the membrane, it then moves to the matrix side of the membrane. At last, it detaches from the matrix side of the membrane. The passage of a mitochondria-targeted antioxidant (MTC) through a membrane is shown schematically in **Figure 1.27**.[197, 198]

As shown in **Figure 1.27**, after binding to the mitochondrial membrane, the cationic targeting moiety is localized on the membrane surface, due to an electrostatic interaction with the negatively charged phosphates. Afterwards, the position of the space linker and the location of the cargo will change depending on their physicochemical properties. Hydrophobic space linkers and cargo will move towards the center of the membrane, whereas the hydrophilic cargo may tend to move towards the aqueous cytosolic phase. The energy barrier for the transfer of the lipophilic cations through the phospholipid bilayer is normally related to the transfer of the membrane-bound compound from one side to the other side of the membrane (step 2 in **Figure 1.27**).[197, 199] Lipophilic cations can more easily infuse the mitochondrial membrane than the plasma membrane. Thus after entering the cell, the depolarized lipophilic compounds will rapidly accumulate in the mitochondria.

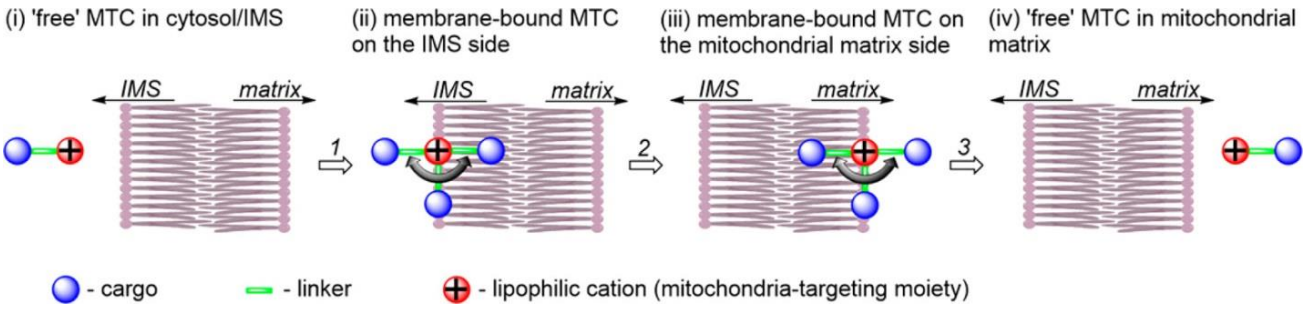

Source: Chem. Rev. 2017, 117, 10043-10120.

Figure 1.27. Schematic representation of the transport of an MTC from the mitochondrial IMS to the matrix through the mitochondrial inner membrane.[190]

1.9 Conclusions

The anticancer and cytotoxicity of numerous α,β-unsaturated ketones and their Mannich bases is an emerging research topic of interest for many of the cancer research scientists who aim to develop novel tumour-selective cytotoxic compounds with enhanced cytotoxicity and improved bioavailability, pharmacokinetic and pharmacodynamic properties. The structural diversity of curcumin related analogues containing the 1,5-diaryl-3-oxo-1,4-pentadienyl pharmacophore mounted on a piperidinyl ring allows the design and development of novel drug candidates to overcome multidrug resistance and show sequential cytotoxicity to malignant cells. This may be achieved by introducing or altering various groups on the aryl rings and the substituents on the piperidyl nitrogen which can react at contiguous binding sites forming van der Waals and hydrogen bonds with cellular constituents which can influence cytotoxic properties. The common issue that was seen in these types of molecules is their hydrophobicity. The hydrophobicity can be reduced by introducing hydrophilic groups on aryl rings or the alkyl/acyl chain linked to the piperidyl nitrogen atom. These structural modifications may produce a molecule with the desired drug-like properties with retained or enhanced tumour-selective cytotoxicity and multidrug resistance. Also, delocalized lipophilic compounds are targeted to the mitochondria and depolarize the MMP in the cancer cells which leads to the dysfunction of mitochondria and thereby to cell death.

The literature review records some of the enormous health problems caused by cancer. In addition, various ways in which treatment takes place are presented. However there are a number of problems with current drug therapy. This review discloses that certain conjugated unsaturated ketones have promising antineoplastic properties and exert their bioactivity, in part at least, to

alkylation of cellular thiols. This review also outlines a variety of quaternary ammonium compounds which display promising cytotoxic properties.

Based on these observations, the objective of the research outlined in this thesis is to prepare a variety of conjugated enones and examine their cytotoxic properties. In addition, the compounds were examined for their capacity to display greater toxicity to neoplasms than to non-malignant cells. Specifically the research work described in this thesis is divided into three principal areas. First, evaluations were made of the cytotoxic properties of various 3,5-bis(benzylidene)-4-piperidones **15** details of which are found in Chapter 2. A series of *N*-acyl analogs **33** of a variety of compounds in series **15** are outlined in Chapter 3. Finally another series of *N*-acyl derivatives **70** were prepared as well as related quaternary ammonium salts **71** which are presented in Chapter 4. These enones are designed to react with cellular thiols and target mitochondria as lipophilic, cationic molecules in tumors with the goal of creating compounds which cause tumor-specific toxicity. Some ideas for future development of these series of compounds were also made.

Hypotheses and Objectives:

Hypotheses

1. The relative cytotoxic potencies of a series of 3,5-bis(benzylidene)-4-piperidones towards Ca9-22, HSC-2, HSC-3 and HSC-4 cells are governed by the magnitude of the electronic properties of the aryl substituents. [Chapter 2].

2. *N*-Acylation of various 3,5-bis(benzylidene)-4-piperidones will increase the in vitro cytotoxic potencies of the precursor ketones towards Ca9-22, HSC-2, HSC-3 and HSC-4 cells. [Chapters 3 and 4].

3. Quaternization of a series of *N*-acyl-3,5-bis(benzylidene)-4-piperidones will lead to compounds with increases in antineoplastic properties and tumor-selective cytotoxicity. [Chapter 4].

Objectives

1. The syntheses of a variety of 3,5-bis(benzylidene)-4-piperidones **15a-t** to evaluate hypothesis 1.

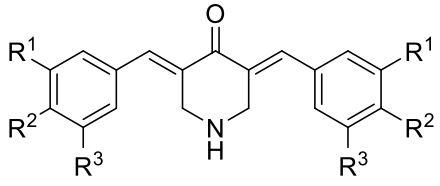

2. The attachment of a 4-dimethylaminoethoxycarbonyl-phenyl group onto the piperidyl nitrogen atom of series **15** to produce compounds **33a-n** to evaluate hypothesis 2.

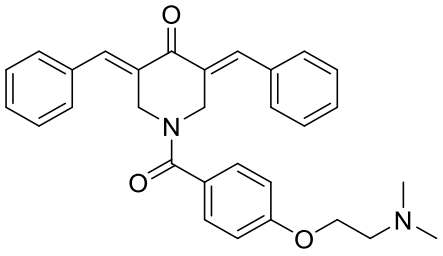

3. The attachment of a 3-(4-oximino-1-piperidyl-1-oxo)-propyl group onto the piperidyl nitrogen atom of series **15** to produce compounds **70a-i** to evaluate hypothesis 2.

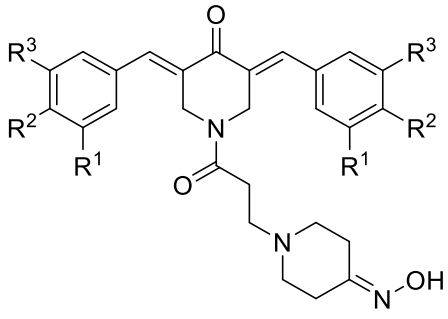

4. The syntheses and bioevaluation of the quaternary ammonium salts **71a-h** derived from series **70a-h** to evaluate hypothesis 3.

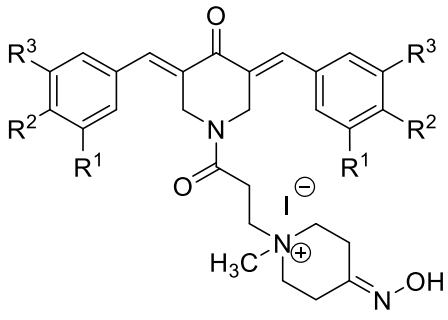

Chapter 2

2.1 Introduction

The goal of this section of the study is to explore the cytotoxicity of a series of 3,5-bis(benzylidene)-4-piperidones **15** towards a number of different neoplastic cell lines. One of the aims is to find potent cytotoxins. In addition, the compounds were planned to be evaluated against some non-malignant cell lines with the goal of finding compounds which display substantially greater potencies to neoplastic cells than to normal cells. In short, one is searching for lead compounds which have high cytotoxic potency for cancers but are well tolerated by normal cells.

An investigation was planned to find if the relative potencies of the cytotoxins are the same irrespective of the cell lines under consideration. Furthermore structure-activity relationships (SAR) and quantitative structure-activity relationships (QSAR) were considered to find the physicochemical properties of the aryl substituents which influence cytotoxic potencies.

2.2 Synthesis of 3,5-bis(arylidene)-4-piperidones

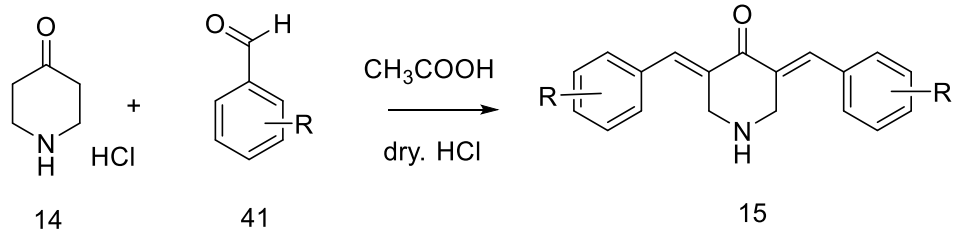

14 41 15

Scheme 2.1. Synthesis of 3,5-bis(arylidene)-4-piperidones.

^{1}H and ^{13}C NMR spectra were obtained using a Bruker 500 MHz spectrometer equipped with a BBO probe. Chemical shifts (δ) are reported in ppm. Melting points of the compounds were determined using a DigiMelt-MPA160 instrument and are uncorrected. The mass spectra were obtained using a JEOL JMS-T100 GCv Accu tof-gcV4G instrument.

2.2.1 General procedure for the synthesis of 3,5-bis(arylidene)-4-piperidones (15)[65]

The aryl aldehyde (**41**) (11.46 mmol) and 4-piperidone hydrochloride monohydrate (**14**) (5.60 mmol) were added to glacial acetic acid (15 mL) and stirred for five minutes. Dry hydrogen chloride gas was passed through this mixture for about 45 minutes till a clear solution was obtained. The reaction mixture was stirred at room temperature for 24 hours. Thin-layer chromatography (TLC) using a mixture of 10% MeOH + 90% $CHCl_3$ as the mobile phase revealed the absence of starting material and the formation of a single compound. The precipitate formed in the reaction was collected by filtration. The precipitate was treated with a mixture of 10 mL of saturated aqueous potassium carbonate solution (25% w/v) and 10 mL of acetone and stirred at room temperature for 45 minutes. The free base was collected by filtration, washed with ice-cold water and dried under vacuum.[65] The compounds **15o** and **15t** were made into their corresponding hydrochloride salts by treating with dry HCl in methanol at 0 °C for 4 hours. The precipitated hydrochloride salts of **15o** and **15t** were filtered and dried under vacuum. The melting points of a number of the compounds in series **15** are identical to those reported in the literature. ^{1}H NMR, ^{13}C NMR (on available compounds), and mass spectra confirm the structures of compounds in series **15**.

2.3 Analytical data

*2.3.1. 3,5-bis(benzylidene)-4-piperidone (**15**)*

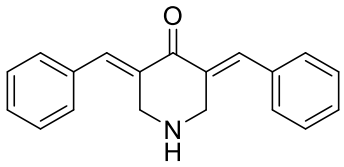

Yield: 89%; mp: 179 °C (lit 178 °C)[65]; ^{1}H NMR (500 MHz, DMSO-d_6) δ ppm 4.25 (br s, 4 H) 7.44-7.54 (m, 10 H)7.76 (s, 2 H). ^{13}C NMR (125 MHz, DMSO-d_6) δ ppm 47.61, 128.67, 129.06, 130.47, 133.73, 134.92, 136.05, 187.70. MS (FD) *m/z* found: 275.1319, calculated *m/z*: 275.1310.

*2.3.2. 3,5-bis(2-methoxybenzylidene)-4-piperidone **(15a)***

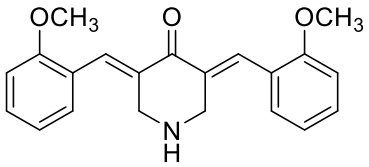

Yield: 68%; mp: 236 °C; ^{1}H NMR (500 MHz, DMSO-d_6) δ ppm 3.87 (s, 6 H) 4.34 (s, 4 H) 7.08 (t, J=7.5 Hz, 2 H) 7.16 (d, J=8.2 Hz, 2 H) 7.26 - 7.34 (m, 2 H) 7.46 - 7.54 (m, 2 H) 8.03 (s, 2 H). ^{13}C NMR (125 MHz, DMSO-d_6) δ ppm 44.06, 55.74, 111.61, 120.46, 122.24, 127.67, 130.22, 132.05, 135.11, 158.11, 182.44. MS (FD) *m/z* found: 335.1528, calculated *m/z*: 335.1521.

*2.3.3. 3,5-bis(3-methoxybenzylidene)-4-piperidone **(15b)***

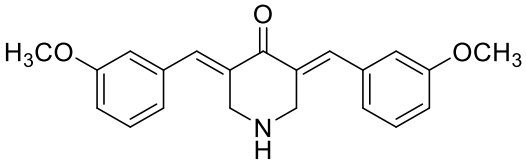

Yield: 79%; mp: 197 °C ; ^{1}H NMR (500 MHz, DMSO-d_6) δ ppm 3.80 (s, 6 H) 3.99 (s, 4 H) 6.97 - 7.06 (m, 6 H) 7.38 (t, *J*=7.9 Hz, 2 H) 7.56 (s, 2 H). ^{13}C NMR (125 MHz, DMSO-d_6) δ ppm 44.2, 55.1, 115.5, 115.7, 122.4, 128.8, 129.9, 134.8, 138.4, 159.2, 182.70. MS (FD) *m/z* found: 335.1519, calculated *m/z*: 335.1521.

2.3.4. 3,5-bis(4-methoxybenzylidene)-4-piperidone ***(15c)***

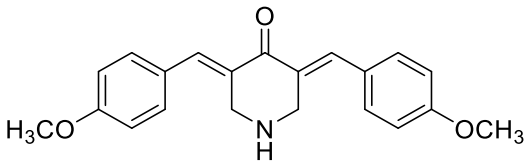

Yield: 84%; mp: 185 °C (lit. 211 °C)[65]; ^{1}H NMR (500 MHz, DMSO-d_6) δ ppm 3.80 (s, 6 H) 3.96 (s, 4 H) 7.02 (d, *J*=8.8 Hz, 4 H) 7.44 (d, *J*=8.8 Hz, 4 H) 7.53 (s, 2 H). ^{13}C NMR (125 MHz, DMSO-d_6) δ ppm 47.67, 55.29, 114.21, 127.55, 132.35, 133.38, 134.00, 159.87, 187.29. MS (FD) *m/z* found: 335.1512, calculated *m/z*: 335.1521.

2.3.5. 3,5-bis(3,4-dimethoxybenzylidene)-4-piperidone ***(15d)***

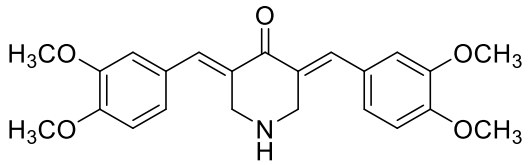

Yield: 73%; mp: 163 °C (lit. 162.2-165.4 °C)[104]; ^{1}H NMR (500 MHz, DMSO-d_6) δ ppm 3.81 (s, 12 H) 4.01 (s, 4 H) 7.05 (s, 4 H) 7.08 (s, 2 H) 7.54 (s, 2 H). ^{13}C NMR (125 MHz, DMSO-d_6) δ ppm 47.66, 55.52, 55.54, 111.59, 114.05, 123.90, 127.79, 133.88, 134.12, 148.50, 149.68, 187.24. MS (FD) *m/z* found: 395.1735, calculated *m/z*: 395.1733.

2.3.6. 3,5-bis(2,5-dimethoxybenzylidene)-4-piperidone ***(15e)***

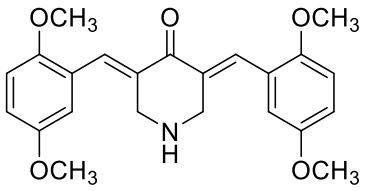

Yield: 53%; mp: 137 °C; ^{1}H NMR (500 MHz, DMSO-d_6) δ ppm 3.76 (s, 6 H) 3.81 (s, 6 H) 4.32 (br s, 4 H) 6.84 (br s, 2 H) 7.08 (br s, 4 H) 7.94 (br s, 2 H). ^{13}C NMR (125 MHz, DMSO-d_6) δ ppm 44.04, 55.67, 56.08, 112.59, 115.74, 116.63, 122.84, 128.04, 135.06, 152.29, 152.73, 182.35. MS (FD) *m/z* found: 395.1735, calculated *m/z*: 395.1733.

2.3.7. 3,5-bis(2,4,6-trimethoxybenzylidene)-4-piperidone ***(15f)***

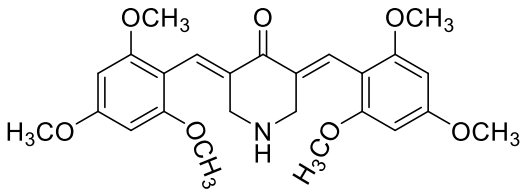

Yield: 43%; mp: 156 °C; ^{1}H NMR (500 MHz, DMSO-d_6) δ ppm 3.38 (s, 4 H) 3.78 (s, 12 H) 3.81 (s, 6 H) 6.27 (s, 4 H) 7.36 (s, 2 H). ^{13}C NMR (125 MHz, DMSO-d_6) δ ppm 48.72, 55.42, 55.57, 90.64, 105.26, 126.47, 136.26, 158.87, 162.12, 187.51. MS (FD) *m/z* found: 455.1956, calculated *m/z*: 455.1944.

2.3.8. 3,5-bis(3,4,5-trimethoxybenzylidene)-4-piperidone ***(15g)***

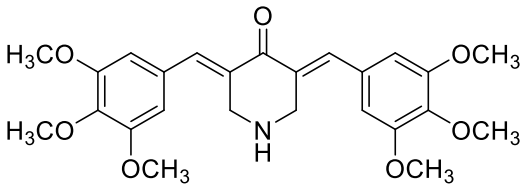

Yield: 76%; mp: 192 °C (lit: 193-194 °C)[104]; ^{1}H NMR (500 MHz, $CDCl_3$-*d*) δ ppm 3.82 (s, 12 H) 3.88 (s, 6 H) 4.52 (br s, 4 H) 6.52 (s, 4 H) 7.88 (s, 2 H) 10.31 (br s, 1 H). MS (FD) *m/z* found: 455.1952, calculated *m/z*: 455.1944.

2.3.9. 3,5-bis(benzo[d][1,3]dioxol-5-ylmethylene)-4-piperidone ***(15h)***

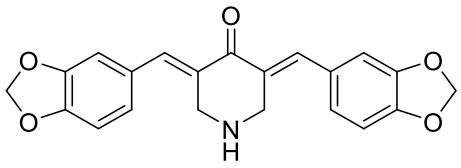

Yield: 89%; mp: 222 °C; ^{1}H NMR (500 MHz, DMSO-d_6) δ ppm 3.95 (br s, 4 H) 6.09 (s, 4 H) 7.01 (d, *J*=0.9 Hz, 4 H) 7.05 (s, 2 H) 7.49 (s, 2 H). ^{13}C NMR (125 MHz, DMSO-d_6) δ ppm 48.13, 102.00, 109.06, 110.51, 126.28, 129.61, 134.08, 134.94, 148.08, 148.51, 186.54. MS (FD) *m/z* found: 363.1107, calculated *m/z*: 363.1107.

2.3.10. 3,5-bis(2-fluorobenzylidene)-4-piperidone ***(15i)***

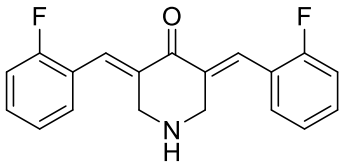

Yield: 89%; mp: 142 °C (lit. 142.5 °C)[104]; ^{1}H NMR (500 MHz, DMSO-d_6) δ ppm 3.96 (s, 4 H) 6.79 - 6.92 (m, 6 H) 7.25 (t, *J*=7.9 Hz, 2 H) 7.47 (s, 2 H). ^{13}C NMR (125 MHz, DMSO-d_6) δ ppm 47.49, 115.65, 115.82, 122.48, 122.58, 124.56, 124.58, 125.82, 125.85, 131.09, 131.39, 131.46, 137.61, 159.44, 161.42, 187.17. MS (FD) *m/z* found: 311.1112, calculated *m/z*: 311.1122.

2.3.11. 3,5-bis(3-fluorobenzylidene)-4-piperidone ***(15j)***

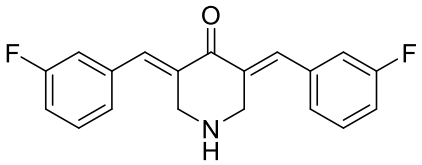

Yield: 84%; mp: 167 °C; ^{1}H NMR (500 MHz, DMSO-d_6) δ ppm 3.98 (s, 4 H) 7.22 - 7.28 (m, 2 H) 7.32 (d, *J*=7.6 Hz, 4 H) 7.48 - 7.53 (m, 2 H) 7.56 (s, 2 H). ^{13}C NMR (125 MHz, DMSO-d_6) δ ppm 44.15, 117.32, 117.62, 127.12, 129.46, 131.51, 136.41, 138.39, 161.00, 164.24, 182.79. MS (FD) *m/z* found: 311.1125, calculated *m/z*: 311.1122.

2.3.12. 3,5-bis(4-fluorobenzylidene)-4-piperidone ***(15k)***

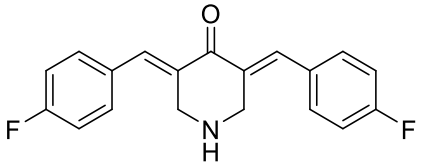

Yield: 91%; mp: 211 °C (lit: 212-213 ˚C)[65]; ^{1}H NMR (500 MHz, DMSO-d_6) δ ppm 4.50 (s, 4 H) 7.31 - 7.45 (m, 4 H) 7.56 - 7.68 (m, 4 H) 7.87 (s, 2 H) 9.85 (br s, 2 H). ^{13}C NMR (125 MHz, DMSO-d_6) δ ppm 43.66, 115.98, 116.16, 127.70, 130.34, 133.13, 138.06, 161.83, 163.81, 182.32. MS (FD) *m/z* found: 311.1110, calculated *m/z*: 311.1122.

2.3.13. 3,5-bis(3,4-difluorobenzylidene)-4-piperidone ***(15l)***

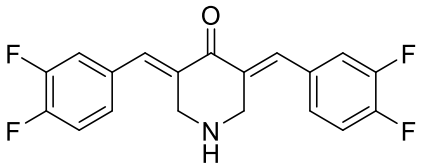

Yield: 77%; mp: 199 °C; ^{1}H NMR (500 MHz, DMSO-d_6) δ ppm 3.97 (s, 4 H) 7.33 - 7.38 (m, 2 H) 7.49 - 7.56 (m, 4 H) 7.60 (dd, *J*=11.9, 7.9 Hz, 1 H) 7.60 (dd, *J*=11.9, 7.9 Hz, 1 H). ^{13}C NMR (125 MHz, DMSO-d_6) δ ppm 47.29, 117.71, 119.36, 127.79, 131.71, 132.58, 136.77, 148.54, 150.62, 187.45. MS (FD) *m/z* found: 347.0932, calculated *m/z*: 347.0933.

2.3.14. 3,5-bis(2,6-difluorobenzylidene)-4-piperidone ***(15m)***

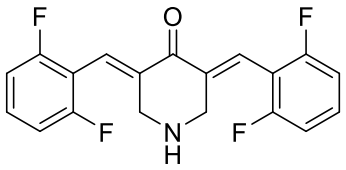

Yield: 81%; mp: 198 °C; ^{1}H NMR (500 MHz, DMSO-d_6) δ ppm 3.60 (br. s., 4 H) 7.22 (t, *J*=8.2 Hz, 4 H) 7.37 (s, 2 H) 7.49 -7.60 (m, 2 H). ^{13}C NMR (125 MHz, DMSO-d_6) δ ppm 48.08, 112.22, 112.34, 112.53, 121.29, 152.37, 182.75. MS (FD) *m/z* found: 347.0947, calculated *m/z*: 347.0933.

2.3.15. 3,5-bis(2-methylbenzylidene)-4-piperidone ***(15n)***

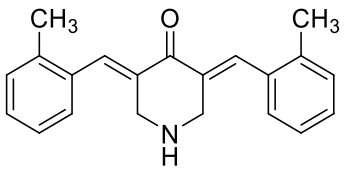

Yield: 91%; mp: 136 °C; ^{1}H NMR (500 MHz, DMSO-d_6) δ ppm 2.31 (s, 6 H) 3.81 (s, 4 H) 7.19 - 7.23 (m, 2 H) 7.24 - 7.32 (m, 6 H) 7.73 (s, 2 H). ^{13}C NMR (125 MHz, DMSO-d_6) δ ppm 19.63, 47.48, 125.72, 128.91, 129.24, 130.28, 132.50, 133.83, 136.07, 137.61, 187.68. MS (FD) *m/z* found: 303.1632, calculated *m/z*: 303.1623.

2.3.16. 3,5-bis(2-nitrobenzylidene)-4-piperidone hydrochloride ***(15o)***

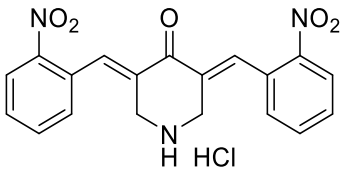

Yield: 86%; mp: 221 °C; ^{1}H NMR (500 MHz, DMSO-d_6) δ ppm 4.23 (d, *J*=1.6 Hz, 4 H) 7.57 (d, *J*=7.6 Hz, 2 H) 7.74 - 7.79 (m, 2 H) 7.91 (td, *J*=7.6, 1.3 Hz, 2 H) 8.17 (s, 2 H) 8.29 (dd, *J*=8.4, 1.1 Hz, 2 H) 9.49 (br s, 1 H). ^{13}C NMR (125 MHz, DMSO-d_6) δ ppm 43.48, 125.29, 128.65, 129.62, 130.70, 130.80, 134.42, 137.51, 147.46, 182.18. MS (FD) *m/z* found: 366.1095, calculated *m/z*: 366.1012.

2.3.17. 3,5-bis(4-hydroxy-3-methoxybenzylidene)-4-piperidone ***(15p)***

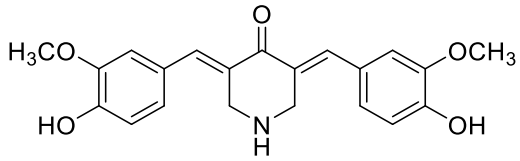

Yield: 74%; mp: 202 °C; ^{1}H NMR (500 MHz, DMSO-d_6) δ ppm 3.82 (s, 6 H) 3.99 (s, 4 H) 6.85 (br s, 2 H) 6.94 (dd, *J*=8.4, 1.73 Hz, 2 H) 7.04 (d, *J*=1.9 Hz, 2 H) 7.51 (s, 2 H). MS (FD) *m/z* found: 367.1426, calculated *m/z*: 367.1420.

2.3.18. 3,5-bis(3-hydroxy-4-methoxybenzylidene)-4-piperidone ***(15q)***

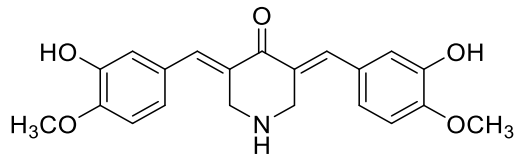

Yield: 79%; mp: 249 °C (dec.); ^{1}H NMR (500 MHz, DMSO-d_6) δ ppm 3.85 (s, 6 H) 4.42 (s, 4 H) 6.96 (s, 2 H) 7.00 (dd, *J*=8.6, 1.9 Hz, 2 H) 7.08 (d, *J*=8.5 Hz, 2 H) 7.71 (s, 2 H) 9.40 (br s, 2 H). ^{13}C NMR (125 MHz, DMSO-d_6) δ ppm 45.33, 55.69, 112.20, 117.15, 123.61, 125.94, 126.61, 138.85, 146.64, 149.67, 182.35. MS (FD) *m/z* found: 367.1433, calculated *m/z*: 367.1420.

2.3.19. 3,5-bis(4-hydroxybenzylidene)-4-piperidone ***(15r)***

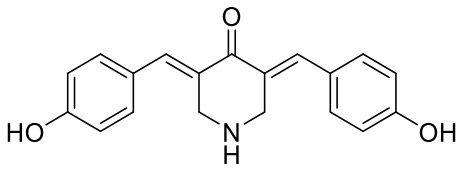

Yield: 67%; mp: >260 °C ((lit. 298.5 °C)[200]; ^{1}H NMR (500 MHz, DMSO-d_6) δ ppm 4.46 (s, 4 H) 6.89 - 6.93 (m, 4 H) 7.38 (d, *J*=8.5 Hz, 4 H) 7.78 (s, 2 H) 10.40 (br s, 2 H). ^{13}C NMR (125 MHz, DMSO-d_6) δ ppm 44.0, 116.0, 124.6, 124.7, 133.0, 139.1, 159.6, 182.0. MS (FD) *m/z* found: 307.1211, calculated *m/z*: 307.1208.

2.3.20. 3,5-bis(3-hydroxybenzylidene)-4-piperidone ***(15s)***

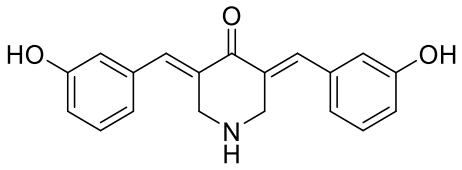

Yield: 39%; mp: 227 °C (lit. 226-230 °C)[200]; ^{1}H NMR (500 MHz, DMSO-d_6) δ ppm 3.94 (s, 4 H) 6.80 (dd, *J*=8.09, 1.79 Hz, 2 H) 6.83 (s, 2 H) 6.88 (d, *J*=7.9 Hz, 2 H) 7.23 - 7.27 (m, 2 H) 7.46 (s, 2 H). ^{13}C NMR (125 MHz, DMSO-d_6) δ ppm 48.14, 116.76, 117.30, 121.83, 130.10, 134.37, 135.86, 136.28, 158.03, 188.12. MS (FD) *m/z* found: 307.1213, calculated *m/z*: 307.1208.

*2.3.21. 3,5-bis(2-chlorobenzylidene)-4-piperidone hydrochloride**(15t)***

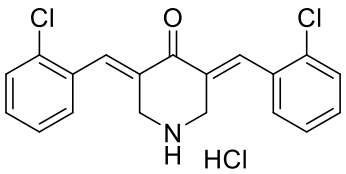

Yield: 83%; mp: 226 °C; ^{1}H NMR (500 MHz, DMSO-d_6) δ ppm 4.37 (d, *J*=1.9 Hz, 4 H) 7.46 - 7.55 (m, 6 H) 7.64 - 7.66 (m, 2 H) 8.00 (s, 2 H) 9.56 (br. s., 1 H). ^{13}C NMR (125 MHz, DMSO-d_6) δ ppm 43.65, 127.57, 129.72, 130.00, 130.82, 131.63, 131.71, 134.11, 135.86, 182.24. MS (FD) *m/z* found: 344.0596, calculated *m/z*: 344.0531.

2.4 Biological results

Table 2.1. Evaluation of **15**, **15a-t** against Ca9-22, HSC-2, and HSC-4 human oral squamous cell carcinoma cell lines.

		Human oral squamous cell carcinoma cell lines							
		Ca9-22		HSC-2		HSC-4		Average	
Compound	R	CC_{50} (μM)[a]	SI[b]	CC_{50} (μM)[a]	SI[b]	CC_{50} (μM)[a]	SI[b]	CC_{50} (μM)[a]	SI[b]
15a	2-OCH_3	0.13± 0.02	40.3	0.33± 0.09	15.9	0.50± 0.04	10.5	0.32± 0.18	22.2
15b	3-OCH_3	0.10± 0.03	18.2	0.02± 0.04	91.0	0.12± 0.02	15.2	0.14± 0.01	41.5
15c	4-OCH_3	3.13± 0.40	17.8	7.97± 0.68	6.98	6.86± 0.77	8.10	5.99± 2.53	10.9
15d	3,4-$(OCH_3)_2$	0.02± 0.01	136	0.24± 0.04	11.3	0.07± 0.00	38.9	0.11± 0.11	62.1
15e	2,5-$(OCH_3)_2$	0.06± 0.01	23.3	0.17± 0.07	8.23	0.18± 0.08	7.78	0.13± 0.07	13.1
15f	2,4,6-$(OCH_3)_3$	6.90± 0.30	5.00	7.95± 0.70	4.34	8.93± 0.75	3.86	7.93± 1.08	4.40
15g	3,4,5-$(OCH_3)_3$	0.04± 0.01	24.3	0.08± 0.01	12.1	0.11± 0.03	8.82	0.08± 0.04	15.1
15h	3,4-OCH_2O	0.16± 0.07	102	0.53± 0.12	30.8	0.71± 0.22	23.0	0.47± 0.28	51.9
15i	2-F	0.16± 0.04	21.4	0.33± 0.23	10.4	0.23± 0.01	14.9	0.24± 0.09	15.6
15j	3-F	0.07± 0.01	26.3	0.13± 0.03	14.2	0.12± 0.05	15.3	0.11± 0.03	18.6
15k	4-F	0.14± 0.06	32.9	0.94± 1.28	4.90	0.16± 0.02	28.8	0.41± 0.45	22.2
15l	3,4-F_2	0.06± 0.03	41.2	0.14± 0.05	17.6	0.07± 0.01	35.3	0.09± 0.04	31.4
15m	2,6-F_2	0.17± 0.02	24.5	0.40± 0.10	10.4	0.31± 0.21	13.5	0.30± 0.11	16.1

15n	2-CH_3	0.45± 0.04	26.4	0.79± 0.19	15.1	1.05± 0.34	11.3	0.76± 0.30	17.6
15o	2-NO_2	0.13± 0.01	20.8	0.31± 0.06	8.71	0.30± 0.15	9.00	0.25± 0.10	12.8
15p	3-OCH_3, 4-OH	0.61± 0.23	13.4	0.61± 0.08	13.4	0.63± 0.16	13.0	0.62± 0.01	13.3
15q	3-OH, 4-OCH_3	0.23± 0.01	214	0.29± 0.06	170	0.31± 0.12	159	0.28± 0.04	181
15r	4-OH	1.67± 0.13	54.1	2.52± 0.19	35.9	3.20± 0.58	28.3	2.47± 0.77	39.4
15s	3-OH	0.18± 0.01	28.2	0.21± 0.01	24.1	0.20± 0.04	25.4	0.20± 0.01	25.9
15t	2-Cl	0.10± 0.04	49.6	0.16± 0.02	31.0	0.25± 0.12	19.8	0.17± 0.08	33.5
15	H	0.27± 0.03	58.1	0.31± 0.05	50.6	0.41± 0.13	38.3	0.33± 0.07	49.0
Doxorubicin		0.24± 0.04	31.5	0.07± 0.00	108	0.08± 0.01	94.5	0.13± 0.10	78.0
Melphalan		27.4± 6.40	6.30	13.9± 3.80	12.4	14.4± 1.70	12.0	18.6± 7.63	10.3

[a] The CC_{50} values are the concentrations of compounds required to kill 50% of the cells.

[b] The letters SI refers to the selectivity index. The SI figures are the ratios of the average CC_{50} value of the compounds towards non-malignant HGF, HPLF and HPC cells (Table 2.2) and the CC_{50} figure of a compound against a specific neoplastic cell line.

Table 2.2. Evaluation of **15**, **15a-t** against HGF, HPLF, and HPC human non-malignant cells.

	Human non-malignant oral cell lines				
	HGF	HPLF	HPC	Average	PSE[b]
compound	CC_{50} (μM)[a]	CC_{50} (μM)[a]	CC_{50} (μM)[a]	CC_{50} (μM)[a]	
15a	2.11 ± 0.13	4.84 ± 3.52	8.77 ± 1.58	5.24 ± 3.35	6944
15b	2.07 ± 0.11	2.47 ± 0.07	0.91 ± 0.08	1.82 ± 0.81	29611
15c	38.1 ± 12.4	>100	28.8 ± 0.52	>55.6 ± 38.7	183
15d	2.06 ± 0.16	2.48 ± 0.28	3.61 ± 2.50	2.72 ± 0.80	56421
15e	1.29 ± 0.60	2.01 ± 0.27	0.91 ± 0.02	1.40 ± 0.56	10087
15f	33.9 ± 8.27	48.0 ± 10.4	21.7 ± 1.72	34.5 ± 13.2	55
15g	1.13 ± 0.79	1.28 ± 0.71	0.51 ± 0.20	0.97 ± 0.40	18830
15h	6.35 ± 0.12	7.91 ± 0.19	34.7 ± 12.2	16.3 ± 15.9	11035
15i	4.40 ± 1.32	3.63 ± 0.57	2.24 ± 1.17	3.43 ± 1.09	6492
15j	2.05 ± 0.16	2.70 ± 0.12	0.78 ± 0.16	1.84 ± 0.98	16901
15k	4.22 ± 1.31	7.07 ± 0.47	2.54 ± 0.14	4.61 ± 2.29	5418
15l	1.68 ± 0.44	3.69 ± 0.64	2.04 ± 0.97	2.47 ± 1.07	34850
15m	2.07 ± 0.30	7.46 ± 0.38	2.97 ± 0.05	4.17 ± 2.89	5378
15n	5.58 ± 0.18	7.27 ± 0.21	22.8 ± 1.85	11.9 ± 9.51	2318
15o	1.71 ± 0.23	2.57 ± 0.07	3.82 ± 1.14	2.70 ± 1.06	5131
15p	5.76 ± 1.20	10.8 ± 1.10	8.08 ± 8.51	8.20 ± 2.50	2145
15q	2.72 ± 0.18	54.6 ± 39.1	90.7 ± 16.2	49.3 ± 44.2	64688
15r	74.0 ± 6.56	>100	97.3 ± 4.62	>90.4 ± 14.3	1596
15s	2.23 ± 0.06	3.45 ± 0.30	9.53 ± 5.17	5.07 ± 3.91	12943
15t	2.25 ± 0.15	5.07 ± 1.99	7.55 ± 1.62	4.96 ± 2.65	19694
15	7.78 ± 0.85	17.0 ± 2.29	22.3 ± 2.61	15.7 ± 7.33	14857
Doxorubicin	2.69 ± 0.35	>10.0	>10 ± 0.00	>7.56 ± 4.22	60000
Melphalan	148.0 ± 0.68	>200	169 ± 18.5	>173 ± 25.8	>55

[a] The CC_{50} values are the concentrations of the compounds required to kill 50% of the cells.

[b] The letters PSE refer to the potency-selectivity expression. These figures are the product of the reciprocal of the average CC_{50} values against Ca9-22, HSC-2 and HSC-4 cells and the average SI value multiplied by 100.

Table 2.3. Evaluation of **15**, **15a-t** towards Colo205, HT-29, CEM and Hs27 cells.

	Human tumour cell lines								Normal cell line	
	Colo205		HT-29		CEM		Average		Hs27	
Compound	CC_{50} (μM)[a]	SI[b]	CC_{50} (μM)[a]	SI[b]	CC_{50} (μM)[a]	SI[b]	CC_{50}[a]	SI[b]	CC_{50} (μM)[a]	PSE[c]
15	10.7± 0.05	1.54	1.57± 0.21	10.5	9.29± 0.11	1.78	7.19	4.61	16.5± 0.35	64
15a	1.32± 0.01	3.10	3.58± 0.21	1.14	0.82± 0.09	4.99	1.91	3.08	4.09± 0.56	161
15b	0.32± 0.11	13.0	5.58± 0.52	0.75	4.51± 0.11	0.92	3.47	4.89	4.16± 0.32	141
15c	14.0± 0.56	6.84	12.6± 0.00	7.60	4.45± 0.03	21.5	10.4	12.0	95.7± 0.11	115
15d	1.36± 0.17	0.65	3.46± 0.46	0.25	0.49± 0.02	1.80	1.77	0.90	0.88± 0.05	51
15e	0.36± 0.01	1.81	0.84± 0.01	0.77	0.42± 0.02	1.55	0.54	1.37	0.65± 0.02	254
15f	16.9± 0.23	1.63	9.63± 0.32	2.87	11.0± 1.06	2.51	12.5	2.34	27.6± 0.79	19
15g	0.27± 0.03	121	2.03± 0.00	16.1	0.31± 0.09	106	0.87	81.0	32.7± 0.56	9310
15h	8.84± 0.08	2.17	7.42± 1.33	2.59	1.88± 0.08	10.2	6.05	4.99	19.2± 2.38	83
15i	2.94± 0.33	0.68	3.46± 0.33	0.58	0.78± 0.04	2.55	2.39	1.27	1.99± 0.17	53
15j	4.19± 0.15	0.44	1.73± 0.15	1.06	0.21± 0.01	8.76	2.04	3.42	1.84± 0.32	168
15k	1.56± 0.28	1.21	5.51± 0.56	0.34	1.68± 0.25	1.13	2.92	0.89	1.89± 0.05	31
15l	1.81± 0.31	16.1	3.50± 0.19	8.34	0.58± 0.05	50.3	1.96	24.9	29.2± 0.08	1270
15m	2.22± 0.00	3.50	7.36± 0.88	1.06	7.88± 0.68	0.99	5.82	1.85	7.77± 0.89	32
15n	1.62± 0.11	30.4	3.54± 0.42	13.9	1.82± 0.10	27.1	2.33	23.8	49.3± 0.23	1022
15o	2.09± 0.33	11.6	2.76± 0.04	8.80	6.14± 0.56	3.96	3.66	8.12	24.3± 0.11	222
15p	1.73± 0.15	1.20	17.8± 1.48	0.12	1.92± 0.53	1.08	7.15	0.80	2.07± 0.07	11
15q	4.58± 0.17	2.73	4.26± 0.01	2.93	4.04± 0.17	3.09	4.29	2.92	12.5± 1.61	68
15r	4.17± 0.32	2.08	19.3± 0.48	0.45	1.99± 0.10	4.36	8.49	2.30	8.68± 0.16	27
15s	2.12± 0.12	0.64	4.18± 0.36	0.32	0.43± 0.04	3.14	2.24	1.37	1.35± 0.08	61
15t	8.19± 0.17	0.08	0.89± 0.07	0.69	4.42± 0.35	0.14	4.50	0.30	0.61± 0.01	7

[a] The CC_{50} values are the concentrations of compounds required to kill 50% of the cells.

[b] The letters SI refers to the selectivity index. The SI figures are the ratios of CC_{50} value of the compounds towards non-malignant Hs27 cells and the CC_{50} figure of a compound against a specific neoplastic cell line.

[c] The letters PSE refer to the potency-selectivity expression. These figures are the product of the reciprocal of the average CC_{50} values against Colo205, HT-29 and CEM cells and the average SI value multiplied by 100.

Table 2.4. Identification of lead molecules based on the data in Tables 2.1 and 2.2.

Table	Bioevaluations	Promising compounds
2.1	Average CC_{50} values	**15d**, **g**, **j**, **l**
2.1	Average SI figures	**15**, **15b**, **d**, **h**
2.2	Low toxicity to normal cells	**15c**, **f**, **q**, **r**
2.2	PSE	**15b**, **d**, **l**, **q**

2.4.1 Methodology

Methodology for determining the cytotoxic activity of 15, 15a-t towards Ca9-22, HSC-2, and HSC-4 tumour cells and HGF, HPLF and HSC human normal cells.

The human oral tumor cell lines used are squamous carcinoma cells HSC-2, HSC-4 and Cellosaurus cell line Ca9-22. The human oral non-malignant cells employed are periodontal ligament fibroblasts (HPLF), gingival fibroblasts (HGF), and hematopoietic precursor cell HPC cells. All cells were cultured in DMEM medium which was supplemented with 10% heat-inactivated FBS. The human normal cells were obtained from periodontal tissues according to the "guidelines of the Meikai University Ethics Committee after obtaining the informed consent from the patient". All cells were incubated for 48 hours at 37 °C with 5% CO_2 at various concentrations of the test samples, and the relative viable cell number was then determined by the MTT assay method and is expressed as the absorbance at 540 nm of the cell lysate. The 50% cytotoxic concentration (CC_{50}) was determined from a dose-response curve.[201] The above bioevaluations data for the compound **15** series in Tables 2.1 and 2.2 are generated at Meikai University Research Institute of Odontology, Japan.

Methodology for determining the cytotoxic activity of 15, 15a-t towards Colo205, HT-29, CEM and Hs27 cells.

In brief, the cells were cultured in DMEM (Colo205, HT29 and Hs-27) or RPMI -1640 (CEM) media supplemented with 10% heat-inactivated fetal bovine serum. Different concentrations of the compounds were added to the cell cultures and then viability was measured by the Differential DNA Staining (DNS) assay after 24 hours incubation.[202, 203] After analysis of the effects of a range of concentrations of the compounds, the CC_{50} (compound concentration needed to kill 50% of the cell population) was determined. After subtracting the percentage of cell death caused by the solvent (DMSO-treated cells), a linear interpolation equation was used to determine the CC_{50} values.[203, 204] The bioevaluations data for series **15** in Tables 2.3 are generated at Department of Biological Sciences and Border Biomedical Research Center, The University of Texas, El Paso, USA.

2.5 Discussion

The cytotoxic evaluation of compounds **15, 15a-t** along with two reference drugs against Ca9-22, HSC-2, and HSC-4 human oral squamous carcinoma cell lines is presented in Table 2.1. The biodata reveals that no less than 86% of the CC_{50} values of **15**, **15a-t** are submicromolar and 14% of the compounds in series **15** have CC_{50} values in the double digit nanomolar range. The average CC_{50} values for **15g, 15l** against the carcinoma cell lines is below 0.1 μM. The unsubstituted compound **15** is a potent cytotoxic compound with CC_{50} value of 0.33 μM; however in total 13 compounds have lower CC_{50} values than **15**. In particular compounds **15d** (3,4-dimethoxy), **15g** (3,4,5-trimethoxy), **15j** (3-fluoro) and **15l** (3,4-difluoro) have the lowest average CC_{50} values and these four compounds are equipotent with doxorubicin, one of the reference drugs used in the assays and are far more potent than the second reference drug melphalan.

Comparisons were made between the compounds having methoxy and fluoro groups in which the substituents are located at the same position on the arylidene aryl rings. Thus **15a** (2-methoxy) was compared with **15i** (2-fluoro), **15b** (3-methoxy) was compared with **15j** (3-fluoro), **15c** (4-methoxy) with **15k** (4-fluoro), and **15d** (3,4-dimethoxy) with **15l** (3,4-difluoro). In each of these comparisons, the fluoro substituted compounds are found to have lower CC_{50} values than the corresponding methoxy substitutions.

Comparisons were also made between **15a**, **15i**, **15n**, **15o**, and **15t** which have different substitutions at the *ortho* position of the arylidene aryl rings. In this comparison **15t** with a 2-chloro substituent has lower average CC_{50} values than the fluoro, nitro, methoxy and methyl analogs at the *ortho* position of the aryl rings. Compound **15n** was found to be the least potent analog among the *ortho* substituted groups.

There are significant differences in the CC_{50} values of several pairs of structural isomers. The average CC_{50} value of **15b** (3-methoxy) is 75 times lower than its corresponding isomer **15c** (4-methoxy). A similar comparison was noted between **15f** (2,4,6-trimethoxy) and **15g** (3,4,5-trimethoxy)**,** where the average CC_{50} value of **15f** is 99 folds higher than its isomer **15g**, while **15s** (3-hydroxy) is 12 times more potent than its structural isomer **15r** (4-hydroxy).

An important factor to consider while developing these compounds is whether they demonstrate tumour-selective toxicity. Consequently, the compounds in series **15** were evaluated against several human non-malignant cells. All of the compounds in series **15** were screened against HGF, HPLF and HSC non-malignant cells and these data are presented in Table 2.2. In this evaluation, the compounds with average CC_{50} values greater than 30 µM which cause the least toxicity are **15c** (4-methoxy), **15f** (2,4,6-trimethoxy), **15q** (3-hydroxy-4-methoxy) and **15r** (4-hydroxy), while the compounds having an average CC_{50} value of less than 2 µM causing the most toxicity to non malignant cells are **15b** (3-methoxy), **15e** (2,5-dimethoxy), **15g** (3,4,5-trimethoxy) and **15j** (3-fluoro). This evaluation revealed that the compounds in series **15** display greater cytotoxicity towards malignant cells than to normal cells.

Under clinical conditions, neoplasms are surrounded by a variety of normal cells in the body. The challenging task is to identify compounds that display greater toxicity to the neoplasms than the surrounding non-malignant cells. In order to evaluate if the compounds in series **15** demonstrate tumor-selective toxicity, selectivity index (SI) values were generated. The SI figures are the ratios of the average CC_{50} value of the compounds towards non-malignant HGF, HPLF and HPC cells and the CC_{50} figure of a compound against a specific neoplastic cell line. The SI figures are presented in Table 2.1 and all of the compounds in series **15** have SI figures greater than 1

demonstrating that they display selective cytotoxicity towards malignant cells. No less than 90% of the compounds shown SI values >10 and the compound **15q** displayed the highest mean SI value of 181 which is 2.3 times more selective than the reference drug doxorubicin and 17.5 times more selective than melphalan. Compounds, **15d** (3,4-dimethoxy), **15h** (3,4-OCH_2O), **15q** (3-hydroxy-4-methoxy) display noteworthy SI figures of, 62.1, 51.9 and 181 respectively and also possess sub-micromolar CC_{50} values; hence these three compounds are considered as leads for further studies.

Potencies and tumour-selective toxicities are two important properties that one should consider in evaluating cytotoxins. Potency Selective Expression (PSE) values were generated in order to identify compounds with these two desirable properties. PSE figures are the product of the reciprocal of the CC_{50} value multiplied by the SI figure times 100 [$PSE = (SI/CC_{50}) \times 100$]. PSE values take into consideration both potency and selectivity indices. In contrast SI values deal only with greater toxicity for neoplastic cells compared to non-malignant ones. The PSE values of series **15** are presented in Table 2.2. Compounds **15b, d, l, q** have PSE values in excess of 25,000. In particular **15q** (3-hydroxy-4-methoxy) has the highest PSE value of 64,688 which is 30 times greater than the value of its structural isomer **15p** (4-hydroxy-3-methoxy).

A summary of lead molecules is presented in Table 2.4. These data reveal that **15d** (3,4-dimethoxy analog) is present in three of the four categories while **15b** (3-methoxy) and **15q** (3-methoxy-4-hydroxy) analogs appear in two of the four divisions. These data suggest that hydroxyl and especially methoxy groups are associated with greater potency than the compounds having halogen substituents.

Since the compounds in series **15** display significant cytotoxic potencies and greater selectivity in harming malignant cells, comparisons were made with the well-known anticancer drugs, doxorubicin which is an antibiotic and melphalan an alkylating agent as reference compounds. The average cytotoxicities CC_{50} towards three malignant cells (Ca9-22, HSC-2 and HSC-4) show that all the compounds **15**, **15a-t** are more potent than melphalan and **15g** is 232 times more potent than melphalan. Other compounds displaying much greater potencies than melphalan are **15l**, **15d**, and **15j** which are 206, 169 and 169 times more potent than melphalan. These four compounds also displayed higher selectivity towards malignant cells than that of melphalan with average SI figures given in parenthesis **15d**(62.1), **15g**(15.1), **15j**(18.6), **15l**(31.4) and melphalan (10.3). All of the compounds in series **15** shown higher cytotoxicities than melphalan towards Ca9-22, HSC-2, and HSC-4 neoplastic cell lines. The average CC_{50} figures in Table 2.1 indicate that four compounds **15d**, **15g**, **15j** and **15l** displayed higher cytotoxicity than doxorubicin while **15e** is equipotent with doxorubicin. In terms of selectivity, **15q** was more sensitive/selective to the neoplastic cells with average an SI figure 181 which is 2.3 times more than doxorubicin and 17.5 times more than melphalan.

In a separate study, the compounds in series **15** were evaluated against three human neoplastic cell lines namely Colo205 and HT-29 colon cancers and CEM leukemia cells. Also, a non-malignant cell line namely human Hs27 fibroblasts was also employed in this screening. The biodata generated are presented in Table 2.3.

The results of this evaluation reveal that 89% of the CC_{50} values are below 10 µM, 73% are below 5µM and 21% have submicromolar CC_{50} values. Thus the three neoplastic cell lines employed in this screening are sensitive towards the compounds in series **15**. The average CC_{50} values were

also examined and two compounds namely **15e** (2,5-dimethoxy) and **15g** (3,4,5-trimethoxy) are the most potent compounds.

There are significant differences in the CC_{50} values between some of the structural isomers The compound **15e** (2,5-dimethoxy) is 3 times more cytotoxic than its structural isomer **15d** (3,4-dimethoxy) and **15g** (3,4,5-trimethoxy) is found to be 14 times more toxic than **15f** (2,4,6-trimethoxy).

To demonstrate if the compounds in series **15** show tumor-selective toxicity, these compounds were also screened against Hs27 fibroblasts which are human non-malignant cells. The selectivity index (SI) values were generated, and the SI figures are the ratios of the average CC_{50} value of the compounds towards non-malignant Hs27 cells and the CC_{50} figure of a compound against a specific neoplastic cell line. The data are presented in Table 2.3 The compounds **15c**, **f**, **g**, **l**, and **n** have the highest CC_{50} values >25 μM towards Hs27 cells. The biodata in Table 2.3 reveal that the dimethoxy analogs **15d** and **15e** are more toxic to the non-malignant cells (average CC_{50} value of 0.77 μM) than to the neoplasms. On the other hand the trimethoxy derivatives **15f**, **g** are 39 times are less toxic towards Hs27 cells (average CC_{50} value of 30.2 μM). The compounds **15c**, **f**, **g**, **l**, and **n** have average SI values greater than 10 and in particular **15g** has a large average SI value of 81.0. Potency Selective Expression (PSE) values were computed and are presented in Table 2.2 in order to identify the compounds with two desirable properties namely potencies and tumor-selective toxicities. Three compounds **15g**, **l**, and **n** have PSE figures greater than 1000. Thus, a number of lead molecules are described in this study and are listed in Table 2.4.

It is possible that the mode of actions of the compounds in series **15** towards the neoplasms are similar and the relative potencies of **15a-u** towards all neoplastic cell lines may be the same. To

investigate this possibility, Kendall's coefficient of concordance (W) was used which is a statistical method for assessing the similarity in rank between a collection of numbers. This methodology was applied initially to the CC_{50} values of the compounds in series **15** against Ca9-22, HSC-2 and HSC-4 malignant cells. In this case, Kendall's coefficient of concordance (W) value is 0.7977 and a p value of 0.0004 indicates that the order of potency towards different neoplastic cell lines is in the same order. Since **15f**, **c**, and **r** are outliers, plots were made by systematically removing the biodata of these three outliers namely **15f**, then **15f**, **c** and finally **15f**, **c**, **r**. The results are as follows namely W=0.7668, p=0.0010 (**15f** removed), W=0.7400, p=0.0021 (**15f**, **c** removed) and W=0.7074, p=0.0045 (**15f, c, r** removed). The same study was repeated with the CC_{50} values of series **15** compounds towards Colo205, HT-29 and CEM cells which generated a W value of 0.5834, and a p value of 0.0200. The data produced when the outliers **15f**, **c**, and **r** were removed are **15f** (W=0.5324, p=0.0475), **15f, c** (W=0.4942, p=0.0850) and **15 f, c, r** (W=0.4788, p=0.1084). The effect on the statistical results of removing the outliers may be explained in the following ways. First, when one or more results are removed, the statistical power is diminished. Second, Kendall's coefficient of concordance deals with rank and is not concerned with potency differences. For example, **15f** is consistently weaker in potency compared to the analogs.

In a separate analysis, Kendall's coefficient of concordance was applied using the CC_{50} values of the six neoplastic cell lines Ca9-22, HSC-2, HSC-4, Colo205, HT29 and CEM cells. Kendall's coefficient of concordance (W) value is 0.6086 and the p figure is 0.0000. When the outliers are systematically eliminated from considerations, the W and p values are as follows W=0.5533, p=0.0000 (excluding **15f**), W=0.5083, p=0.0000 (excluding **15f, c**) and W=0.4813, p=0.0001(excluding **15f, c, r**). This observation provides strong evidence that the modes of action

of series **15** are similar and one is justified in taking the average CC_{50} values of each compound against the six neoplastic cell lines in the search for finding correlations between some of the physicochemical properties of the aryl substituents and the cytotoxic potencies (CC_{50}). In other words, if there was no concordance, then one would need to plot the CC_{50} values towards each cell line against a physicochemical parameter such as Hammett sigma values (σ). However no concordance has been demonstrated, the average CC_{50} value can be used and plotted directly against σ values.

In order to find if one or more physicochemical properties of the aryl substituents influence the cytotoxic properties, linear and semilogarithmic plots were generated between the average CC_{50} values of series **15** towards the six neoplastic cell lines and the sigma/sigma star (σ/σ*), pi (π) and molecular refractivity (MR) values of the aryl substituents. The physicochemical constants σ/σ*, π and MR values reflect the electronic, hydrophobic, and steric properties of the aryl groups, respectively. The sigma / sigma star (σ/σ*), pi (π) and MR values used in the QSAR studies were taken from a reference source.[205, 206]

In a linear plot, a negative correlation was noted between the σ/σ* values and cytotoxic potencies ($p=0.02$). No other correlations ($p<0.05$) nor trends to a correlation (<0.10) were observed. This observation indicates that the cytotoxic potency increases as the magnitude of the electron-withdrawing properties of the aryl substituents rise. The explanation for this observation may be due to a reduction of the electron densities on the olefinic carbon atoms as the σ/σ* values rise. Hence the reactivity of these compounds towards cellular thiols will increase and thus the extent of cell death. In future studies, therefore strongly electron-attracting groups should be placed in

the aryl rings which may generate compounds with even higher cytotoxicities towards malignant cells.

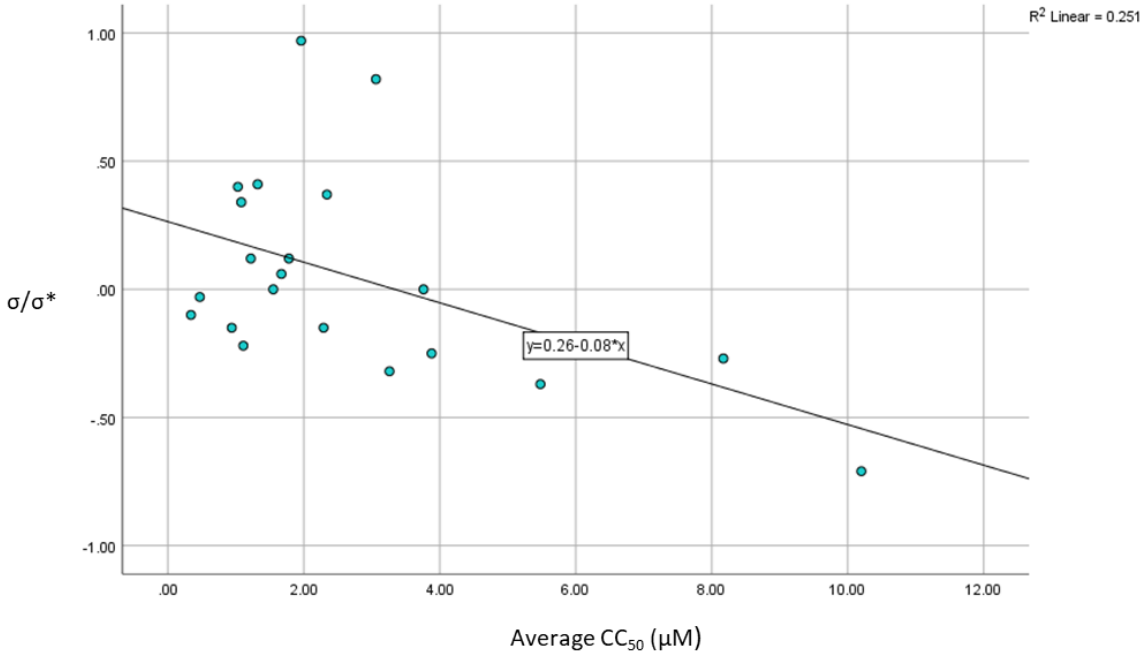

Plot 2.1 Linear plot between the average CC_{50} values of series **15** towards the six neoplastic cell lines and the sigma/sigma star (σ/σ*) values.

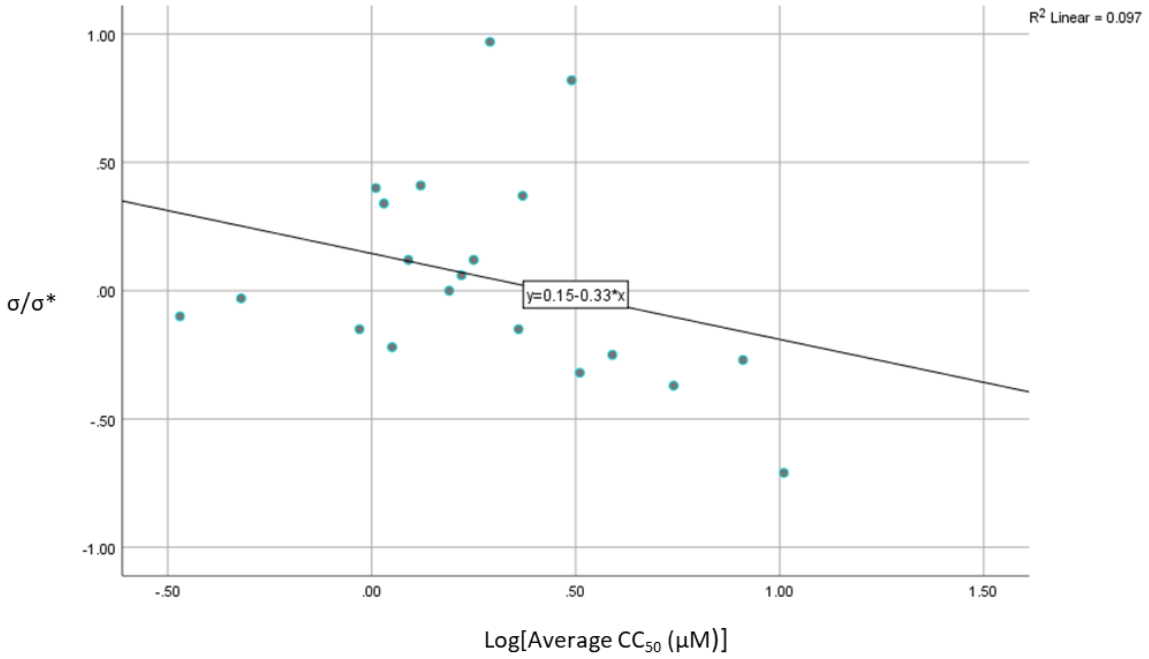

Plot 2.2 Semilogarithmic plot between the average CC50 values of series **15** towards the six neoplastic cell lines and the sigma/sigma star (σ/σ*).

Prior to leaving this section of the thesis which outlines the cytotoxic properties of a number of 3,5-bis(benzylidene)-4-piperidones, mention will be made of an unusual reaction which was observed in an attempt to prepare a series of 2,2,6,6-tetramethyl-3,5-bis(benzylidene)-4-piperidones".

2.6 Unusual reactions observed in the 2,2,6,6-tetramethyl-4-piperidone (TMP) project.

It is known that changes in the conformations of drugs will affect the corresponding biological responses at the binding sites of the receptors.[57] The hypothesis is that the conformational changes in representative 3,5-bis(benzylidene)-4-piperidones will affect their cytotoxic potencies. There is a non-bonding interaction between the equatorial hydrogen atom at position 2 of the 4-piperidone with the *ortho* proton of the aryl ring as indicated in **Figure 2.1** which increases the interplanar

angle θ_A .[56] Therefore, if the equatorial protons in the 4-piperidone ring are replaced with bulky methyl groups for example, the magnitude of the non-bonding interaction between the methyl group and protons at the ortho position of the aryl ring will increase and thereby the θ_A value should change. This results in overall conformational changes in the molecule (**Figure 2.1**) which may show a variation in the cytotoxic potencies compared to the present compounds.

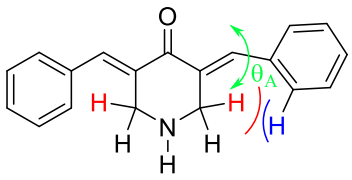

15

Figure 2.1. 3,5-Bis(benzylidene)-4-piperidone showing interaction between equatorial hydrogen atom at position 2 of the 4-piperidone with the *ortho* proton of the aryl ring.

Initially, the synthesis of 3,5-dibenzylidene-2,2,6,6-tetramethylpiperidin-4-one was attempted using the reported procedure of condensing aromatic aldehydes with piperidine-4-one under acidic conditions.[79] The reaction did not proceed even at higher temperatures.

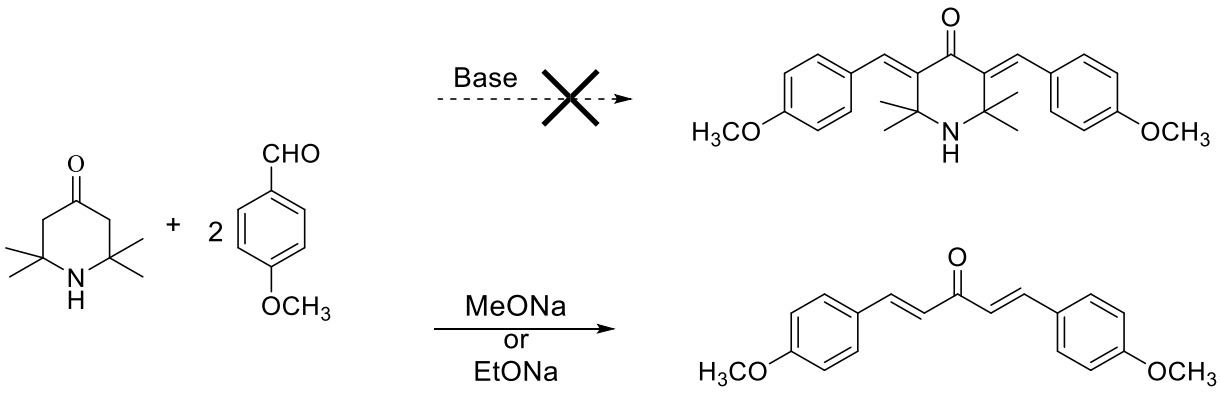

Scheme 2.2. Attempted synthesis of 3,5-dibenzylidene-2,2,6,6-tetramethylpiperidin-4-one.

A general synthetic procedure was tried under basic conditions for the synthesis of 3,5-dibenzylidene-2,2,6,6-tetramethylpiperidin-4-ones which did not produce any desired product. Many trials were carried out with TMP, 4-methoxybenzaldehyde in the presence of different bases viz., NaH, piperidine/AcOH, NaOH at different temperature conditions, but none of them produced the desired product.

The reactions using NaOEt and NaOMe as bases, at 50-55 °C produced a compound which was isolated by column chromatography and characterized by ^{1}H NMR. Analysis of the ^{1}H NMR spectra revealed the isolated compound to be 1,5-bis(4-methoxyphenyl)-penta-1,4-dien-3-one which is not the desired compound. The % yields of 1,5-bis(4-methoxyphenyl)-penta-1,4-dien-3-one under different reaction conditions are summarized in Table 2.5.

2.7 Plausible Reaction Mechanism:

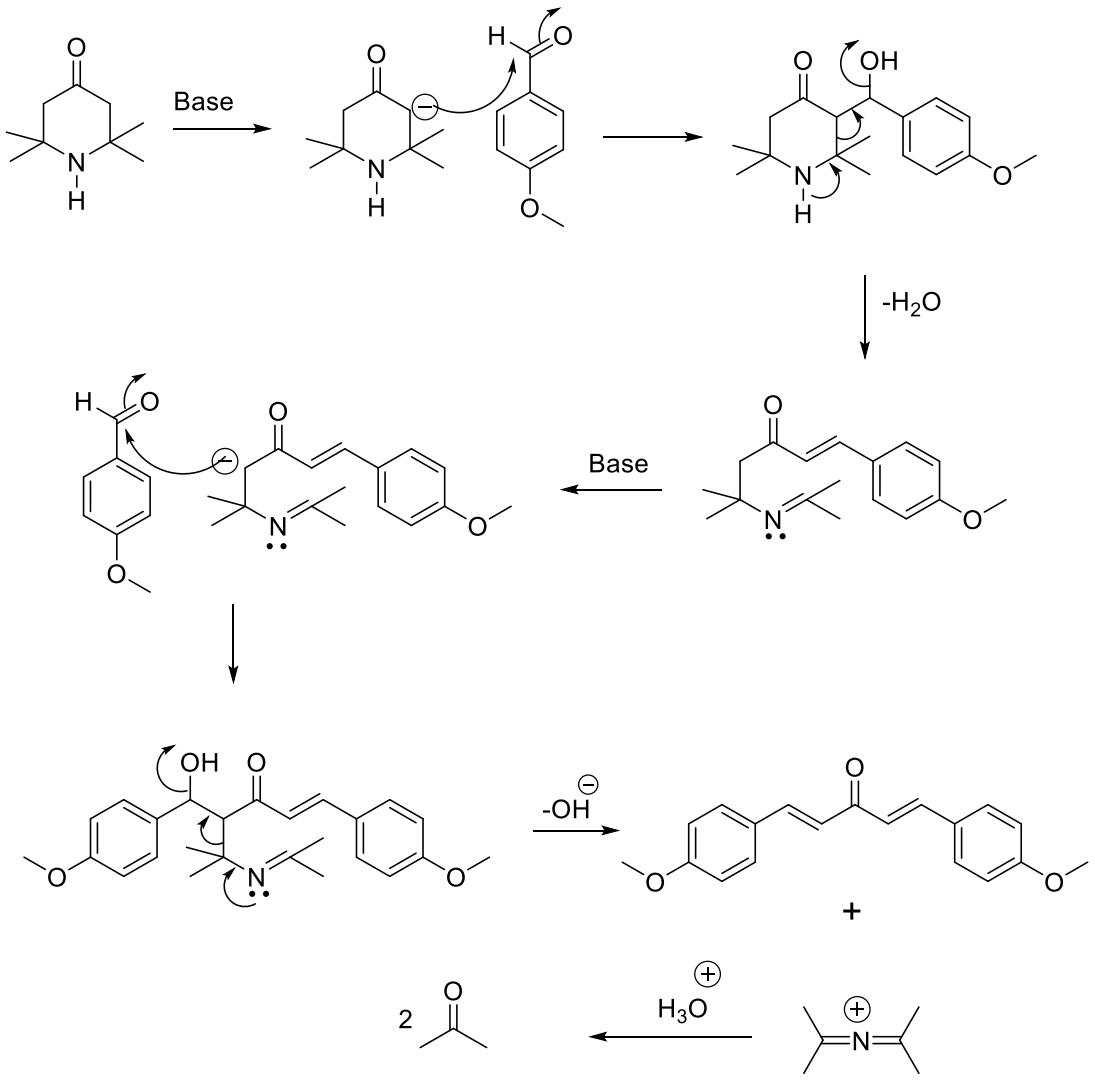

Scheme 2.3. Plausible reaction mechanism for the formation of unusual acyclic compounds.

The mechanism for the formation of 1,5-bis(4-methoxyphenyl)-penta-1,4-dien-3-one was proposed, and a detailed investigation will be carried out in the future with different aryl aldehydes to establish an alternative route for the synthesis of 1,5-bis(aryl)-1,4-dien-3-ones.

In future, to overcome the formation of the undesired 1,5-bis(4-methoxyphenyl) penta-1,4-dien-3-one, the proposed plan is to protect the basic nitrogen of TMP with electron-withdrawing groups viz., benzoyl chloride, 4-nitro benzoyl chloride and condensing the *N*-protected TMP with aryl aldehydes.

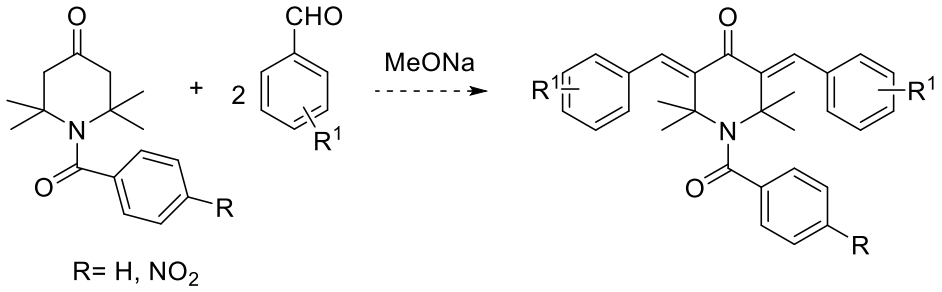

Scheme 2.4. Proposed synthetic route for 3,5-dibenzylidene-2,2,6,6-tetramethylpiperidin-4-ones.

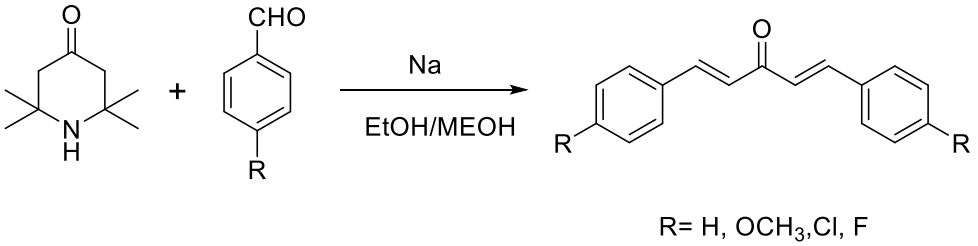

Scheme 2.5. Synthesis of 1,5-bis(aryl)-1,4-pentadien-3-one compounds.

2.7.1 General procedure for the synthesis of 1,5-bis(aryl)-1,4-pentadien-3-ones

The aryl aldehyde (2.64 mmol) and 2,2,6,6-tetramethyl-4-piperidone (1.28 mmol) were dissolved in absolute ethanol or methanol (20 mL) and stirred at room temperature for 5 minutes. Sodium metal (4.5 mmol) was added slowly to the reaction mixture at 0 °C. After all the sodium metal dissolved, the reaction mixture was stirred at room temperature for 1 hour and then heated to 50-55 °C overnight. The reaction mixture was cooled to 5-10 °C and 5 mL 6N hydrochloric acid was

slowly added. The organic solvent was completely evaporated, and the residue was extracted with ethyl acetate. The organic extract were dried over anhydrous Na_2SO_4 and concentrated to get the crude compound which was purified by silica gel-60, (0.040-0.063 mm, 230-400 mesh) column chromatography using 5% ethyl acetate in hexane as the mobile phase.

The compounds formed in these unusual reactions were not tested for cytotoxicity as we are not interested in evaluating the biological properties of these compounds in these studies.

Table 2.5. Reaction conditions and % yields of unusual reactions

Aryl substituent	TMP (mmol)	Aryl aldehyde (mmol)	Sodium metal (mmol)	Solvent	Temp	Time	Yield
H	1.28	2.64	4.5	Ethanol	55 °C	15 h	22%
OCH_3	1.28	2.64	4.5	Ethanol	55 °C	14 h	37%
OCH_3	1.28	2.64	4.5	Methanol	55 °C	18 h	26%
Cl	1.28	2.64	4.5	Ethanol	55 °C	14 h	41%
F	1.28	2.64	4.5	Ethanol	55 °C	14 h	29%

2.8 Analytical data

2.8.1. (1E,4E)-1,5-Diphenylpenta-1,4-dien-3-one[207]

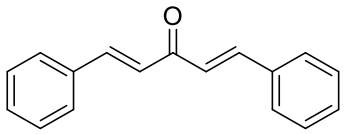

Yield: 22 %; mp: 112 °C(lit 98 °C)[207]; ^{1}H NMR (500 MHz, DMSO-d_6) δ ppm 7.09 (d, *J*=15.9 Hz, 2 H), 7.37 -7.46 (m, 6 H), 7.58 - 7.65 (m, 4 H), 7.74 (d, *J* =15.9 Hz, 2 H). MS (FD) *m/z* found: 234.1057, calculated *m/z*: 234.1045.

2.8.2. (1E,4E)-1,5-bis(4-Methoxyphenyl)penta-1,4-dien-3-one

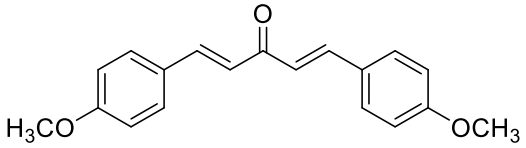

Yield: 26%; mp: 122 °C; ^{1}H NMR (500 MHz, DMSO-d_6) δ ppm 3.80 (s, 6 H) 7.01 (d, *J* = 8.8 Hz, 4 H) 7.20 (s, 1 H) 7.17 (s, 1 H) 7.71 (s, 1 H) 7.72 - 7.75 (m, 5 H). MS (FD) *m/z* found: 294.1271, calculated *m/z*: 294.1256.

2.8.3. (1E,4E)-1,5-bis(4-Chlorophenyl)penta-1,4-dien-3-one

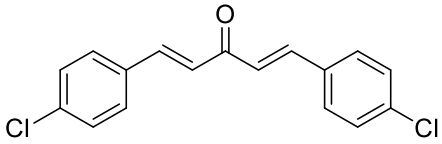

Yield: 41%; mp: 193 °C; ^{1}H NMR (500 MHz, $CDCl_3$) δ ppm 7.04 (d, *J*=15.9 Hz, 2 H), 7.40 (dd, *J*=8.6 Hz, 4 H), 7.56 (d, *J*=8.6 Hz, 4 H), 7.70 (d, *J*=15.9 Hz, 2 H). ^{13}C NMR (125 MHz, $CDCl_3$) δ

126.0, 128.7, 128.7, 129.3, 129.3, 133.3, 136.5, 142.1, 188.3. MS (FD) *m/z* found: 302.0279, calculated *m/z*: 302.0265.

2.8.4. (1E,4E)-1,5-bis(4-Fluorophenyl)penta-1,4-dien-3-one

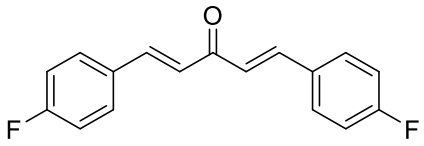

Yield: 29%; mp: 148 °C; ^{1}H NMR (500 MHz, $CDCl_3$) δ ppm 7.00 (d, *J*=15.9 Hz, 2 H), 7.11 (dd, *J*=8.7 Hz, 4 H), 7.60 (d, *J*=8.7 Hz, 4 H), 7.71 (d, *J*=15.9 Hz, 2 H). ^{13}C NMR (125 MHz, $CDCl_3$) δ 115.8, 125.4, 130.8, 141.5, 161.6, 164.9, 188.3. MS (FD) *m/z* found: 270.094, calculated *m/z*: 270.085.

Chapter 3

3.1 Introduction

The aim of this portion of the investigation was to prepare a series of *N*-aroyl analogs of a number of 3,5-bis(benzylidene)-4-piperidones in order to examine their potential as antineoplastic agents. The hypothesis 2 was formulated that the presence of an acyl group attached on to the piperidyl nitrogen atom of 3,5-bis(benzylidene)-4-piperidones may interact with an additional binding site and thereby enhancing cytotoxic potencies and tumor selectivities. An aryl ring in the *N*-acyl function was chosen since it may allow van der Waal bonding at auxiliary binding site. An aminoalkoxy group was placed on the aromatic ring would interact at a complementary area of the binding site may increase the cytotoxic potencies. The nitrogen atom of aminoalkoxy group in series **33** may interact with an additional binding site thereby enhancing cytotoxic potencies. A variety of substituents were placed on the arylidene aryl rings in order to seek correlations between some of their physicochemical properties and the magnitude of the cytotoxic potencies. These evaluations would be made using SAR and QSAR approaches.

In order to evaluate whether these compounds in series **33** display tumor-selective cytotoxicity, they were also evaluated against several non-malignant cell lines. The enone **33g** was planned to be examined as a possible initiator of apoptosis in HL-60 leukemic cells.

3.2 Syntheses of *N*-aroyl analogs of 3,5-bis(arylidene)-4-piperidones

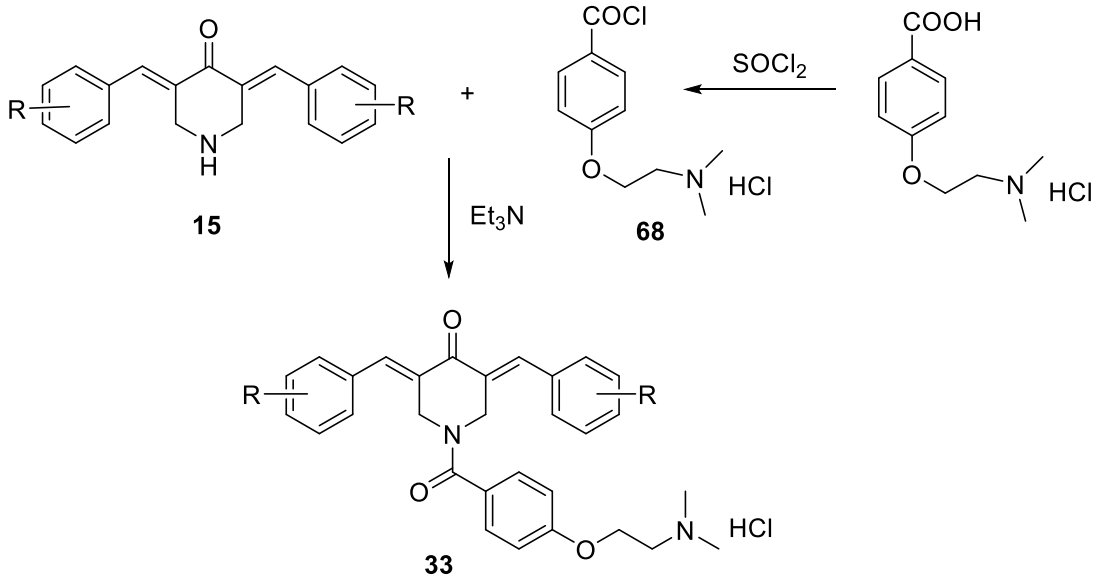

Scheme 3.1. Syntheses of *N*-aroyl analogs of 3,5-bis(arylidene)-4-piperidones.

Melting points were determined on a DigiMelt-MPA160 instrument and are uncorrected. ^{1}H NMR and ^{13}C NMR spectra were obtained using a Bruker 500 MHz spectrometer equipped with a BBO probe. Chemical shifts (δ) are reported in ppm. Mass spectra were obtained using a Jeol JMS-T100 GCv tof-gcV4G instrument.

3.2.1 General procedure for the synthesis of 3,5-bis(arylidene)-4-piperidones (15a-n)

The intermediate ketones **15a**-**n** were prepared by modifications of a literature procedure.[104] A mixture of an aryl aldehyde (11.5 mmol) and 4-piperidone hydrochloride monohydrate (5.60 mmol) in glacial acetic acid (15 mL) was stirred for 5 minutes. Dry hydrogen chloride gas was passed through the mixture for approximately 45 minutes and the reaction mixture was then stirred at room temperature for 24 hours. The resultant precipitate was collected by filtration and washed with a mixture of aqueous potassium carbonate solution (25 % w/v, 10

mL) and acetone (10 mL) and stirred at room temperature for 45 minutes. The product was collected by filtration, washed with ice cold water and dried. The compounds were taken for the reaction with the acid chloride **68**[81] without further purification. The melting points, yields and ^{1}H NMR spectra of **15a**-**m** are presented in the previous chapter. ^{1}H NMR spectroscopy revealed the presence of **15n** along with some impurities. The crude product was pure enough to carry forward to the next step in the synthesis of **33n**.

3.2.2 General procedure for the synthesis of *N*-aroyl analogs of 3,5-bis(arylidene)-4-piperidones (33a-n)

4-(2-Dimethylaminoethyl)benzoic acid hydrochloride (4.8 mmol) prepared by a literature method[81] was treated with thionyl chloride (10 mL) and heated under reflux for 4 hours. Excess thionyl chloride was evaporated under inert conditions to produce the crude acid chloride **68** which was used without further purification. This compound was dissolved in 1,2-dichloroethane (10 mL) and added slowly to a mixture of the appropriate 3,5-bis(benzylidene)-4-piperidones (3.21 mmol) and trimethylamine (1.6 mL, 12 mmol) in 1,2-dichloroethane (10 mL). During the addition process, the external temperature was maintained at 10 °C. After the addition of the acid chloride, the reaction mixture was stirred at room temperature overnight. Removal of the solvent by evaporation afforded a residue which was stirred with aqueous potassium carbonate solution (10 % w/v) for 5 hours. The resultant solid was collected by filtration, vacuum dried and crystallized from mixtures of chloroform and 2-propanol (**33a**-**g**, **n**), chloroform and ethanol (**33h**-**l**) and hexane and ethanol (**33m**).

3.3 Analytical data

*3.3.1. 1-[4-(2-dimethylaminoethoxy)benzoyl-3,5-bis(2-methoxybenzylidene)-4-piperidone hydrochloride (**33a**)*

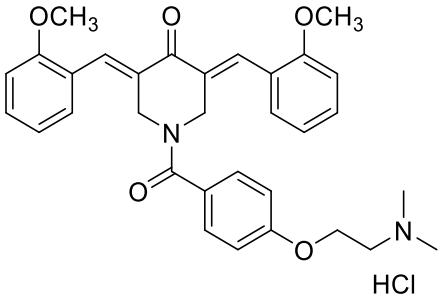

Yield: 69%; mp: 236 °C (dec.); ^{1}H NMR (500 MHz, DMSO-d_6) δ ppm 2.82 (s, 6 H) 3.47 (br s, 2 H) 3.88 (s, 6 H) 4.25 (t, *J*=4.9 Hz, 2 H) 4.73 (br s, 4 H) 6.71 (d, *J*=8.8 Hz, 2 H) 7.01 (br s, 2 H) 7.05 - 7.15 (m, 4 H)7.16 (d, *J*=8.8 Hz, 2 H) 7.44 (br s, 2 H) 7.90 (br s, 2 H). ^{13}C NMR (125 MHz, DMSO-d_6) δ ppm 42.64, 54.97, 55.72, 62.36, 111.38, 113.15, 113.94, 120.26, 122.74, 127.26, 128.62, 130.16, 131.47, 132.19, 157.98, 158.44, 168.67, 186.00. MS (FD) *m/z* found: 527.2483, calculated *m/z*: 527.2468.

*3.3.2. 1-[4-(2-dimethylaminoethoxy)benzoyl)-3,5-bis(3-methoxybenzylidene)-4-piperidone hydrochloride **(33b)***

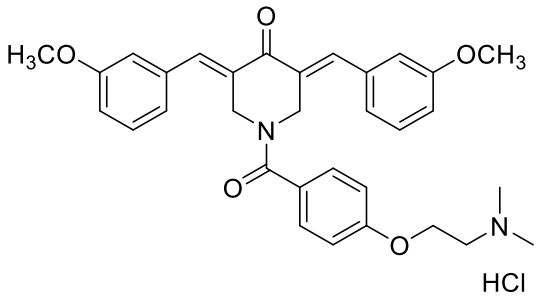

Yield: 87%; mp: 166 °C; ^{1}H NMR (500 MHz, DMSO-d_6) δ ppm 2.21, (s, 6 H) 2.60 (t, *J*=5.7 Hz, 2 H) 3.90 (s, 6 H) 3.95 (t, *J*=5.7 Hz, 2 H) 4.85 (br s, 4 H) 6.64 (d, *J*=8.6 Hz, 2 H) 7.00 (br s, 6 H) 7.14 (d, *J*=8.6 Hz, 2 H) 7.37 (br s, 2 H) 7.73 (s, 2 H). ^{13}C NMR (125 MHz, DMSO-d_6) δ ppm 45.38, 55.26, 57.36, 65.62, 113.80, 115.46, 122.55, 126.30, 128.79, 29.84, 132.76, 135.58, 159.31, 159.53, 169.01, 185.93. MS (FD) *m/z* found: 527.2453, calculated *m/z*: 527.2468.

3.3.3. 1-[4-(2-dimethylaminoethoxy)benzoyl)-3,5-bis(4-methoxybenzylidene)-4-piperidone hydrochloride ***(33c)***

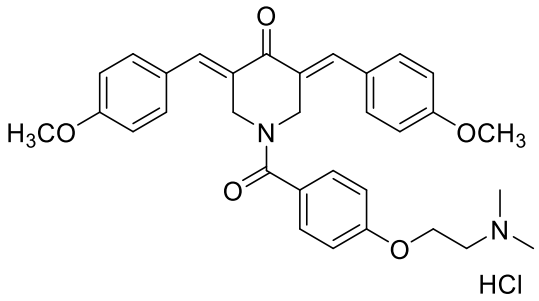

Yield: 88%; mp: 158 °C; ^{1}H NMR (500 MHz, DMSO-d_6) δ ppm 3.80 (s, 6 H) 3.96 (s, 4 H) 7.25 (d, *J*=8.8 Hz, 4 H) 7.44 (d, *J*=8.8 Hz, 4 H) 7.53 (s, 2 H). ^{13}C NMR (125 MHz, DMSO-d_6) δ ppm 45.47, 55.37, 57.45, 65.77, 113.76, 114.35, 126.27, 126.85, 128.76, 130.53, 159.56, 160.37, 168.84, 185.61. MS (FD) *m/z* found: 527.2464, calculated *m/z*: 527.2468.

3.3.4. 1-[4-(2-dimethylaminoethoxy)benzoyl)-3,5-bis(3,4-dimethoxybenzylidene)-4-piperidone hydrochloride ***(33d)***

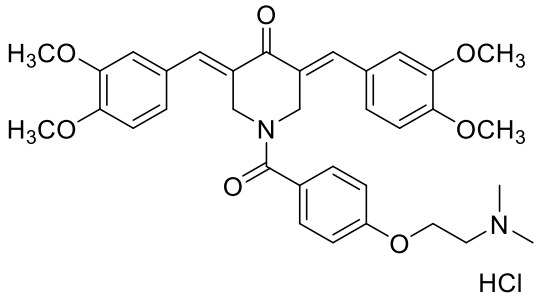

Yield: 52%; mp: 129 °C; ^{1}H NMR (500 MHz, DMSO-d_6) δ ppm 2.19 (s, 6 H) 2.57 (t, *J*=5.7 Hz, 2 H) 3.81 (s, 12 H) 3.94 (t, *J*=5.7 Hz,2 H) 4.85 (br s, 4 H) 6.69 (d, *J*=8.2 Hz, 2 H) 7.04 (br s, 6 H) 7.18 (d, *J*=8.5 Hz, 2 H) 7.71 (br s, 2 H). ^{13}C NMR (125 MHz, DMSO-d_6) δ ppm 45.50, 55.61, 55.62, 57.49, 65.78, 111.67, 113.82, 116.88, 124.07, 126.44, 128.81, 130.60, 148.60, 150.18, 159.59, 168.95, 185.56. MS (FD) *m/z* found: 587.2658, calculated *m/z*: 587.2679.

3.3.5. 1-[4-(2-dimethylaminoethoxy)benzoyl)-3,5-bis(2,5-dimethoxybenzylidene)-4-piperidone hydrochloride ***(33e)***

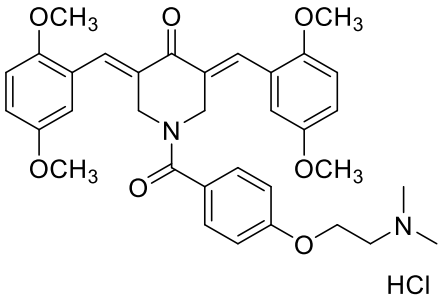

Yield: 57%; mp: 159 °C; ^{1}H NMR (500 MHz, DMSO-d_6) δ ppm 2.71 (s, 6 H) 3.38(t, *J*=5.2 Hz 2 H) 3.76 (s, 6 H) 3.82 (s, 6 H) 4.23 (t, *J*=5.3 Hz 2 H) 4.38 (br s, 4 H) 6.86 (d, *J*=2.2 Hz, 2 H) 6.94

- 6.97 (m, 2 H) 7.08 - 7.10 (m, 2 H) 7.76 - 7.79 (m, 2 H) 7.98 (s, 2 H) 9.38 (br s, 1 H). MS (FD) *m/z* found: 587.2687, calculated *m/z*: 587.2679.

3.3.6. 1-[4-(2-dimethylaminoethoxy)benzoyl)-3,5-bis(2,4,6-trimethoxybenzylidene)-4-piperidone hydrochloride ***(33f)***

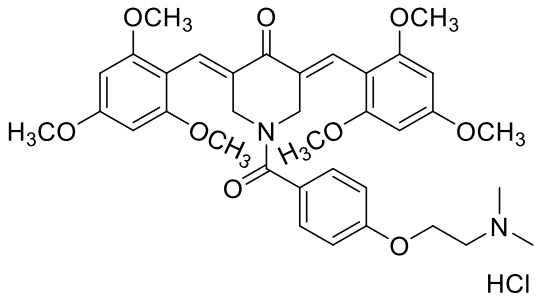

Yield: 86%; mp: 183 °C; ^{1}H NMR (500 MHz, DMSO-d_6) δ ppm 2.20 (s, 6 H) 2.58 (t, *J*=5.7 Hz, 2 H) 3.82 (s, 18 H) 3.94 (t, *J*=5.8 Hz, 2 H) 4.27 (br s, 4 H) 6.6 (d, *J*=8.2 Hz, 2 H) 7.02 (d, *J*=8.2 Hz, 2 H) 7.54 (br s, 2 H). MS (FD) *m/z* found: 647.2909, calculated *m/z*: 647.2890.

3.3.7. 1-[4-(2-dimethylaminoethoxy)benzoyl)-3,5-bis(3,4,5-trimethoxybenzylidene)-4-piperidone hydrochloride ***(33g)***

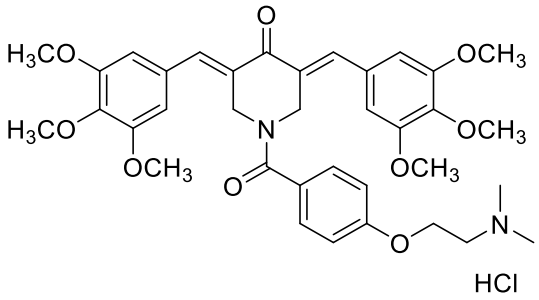

Yield: 69%; mp: 196 °C; ^{1}H NMR (500 MHz, DMSO-d_6) δ ppm 2.19 (s, 6 H) 2.57 (t, *J*=5.8 Hz, 2 H) 3.71 (s, 6 H) 3.79 (s, 12 H) 3.97 (t, *J*=5.8 Hz, 2 H) 4.93 (br s, 4 H) 6.72 (d, *J*=5.1 Hz, 2 H) 6.95

(br s, 4 H) 7.23 (d, *J*=5.4 Hz, 2 H) 7.69 (br s, 2 H). ^{13}C NMR (125 MHz, DMSO-d_6) δ ppm 45.51, 56.09, 57.52, 60.18, 65.81, 108.14, 113.82, 26.50, 128.92, 131.76, 138.84, 152.84, 159.66, 169.11, 185.76. MS (FD) *m/z* found: 647.2879, calculated *m/z*: 647.2890.

3.3.8. 1-[4-(2-dimethylaminoethoxy)benzoyl)-3,5-bis(benzo[d][1,3]dioxol-5-ylmethylene)-4-piperidone hydrochloride ***(33h)***

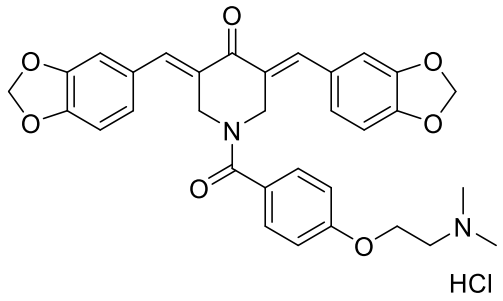

Yield: 89%; mp: 198 °C; ^{1}H NMR (500 MHz, DMSO-d_6) δ ppm 2.19 (s, 6 H) 2.56 - 2.61 (m, 2 H) 3.32 (s, 6 H) 3.96 (t, *J*=5.8 Hz, 2 H) 4.85 (br s, 4 H) 6.06 - 6.13 (m, 5 H) 6.66 - 6.71 (m, 2 H) 7.12 - 7.16 (m, 3 H) 7.65 (s, 2 H). ^{13}C NMR (125 MHz, DMSO-d_6) δ ppm 45.49, 55.12, 57.45, 65.82, 101.68, 108.66, 109.97, 113.26, 113.77, 126.33, 128.41, 128.74, 147.69, 148.52, 159.57, 168.96, 185.62. MS (FD) *m/z* found: 555.2044, calculated *m/z*: 555.2053.

3.3.9. 1-[4-(2-dimethylaminoethoxy)benzoyl)-3,5-bis(2-fluorobenzylidene)-4-piperidone hydrochloride ***(33i)***

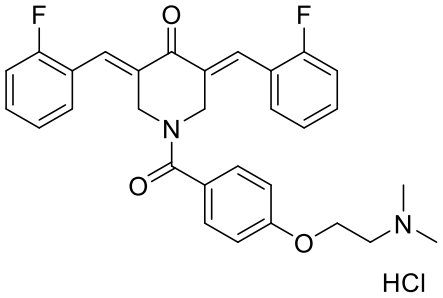

Yield: 79%; mp: 117 °C; ^{1}H NMR (500 MHz, DMSO-d_6) δ ppm 2.83 (s, 6 H) 3.52 (t, *J*=5.4 Hz, 2 H) 3.90 (s, 4 H) 4.41 - 4.46 (m, 2H) 7.07 - 7.10 (m, 2 H) 7.28 - 7.35 (m, 4 H) 7.43 - 7.52 (m, 4 H) 7.65 (s, 2 H) 7.90 - 7.94 (m, 2 H). ^{13}C NMR (125 MHz, DMSO-d_6) δ ppm 45.53, 55.16, 57.46, 65.84, 113.20, 113.72, 115.80, 115.97, 121.84, 121.94, 124.70, 126.13, 128.57, 128.82, 130.98, 131.95, 134.33, 159.58, 169.15, 185.42. MS (FD) *m/z* found: 503.2062, calculated *m/z*: 503.2068.

3.3.10. 1-[4-(2-dimethylaminoethoxy)benzoyl)-3,5-bis(3-fluorobenzylidene)-4-piperidone hydrochloride ***(33j)***

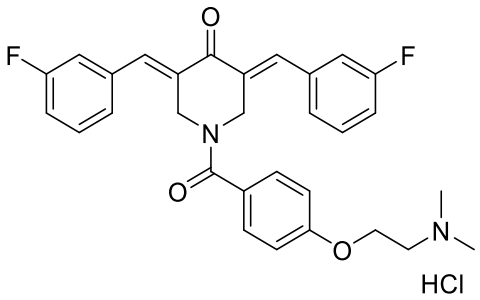

Yield: 66%; mp: 136 °C; ^{1}H NMR (500 MHz, DMSO-d_6) δ ppm 2.14 (s, 6 H) 2.59 (t, *J*=5.4 Hz, 2 H) 3.94 (t, *J*=5.5 Hz, 2 H) 4.85 (br s, 4 H) 6.65 (d, *J*=8.5 Hz, 2 H) 6.78 - 6.94 (m, 2 H) 6.94 - 7.10

(m, 4 H) 7.14 (d, *J*=8.5 Hz, 2 H) 7.37 (d, *J*=6.6 Hz, 2 H) 7.73 (br s, 2 H). ^{13}C NMR (125 MHz, DMSO-d_6) δ ppm 45.48, 55.26, 57.43, 65.75, 113.79, 115.47, 126.26, 128.78, 129.83, 132.76, 135.58, 159.31, 159.57, 169.02, 185.94. MS (FD) *m/z* found: 503.2064, calculated *m/z*: 503.2068.

3.3.11. 1-[4-(2-dimethylaminoethoxy)benzoyl)-3,5-bis(4-fluorobenzylidene)-4-piperidone hydrochloride ***(33k)***

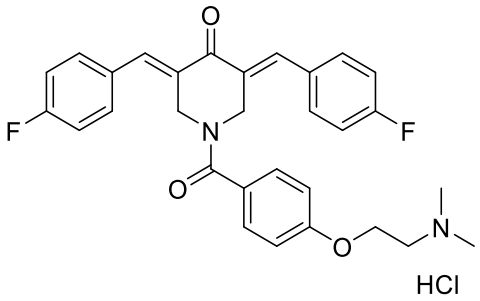

Yield: 84%; mp: 149 °C; ^{1}H NMR (500 MHz, DMSO-d_6) δ ppm 2.21 (s, 6 H) 2.60 (t, *J*=5.7 Hz, 2 H) 3.93 (t, *J*=5.8 Hz, 2 H) 4.83 (br s, 4 H) 6.64 (d, *J*=8.8 Hz, 2 H) 7.02 (br s, 4 H) 7.13 (d, *J*=8.5 Hz, 2 H) 7.31-7.34 (br s, 4 H) 7.71 (s, 2 H). ^{13}C NMR (125 MHz, DMSO-d_6) δ ppm 39.02, 39.19, 39.35, 39.68, 39.85, 40.02, 45.29, 55.36, 57.29, 65.53, 113.77, 114.34, 126.32, 126.85, 128.76, 159.49, 160.36, 168.82, 185.60. MS (FD) *m/z* found: 503.2089, calculated *m/z*: 503.2068.

3.3.12. 1-[4-(2-dimethylaminoethoxy)benzoyl)-3,5-bis(3,4-difluorobenzylidene)-4-piperidone hydrochloride ***(33l)***

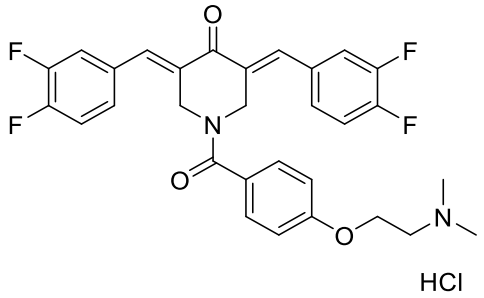

Yield: 72%; mp: 178 °C; ^{1}H NMR (500 MHz, DMSO-d_6) δ ppm 2.18 (s, 6 H) 2.57 (t, *J*=5.5 Hz, 2 H) 3.94 (t, *J*=5.8 Hz, 2 H) 4.82 (br s, 4 H) 6.66 (d, *J*=8.5 Hz, 2 H) 7.11 (d, *J*=8.5 Hz, 2 H) 7.53 (br s, 6 H) 7.69 (br s, 2 H). ^{13}C NMR (125 MHz, DMSO-d_6) δ ppm 45.44, 57.42, 65.78, 113.74, 126.21, 128.63, 131.84, 133.37, 159.58, 169.30, 185.81. MS (FD) *m/z* found: 539.1898, calculated *m/z*: 539.1880.

3.3.13. 1-[4-(2-dimethylaminoethoxy)benzoyl)-3,5-bis(2,6-difluorobenzylidene)-4-piperidone hydrochloride ***(33m)***

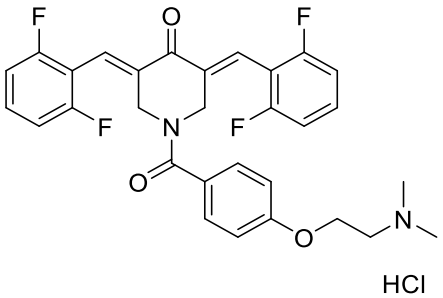

Yield: 71%; mp: 127 °C; ^{1}H NMR (500 MHz, DMSO-d_6) δ ppm 2.21 (S, 6 H) 2.59 (t, *J*=5.7 Hz, 2 H) 3.93 (t, *J*=5.7 Hz, 2 H) 4.47 (br s, 4 H) 6.61 (d, *J*=8.8 Hz, 2 H) 7.06 (d, *J*=8.8 Hz, 2 H) 7.22

(br s, 4 H) 7.52 (br s, 4 H). ^{13}C NMR (125 MHz, DMSO-d_6) δ ppm 45.47, 57.42, 65.80, 111.94, 112.13, 113.62, 126.17, 128.31, 136.73, 158.53, 159.52, 160.52, 169.31, 184.69. MS (FD) *m/z* found: 539.1868, calculated *m/z*: 539.1880.

3.3.14. 1-[4-(2-dimethylaminoethoxy)benzoyl-3,5-bis(2,5-difluorobenzylidene)-4-piperidone hydrochloride ***(33n)***

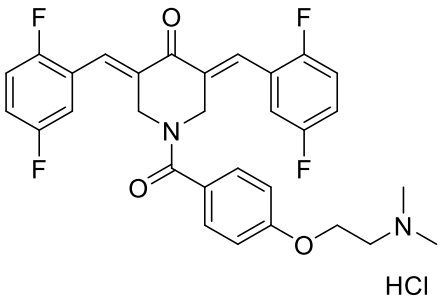

Yield: 74%; mp: 138 °C; ^{1}H NMR (500 MHz, DMSO-d_6) δ ppm 2.23 (s, 6 H) 2.63 (t, *J*=5.5 Hz, 2 H) 3.96 (t, *J*=5.7 Hz, 2 H) 6.67 (d, *J*=8.5 Hz, 2 H) 7.12 (d, *J*=8.5 Hz, 2 H) 7.39 (br s, 6 H) 7.66 (br s, 2 H). ^{13}C NMR (125 MHz, DMSO-d_6) δ ppm 45.36, 49.62, 57.33, 65.65, 113.74, 116.94, 117.14, 126.19, 128.56, 128.71, 135.25, 156.84, 159.56, 169.42, 185.33. MS (FD) *m/z* found: 539.1902, calculated *m/z*: 539.1880.

3.4 Biological results

Table 3.1. Evaluation of **33, 33a-n** against four human tumour cell lines

Compound		Human tumour cell lines, CC_{50} (μM)[a]									
	R	Ca9-22	SI[b]	HSC-2	SI[b]	HSC-3	SI[b]	HSC-4	SI[b]	Avg CC_{50}	Avg SI
33	H	0.26 ± 0.12	40.4	0.45 ± 0.09	23.3	1.00 ± 0.09	10.5	0.07 ± 0.04	150	0.45 ± 0.40	56.1
33a	2-OCH_3	0.10 ± 0.06	57.0	0.20 ± 0.00	22.8	0.27 ± 0.01	21.1	0.06 ± 0.02	95.0	0.17 ± 0.10	49.0
33b	3-OCH_3	0.21 ± 0.02	29.6	0.27 ± 0.03	23.0	0.64 ± 0.23	9.72	0.02 ± 0.01	311	0.29 ± 0.26	93.3
33c	4-OCH_3	0.63 ± 0.05	14.1	1.66 ± 0.10	5.36	1.49 ± 0.26	5.97	0.40 ± 0.10	22.3	1.05 ± 0.62	11.9
33d	3,4-$(OCH_3)_2$	0.24 ± 0.04	31.2	0.85 ± 0.03	8.80	0.74 ± 0.02	10.1	0.15 ± 0.02	49.9	0.49 ± 0.35	25.0
33e	2,5-$(OCH_3)_2$	0.12 ± 0.05	22.3	0.24 ± 0.03	11.1	0.22 ± 0.03	12.1	0.41 ± 0.11	6.51	0.25 ± 0.12	13.0
33f	2,4,6-$(OCH_3)_3$	6.70 ± 0.46	3.09	15.6 ± 1.50	1.33	6.15 ± 0.60	3.37	11.8 ± 4.99	1.75	10.1 ± 4.49	2.39
33g	3,4,5-$(OCH_3)_3$	0.02 ± 0.00	75.5	0.07 ± 0.02	21.6	0.03 ± 0.00	50.3	0.04 ± 0.01	37.8	0.04 ± 0.02	46.3
33h	3,4-OCH_2O	0.56 ± 0.08	18.0	0.76 ± 0.48	13.3	1.37 ± 0.42	7.37	0.41 ± 0.09	24.6	0.77 ± 0.42	15.8
33i	2-F	0.20 ± 0.02	28.6	0.46 ± 0.08	12.4	0.70 ± 0.03	8.16	0.07 ± 0.03	81.6	0.36 ± 0.28	32.7
33j	3-F	0.32 ± 0.09	20.9	0.75 ± 0.36	8.92	1.03 ± 0.29	6.50	0.07 ± 0.02	95.6	0.54 ± 0.43	33.0
33k	4-F	1.12 ± 0.57	13.5	1.64 ± 0.37	9.45	2.25 ± 0.22	6.89	0.49 ± 0.16	31.6	1.38 ± 0.75	15.4
33l	3,4-F_2	0.09 ± 0.04	60.0	0.37 ± 0.11	14.6	0.74 ± 0.11	7.30	0.08 ± 0.02	67.5	0.32 ± 0.31	37.4
33m	2,6-F_2	0.12 ± 0.04	56.7	0.28 ± 0.11	24.3	1.05 ± 0.30	6.48	0.14 ± 0.10	48.6	0.40 ± 0.44	34.0
33n	2,5-F_2	0.59 ± 0.06	29.8	0.81 ± 0.15	21.7	1.31 ± 0.56	13.4	0.15 ± 0.03	117	0.71 ± 0.48	45.5
Melphalan		38.7 ± 2.10	>4.88	13.0 ± 5.27	>14.5	13.3 ± 2.22	>14.2	17.1 ± 1.69	>11.1	20.5 ± 12.3	>11.2
5-Fluorouracil		19.2 ± 4.37	>51.2	>1000	>0.98	>1000	>0.98	>1000	>0.98	>755 - - -	>13.5
Methotrexate		>400	- - -	>400	- - -	0.44 ± 0.29	>909	33.7 ± 25.4	>11.9	>209 - - -	- - -
Doxorubicin		0.29 ± 0.04	>28.4	0.31 ± 0.39	>26.6	0.16 ± 0.06	>51.4	0.15 ± 0.09	>54.9	0.28 ± 0.08	>40.3

[a]The CC_{50} values are the concentrations of the compounds required to kill 50% of the cells. (Avg= Average).

[b]The SI figures refer to the selectivity indices which are computed by dividing the average CC_{50} figure for the nonmalignant cells by the CC_{50} value of a specific compound towards a tumour cell line.

Table 3.2. Evaluation of **33**, **33a-n** against HGF, HPLF, and HPC human normal cell lines

	Human normal cell lines, CC_{50} (μM)[a]				
Compound	HGF	HPLF	HPC	Average CC_{50}	PSE[b]
33	8.80 ± 0.30	13.1 ± 3.01	9.57 ± 3.85	10.5	12,467
33a	7.27 ± 0.15	7.70 ± 0.28	2.12 ± 0.48	5.70	28,824
33b	7.03 ± 0.95	8.88 ± 0.85	2.75 ± 0.54	6.22	32,172
33c	6.80 ± 0.10	14.6 ± 3.3	5.29 ± 0.53	8.90	1133
33d	7.83 ± 0.12	9.01 ± 0.31	5.61 ± 1.14	7.48	5000
33e	2.11 ± 0.02	2.45 ± 0.32	3.44 ± 0.51	2.67	5200
33f	20.2 ± 0.06	22.8 ± 0.32	19.0 ± 9.25	20.7	239
33g	2.09 ± 0.11	1.90 ± 0.09	0.55 ± 0.03	1.51	115,750
33h	7.79 ± 0.37	15.0 ± 2.85	7.48 ± 0.42	10.1	2026
33i	7.16 ± 0.06	6.46 ± 0.22	3.52 ± 1.01	5.71	9083
33j	7.53 ± 0.25	7.49 ± 0.19	5.06 ± 0.17	6.69	6111
33k	19.2 ± 0.67	20.1 ± 0.46	7.12 ± 0.28	15.5	1116
33l	6.63 ± 0.48	6.23 ± 0.50	3.33 ± 0.39	5.40	11,688
33m	7.59 ± 0.23	7.55 ± 0.13	5.25 ± 0.27	6.80	8500
33n	20.9 ± 1.33	21.2 ± 0.70	10.6 ± 0.49	17.6	6319
Melphalan	192 ± 13.3	>200 - - -	174 ± 10.7	>189	>54.6
5-Fluorouracil	>988 - - -	>1000 - - -	>961 - - -	>983	- - -
Methotrexate	>400 - - -	>400 - - -	>400 - - -	>400	- - -
Doxorubicin	6.00 ± 4.39	>10 - - -	8.69 ± 1.15	>8.23	>17,522

[a]The CC_{50} values are the concentrations of the compounds required to kill 50% of the cells.

[b]The potency selectivity expression (PSE) is the product of the reciprocal of the average CC_{50} value towards the four neoplastic cell lines and the average SI figures multiplied by 100.

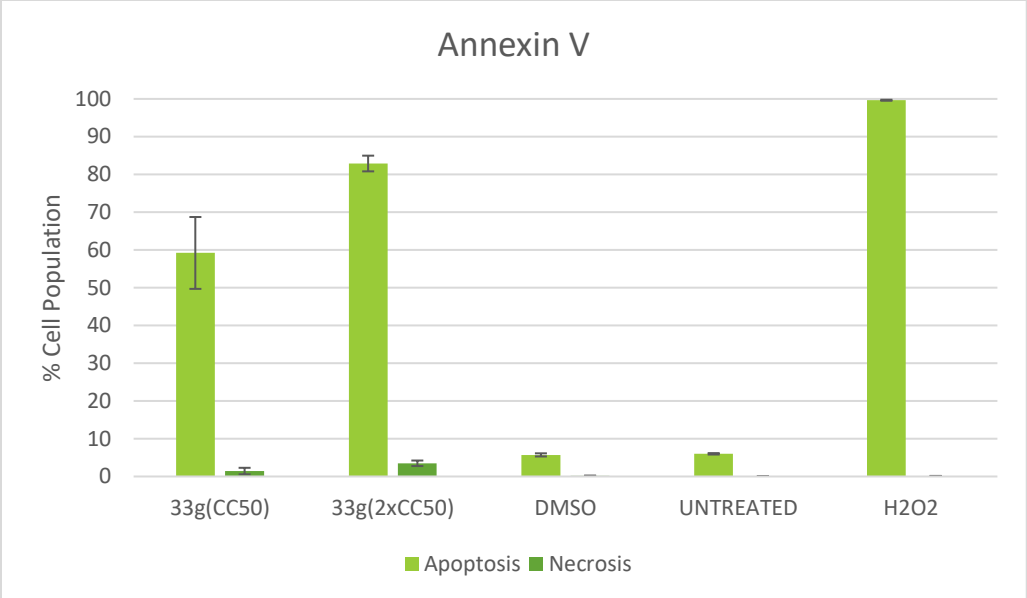

Figure 3.1. Apoptosis by **33g** in HL-60 cells.

3.4.1 Methodology

Methodology for determining the cytotoxic activity of 33, 33a-n towards Ca9-22, HSC-2, HSC-3, and HSC-4 tumour cells and HGF, HPLF and HPC human normal cells

The human oral tumor cell lines used are squamous carcinoma cells HSC-2, HSC-3, HSC-4 and Cellosaurus cell line Ca9-22. The human oral non-malignant cells employed are periodontal ligament fibroblasts (HPLF), gingival fibroblasts (HGF), and hematopoietic precursor cell HPC cells. All cells were cultured in DMEM medium which was supplemented with 10% heat-inactivated FBS. The human normal cells were obtained from periodontal tissues according to the "guidelines of the Meikai University Ethics Committee after obtaining the informed consent from the patient". All cells were incubated for 48 hours at 37 °C with 5% CO_2 at various concentrations of the test samples, and the relative viable cell number was then determined by the MTT assay method and is expressed as the absorbance at 540 nm of the cell lysate. The 50% cytotoxic

concentration (CC_{50}) was determined from a dose-response curve.[208] The bioevaluations data for the compounds **33** series in Table 3.1 and Table 3.2 are generated at Meikai University Research Institute of Odontology, Japan.

Methodology for determining apoptosis in HL-60 cells

An annexin V-FITC Kit was used to determine phosphatidylserine externalization (Beckman Coulter, Miami, FL, USA). HL-60 Cells with ≥ 95% of viability were seeded at 100,000 cells in 1000 µL of growth media per well in 24-well plates. Then the cells were left overnight under cell culture conditions and then treated with 0.1% v/v DMSO as a vehicle and 1.6 mM H_2O_2 as a positive control. The untreated cells are used as negative controls. For compound treatment, the CC_{50} and 2 x CC_{50} values of the compounds were used. After 24 hours of incubation in the presence of the test compound, the cells were collected in cold flow cytometry tubes (5 mL tubes) and centrifuged at 1200 rpm for 5 minutes at 4 °C. The supernatant solution formed was removed and cells were gently resuspended with a mixture containing 100 µL of 1x binding, buffer, 1 µL of annexin V-FITC and 2.5 µL of propidium iodide (PI). The cells were incubated for another 15 minutes in ice cold conditions in the dark. After this incubation, 300 µL of 1x binding buffer was added to each tube and examined by flow cytometry (Cytomics FC 500, Beckman Coulter). FL1 and FL2 detectors were used to capture the signals emitted by FITC and PI. Cells positive for just FITC were considered as early apoptotic cells, whereas cells stained by PI alone indicate necrotic cells. The FITC and PI double positive cells represent late stages of apoptosis.[208] The data for the compound **33** series in Table 3.1 and apoptosis by **33g** in HL-60 cells are generated at Department of Biological Sciences and Border Biomedical Research Center, The University of Texas, El Paso, USA.

3.5 Discussion

The cytotoxic evaluation of compounds **33a-n** as well as **33** and four reference drugs against Ca9-22, HSC-2, HSC-3, and HSC-4 tumour cell lines is presented in Table 3.1. These biodata reveal that the compounds in series **33** are highly potent cytotoxins except **33f**. No less than 75% of the compounds in series **33** have CC_{50} values in the submicromolar range. If the CC_{50} value of **33f** is excluded from the consideration, then the figure rises to 81%. A particular objective of this investigation is to find compounds in series **33** with CC_{50} values below 0.1 μM towards the neoplastic cell lines. Six compounds achieved this criterion (cell line in parentheses) namely **33a** (HSC-4), **33b** (HSC-4), **33g** (Ca9-22, HSC-2, HSC-3, HSC-4), **33i** (HSC-4), **33j** (HSC-4) and **33l** (Ca9-22, HSC-4). Thus, 17% of the compounds in series **33** have CC_{50} values which are less than 0.1 μM.

Comparisons were made between compounds having methoxy and fluoro groups in which the substituents are located at the same position on the arylidene aryl rings. Thus **33a** (2-methoxy) was compared with **33i** (2-fluoro), **33b** (3-methoxy) with **33j** (3-fluoro) and **33c** (4-methoxy) with **33k** (4-fluoro). In each of these comparisons, the methoxy substituted compounds are found to have lower average CC_{50} values than the corresponding fluoro analogs. Due to the high standard deviations of the average CC_{50} figures, the differences in the average cytotoxic potencies are not statistically significant.

Compound **33** is a potent cytotoxin. Some of the following compounds with substituents on the arylidene aryl ring have lower CC_{50} values than **33** (bioassay in parentheses) namely **33g**, **l** (Ca9-22), **33a, b**, **e**, **g** (HSC-2) and **33a**, **b**, **d**, **e**, **g**, **i, l** (HSC-3). In addition **33a, b, g, i, j, l, m** are

equipotent with **33** towards HSC-4 cells. Thus the dienones **33** and **33a-n** differ in their toxicity to various neoplasms which may reflect the ability of these compounds to display greater toxicity to tumours than non-malignant cells. Hence the next phase of the investigation was to examine this possibility in more detail.

Tumour-selective toxicity is an important factor to consider when developing these compounds as cytotoxic agents. Consequently in order to investigate if these compounds in series **33** demonstrate tumour-selective toxicity, evaluation of these molecules against HGF, HPLF and HSC human non-malignant cells was considered. All compounds in series **33** were screened against these non-malignant cells and the data is presented in Table 3.2. The following compounds namely **33c** (HPLF), **33f** (HGF, HPLF, HPC), **33h** (HPLF), **33k** (HGF, HPLF) and **33n** (HGF, HPLF, HPC) have CC_{50} values greater than 10 μM (bioassay in parentheses). A similar trend was noticed with three compounds namely **15c, f** (HGF, HPLF, HPC), **15n** (HPC) in series **15** bearing the same aryl substituents as in **33c**, **33f** and **33n**. However, **15k** displayed toxicity towards non-malignant cells in contrast to **33k**. Hence, for further development of these compounds as cytotoxic agents, the aryl substituent pattern of **33c**, **f**, **h**, **k**, **n** should be taken into consideration in the design of new molecules in regard to reducing the toxicity to non-malignant cells and making the candidate cytotoxins more toxic to tumors.

Under clinical conditions, tumours are surrounded by a variety of non-malignant cells in the body. Protecting or reducing harm to non-malignant cells from cytotoxic agents in the development stage requires the identity of compounds which display greater toxicity to the neoplasms than the surrounding non-malignant cells. In order to evaluate if the compounds in series **33** demonstrate tumor-selective toxicity, the selectivity index (SI) values were generated. The SI figures are the

ratios of the average CC_{50} value of the compounds towards non-malignant HGF, HPLF and HPC cells and the CC_{50} figure of a compound against a specific neoplastic cell line. The SI figures are presented in Table 3.1. The following observations were made. All compounds in the series **33** have SI figures greater than one demonstrating that they displayed selective cytotoxicity towards the malignant cells. No less than 70% of the SI values are greater than ten indicating these are more tumor-selective and the highest average SI value was displayed by compound **33b** with a figure of 93.3. The compounds **33a**, **33g**, and **33n** displayed noteworthy average SI values of 49.0, 46.3 and 45.5 respectively. These compounds may be considered as valuable leads for further studies.

In view of the significant cytotoxic potency and tumor-selective toxicity of the compounds in series **33**, the decision was made to compare these results with that of established anticancer drugs. Four reference drugs were chosen from three different classes of anticancer drugs namely melphalan which is an alkylating agent, 5-fluorouracil and methotrexate are antimetabolites and doxorubicin is an antibiotic. The cytotoxicities of these four drugs towards neoplastic and non-malignant cells are presented in Tables 3.1 and 3.2.

The compounds **33a-n** are more potent than the reference drug melphalan except **33f,** which is equipotent with melphalan in the HSC-2 and HSC-4 bioassays while in the Ca9-22 and HSC-3, all compounds are more potent than melphalan. All the compounds in series **33** are more potent towards Ca9-22, HSC-2, HSC-3 and HSC-4 malignant cell lines than 5-fluorouracil. In another comparison, the compounds in series **33** are more cytotoxic than methotrexate towards Ca9-22 and HSC-2 cells. The compound **33g** is more potent than methotrexate while the compounds **33a**, **b**, **d**, **e**, **i**, and **l** are equipotent to methotrexate in the HSC-3 bioassay. The anticancer drug

doxorubicin displayed marked potencies towards Ca9-22, HSC-2, HSC-3 and HSC-4 malignant cells with an average CC_{50} value of 0.28 μM. The average CC_{50} figures for compounds **33a-n** are presented in Table 3.1 which reveals that compound **33g** is more cytotoxic than doxorubicin while the compounds **33a**, **b**, **d**, **e, h**, **i**, **j**, **l**, **m**, and **n** are equipotent with this established drug. The three reference drugs namely melphalan, 5-fluorouracil, and methotrexate display little toxicity to non-malignant cells except doxorubicin. In summary, the compounds in series **33** are much more potent than melphalan, 5-fluorouracil and methotrexate and in general are equipotent with doxorubicin.

There is a significant difference between the cytotoxic potencies of the structural isomers **33f** and **33g**. The average CC_{50} value of **33g** against four neoplastic cell lines is 0.04 μM and the average CC_{50} figure for **33f** against the same cells is 10.1 μM which is 253 times more potent than its corresponding isomer. Therefore, attempts were made to find some of the possible reasons for this observation which could be of assistance in future for developing this series of compounds. A previous X-ray crystallographic study of some 3,5-bis(benzylidene)-4-piperidones by Dimmock *et. al* revealed that non-bonding interactions occurred between one of the *ortho* protons in each of the aryl rings and the equatorial hydrogen atoms at the 2 and 6 positions of the piperidine ring[209] resulting in a lack of coplanarity of the aryl rings and the adjacent olefinic group. In the present situation, the presence of two ortho methoxy substituents in **33f** can cause larger interplanar angles between the aryl rings and the adjacent olefinic groups than in the case of **33g**, which could affect the cytotoxic activity. In future studies, interplanar angles can be determined and linear and semilogarithmic plots can be generated to investigate any correlations between the cytotoxic potencies and interplanar angles.

In addition to differences in shape, there are other possible reasons why **33f** and **33g** display such varied cytotoxic potencies towards human non-malignant cells. The first consideration is the electronic effects of the aryl substituents: These compounds were developed as thiol alkylators in which the olefinic carbon atoms react with the mercapto (-SH) groups of cellular constituents. The electronic properties of the aryl substituents are likely to affect the relative rates of reaction with cellular thiols. The combined Hammett (σ) and Taft (σ*) values of the arylidene aryl substituents are -0.71 for **33f** and -0.03 for **33g** suggesting that the lower negative charge in **33g** may contribute to its having lower CC_{50} values than **33f**. A second factor to consider is the steric effects. The enone **33g** has two *ortho* protons on each of the arylidene aryl rings whereas **33f** has two methoxy groups in *ortho* locations. These ortho methoxy groups could exert a steric hindrance to nucleophilic attack by cellular thiols. Third, the possibility exists that **33g** is much more effective than **33f** in causing apoptosis. In order to evaluate this hypothesis, HSC-2 cells were incubated with **33f** and **33g** and then subjected to a western blot analysis. The result reveals that **33g** induced apoptosis in HSC-2 cells at much lower concentrations than **33f** and thus making **33g** more potent. Finally the 3,4,5-trimethoxyphenyl group present in **33g** is also found in colchicine and hence **33g** but probably not **33f** could interact at the colchicine binding site in tubulin.[210]

Potencies and tumour-selective toxicities are two important properties that one should consider in evaluating cytotoxins. Hence, potency selective expression (PSE) values were generated in order to identify one or more lead compounds with these two desirable properties. PSE figures are the product of the reciprocal of the CC_{50} value multiplied by the SI figure times 100 [$PSE = (SI/CC_{50}) \times 100$]. The PSE values of series **33** are presented in Table 3.2. Five compounds namely **33, 33a**, **b, g**, and **l** have PSE figures of over 10,000 and are clearly lead molecules as shown by this

study. In particular, for the compound **33g** the PSE figure is outstanding and 484 times greater than the value for its structural isomer **33f**. The unsubstituted analog **33** having a PSE figure of 12,467 displayed good cytotoxic potency and favourable SI values. This PSE figure for **33** is however less than the value of **33a**, **b**, **g** and doxorubicin.

An objective of this study is to make predictions regarding the design of future analogs with greater potencies and selective toxicities than **33a**-**n**. The aryl substituents on the arylidene rings of the compounds in series **33** might have an effect on potencies and selectivity indices as well. In order to investigate this, an attempt was made to determine whether the cytotoxic potencies (CC_{50}'s) and selectivity indices (SI) are related to one or more physicochemical properties of the aryl substituents. The physicochemical constants utilised are the Hammett sigma (σ) and Taft sigma star (σ*), Hansch pi (π) values and molar refractivity (MR) values of the aryl groups reflect the electronic, hydrophobic, and steric properties, respectively.[205,206] The general approach undertaken is as follows. A statistical analysis for correlations ($p<0.05$) and trends to a correlation ($p<0.1$) are considered initially with the CC_{50} values generated. Linear (l) and semilogarithmic plots (sl) were generated between the CC_{50} values of each of the four neoplastic cell lines (Ca9-22, HSC-2, HSC-3 and HSC-4) and the sigma/sigma star (σ/σ*), pi (π) and molecular refractivity (MR) values of the aryl substituents. Also plots are generated with the average CC_{50} values of the compounds against all four cell lines and physicochemical parameters. This process was repeated using the SI values, i.e., the physicochemical constants were plotted against the SI figures of four individual cell lines and also the average SI values.

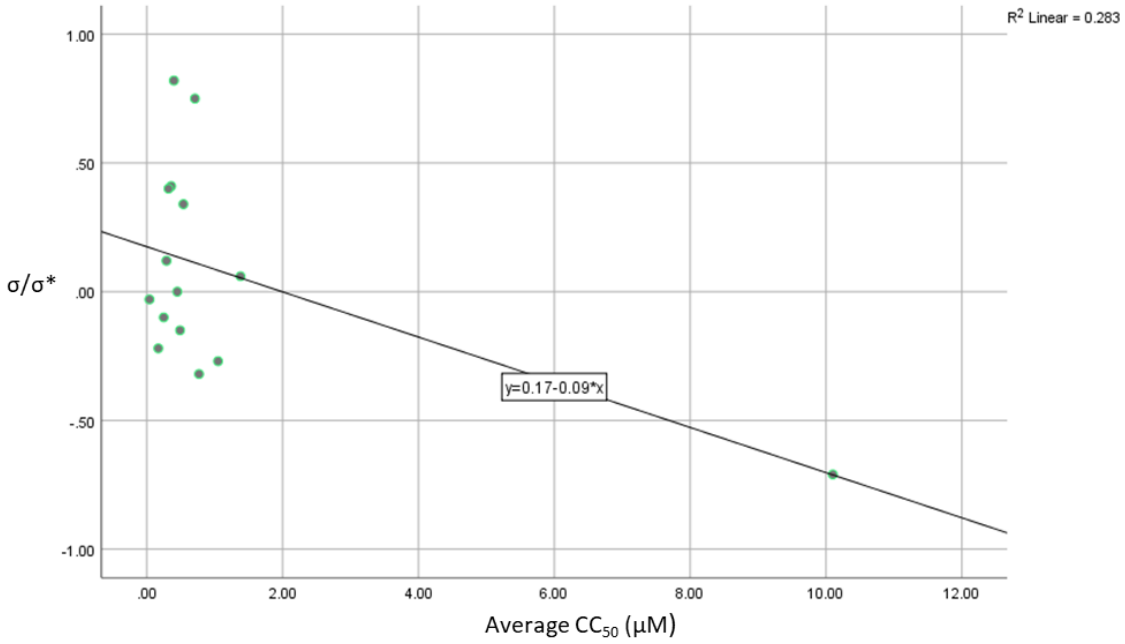

Plot 3.1. Linear plot between the average CC_{50} values of series **33** towards the four neoplastic cell lines and the sigma/sigma star (σ/σ*) values.

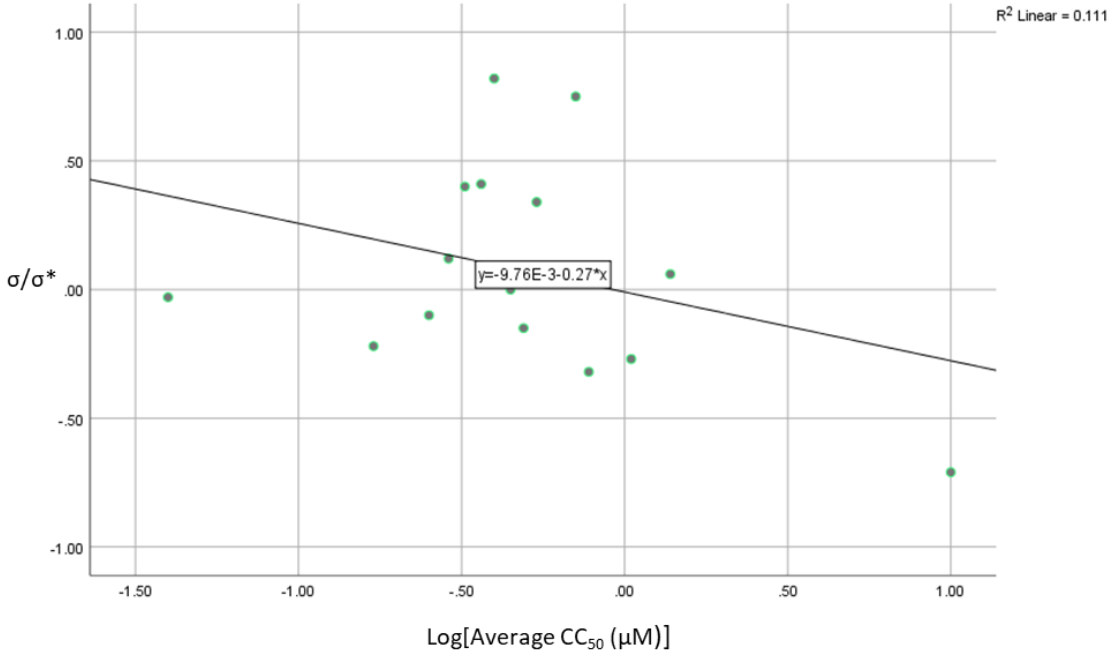

Plot 3.2. Semilogarithmic plot between the average CC_{50} values of series **33** towards the four neoplastic cell lines and the sigma/sigma star (σ/σ*) values.

The result generated from the plots between the σ/σ* values of the aryl substituent groups and the CC_{50} values of **33a-n** in the Ca9-22 (l), HSC-2 (l) and HSC-4 (l, sl) screens, indicates a negative correlation between CC_{50} figures and σ/σ*. This result reveal that the CC_{50} figures decrease (cytotoxic potencies increases) as the magnitude of the σ and σ* values increase. Therefore in the future design of new cytotoxic compounds, strongly electron attracting groups should be placed in the arylidene aryl rings. Also a negative correlation was noted when the σ/σ* constants were plotted against the average CC_{50} values (l). The plots generated between the π values of the arylidene aryl substituents of **33a-n** and the CC_{50} figures generated against the four neoplastic (Ca9-22, HSC-2, HSC-3 and HSC-4) cell lines did not reveal any correlations. When the plots between the π values and the average CC_{50} figures of **33a-n** were considered, no correlations were noted. There was a trend to a positive linear correlation ($p<0.1$) between the MR constants of the arylidene aryl rings of **33a-n** and the CC_{50} values in the HSC-2 and HSC-4 bioassays suggesting smaller aryl substituents may be favourable. No correlation was observed between the average CC_{50} figures of **33a-n** and the MR values ($p>0.10$).

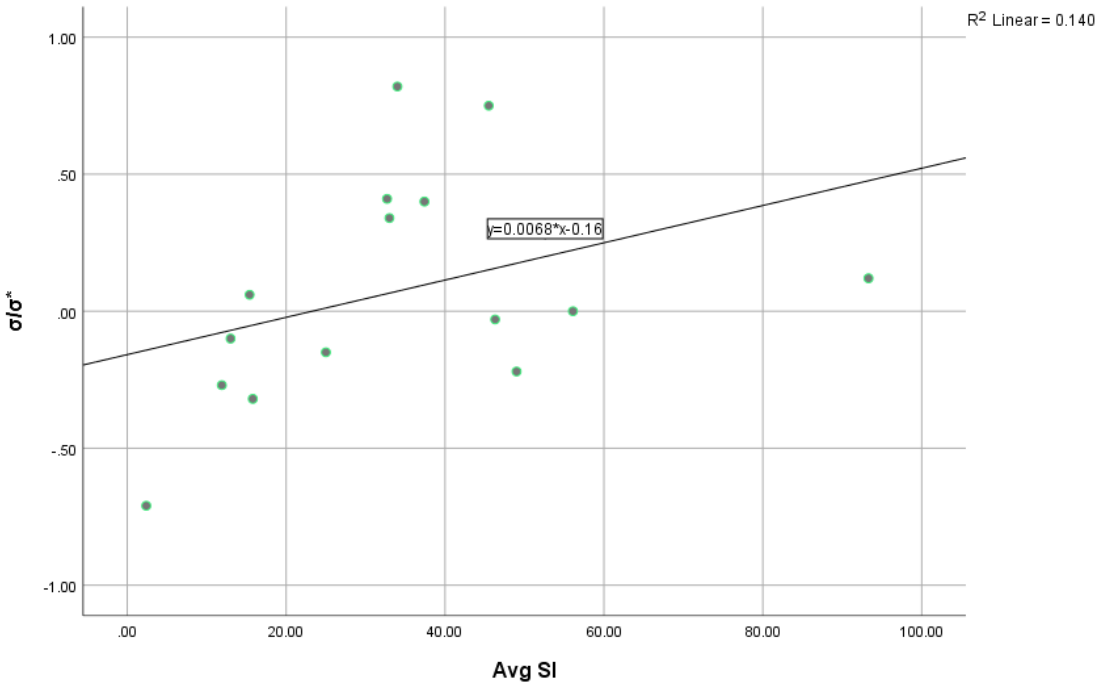

Plot 3.3. Linear plot between the average CC_{50} values and the average SI values of series **33** towards the four neoplastic cell lines.

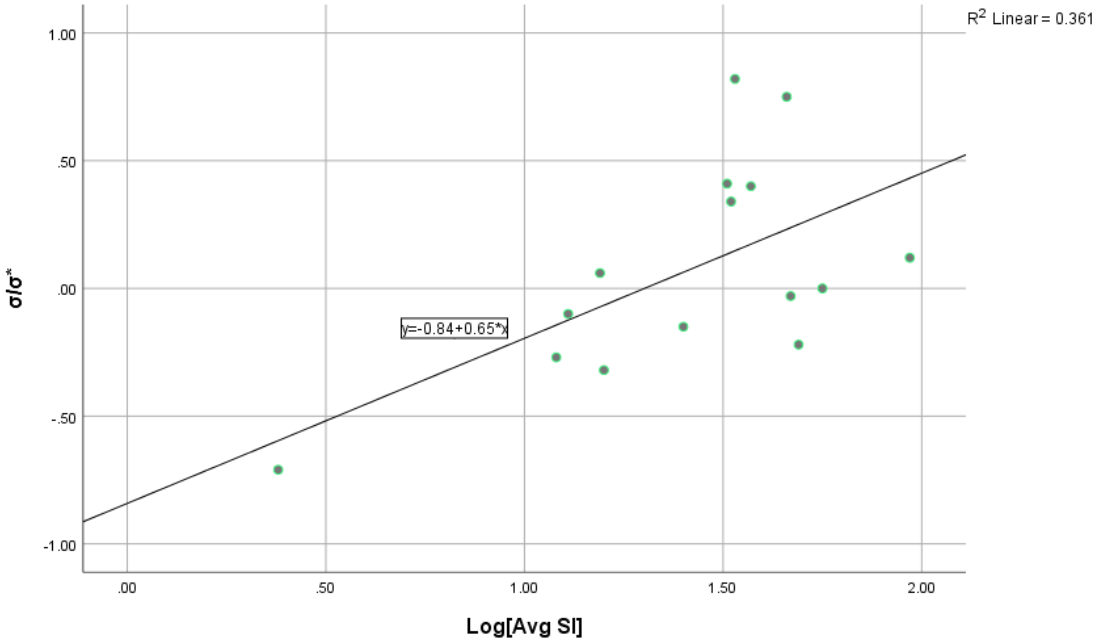

Plot 3.4. Semilogarithmic plot between the average CC_{50} values and the average SI values of series **33** towards the four neoplastic cell lines.

To seek further correlations, linear and semilogarithmic plots were made between the SI values for **33a-n** and the physicochemical constants (σ/σ*, π and MR). From semilogarithmic plots between the SI figures and the σ/σ* constants of **33a-n** in the Ca9-22, HSC-2 and HSC-4 bioassays, positive correlations ($p<0.05$) were observed. A positive correlation between the average SI values and the σ/σ* figures was also noted from a semilogarithmic plot. In addition, a positive correlation was observed between a linear plot of the σ/σ* values and the SI figures for HSC-2 cells. These results indicate that selective toxicity towards non-malignant cells rises as the σ/σ* values increase. From the linear and semilogarithmic plots, no correlations were noted between the π values and the SI figures generated in the Ca9-22, HSC-2, HSC-3 and HSC-4 screens nor the average SI figures for these four cells. Only one positive correlation was noted from a semilogarithmic plot between the SI values of **33a-n** against HSC-4 cells and MR values. No correlation was observed between the average SI values and the MR figures of the arylidene aryl substituents.

The conclusions to be drawn from the QSAR study are as follows. (1). The magnitude of the electronic properties of the arylidene aryl rings of **33a-n** has a profound influence on potencies while the π values have no discernable effects and the MR values exert only a marginal influence on cytotoxic potencies. (2). In the case of selective toxicities, the major correlation is that the electronic nature of the substituents in the arylidene aryl rings influences the selective toxicity (SI values which increase as the magnitude of the σ/σ*values are elevated) and the SI figures are influenced to a marginal extent by the relative sizes of the various substituent group

Chapter 4

4.1 Introduction

The two final series of compounds in this report, which are designated as series **70** and **71**, were prepared as having the potential to undergo deamination to produce compounds which have an additional centre for thiol alkylation. In addition, an oxime group is incorporated into the design of the molecules which will permit conversion to a variety of analogs which could deal with issues of solubility and chemical reactivity.

It was planned to evaluate the compounds in series **70** and **71** against neoplastic and non-malignant cell lines in probing for tumor-selective cytotoxins. In the case of series **71**, the possibility exists that these molecules will affect the mitochondrial membrane potential and the proposal was made to examine two members of series **71** for this property.

4.2 Synthesis of 4-piperidone-oxime

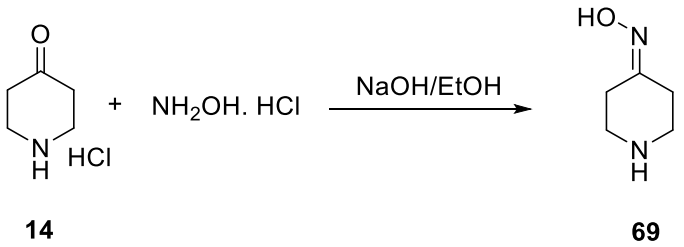

14 **69**

Scheme 4.1. Synthesis of 4-piperidone-oxime.

^{1}H NMR and ^{13}C NMR spectra were obtained using a Bruker 500 MHz spectrometer equipped with a BBO probe. Chemical shifts (δ) are reported in ppm. Melting points of the compounds were determined using a DigiMelt-MPA160 instrument and the mass spectra were obtained using a JEOL JMS-T100 GCv Accu tof-gcV4G spectrometer.

4.2.1 General procedure for the synthesis of 4-piperidone-oxime

To a mixture of hydroxylamine hydrochloride (6.79 g, 97.65 mmol) and 200 mL of ethanol, a solution of NaOH (7.81 g, 195.3 mmol) was added and stirred at room temperature for 15 minutes. To the resultant mixture, piperidin-4-one hydrochloride (**14**) (10 g, 65.1 mmol) was added and stirred at reflux temperature for 2 hours. The solvent was completely evaporated under reduced pressure, and the residue obtained was diluted with water (250 mL) and extracted with ethyl acetate (250 mL x3). The organic layer was separated, washed with water and brine and dried over anhydrous Na_2SO_4. The organic layer was concentrated to produce 4-piperidone-oxime (**69**).[211]

Yield: 52%; mp: 236 °C (dec.); ^{1}H NMR (500 MHz, DMSO-d_6) δ ppm 1.73 (s, 1 H) 2.07 - 2.11 (m, 2 H) 2.33 - 2.38 (m, 2 H) 2.68 (t, *J*=5.9 Hz, 2 H) 2.75 (t, *J*=5.9 Hz, 2 H).

4.3 Synthesis of oximes and quaternary salts

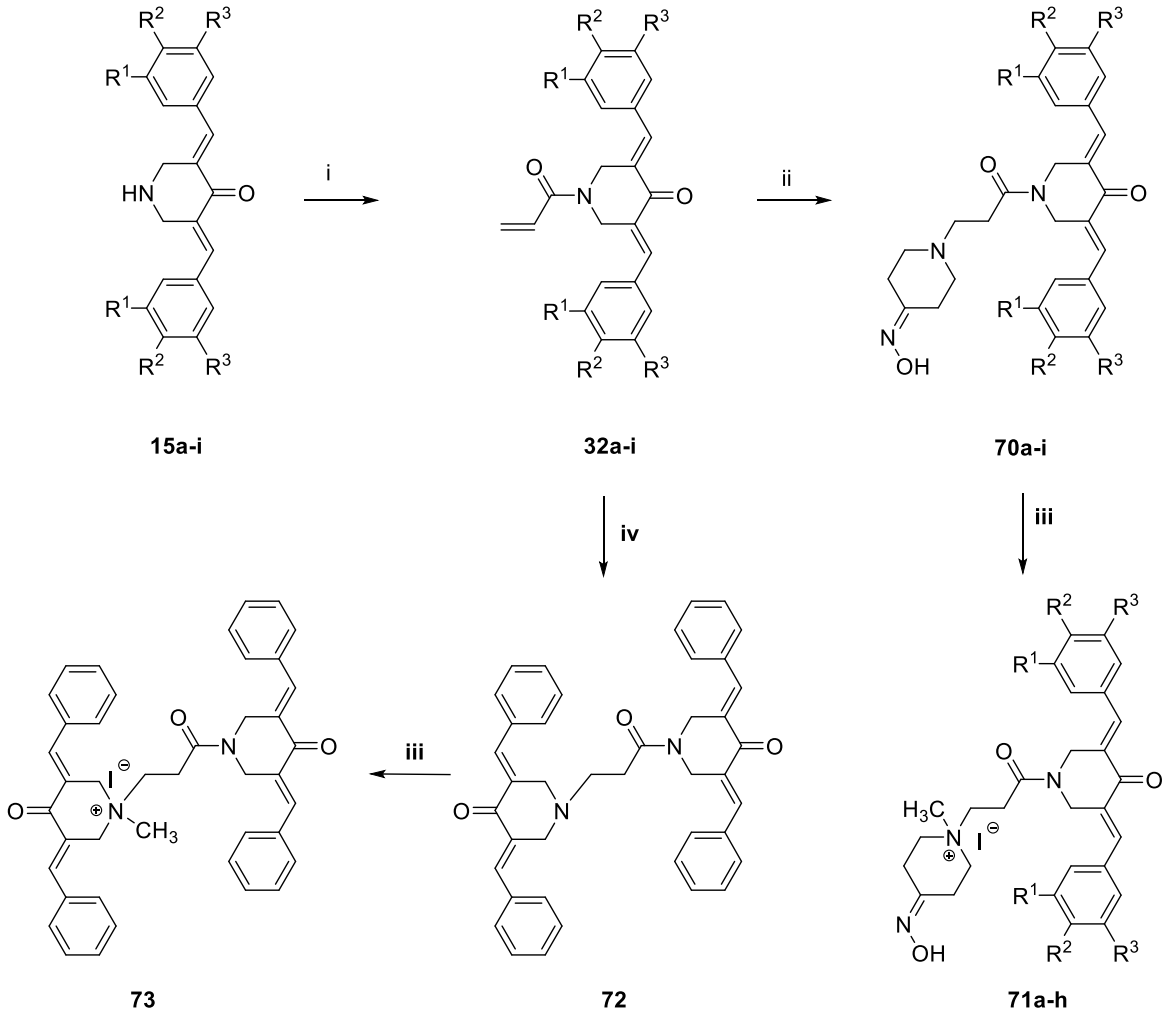

Reagents: i = acryloyl chloride, K_2CO_3; ii= piperidone-4-oxime, K_2CO_3; iii = CH_3I; iv = **15a**

Scheme 4.2. Syntheses of oximes and their corresponding quaternary salts including the dimeric compounds **72** and **73**.

4.3.1 Synthesis of compounds 32a-i

The 3,5-bis(benzylidene)-4-piperidones **15a-i** were prepared by a literature method[65] and their structures confirmed by ^{1}H NMR spectroscopy.

Acryloyl chloride (0.9 mL, 10.9 mmol) was added dropwise to a stirring mixture of 3,5-diarylidenepiperidin-4-ones (2.0g, 7.26 mmol), potassium carbonate (1.61g, 11.62 mmol) and acetone (15 mL) in an ice bath. The reaction continued for 24 hours at ambient temperature. After the starting material was completely consumed, the reaction mixture was poured into ice. The precipitate obtained was filtered and washed with water to afford the appropriate 1-acryloyl-3,5-bis(benzylidene)-4-piperidones **32a-i** as yellow solids. These compounds were identified using ^{1}H NMR and ^{13}C NMR spectroscopy as well as mass spectrometry.

4.3.2 Synthesis of compounds 70a-i

To a mixture of 4-piperidone-oxime (0.41 g, 3.64 mmol) and dry potassium carbonate (0.84 g, 6.07 mmol) in anhydrous tetrahydrofuran (10 mL), the appropriate 1-acryloyl-3,5-bis(benzylidene)-4-piperidone **32a-i** (1.0 g, 3.04 mmol) was added and stirred at reflux temperature for 24 hours. After the disappearance of the starting material, the solvent was completely evaporated and the residue obtained was washed with cold water. The obtained products **70a-i** were vacuum dried and recrystallized in ethanol. The compounds **70a-d**, **70f**, and **70g**, were dissolved in a mixture of chloroform (10 mL) and ethanol (10 mL) and converted into hydrochlorides by passing dry hydrogen chloride gas into the solution for 1 hour and evaporating the solvent under vacuum. The corresponding hydrochlorides were recrystallized in ethanol.

4.4 Analytical data

4.4.1. (3~{E},5~{E})-3,5-bis-benzylidine-1-[3-(4-Hydroximino-1-piperidyl)propanoyl]piperidin-4-one hydrochloride ***(70a)***

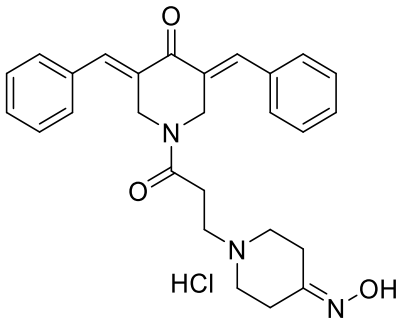

Yield: 88%; mp: 172.3 °C; ^{1}H NMR (500 MHz, DMSO-d_6) δ ppm 2.00 - 2.07 (m, 2 H) 2.09 - 2.16 (m, 2 H) 2.16 - 2.22 (m, 2 H) 2.27 - 2.35 (m, 4 H) 2.36 - 2.41 (m, 2 H) 3.33 (s, 4 H) 3.42 - 3.48 (m, 1 H) 4.81 - 4.88 (m, 4 H) 7.46 - 7.55 (m, 7 H) 7.56 - 7.59 (m, 4 H) 7.68 - 7.74 (m, 2 H) 10.25 (s, 1 H). ^{13}C NMR (125 MHz, DMSO- d_6) δ ppm 23.98, 30.93, 42.70, 46.24, 51.58, 52.98, 128.88, 129.63, 130.56, 132.69, 132.89, 134.16, 134.38, 135.93, 136.40, 154.37, 170.16, 186.22. MS (FD) *m/z* found: 444.2283, calculated *m/z*: 444.2209.

4.4.2. (3~{E},5~{E})-3,5-bis[(4-Fluorophenyl)methylene]-1-[3-(4-hydroximino-1-piperidyl)propanoyl]piperidin-4-one hydrochloride ***(70b)***

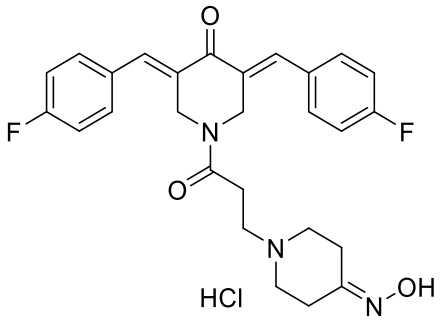

Yield: 84%; mp: 213.4 °C; ^{1}H NMR (500 MHz, DMSO-d_6) δ ppm 2.03 - 2.07 (m, 2 H) 2.15 (t, *J*=5.99 Hz, 2 H) 2.21 (t, *J*=5.9 Hz, 2 H) 2.29 - 2.36 (m, 4 H) 2.37 - 2.42 (m, 2 H) 4.82 (s, 4 H) 7.36 (t, *J*=8.8 Hz, 4 H) 7.65 (t, *J*=6.6 Hz, 4 H) 7.70 (s, 2 H) 10.26 (br s, 1 H). ^{13}C NMR (125 MHz, DMSO-d_6) δ ppm 23.95, 25.56, 30.25, 30.92, 42.54, 46.15, 51.66, 53.00, 53.03, 114.54, 115.84, 116.01, 130.73, 130.94, 132.45, 132.67, 132.97, 133.04, 134.83, 135.23, 154.19, 161.58, 163.56, 163.65, 170.20, 174.56, 186.15. MS (FD) *m/z* found: 480.2090, calculated *m/z*: 480.2020.

4.4.3. (3~{E},5~{E})-3,5-bis[(4-Chlorophenyl)methylene]-1-[3-(4-hydroximino-1-piperidyl)propanoyl]piperidin-4-one hydrochloride ***(70c)***

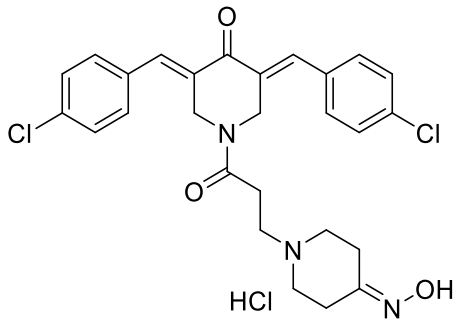

Yield: 79%; mp: 167.9 °C; ^{1}H NMR (500 MHz, DMSO-d_6) δ ppm 2.04 - 2.07 (m, 2 H) 2.15 (t, *J*=5.9 Hz, 2 H) 2.20 (t, *J*=5.9 Hz, 2 H) 2.30 - 2.35 (m, 4 H) 2.37 - 2.42 (m, 2 H) 4.81 (s, 4 H) 7.57 - 7.63 (m, 9 H) 7.68 (s, 2 H) 10.25 (s, 1 H). ^{13}C NMR (125 MHz, DMSO-d_6) δ ppm 42.71, 55.09, 62.30, 113.53, 114.04, 127.13, 128.78, 132.54, 158.50, 168.78, 185.92. MS (FD) *m/z* found: 512.1507, calculated *m/z*: 512.1429.

4.4.4. (3~{E},5~{E})-3,5-bis[(3,4-Dichlorophenyl)methylene]-1-[3-(4-hydroximino-1-piperidyl)propanoyl]piperidin-4-one hydrochloride ***(70d)***

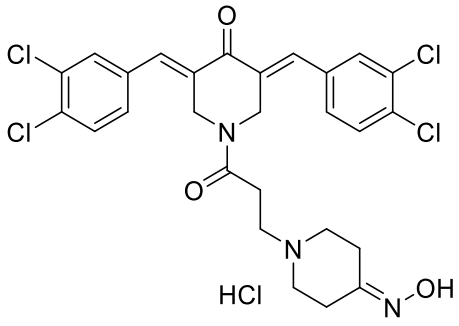

Yield: 82%; mp: 194.1 °C; ^{1}H NMR (500 MHz, DMSO-d_6) δ ppm 2.05 - 2.09 (m, 2 H) 2.18 (t, *J*=5.9 Hz, 2 H) 2.23 (t, *J*=5.9 Hz, 2 H) 2.31 - 2.37 (m, 4 H) 2.38 - 2.43 (m, 2 H) 4.80 (s, 4 H) 7.57 (dd, *J*=8.4, 1.9 Hz, 2 H) 7.66 (s, 2 H) 7.78 (d, *J*=8.4 Hz, 2 H) 7.89 (s, 2 H) 10.25 (s, 1 H). ^{13}C NMR (125 MHz, DMSO-d_6) δ ppm 23.98, 30.25, 30.93, 39.03, 42.44, 46.06, 51.72, 53.00, 53.04, 130.28, 130.91, 131.60, 131.62, 131.67, 132.16, 132.24, 133.66, 133.95, 134.18, 134.36, 134.82, 134.98, 154.27, 170.32, 185.96. MS (FD) *m/z* found: 580.0621, calculated *m/z*: 580.0650.

4.4.5. (3~{E},5~{E})-1-[3-(4-Hydroximino-1-piperidyl)propanoyl]-3,5-bis[(4-nitrophenyl)methylene]piperidin-4-one ***(70e)***

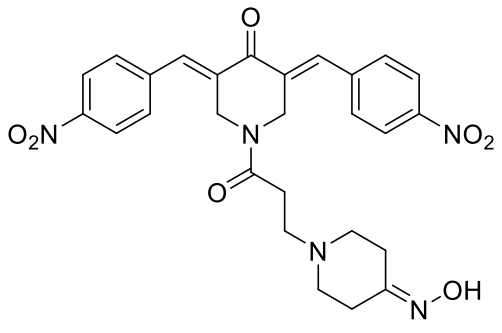

Yield; 72%; mp: 114.1 °C; ^{1}H NMR (500 MHz, DMSO-d_6) δ ppm 2.00 - 2.04 (m, 2 H) 2.12 - 2.17 (m, 2 H) 2.20 (t, *J*=5.9 Hz, 2 H) 2.28 (t, *J*=5.9 Hz, 2 H) 2.32 - 2.40 (m, 4 H) 4.87 (d, *J*=8.3 Hz, 4 H) 7.80 (s, 2 H) 7.86 (br s, 4 H) 8.34 (d, *J*=8.5 Hz, 4 H) 10.27 (s, 1 H). ^{13}C NMR (125 MHz, DMSO-d_6) δ ppm 18.59, 23.90, 30.20, 30.85, 42.50, 46.19, 51.73, 52.75, 52.93, 53.08, 53.20, 56.05, 109.58, 114.54, 123.79, 131.54, 131.68, 133.87, 134.15, 135.51, 135.63, 140.63, 140.78, 147.38, 154.26, 170.36, 186.11. MS (FD) *m/z* found: 533.1928, calculated *m/z*: 533.1910.

4.4.6. (3~{E},5~{E})-3,5-bis[(4-Methylphenyl)methylene]-1-[3-(4-hydroximino-1-piperidyl)propanoyl]piperidin-4-one hydrochloride ***(70f)***

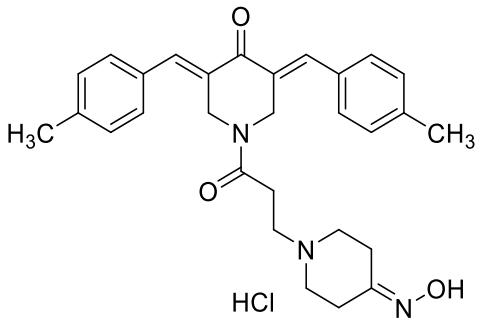

Yield: 91%; mp: 195.4 °C; ^{1}H NMR (500 MHz, DMSO-d_6) δ ppm 2.01 - 2.07 (m, 2 H) 2.10 (t, *J*=5.9 Hz, 2 H) 2.18 (t, *J*=5.9 Hz, 2 H) 2.27 - 2.34 (m, 4 H) 2.37 (br s, 2 H) 2.38 (s, 6 H) 4.82 (d, *J*=8.7 Hz, 4 H) 7.34 (d, *J*=8.0 Hz, 4 H) 7.47 (d, *J*=8.0 Hz, 4 H) 7.68 (s, 2 H) 10.25 (s, 1 H). ^{13}C NMR (125 MHz, DMSO-d_6) δ ppm 21.05, 23.96, 30.23, 30.93, 39.03, 42.80, 46.24, 51.50, 52.95, 52.98, 113.86, 129.49, 130.61, 130.68, 131.41, 131.65, 131.90, 132.14, 135.84, 136.41, 139.62, 139.65, 154.33, 170.08, 186.04. MS (FD) *m/z* found: 472.2589, calculated *m/z*: 472.2528.

4.4.7. (3~{E},5~{E})-3,5-bis[(4-Methoxyphenyl)methylene]-1-[3-(4-hydroximino-1-piperidyl)propanoyl]piperidin-4-one hydrochloride ***(70g)***

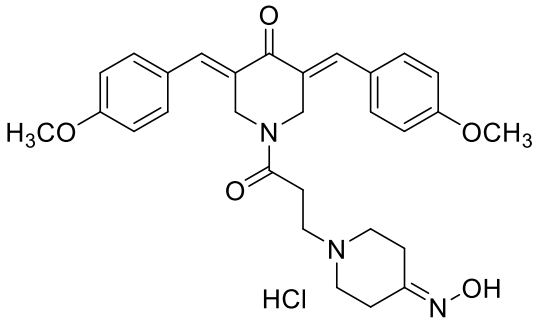

Yield: 74%; mp: 186.2 °C; ^{1}H NMR (500 MHz, DMSO-d_6) δ ppm 2.01 - 2.09 (m, 2 H) 2.14 (t, *J*=5.9 Hz, 2 H) 2.20 (t, *J*=5.9 Hz, 2 H) 2.26 - 2.32 (m, 2 H) 2.32 - 2.45 (m, 3 H) 3.84 (s, 6 H) 4.82 (d, *J*=6.4 Hz, 4 H) 7.08 (d, *J*=8.8 Hz, 4 H) 7.55 (d, *J*=8.8 Hz, 4 H) 7.66 (s, 2 H) 10.24 (s, 1 H). ^{13}C NMR (125 MHz, DMSO-d_6) δ ppm 20.87, 23.97, 30.34, 30.93, 42.37, 42.77, 46.29, 47.01, 51.59, 53.00, 53.05, 55.37, 114.41, 126.75, 127.01, 130.42, 130.58, 130.87, 132.59, 132.62, 135.58, 135.71, 135.96, 136.10, 154.36, 160.37, 168.63, 170.08, 185.82. MS (FD) m/z found: 504.2478, calculated *m/z*: 504.2420.

*4.4.8. (3~{E},5~{E})-1-[3-(4-Hydroximino-1-piperidyl)propanoyl]-3,5-bis[(3,4,5-trimethoxyphenyl)methylene]piperidin-4-one (**70h**)*

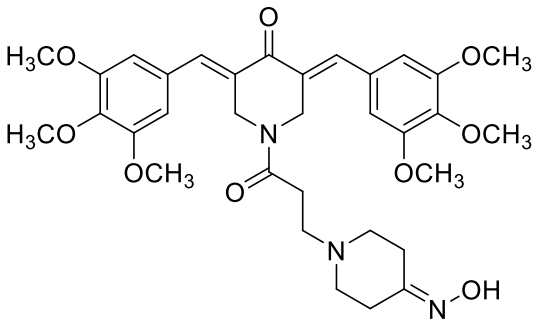

Yield: 71%: mp: 177.8 °C; ^{1}H NMR (500 MHz, DMSO-d_6) δ ppm 2.05 (t, *J*=5.87 Hz, 2 H) 2.18 (t, *J*=5.9 Hz, 2 H) 2.23 (t, *J*=5.9 Hz, 2 H) 2.30 - 2.33 (m, 2 H) 2.41 (s, 4 H) 3.74 (s, 6 H) 3.85 (d, *J*=5.6 Hz, 12 H) 4.88 (s, 4 H) 6.89 (s, 2 H) 6.87 (s, 2 H) 7.68 (s, 2 H) 10.24 (s, 1 H). ^{13}C NMR (125 MHz, DMSO-d_6) δ ppm 23.96, 30.47, 30.90, 42.62, 46.37, 51.66, 53.00, 56.08, 60.17, 108.10, 108.15, 129.71, 129.93, 131.99, 132.22, 136.41, 136.75, 138.79, 152.89, 154.28, 170.31, 185.99. MS (FD) *m/z* found: 623.2846, calculated *m/z*: 623.2843.

4.4.9. (3~{E},5~{E})-3,5-bis[(4-Hydroxyphenyl)methylene]-1-[3-(4-hydroximino-1-piperidyl)propanoyl]piperidin-4-one ***(70i)***

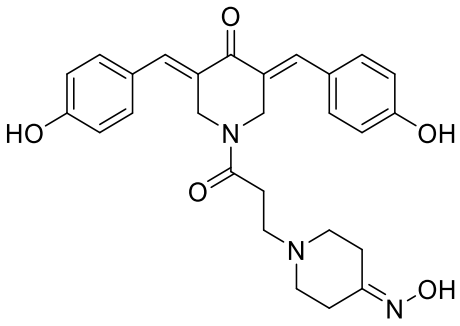

Yield: 68%; mp: 216.6 °C; ^{1}H NMR (500 MHz, DMSO-d_6) δ ppm 2.05 (t, *J*=5.9 Hz, 2 H) 2.17 (t, *J*=5.9 Hz, 2 H) 2.22 (t, *J*=5.7 Hz, 2 H) 2.29 - 2.33 (m, 2 H) 2.34 - 2.42 (m, 4 H) 4.80 (d, *J*=6.3 Hz, 4 H) 6.90 (d, *J*=8.5 Hz, 4 H) 7.43 (dd, *J*=8.0, 3.74 Hz, 4 H) 7.61 (s, 2 H) 10.13 (br. s., 1 H) 10.27 (s, 1 H). ^{13}C NMR (125 MHz, DMSO-d_6) δ ppm 24.00, 30.39, 30.93, 42.84, 46.32, 51.71, 53.05, 53.09, 115.82, 125.24, 125.55, 129.74, 130.01, 132.79, 132.89, 135.88, 136.40, 154.42, 159.08, 159.16, 170.08, 185.77. MS (FD) *m/z* found: 475.2189, calculated *m/z*: 475.2107.

4.5 Synthesis of compound 72

4.5.1. (3~{E},5~{E})-3,5-dibenzylidene-1-[3-[3~{E},5~{E})-3,5-dibenzylidene-4-oxo-1-piperidyl]-3-oxo-propyl]piperidin-4-one ***(72)***

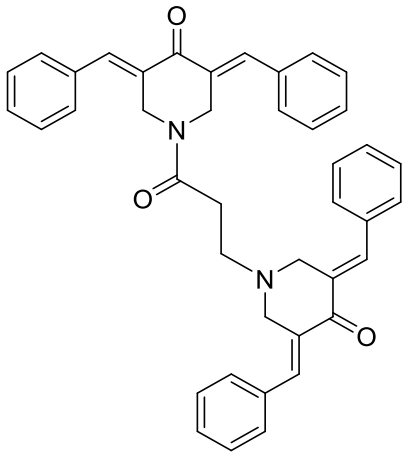

To a mixture of 3,5-bis(benzylidene)-4-piperidone **15a** (1.0 g, 3.64 mmol) and dry potassium carbonate (0.84 g, 6.07 mmol) in anhydrous tetrahydrofuran (10 mL), the appropriate 1-acryloyl-3,5-bis(benzylidene)-4-piperidone **32a** (1.0 g, 3.04 mmol) was added and stirred at reflux temperature for 24 hours. After the disappearance of the starting material, the solvent was completely evaporated and the residue obtained was washed with cold water. Compound **72** was vacuum dried and recrystallized in ethanol.

Yield: 91%; mp: 247 °C; ^{1}H NMR (500 MHz, DMSO-d_6) δ ppm 2.85 - 2.91 (m, 2 H) 3.06 (dd, *J*=13.2, 3.4 Hz, 2 H) 3.16 (dd, *J*=9.8, 5.0 Hz, 2 H) 3.63 - 3.68 (m, 2 H) 3.77 (d, *J*=12.1 Hz, 4 H) 3.89 - 3.94 (m, 2 H) 4.69 (d, *J*=15.9 Hz, 2 H) 4.87 (d, *J*=17.1 Hz, 2 H) 5.05 (d, *J*=16.2 Hz, 2 H) 5.22 (d, *J*=16.9 Hz, 2 H) 6.37 (s, 2 H) 6.43 (s, 2 H) 7.14 - 7.23 (m, 12 H) 7.31 - 7.40 (m, 10 H) 7.42 - 7.46 (m, 2 H) 7.50 (q, *J*=7.9 Hz, 8 H) 7.53 - 7.57 (m, 4 H) 7.60 (d, *J*=7.6 Hz, 4 H) 7.72 (s,

2 H) 7.68 (s, 2 H). ^{13}C NMR (125 MHz, DMSO-d_6) δ ppm 43.16, 45.72, 46.97, 52.11, 55.20, 55.91, 75.00, 117.23, 118.91, 126.05, 126.28, 128.40, 128.43, 128.47, 128.50, 128.75, 128.80, 129.44, 129.52, 130.45, 130.55, 132.91, 133.33, 134.40, 134.49, 135.48, 136.07, 136.86, 137.15, 141.92, 145.09, 170.59, 186.39. MS (FD) *m/z* found: 604.2734, calculated *m/z*: 604.2726.

4.6 Synthesis of compounds 71a-h, and 73

The appropriate compounds (free bases) in series **70** or **72** (1.13 mmol) was added to a solution of methyl iodide (0.24 g, 1.69 mmol) in chloroform (10 mL). The mixture was heated under reflux for 24 hours after which time the solvent was evaporated and **71a-h** and **73** were recrystallized from ethanol.

Attempts to synthesize compound **71i** were made following the general synthetic procedure as **71a-h** but were not successful. The colour of the reaction mixture turned dark during the reaction in contrast to other compounds and the TLC shown multiple spots. No alternate synthetic routes were tried due to the approaching timeline to finish the project. The synthetic study and bioevalutions of compound **71i** can be taken up for future work.

4.7 Analytical data

4.7.1. (3~{E},5~{E})-3,5-bis-benzylidine-1-[3-(4-Hydroximino-1-piperidyl)propanoyl]piperidin-4-one methiodide ***(71a)***

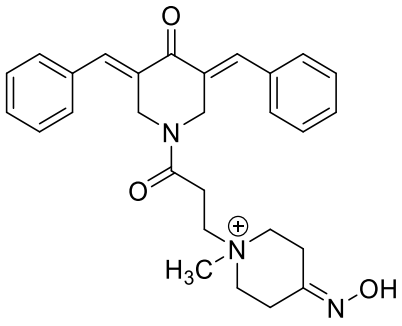

Yield: 81%; mp: 173 °C; ^{1}H NMR (500 MHz, DMSO-d_6) δ ppm 2.56 - 2.68 (m, 2 H) 2.86 - 2.92 (m, 1 H) 2.95 (t, *J*=7.7 Hz, 2 H) 3.02 (s, 3 H) 3.36 - 3.49 (m, 3 H) 3.59 (t, *J*=7.7 Hz, 2 H) 4.85 (br s, 2 H) 4.95 (br s, 2 H) 7.46 - 7.59 (m, 9 H) 7.64 (d, *J*=5.8 Hz, 2 H) 7.66 (br s, 1 H) 7.72 (s, 1 H) 10.94 (s, 1 H). ^{13}C NMR (125 MHz, DMSO-d_6) δ ppm 18.69, 24.79, 25.22, 41.85, 46.16, 58.05, 59.12, 59.16, 128.80, 128.93, 129.54, 129.68, 130.33, 130.84, 132.40, 132.56, 134.16, 134.24, 135.83, 136.29, 148.05, 167.51, 186.71. MS (FD) *m/z* found: 458.2461, calculated *m/z*: 458.2438.

4.7.2. (3~{E},5~{E})-3,5-bis[(4-Fluorophenyl)methylene]-1-[3-(4-hydroximino-1-piperidyl)propanoyl]piperidin-4-one methiodide ***(71b)***

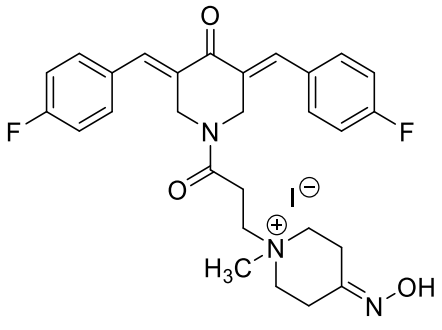

Yield: 86%; mp: 163 °C; ^{1}H NMR (500 MHz, DMSO-d_6) δ ppm 2.57 - 2.70 (m, 2 H) 2.90 (d, *J*=16.6 Hz, 1 H) 2.94 - 2.99 (m, 2 H) 3.04 (s, 3 H) 3.39 - 3.49 (m, 4 H) 3.60 (t, *J*=7.2 Hz, 2 H) 4.81 (br s, 2 H) 4.92 (br s, 2 H) 7.38 (d, *J*=8.5 Hz, 4 H) 7.64 (br s, 3 H) 7.72 (d, *J*=8.8 Hz, 3 H) 10.95 (s, 1 H). ^{13}C NMR (125 MHz, DMSO-d_6) δ ppm 18.73, 24.83, 25.25, 41.66, 46.17, 58.10, 59.15, 59.20, 113.84, 115.83, 115.93, 116.01, 116.10, 130.82, 130.85, 132.24, 132.74, 132.81, 133.35, 133.42, 134.73, 135.30, 148.13, 161.63, 163.61, 167.60, 186.60. MS (FD) *m/z* found: 494.2238, calculated *m/z*: 494.2250.

4.7.3. (3~{E},5~{E})-3,5-bis[(4-Chlorophenyl)methylene]-1-[3-(4-hydroximino-1-piperidyl)propanoyl]piperidin-4-one methiodide ***(71c)***

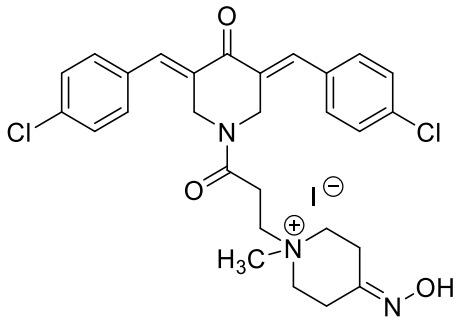

Yield: 89%; mp: 192 °C; ^{1}H NMR (500 MHz, DMSO-d_6) δ ppm 2.53 - 2.56 (m, 1 H) 2.57 - 2.69 (m, 2 H) 2.87 - 2.92 (m, 1 H) 2.95 (t, *J*=7.7 Hz, 2 H) 3.37 - 3.50 (m, 4 H) 3.59 (t, *J*=7.7 Hz, 2 H) 4.81 (s, 2 H) 4.92 (br s, 2 H) 7.57 - 7.65 (m, 7 H) 7.68 (d, *J*=8.8 Hz, 3 H) 10.95 (s, 1 H). ^{13}C NMR (125 MHz, DMSO-d_6) δ ppm 18.73, 24.83, 25.23, 41.70, 46.13, 58.10, 59.15, 59.20, 79.21, 114.16, 128.90, 128.97, 132.10, 132.64, 132.94, 133.08, 133.14, 134.30, 134.44, 134.60, 135.16, 148.14, 167.62, 186.51. MS (FD) *m/z* found: 526.1652, calculated *m/z*: 526.1659.

4.7.4. (3~{E},5~{E})-3,5-bis[(3,4-Dichlorophenyl)methylene]-1-[3-(4-hydroximino-1-piperidyl)propanoyl]piperidin-4-one methiodide ***(71d)***

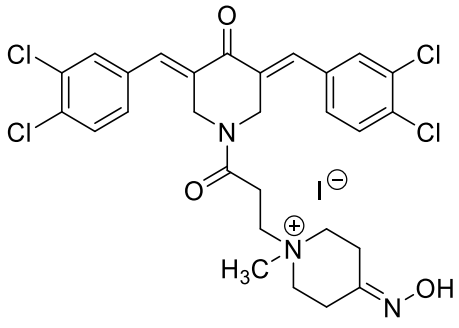

Yield: 88%; mp: 177.2 °C; ^{1}H NMR (500 MHz, DMSO-d_6) δ ppm 2.54 (d, *J*=5.7 Hz, 1 H) 2.58 - 2.70 (m, 2 H) 2.88 - 2.93 (m, 1 H) 2.96 (t, *J*=7.6 Hz, 2 H) 3.05 (s, 3 H) 3.37 - 3.50 (m, 4 H) 3.60 (t, *J*=7.6 Hz, 2 H) 4.79 (br s, 2 H) 4.92 (br s, 2 H) 7.57 (d, *J*=8.1 Hz, 1 H) 7.60 - 7.65 (m, 2 H) 7.67 (s, 1 H) 7.79 (dd, *J*=8.0, 2.40 Hz, 2 H) 7.90 (s, 1 H) 7.94 (s, 1 H) 10.95 (s, 1 H). ^{13}C NMR (125 MHz, DMSO-d_6) δ ppm 18.74, 24.83, 25.26, 41.69, 46.19, 58.10, 59.11, 59.20, 115.70, 130.17, 130.42, 130.98, 131.59, 131.67, 131.93, 132.13, 132.23, 132.58, 133.46, 133.86, 134.06, 134.19, 134.86, 134.92, 148.12, 167.72, 186.29. MS (FD) *m/z* found: 594.0859, calculated *m/z*: 594.0879.

4.7.5. (3~{E},5~{E})-1-[3-(4-Hydroximino-1-piperidyl)propanoyl]-3,5-bis[(4-nitrophenyl)methylene]piperidin-4-one methiodide ***(71e)***

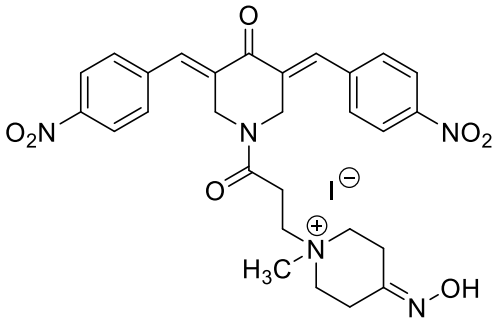

Yield: 77%; mp: 189.8 °C; ^{1}H NMR (500 MHz, DMSO-d_6) δ ppm 2.56 - 2.68 (m, 2 H) 2.89 (dt, *J*=16.8, 5.3 Hz, 1 H) 2.95 (t, *J*=7.7 Hz, 2 H) 3.02 (s, 3 H) 3.38 - 3.50 (m, 4 H) 3.58 (t, *J*=7.7 Hz, 2 H) 4.85 (br s, 2 H) 4.98 (br s, 2 H) 7.75 (br s, 1 H) 7.81 (br s, 1 H) 7.85 (d, *J*=8.5 Hz, 2 H) 7.92 (d, *J*=8.5 Hz, 2 H) 8.35 (d, *J*=7.3 Hz, 4 H) 10.94 (s, 1 H). ^{13}C NMR (125 MHz, DMSO-d_6) δ ppm 18.72, 24.80, 25.24, 41.72, 46.19, 58.10, 59.03, 59.20, 114.06, 123.81, 131.39, 131.87, 133.78, 134.34, 135.09, 135.46, 140.61, 140.75, 147.42, 148.12, 167.75, 186.43. MS (FD) *m/z* found: 548.2139, calculated *m/z*: 548.2145.

4.7.6. (3~{E},5~{E})-3,5-bis[(4-Methylphenyl)methylene]-1-[3-(4-hydroximino-1-piperidyl)propanoyl]piperidin-4-one methiodide ***(71f)***

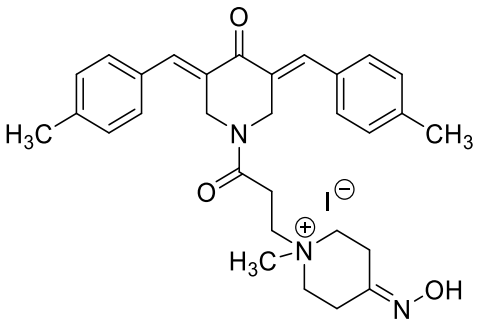

Yield: 95%; mp: 183.9 °C; ^{1}H NMR (500 MHz, DMSO-d_6) δ ppm 2.39 (d, *J*=6.8 Hz, 7 H) 2.56 - 2.67 (m, 2 H) 2.84 - 2.91 (m, 1 H) 2.92 - 2.96 (m, 2 H) 3.37 - 3.47 (m, 3 H) 3.59 (t, *J*=7.6 Hz, 2 H) 4.84 (s, 2 H) 4.92 (br s, 2 H) 7.32 - 7.36 (m, 5 H) 7.46 (d, *J*=8.0 Hz, 2 H) 7.55 (d, *J*=7.8 Hz, 2 H) 7.60 (s, 1 H) 7.68 (s, 1 H) 10.95 (s, 1 H). ^{13}C NMR (125 MHz, DMSO-d_6) δ ppm 18.72, 21.06, 24.82, 25.25, 41.95, 46.08, 46.26, 58.04, 59.17, 59.22, 113.83, 129.47, 129.60, 130.49, 131.00, 131.48, 131.53, 131.69, 131.74, 135.88, 136.28, 139.59, 139.77, 148.13, 167.51, 186.57. MS (FD) *m/z* found: 486.2744, calculated *m/z*: 486.2751.

4.7.7. (3~{E},5~{E})-3,5-bis[(4-Methoxyphenyl)methylene]-1-[3-(4-hydroximino-1-piperidyl)propanoyl]piperidin-4-one methiodide ***(71g)***

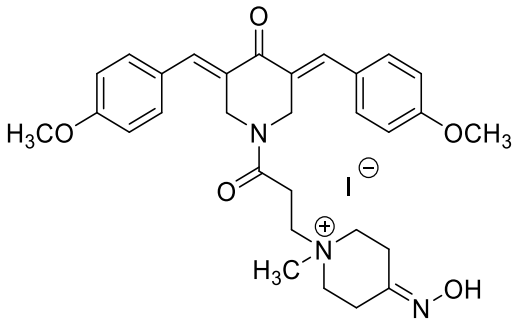

Yield: 81%; mp: 179.5 °C; ^{1}H NMR (500 MHz, DMSO-d_6) δ ppm 2.57 - 2.68 (m, 2 H) 2.87 - 2.94 (m, 1 H) 2.97 (t, *J*=7.5 Hz, 2 H) 3.04 (s, 3 H) 3.37 - 3.51 (m, 4 H) 3.61 (t, *J*=7.5 Hz, 2 H) 3.85 (s, 3 H) 3.84 (s, 3 H) 4.84 (br s, 2 H) 4.92 (br s, 2 H) 7.09 (t, *J*=7.5 Hz, 4 H) 7.54 (d, *J*=8.5 Hz, 2 H) 7.62 (s, 1 H) 7.59 (s, 1 H) 7.66 (s, 1 H) 7.64 (s, 1 H) 10.92 - 10.98 (m, 1 H). ^{13}C NMR (125 MHz, DMSO-d_6) δ ppm 18.74, 24.84, 25.32, 41.90, 46.13, 46.32, 55.41, 55.47, 58.09, 59.21, 59.25, 113.38, 114.40, 114.50, 126.87, 130.27, 130.39, 132.42, 133.03, 135.56, 136.02, 148.14, 160.34, 160.41, 167.47, 186.31. MS (FD) *m/z* found: 518.2676, calculated *m/z*: 518.2649.

4.7.8. (3~{E},5~{E})-1-[3-(4-Hydroximino-1-piperidyl)propanoyl]-3,5-bis[(3,4,5-trimethoxyphenyl)methylene]piperidin-4-one methiodide ***(71h)***

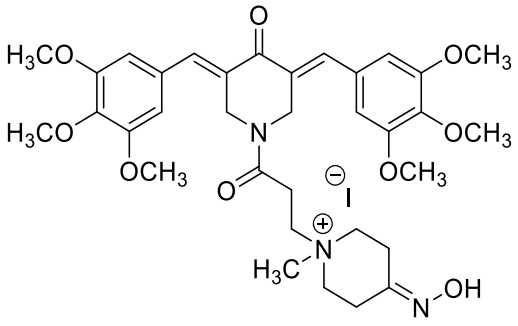

Yield: 79%; mp: 207 °C; ^{1}H NMR (500 MHz, DMSO-d_6) δ ppm 2.53 - 2.62 (m, 3 H) 2.62 - 2.70 (m, 2 H) 2.86 - 2.92 (m, 1 H) 2.99 (t, *J*=7.5 Hz, 2 H) 3.03 (s, 3 H) 3.39 - 3.48 (m, 4 H) 3.62 (t, *J*=7.5 Hz, 2 H) 3.74 (s, 6 H) 3.84 (s, 6 H) 3.88 (s, 6 H) 4.89 (s, 2 H) 4.98 (br s, 2 H) 6.91 (s, 2 H) 6.94 (s, 2 H) 7.62 (s, 1 H) 7.68 (s, 1 H) 10.95 (s, 1 H). ^{13}C NMR (125 MHz, DMSO-d_6) δ ppm 18.73, 24.82, 25.29, 46.30, 56.13, 58.12, 58.98, 59.22, 60.19, 108.03, 108.49, 113.56, 129.75, 129.82, 131.67, 138.86, 148.12, 152.91, 167.75, 186.42. MS (FD) *m/z* found: 638.3079, calculated *m/z*: 638.3072.

4.7.9. (3~{E},5~{E})-3,5-dibenzylidene-1-[3-[3~{E},5~{E})-3,5-dibenzylidene-4-oxo-1-piperidyl]-3-oxo-propyl]piperidin-4-one) methiodide ***(73)***

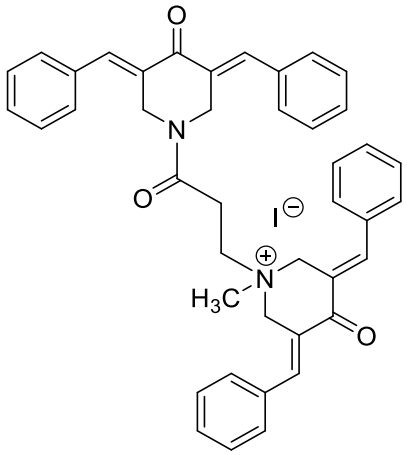

Yield: 89%; mp: 194 °C; ^{1}H NMR (500 MHz, DMSO-d_6) δ ppm 3.18 (d, *J*=5.3 Hz, 1 H) 3.23 (s, 3 H) 3.45 (qd, *J*=7.0, 5.12 Hz, 1 H) 3.57 (dd, *J*=10.1, 4.5 Hz, 1 H) 3.73 (t, *J*=10.6 Hz, 1 H) 3.81 - 3.87 (m, 1 H) 4.64 - 4.76 (m, 2 H) 4.77 - 4.90 (m, 4 H) 4.96 - 5.03 (m, 2 H) 5.17 (d, *J*=16.8 Hz, 1 H) 6.46 (s, 1 H) 6.51 (s, 1 H) 6.68 (s, 1 H) 7.15 (d, *J*=7.4 Hz, 2 H) 7.19 (d, *J*=7.4 Hz, 2 H) 7.29 - 7.36 (m, 2 H) 7.39 - 7.42 (m, 2 H) 7.44 - 7.49 (m, 6 H) 7.52 - 7.57 (m, 4 H) 7.61 - 7.64 (m, 2 H) 7.72 (d, *J*=7.1 Hz, 2 H). ^{13}C NMR (125 MHz, DMSO-d_6) δ ppm 18.58, 43.17, 43.48, 47.42, 51.65, 56.03, 60.56, 62.55, 63.40, 72.96, 113.29, 114.54, 120.27, 121.77, 127.53, 127.73, 128.53, 128.76, 128.79, 128.82, 129.47, 130.23, 130.36, 130.50, 132.59, 132.67, 132.96, 134.34, 134.57, 134.75, 134.98, 135.74, 136.04, 167.52, 186.22. MS (FD) *m/z* found: 619.2916, calculated *m/z*: 619.2944.

4.8 Biological results

Table 4.1. Evaluation of **70a-h**, **71a-h**, **71** and **72** against Ca9-22, HSC-2 and HSC-4 neoplastic cells

Compound		Ca9-22		HSC-2		HSC-4		Average	
		CC_{50} (μM)[a]	SI[b]	CC_{50} (μM)[a]	SI[b]	CC_{50} (μM)[a]	SI[b]	CC_{50} (μM)[a]	SI[b]
70a	H	0.65 ± 0.07	16.9	0.89 ± 0.06	12.4	0.44 ± 0.16	25.0	0.66	18.1
70b	4-F	0.37 ± 0.19	28.1	0.73 ± 0.13	14.3	0.20 ± 0.08	52.0	0.43	31.5
70c	4-Cl	0.12 ± 0.08	113	0.66 ± 0.14	20.5	0.18 ± 0.03	75.0	0.32	69.5
70d	3,4-Cl_2	0.02 ± 0.01	180	0.10 ± 0.02	35.9	0.07 ± 0.00	51.3	0.06	89.1
70e	4-NO_2	0.03 ± 0.00	109	0.12 ± 0.09	27.3	0.09 ± 0.02	36.3	0.08	57.5
70f	4-CH_3	0.47 ± 0.04	15.3	0.75 ± 0.04	9.57	0.43 ± 0.12	16.7	0.55	13.9
70g	4-OCH_3	0.59 ± 0.06	18.3	1.56 ± 0.55	6.92	0.65 ± 0.02	16.6	0.93	13.9
70h	3,4,5-$(OCH_3)_3$	0.07 ± 0.03	43.9	0.23 ± 0.02	13.4	0.30 ± 0.15	10.2	0.20	22.5
70i	4-OH	16.5 ± 2.35	5.10	18.0 ± 2.06	4.68	19.3 ± 1.61	4.36	17.9	4.71
71a	H	0.56 ± 0.01	30.4	1.45 ± 0.16	11.7	0.58 ± 0.04	29.3	0.86	23.8
71b	4-F	0.29 ± 0.23	28.7	0.42 ± 0.14	19.8	0.21 ± 0.01	39.6	0.31	29.4
71c	4-Cl	0.02 ± 0.01	202	0.06 ± 0.01	67.3	0.09 ± 0.03	44.9	0.06	105
71d	3,4-Cl_2	0.01 ± 0.00	236	0.03 ± 0.00	78.7	0.03 ± 0.00	78.7	0.02	131
71e	4-NO_2	0.02 ± 0.00	104	0.05 ± 0.01	41.4	0.06 ± 0.01	34.5	0.04	60.0
71f	4-CH_3	0.18 ± 0.02	53.1	0.46 ± 0.10	20.8	0.40 ± 0.23	23.9	0.35	32.6
71g	4-OCH_3	0.31 ± 0.17	41.0	0.68 ± 0.04	18.7	0.66 ± 0.05	19.2	0.55	26.3
71h	3,4,5-$(OCH_3)_3$	0.07 ± 0.01	20.4	0.22 ± 0.04	6.50	0.18 ± 0.04	7.94	0.16	11.6

72	>100 - - -	- - -	0.61 ± 0.04	>137	0.60 ± 0.30	>139	>33.7	---
73	0.03 ± 0.01	171	0.20 ± 0.02	25.7	0.07 ± 0.03	73.3	0.10	90.0
Melphalan	48.5 ± 1.33	>3.79	14.4 ± 2.08	>12.8	17.4 ± 0.88	>10.6	26.7	>9.06
Doxorubicin	0.47 ± 0.12	15.6	0.11 ± 0.01	66.5	0.15 ± 0.05	48.7	0.24	43.6

[a] The CC_{50} values are the concentrations of compounds required to kill 50% of the cells.

[b] The letters SI refers to the selectivity index. The SI figures are the ratios of the average CC_{50} value of the compounds towards non-malignant HGF, HPLF and HPC cells (Table 4.2) and the CC_{50} figure of a compound against a specific neoplastic cell line.

Table 4.2. Evaluation of **70a-i**, **71a-h**, **71** and **72** against HGF, HPLF and HPC non-malignant cells

Compound	CC_{50} (μM)[a]				PSE[b]
	HGF	HPLF	HPC	Avg CC_{50} (μM)[a]	
70a H	7.11 ± 0.47	14.3 ± 3.79	11.5 ± 2.57	11.0	2,742
70b 4-F	7.12 ± 0.04	9.73 ± 0.23	14.2 ± 2.00	10.4	7,326
70c 4-Cl	6.40 ± 0.35	8.03 ± 0.06	26.1 ± 35.9	13.5	21,719
70d 3,4-Cl_2	1.91 ± 0.22	3.90 ± 1.42	4.97 ± 0.89	3.59	148,500
70e 4-NO_2	1.67 ± 0.31	3.06 ± 0.16	5.07 ± 0.21	3.27	71,875
70f 4-CH_3	5.70 ± 0.65	8.00 ± 0.20	7.85 ± 7.10	7.18	2,527
70g 4-OCH_3	6.63 ± 0.06	12.1 ± 1.79	13.6 ± 0.60	10.8	1,495
70h 3,4,5-$(OCH_3)_3$	2.18 ± 0.23	5.22 ± 0.69	1.80 ± 0.60	3.07	11,250
70i 4-OH	64.9 ± 5.66	88.3 ± 4.56	99.3 ± 1.16	84.2	26.3
71a H	9.65 ± 1.23	24.6 ± 1.10	16.8 ± 0.68	17.0	2,767
71b 4-F	4.50 ± 1.39	9.13 ± 0.48	11.3 ± 2.59	8.31	9,484
71c 4-Cl	1.65 ± 0.17	4.17 ± 1.44	6.30 ± 0.70	4.04	175,000
71d 3,4-Cl_2	1.15 ± 0.41	2.12 ± 0.20	3.81 ± 0.02	2.36	655,000
71e 4-NO_2	1.15 ± 0.35	2.59 ± 0.27	2.46 ± 1.23	2.07	150,000
71f 4-CH_3	5.12 ± 0.24	8.37 ± 0.81	15.2 ± 1.90	9.56	9,314
71g 4-OCH_3	6.30 ± 0.27	16.2 ± 4.05	15.6 ± 3.16	12.7	4,782
71h 3,4,5-$(OCH_3)_3$	0.62 ± 0.06	1.32 ± 0.04	2.35 ± 0.82	1.43	7,250
72	53.3 ± 6.43	97.3 ± 4.62	>100 - - -	>83.5	- - -
73	2.78 ± 0.37	6.40 ± 1.05	6.20 ± 0.78	5.13	90,000
Melphalan	157 ± 38.2	195 ± 4.04	>200 - - -	184	>33.9
Doxorubicin	3.44 ± 0.53	9.73 ± 0.47	8.77 ± 2.14	7.31	18,167

[a] The CC_{50} values are the concentrations of the compounds required to kill 50% of the cells.

[b] The letters PSE refer to the potency-selectivity expression. These figures are the product of the reciprocal of the average CC_{50} values against Ca9-22, HSC-2 and HSC-4 cells and the average SI value multiplied by 100.

Table 4.3. Evaluation of **70a-i**, **71a-h**, **72** and **73** against human CEM cells

Compound	CC_{50}(μM)[a]	Compound	CC_{50}(μM)[a]
70a H	5.39 ± 0.26	**71a** H	7.62 ± 1.44
70b 4-F	1.78 ± 0.21	**71b** 4-F	1.05 ± 0.38
70c 4-Cl	15.9 ± 0.94	**71c** 4-Cl	4.96 ± 0.28
70d 3,4-Cl_2	8.49 ± 0.34	**71d** 3,4-Cl_2	5.19 ± 0.66
70e 4-NO_2	11.6 ± 0.31	**71e** 4-NO_2	0.87 ± 0.02
70f 4-CH_3	8.42 ± 1.10	**71f** 4-CH_3	4.18 ± 0.65
70g 4-OCH_3	4.35 ± 0.20	**71g** 4-OCH_3	13.0 ± 0.95
70h 3,4,5-$(OCH_3)_3$	2.31 ± 0.30	**71h** 3,4,5-$(OCH_3)_3$	5.12 ± 0.14
70i 4-OH	11.1 ± 1.01	**72**	12.2 ± 1.49
		73	4.44 ± 0.23

[a] The CC_{50} values are the concentrations of the compounds required to kill 50% of the cells.

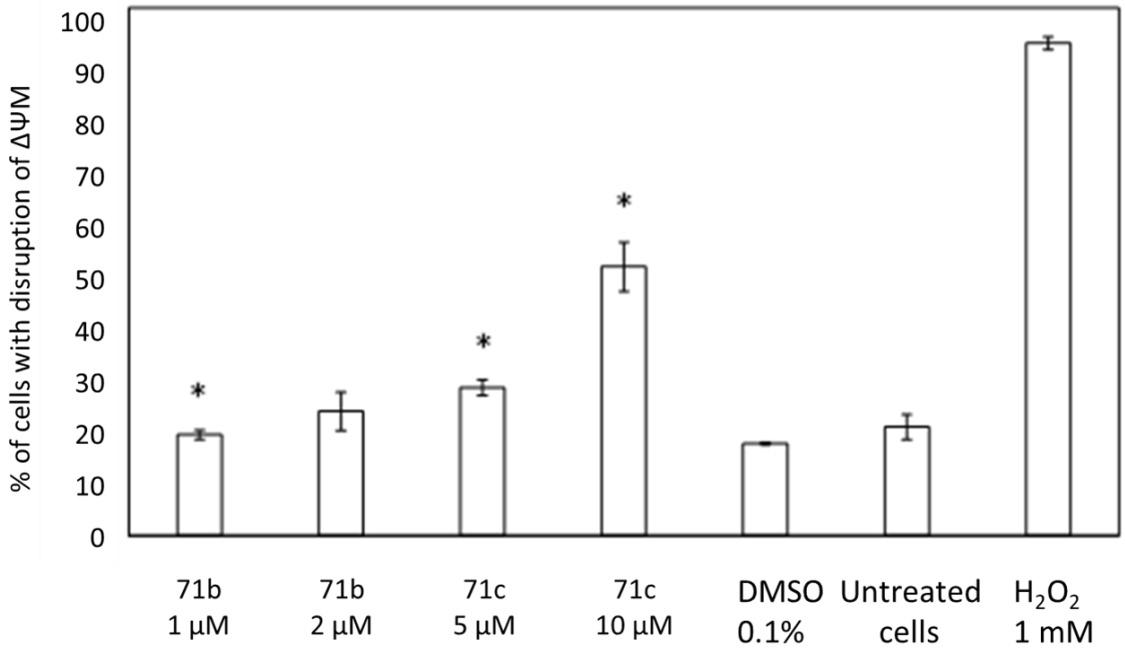

Figure 4.1. Disruption of MMP in the cells with **71b** and **71c**.

Table 4.4. Evaluation of **70a-h** and **72** against a panel of human tumor cells

Compound	Leukemia cells, IC_{50}(μM)					
	HL-60(TB)	K-562	Molt-4	RPMI-8226	SR	Average
70a H	2.60	0.40	0.69	0.32	0.33	0.85
70b 4-F	1.55	0.35	0.33	0.29	0.25	0.52
70c 4-Cl	0.56	0.16	0.28	0.16	0.04	0.24
70d 3,4-Cl_2	1.00	0.25	0.32	0.23	0.10	0.37
70e 4-NO_2	1.55	0.28	0.40	0.30	0.10	0.50
70f 4-CH_3	1.70	0.32	0.37	0.30	0.31	0.55
70g 4-OCH_3	2.82	1.20	2.95	0.65	0.62	1.88
70h 3,4,5-$(OCH_3)_3$	0.27	0.32	0.29	0.32	0.30	0.30
72	10.96	0.36	1.10	0.05	0.28	2.20

Table 4.5. Evaluation of **70a-h** and **72** against some human colon cancer cells.

Compound	All cell lines, IC_{50}(μM)	Colon cancer cells, IC_{50}(μM)							
		Colo205	HCC-2998	HCT-116	HCT-15	HT29	KM12	SW-620	Avg
70a H	1.51	1.70	1.74	0.68	1.38	1.20	0.66	0.32	1.10
70b 4-F	1.15	1.50	1.41	0.22	0.37	0.32	0.23	0.20	0.61
70c 4-Cl	1.62	0.35	0.31	0.21	0.27	0.30	0.22	0.15	0.26
70d 3,4-Cl_2	1.30	0.39	0.36	0.32	0.27	0.32	0.25	0.23	0.31
70e 4-NO_2	1.79	0.40	1.17	0.49	0.36	0.33	0.29	0.20	0.46
70f 4-CH_3	1.23	1.15	1.58	0.36	0.55	0.35	0.28	0.29	0.65
70g 4-OCH_3	1.28	2.04	1.86	1.74	2.14	2.04	1.74	1.38	1.84
70h 3,4,5-$(OCH_3)_3$	1.22	0.26	0.21	0.21	1.23	0.33	0.20	0.30	0.39
72	3.15	3.02	1.05	0.31	0.66	0.45	0.35	0.37	0.89

Table 4.6. Evaluation of **70c**, **d**, **71c-e** for some drug-like properties and oral bioavailability[a]

Compound	MW (g/mol)	log P	HBA	HBD	RB	PSA ($Å^2$)	Oral bioavailability score
70c	512.43	4.31	5	1	6	73.21	0.56
70d	581.32	5.37	5	1	6	73.21	0.17
71c	654.37	2.67	4	1	6	69.97	0.56
71d	723.26	3.70	4	1	6	69.97	0.56
71e	675.47	0.88	8	1	8	161.61	0.17
Ideal compound	⩾500	⩾5	⩾10	⩾5	<10	<140$Å^2$	> 0.50

[a]The abbreviations in some of the headings of each column refer to molecular weight (MW), logarithm of the partition coefficient (log P), hydrogen bond acceptor atoms (HBA), hydrogen bond donor atoms (HBD), rotatable bonds (RB) and polar surface area (PSA).

4.8.1 Methodology

Methodology for determining cytotoxic activity of the Ca9-22, HSC-2, and HSC-4 tumour cells and HGF, HPLF and HPC human non-malignant cells

Human oral tumor cell lines, oral squamous cell carcinoma cells HSC-2, and HSC-4 and Cellosaurus cell line Ca9-22, and human oral normal cells, periodontal ligament fibroblast (HPLF), and gingival fibroblast (HGF) (5-7 population doubling levels), and hematopoietic precursor cell HPC, were cultured in DMEM medium which is supplemented with 10% heat-inactivated FBS. The human normal cells were obtained from the periodontal tissues according to the "guidelines of the Meikai University Ethics Committee after obtaining the informed consent from the patient". All cells were incubated for 48 hours at 37 °C with 5% CO_2 at various concentrations of the test samples, and the relative viable cell number was then determined by the MTT assay method and is expressed as absorbance at 540 nm of the cell lysate. The 50% cytotoxic concentration (CC_{50}) was determined from the dose-response curve.[201] The data for the series **70** in Tables 4.1 and 4.2 are generated at Meikai University Research Institute of Odontology, Japan.

Methodology for determining the cytotoxic activity of 70a-i, 71a-h, 72 and 73 against human CEM cells.

In brief, the cells were cultured in RPMI-1640 (CEM) media supplemented with 10% heat-inactivated fetal bovine serum. Different concentrations of the compounds were added to the cell cultures and then viability was measured by the Differential DNA Staining (DNS) assay after 24 hours incubation.[202, 203] After analysis of the effects of a range of concentrations of the compounds, the CC_{50} (compound concentration needed to kill 50% of the cell population) was determined. After subtracting the percentage of cell death caused by the solvent (DMSO-treated cells), a linear

interpolation equation was used to determine the CC_{50} values.[203, 204] The data for the compounds **70a-i, 71a-h, 72 and 73** in Table 4.3 are generated at Department of Biological Sciences and Border Biomedical Research Center, The University of Texas, El Paso, USA.

Methodology of mitochondrial membrane potential assay for the disruption of MMP in the cells with 71b and 71c.

The mitochondrial membrane potential (MMP) was analyzed by using the MitoProbe JC-1 assay kit (Molecular Probes, M34152). HL-60 cells were seeded in 24-well plates at a density of 100,000 cells per mL in each well and were left under cell culture conditions overnight. Cells were treated with 0.1% v/v DMSO and 1.6 mM of H_2O_2, as a vehicle and cytotoxicity controls, respectively, and incubated for 7 hours. Treatments with the compounds were CC_{50} and 2 x CC_{50}. After incubation, cells were collected in 5 ml tubes and were spun down at 1200 rpm for 5 minutes at room temperature. The supernatant was discarded, and cells were resuspended with 400 µL of PBS containing 2 µM of JC-1 and incubated under normal cell culture conditions for 45 minutes. After incubation, cells were washed with 3000 µL of warm PBS (37 °C) and centrifuged. The supernatant was discarded, and cells were resuspended in 400 µL of warm PBS to be read immediately by flow cytometry.[212] The results of mitochondrial membrane potential assay are generated at Department of Biological Sciences and Border Biomedical Research Center, The University of Texas, El Paso, USA.

Methodology for the half maximal inhibitory concentration (IC_{50})

The data in Tables 4.4 and 4.5 were generated in the NCI-60 screen under the auspices of the National Cancer Institute, USA.[213] In brief, compounds are screened at five concentrations of log 10^{-8} to 10^{-4} M and the result expressed as $\log_{10} GI_{50}$ values which were converted into IC_{50} figures. Compounds were screened against approximately 60 different neoplastic conditions including leukemia and colon cancers.

4.9 Discussion

The compounds in series **70** and **71** were synthesized as follows. At first, the acid catalyzed condensation reaction between a variety of substituted aryl aldehydes and 4-piperidone produced series **15.** The compounds in series **15** were treated with acryloyl chloride to generate series **32** which were then are reacted with 4-piperidone oxime to yield the oximes (series **70**). The quaternization of compounds in series **70** with methyl iodide led to the formation of series **71**. During the quaternization, there was the possibility that methylation could take place on the piperidyl nitrogen atom or on the hydroxyl group of the oxime. The confirmation that methylation took place on the piperidyl nitrogen atom and not on the oxime hydroxyl was obtained by using a NMR-heteronuclear multiple bond correlation (HMBC) technique. In this case, the HMBC cross peak of the exocyclic methylene group attached to the piperidyl nitrogen atom with the carbon atom of the methyl group was observed.

The cytotoxic evaluations of the compounds in series **70** and **71** against the neoplastic Ca9-22, HSC-2 and HSC-4 cells lines was carried out and the CC_{50} values of these enones in series **70** and **71** are presented in Table 4.1. All of the compounds in series **70** and **71** are found to be potent cytotoxins with the exclusion of **70i** . Indeed 96 % of the CC_{50} values of **70a-h** and **71a-h** are submicromolar and if the outlier **70i** is considered, this figure falls to 90 %. For compounds **70a-i** and **71a-h,** 29 % of the CC_{50} values are in the double digit nanomolar range (10^{-8} M). From this evaluation, the most potent compounds (average CC_{50} figures in μM in parentheses) are **70d** (0.06), **70e** (0.08), **71c** (0.06), **71d** (0.02) and **71e** (0.04). The average CC_{50} values of **70a-h** towards the three malignant cell lines is 0.40 μM and for **71a-h** the value is 0.29 μM suggesting that in general the quaternary ammonium compounds **71** are more cytotoxic than the precursor oximes **70**. The

compounds **70d**, **70e**, **71c**, **71d** and **71e** can be considered as lead molecules for the further development of the compounds and future studies. In the section entitled "Conclusions", a comparison of the aryl substitution pattern in the lead molecules in series **15**, **33**, **70** and **71** is made.

The cytotoxic potencies of the compounds in series **70** and **71** were compared with that of two established anticancer drugs namely doxorubicin and melphalan. Doxorubicin is an antibiotic and was chosen as a reference compound since it is a potent anticancer drug. Melphalan was chosen as a reference drug in this evaluation, since it is an alkylating agent and the compounds in series **70** and **71** contain the 1,5-diaryl-3-oxo-1,4-pentadienyl group, which is considered a pharmacophore which alkylates cellular thiols.[214] The compounds which rival the efficacy of these two drugs are useful lead molecules to consider. All the compounds in series **70** and **71,** with the exception of **70i**, are substantially more potent than melphalan. For example, the average CC_{50} values of **70d** and **71d** are 445 and 1335 times lower than the corresponding CC_{50} value for melphalan. Doxorubicin having an average CC_{50} value of 0.24 μM towards these three cell lines, is more potent than melphalan. It may be concluded that a number of compounds in series **70** and **71** exceed the cytotoxic potencies (CC_{50} values) of these two reference anticancer agents towards the Ca9-22, HSC-2 and HSC-4 cell lines and are considered as prototypes for analog development.

The cytotoxic potencies of the oximes **70a**-**h** and the related quaternary ammonium compounds **71a**-**h** were compared when the same substituents are present in the aryl rings. Thus the CC_{50} values of **70a** and **71a, 70b** and **71b**, **70c** and **71c** in the Ca9-22 screen were compared and so forth. The standard deviations were taken into consideration for these evaluations. The following compounds have the greater potencies (bioassay in parentheses) namely **71a**, **c**, **e**, **f**, **g** (Ca9-22),

71b, **c**, **d**, **f**, **g** and **70a** (HSC-2) and **71c**, **d** (HSC-4). For the other comparisons, equipotency was observed. Hence in 50% of the comparisons, the quaternary ammonium compounds in series **71** are more potent than the corresponding analogs in series **70** while in 4% of the comparisons an oxime has a lower CC_{50} value. Equipotency was noted in 46% of the comparisons made. This evaluation reveals that in general the quaternary ammonium salts are either more potent than the analogs in series **70** or are equipotent.

An important factor to consider for developing cytotoxic agents is whether they demonstrate tumour-selective toxicity. i.e., whether the compounds have greater toxicity towards neoplasms than towards non-malignant cells. To evaluate whether tumour selectivity is demonstrated, the compounds in series **70** and **71** were evaluated against non-malignant HGF, HPLF and HPC cells. The data are portrayed in Table 4.2 and the following observations were made. In this evaluations, low toxicity towards non-malignant cell lines is favoured and 29% of the CC_{50} values for series **70** and **71** are above 10 µM. Compound **70i** is again an outlier displaying low cytotoxicity, which might be due to the presence of the polar hydroxyl groups on the aryl rings hindering the penetration of the molecule into the cells. The lowest toxicity is demonstrated by **70a**, **b**, **c**, **g** and **71a**, **g** with average CC_{50} values greater than 10 µM. A comparison of the results obtained with that of established two reference drugs demonstrated favourable results for doxorubicin but not for melphalan.

Comparison was made between **70a-h,** and the related quaternary ammonium compounds **71a-h** in terms of their toxicity towards HGF, HPLF and HPC non-malignant cells. The compounds with the higher CC_{50} values are preferable since they demonstrate less toxicity to normal cells. The CC_{50} values in each bioassay of the compounds in series **70** are compared with the corresponding

analogs in series **71** with the same aryl substituents. The compounds namely **70b, c, d**, **h**, and **71a** in HGF cell lines, **70c**, **d**, **e**, **h**, and **71a** in HPLF and **70d**,**e**, and **71a** in HPC bioassays have higher CC_{50} values, which means these compounds are less toxic to non-malignant cells. Equipotency was noted in the remaining comparisons. Thus 42% of the compounds in series **70** and 12% of the compounds in series **71** have higher CC_{50} values towards HGF, HPLF and HPC non-malignant cells, while equipotency was noted in 46% of the comparisons. Therefore, from these comparisons, in general the quaternary ammonium salts i.e., series **71** are more cytotoxic to non-malignant cells than the corresponding oximes **70**. In summary, the quaternary ammonium salts are in general more toxic than the corresponding oximes to both Ca9-22, HSC-2 and HSC-4 neoplasms as well as HGF, HPLF and HPC non-malignant cells.

A significant factor one must consider in expanding these series of cytotoxic agents is whether they demonstrate tumour-selective toxicity i.e., these agents cause more damage to malignant cells than normal cells. In the in vivo situation, a tumour is surrounded by a number of non-malignant cells. Hence, to assess whether the compounds in series **70** and **71** are more toxic to neoplasms than non-malignant cells, selective index (SI) figures were calculated, and these SI values were obtained by dividing the average CC_{50} values for the HGF, HPLF and HPC non-malignant cells by the CC_{50} figure against a specific neoplastic cell line. The data are presented in Table 4.1.

All the compounds in series **70** and **71** have SI figures greater than 1, indicating that the compounds display greater toxicity towards the neoplasms than non-malignant cells. In particular the compounds **70c**, **d**, **e** and **71c**, **d**, **e** have SI figures greater than 100 towards Ca9-22 cells indicating that these compounds cause more damage to neoplasms than non-malignant cells. The average SI values are portrayed in Table 4.1 and the compounds **70c**, **d**, **e** and **71c**, **d**, **e** possess the SI figures

more than 50. In particular, for the compounds **71c** and **71d,** the average SI figures are over 100, reemphasizing the identity of these two compounds as lead molecules.

A comparison was made between the SI data of the oximes **70a-h** and the quaternary ammonium salts **71a-h** when the aryl substituents are identical. From these comparisons, the compounds **71a, b, c**, **d**, **f**, **g** in Ca9-22, **71b, c, d, e, f, g** in HSC-2 and **71a**, **c, d, e, f, g** in HSC-4 bioassay's have higher SI values. Thus, in the comparisons made, greater selectivity was displayed by the compounds in series **71**.

Potency-selectivity expression (PSE) values were computed to identify the most promising lead compounds in terms of both cytotoxic potencies and favourable SI values. PSE values are the products of the reciprocal of the average CC_{50} value against Ca9-22, HSC-2 and HSC-4 cells and the average SI figure multiplied by 100 [PSE= (SI/Avg CC_{50}) x 100]. These values are presented in Table 4.2. Four compounds namely **70d**, and **71c**, **d**, **e** have an outstanding PSE values in excess of 100,000. In a comparison between the PSE figures of **70a-h** and **71a-h** which have the same aryl substituents revealed higher PSE values for **71a-g** than **70a-g** while **70h** has a higher PSE value than **71h**. From this comparison study, once again it reinforces the superior cytotoxic properties of the quaternary ammonium compounds in series **71** than the oximes in series **70**. In this case, one may also observe that the very low PSE value for **70i** revealing the negative influence on both cytotoxic potency and selectivity of a 4-hydroxy substituent in the aryl rings.

In view of the encouraging result with Ca9-22, HSC-2, HSC-4 and CEM leukemic cells, consideration was given to an assessment in the National Cancer Institute (NCI) in vitro screening program.[215] The request for screening the compounds in series **70** and **71** was made to the NCI. However, the oximes **70a-h**, were accepted for bioevaluations but not the quaternary ammonium

salts **71**. Examination of the mean graphs[216] from the NCI screening results confirms the sensitivity of leukemic cells to these compounds. These data are presented in Table 4.4.

The results from the NCI screening reveal that **70a-h** are potent inhibitors of the growth of a number of leukemic cell lines. From the biodata generated, 78% of the IC_{50} values are submicromolar. The compounds **70c** with a 4-chloro aryl substituent and **70h** with 3,4,5-trimethoxy aryl substituent have the lowest average IC_{50} values. Compound **70c** is exceptional with an average IC_{50} value of 40 nM against SR leukemic cells. A previous report indicated that the drug melphalan, which is used in treating leukemias, has an average IC_{50} value of 56.7 μM towards HL-60 (TB), K-562, RPMI-8226 and SR cells.[217] The results demonstrate that the compounds in series **70** are far more potent than melphalan towards these leukemic cell lines.

The results from the NCI screen revealed that the compounds **70a-h** are not only sensitive towards leukemic cells but also are highly toxic towards colon cancers. These data are presented in Table 4.5. It is noted that some 70% of the IC_{50} values and 75% of the average IC_{50} values are in the submicromolar range. A previous report indicated that the drug 5-fluorouracil, which is used in treating colon cancers has an average IC_{50} value of 8.46 μM against Colo205, HCC-2998, HCT-15, KM12 and SW-620 cells.[217] This value is substantially higher than the IC_{50} figures of the compounds in series **70**. The compounds **70c** and **70d** having 4-chloro and 3,4-dichloro aryl substituents show the lowest average IC_{50} values. Thus, the bioevaluation indicates that the compounds in series **70** are novel potent cytotoxins.

A further question to resolve is whether the quaternary ammonium compounds **71** have an effect on the mitochondrial membrane potential (MMP). In order to investigate the effect on MMP, two compounds **71b** and **71c** were chosen which have a fivefold difference in potencies towards CEM

cells as indicated in Table 4.3. For this study, **71b** and **71c** were studied using the CC_{50} and twice CC_{50} concentrations towards CEM cells. The results revealed that both compounds interfered with the MMP. The MMP effect is more noticeable with **71c** suggesting this biochemical effect is a greater contributor to its cytotoxicity than is the case with **71b.** The isosteric replacement of the fluoro atom in **71b** by a chloro group to produce **71c** leads to differences not only in potency but also in the effect on the MMP. These observations illustrate the varying sensitivity of cells to compounds with different aryl substituents.

The stabilities of a representative oxime **70a** and the quaternary ammonium compound **71a** were determined on using a NMR technique in a solvent mixture of 9:1 deuterated dimethylsulfoxide and deuterium oxide. ^{1}H NMR spectra were determined in dissolution and after 48 hours of incubation at 37 ℃ (the same time and temperature as used for the cytotoxicity assays) and found to be identical. This result indicates the compounds are stable under these conditions. Hence cytotoxicity may be due to the compounds and not with any breakdown products.

The biodata generated for the compounds in series **70** and **71** are most encouraging and in considering future development of these compounds as antineoplastic agents, one must look into whether these compounds (and especially lead molecules) possess drug-like properties. In series **70** and **71**, the most favourable biodata is demonstrated by the compounds **70c**, **d** and **71c**, **d**, **e** in terms of potency, selectivity and PSE figures. For good ADME properties, lead molecules are recommended to have a molecular weight not exceeding 500 and a logP value below 5 while the number of hydrogen bond acceptor and donor atoms should not exceed 10 and 5, respectively.[218] For good oral bioavailability the polar surface area should not exceed 140 A˚ and the number of rotatable bonds should be less than 10.[219] The relevant data for these compounds is presented in

Table 4.6. For the compounds in series **70** and **71**, apart from the molecular weight of the compounds being over 500, display no other violations. These observations reveal that **70c, d** and **71c, d, e** have drug-like properties illustrating the necessity to proceed further with the development of this series of compounds as antineoplastic agents.

The compounds described in series **15**, **33**, **70** and **71** have two sites for alkylation of cellular thiols. The enones **72** and **73**, whose structures are presented in Scheme 4.2, are molecules with four sites which are capable of reacting with thiols. In order to obtain some appreciation of the potencies of these two compounds, **72** and **73** were evaluated for cytotoxic properties and the results are portrayed in Tables 4.1, 4.2 and 4.3 while data for **72** is also present in Tables 4.4 and 4.5. The quaternary ammonium compound **73** is more potent than **72** and coupled with its selective indices and PSE value serves as a lead molecule for further studies.

Conclusions and future work

This thesis describes the successful completion of work undertaken on three separate projects. These studies were designed with the goal of producing novel cytotoxins that display more significant toxicity to neoplasms than towards non-malignant cells. First, a series of 3,5-bis(benzylidene)-4-piperidones **15** were prepared and in general, demonstrated significant potencies to a number of different neoplastic cells. Second, series **33** are a novel cluster of cytotoxins which led to the identification of various lead compounds. The third project examined the hypothesis that the quaternary ammonium compounds are more potent than the precursor amines. These comments comprise an overview of what has been achieved. The remaining comments expand on these ideas and record possible future work with these groups of molecules.

In general, the compounds in series **15** are highly toxic to a range of neoplastic cells and most of them displayed lower toxicity towards various non-malignant cells. From these determinations, a number of lead compounds were identified, which may be considered for molecular modifications to enhance cytotoxic potencies and tumor selectivity. In this series of compounds, the cytotoxic potencies increased as the electron-withdrawing properties of the aryl substituents were raised. However, the pi (π) and MR values of the aryl groups did not show any affect on the magnitude of the CC_{50} values. In future, analogs of series **15** will be prepared with the substituents having increased electron-withdrawing properties, for example the 3-nitro-4-trifluoromethyl derivative ($\Sigma\sigma$ =1.25). Further attempts can be made to introduce methyl groups at the 2 and 6 positions of the piperidine ring and to compare their cytotoxicity with the analogs in series **15**.

The majority of compounds in series **33** display submicromolar CC_{50} values towards the neoplasms. The CC_{50} figures for some of the compounds are less than 10^{-7} M. In general, series **33** have much lower CC_{50} values than the reference drugs melphalan, 5-fluorouracil and methotrexate while some compounds displayed equitoxicity with doxorubicin. The compounds are less toxic to the non-malignant cells demonstrating tumor-selectivity. Compounds **33a, b, g, i, j, l,** are potent cytotoxins, with CC_{50} figures of <0.1 µM towards some or all of the four malignant cell lines. The higher PSE value of **33g** indicates that it is a principal lead molecule (with an average CC_{50} value of 0.04 µM towards four malignant cell lines and a selectivity index of 46.3) to take forward for further preclinical evaluations. In future studies, molecular modifications of **33g** could be done to achieve greater tumor-selective toxicity. Thiol adducts at the olefinic carbon atoms can be considered to form a prodrug which may release the 1,5-diaryl-3-oxo-1,4-pentadienyl pharmacophoric group slowly.

A number of novel oximes **70a-h** and related quaternary ammonium compounds **71a-h** have been prepared. The bioevaluations revealed that these compounds are potent cytotoxins which in general have much greater potencies than melphalan while some of these molecules rival doxorubicin in potency. In the majority of the cases, the quaternary ammonium salts **71a-h** are more toxic to neoplasms than the related oximes **70a-h**. The design of the quaternary ammonium salts in series **71** took into consideration the possibility of the MMP as a cellular target for these candidate antineoplastics. Two representative quaternary ammonium salts **71b** and **71c** caused a reduction in the MMP in CEM cells which likely contributes to the toxic effect thereby strengthening the hypothesis that quaternary ammonium salts might interfere with the MMP of the cancer cells. The compounds in series **70** and **71** displayed greater cytotoxicity towards several neoplastic cell lines than to non-malignant cells thus demonstrating tumor-selectivity. Compounds in series **70** and **71**

are structurally divergent from the contemporary anticancer drugs and thus drug-resistant tumours may be sensitive to these compounds. In addition, in NCI evaluations the compounds **70a-h** demonstrated cytotoxic potencies towards a number of leukemic and colon cancer cells. Several lead molecules namely **70c, d, 71c-e** have been identified which have drug-like characteristics and serve as prototypes for further studies.

A review of the PSE values in each of the four series **15**, **33**, **70** and **71** was conducted with a view to finding which aryl substituents are present in the compounds with the highest PSE scores. Such information will be useful in the design of future compounds based on the biodata generated in this study.

The four compounds in each series with the highest PSE values were arranged in descending order of the magnitude of the PSE values. In the case of series 15, the compounds with the greatest PSE figures are **15q** (3-OH,4-OCH_3) > **15d** [3,4-$(OCH_3)_2$] > **15l** (3,4-F_2) > **15b** (3-OCH_3). In series **33**, one finds the following relative values namely **33g** [3,4,5-$(OCH_3)_3$] > **33b** (3-OCH_3) > **33a** (2-OCH_3) > **33** (H). On the other hand, in series **70** the PSE figures are in the sequence of **70d** (3,4-Cl_2) > **70e** (4-NO_2) > **70c** (4-Cl) > **70h** [3,4,5-$(OCH_3)_3$]. Finally in series **71**, the following relative PSE figures are **71d** (3,4-Cl_2) > **71c** (4-Cl) > **71e** (4-NO_2) > **71f** (4-F).

The aryl substituents of the compounds with the highest PSE values 15 and 33 are in general relative large groups where methoxy groups predominate over the presence of halogens. In these series it is possible that an oxygen atom adjacent to the aryl ring is important and in the future larger *O*-alkyl and *O*-aryl groups could be placed on the aryl rings. In contrast, the PSE values in series **70** and **71** are increased with halogens and electron-withdrawing nitro groups. The

outstanding PSE values of **70d** and **71d** which possess a 3,4-dichloro substituent suggest the preparation and bioevaluation of the 3,4-difluoro analogs for future evaluations.

But an effort should be made to create new series of compounds in addition to dealing with the effect on cytotoxicity by changes in the aryl substitution pattern. The development of different series is based on the lead molecule **71a**. The general structure of a series of compounds **74** are indicated in the **Figure 5.1**.

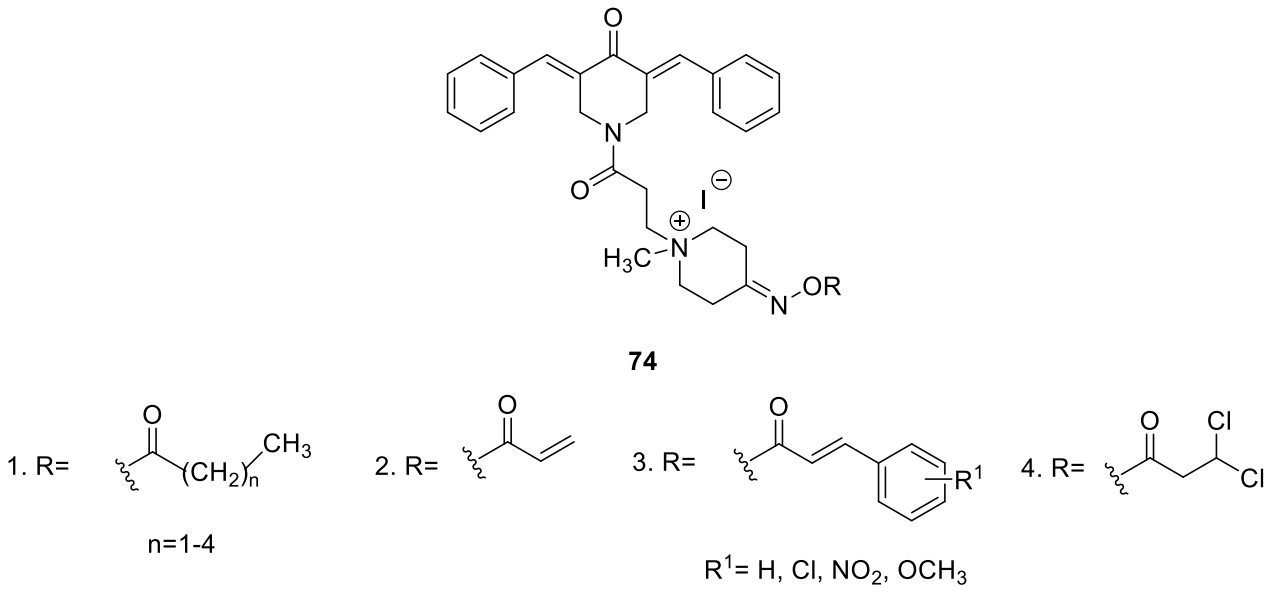

Scheme 5.1. General structure of the proposed series of compounds.

The reasons for suggesting these novel compounds are as follows.

(1) When R=H (**71a**), a polar OH group is present which may impede the compound from entering the neoplastic cell. Hence the process may be prevented by acylation.

(2) The introduction of an acryloyl group provides an additional location for the molecule to react with cellular thiols. Also the rates of reaction at the olefinic groups attached to the aryl rings and

on the acryloyl carbon will be different which, if the theory of sequential cytotoxicity is valid, will enhance tumour-selective toxicity.

(3) Another approach is to have variation on the electron densities on the olefinic carbon atoms in series **3** where the atomic charges on the 3-aryl-prop-1-en-3-one group will be influenced by the nature of the R^1 group.

(4) Hydrolysis of the dichloroacetyl group will liberate dichloroacetic acid which has anticancer properties.[220]

(5) In view of observation that the dimers of certain 3,5-bis(benzylidene)-4-piperidone are potent cytotoxins[167] the dimerization of **71a** was planned to give series **75**.

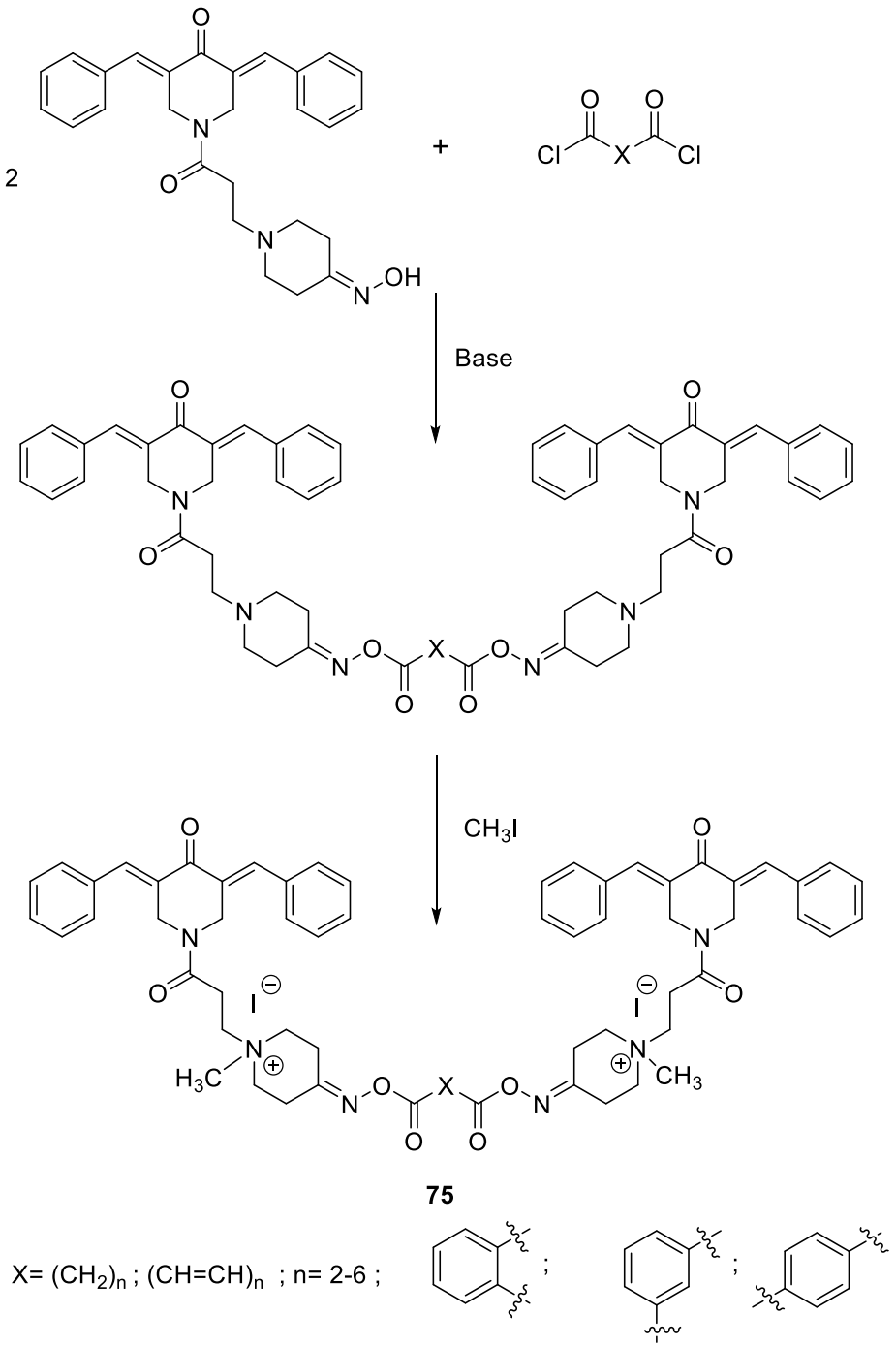

Scheme 5.2. Syntheses of the proposed series **75**.

(6) An important approach would be to form thiol adducts with **71a** and determine if there was a slow release of the cytotoxin in vitro.[60] This prodrug approach is illustrated in Scheme 5.3.

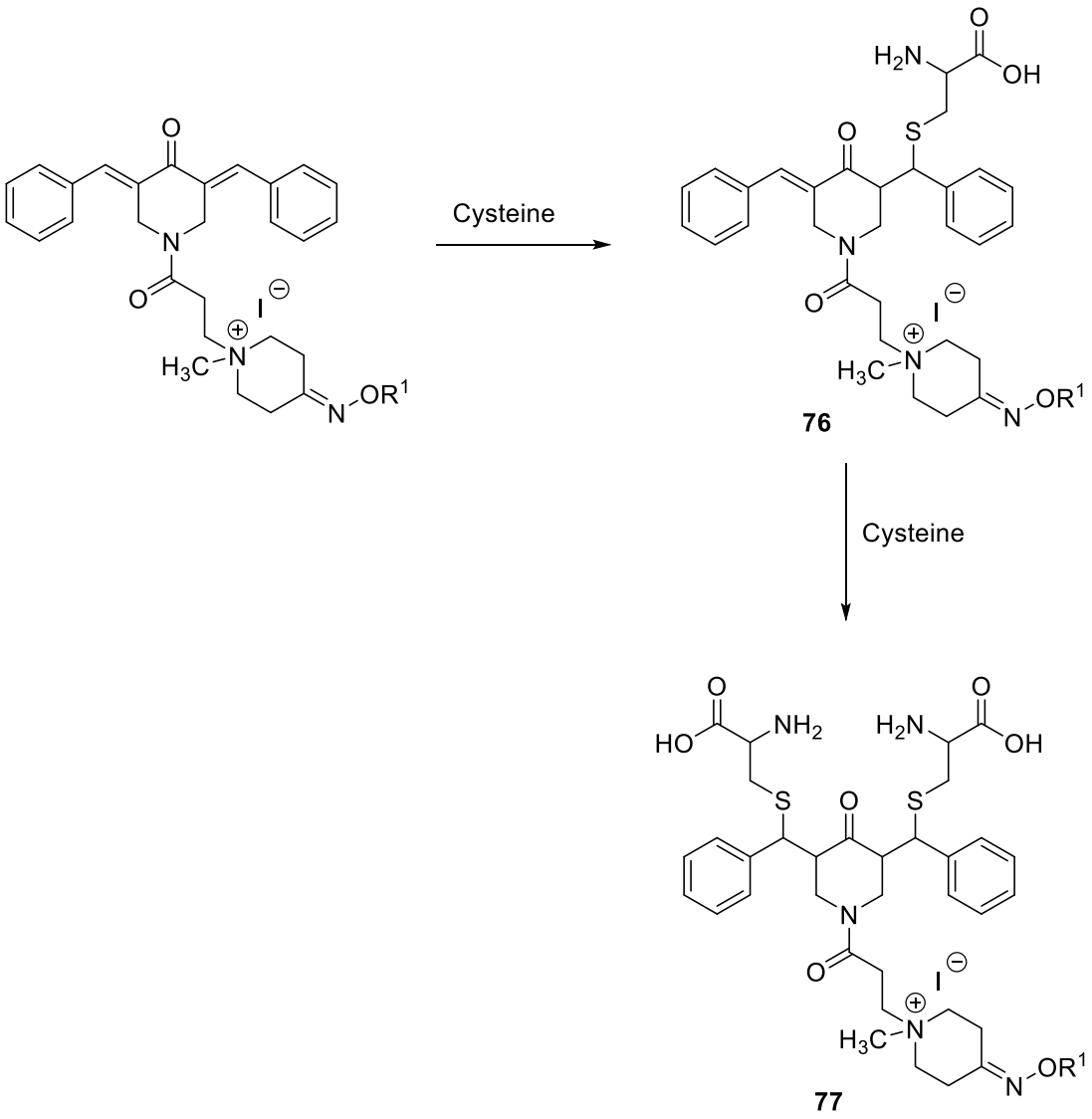

Scheme 5.3. Reaction of **71** analogs with cysteine to form mono adducts **76** and bis adducts **77**.

References

(1). Canadian Cancer Statistics 2019. http://cancer.ca/Canadian-Cancer-Statistics-2019-EN (accessed July 10, 2020).

(2). Public Health Agency of, C.; Statistics, C.; Canadian Cancer, S.; provincial/territorial cancer, r., Release notice - Canadian Cancer Statistics 2019. *Health promotion and chronic disease prevention in Canada : research, policy and practice* **2019,** *39*, 255-255.

(3). Brazier, Y. What are the different types of tumor? https://www.medicalnewstoday.com/articles/249141 (accessed July 10, 2020).

(4). Nordqvist, C. What are the different types of tumors? https://www.medicalnewstoday.com/articles/249141.php (accessed August 27, 2018).

(5). Understanding cancer. https://www.ncbi.nlm.nih.gov/books/NBK20362/ (accessed August 27, 2018).

(6). Cancer facts & figures 2017. https://www.cancer.org/research/cancer-facts-statistics/all-cancer-facts-figures/cancer-facts-figures-2017.html (accessed January 9, 2018).

(7). Brenner, D. R.; Weir, H. K.; Demers, A. A.; Ellison, L. F.; Louzado, C.; Shaw, A.; Turner, D.; Woods, R. R.; Smith, L. M., Projected estimates of cancer in Canada in 2020. *Canadian Medical Association Journal* **2020,** *192*, E199.

(8). Canadian Cancer Statistics 2018. http://www.cancer.ca/~/media/cancer.ca/CW/cancer%20information/cancer%20101/Canadian%20cancer%20statistics/Canadian-Cancer-Statistics-2018-EN.pdf?la=en (accessed September 09, 2018).

(9). Wei, E. K.; Giovannucci, E.; Wu, K.; Rosner, B.; Fuchs, C. S.; Willett, W. C.; Colditz, G. A., Comparision of risk factors for colon and rectal cancer. *International Journal of Cancer* **2004,** *108*, 433-442.

(10). Austin, H.; Henley, S. J.; King, J.; Richardson, L. C.; Eheman, C., Changes in colorectal cancer incidence rates in young and older adults in the United States: what does it tell us about screening. *Cancer Causes & Control* **2014,** *25*, 191-201.

(11). Patel, P.; De, P., Trends in colorectal cancer incidence and related lifestyle risk factors in 15-49 year olds in Canada, 1969-2010. *Cancer Epidemiology* **2016,** *42*, 90-100.

(12). Chemotherapy to Treat Cancer. https://www.cancer.gov/about-cancer/treatment/types/chemotherapy (accessed June 14, 1018).

(13). Yap, T. A.; Omlin, A.; Bono, J. S. D., Development of therapeutic combinations targeting major cancer signaling pathways. *Journal of Clinical Oncology* **2013,** *31*, 1592-1605.

(14). Nawara, H. M.; Afify, S. M.; Hassan, G.; Zahra, M. H.; Atallah, M. N.; Mansour, H.; Quora, H. A. A.; Alam, M. J.; Osman, A.; Kakuta, H.; Hamada, H.; Seno, A.; Seno, M., Paclitaxel and sorafenib: The effective combination of cuppressing the self-Renewal of cancer stem cells. *Cancers* **2020,** *12*, 1360.

(15). Reza B. Mokhtari, T. S. H., Narges. B, Evgeniya.; M, S. K., Bikul. D, and Herman. Y, Combination therapy in combating cancer. *Oncotarget,* **2017,** *8*, 38022-38043.

(16). Ann H. Partridge, H. J. B., Eric P. Winer, Side effects of chemotherapy and combined chemohormonal therapy in women with early-stage breast cancer *Journal of the National Cancer Institute Monographs* **2001,** *30*, 135-142.

(17). Mokhtari, R. B.; Kumar, S.; Islam, S. S.; Yazdanpanah, M.; Adeli, K.; Cutz, E.; Yeger, H., Combination of carbonic anhydrase inhibitor, acetazolamide, and sulforaphane, reduces the viability and growth of bronchial carcinoid cell lines. *BMC Cancer* **2013,** *13*, 378.

(18). Blagosklonny, M. V., Overcoming limitations of natural anticancer drugs by combining with artificial agents. *Trends in Pharmacological Sciences* **2005,** *26*, 77-81.

(19). Khdair, A.; Di, C.; Patil, Y.; Ma, L.; Dou, Q. P.; Shekhar, M. P. V.; Panyam, J., Nanoparticle-mediated combination chemotherapy and photodynamic therapy overcomes tumor drug resistance. *Journal of Controlled Release* **2010,** *141*, 137-144.

(20). Gottesman, M. M.; Fojo, T.; Bates, S. E., Multidrug resistance in cancer: Role of ATP–dependent transporters. *Nature Reviews Cancer* **2002,** *2*, 48-58.

(21). Hanahan, D.; Bergers, G.; Bergsland, E., Less is more, regularly: Metronomic dosing of cytotoxic drugs can target tumor angiogenesis in mice. *Journal of Clinical Investigation* **2000,** *105*, 1045-1047.

(22). Mello, F. V. C.; Moraes, G. N. d.; Maia, R. C.; Kyeremateng, J.; Iram, S. H.; Santos-Oliveira, R., The Effect of Nanosystems on ATP-Binding Cassette Transporters: Understanding the Influence of Nanosystems on Multidrug Resistance Protein-1 and P-glycoprotein. *International Journal of Molecular Sciences* **2020,** *21*, 2630.

(23). Cancer treatment-side effects. https://www.cancer.gov/about-cancer/treatment/side-effects (accessed January 8, 2018).

(24). Mellinger, E.; Skinker, L.; Sears, D.; Gardner, D.; Shult, P., Safe handling of chemotherapy in the perioperative setting. *AORN Journal* **2010,** *91*, 435-453.

(25). Gehdoo, R., Anticancer chemotherapy and it's anaesthetic implications (current concepts). *Indian Journal of Anaesthesia* **2009,** *53*, 18-29.

(26). Bovelli, D.; Plataniotis, G.; Roila, F.; Group, E. G. W., Cardiotoxicity of chemotherapeutic agents and radiotherapy-related heart disease: ESMO Clinical Practice Guidelines. *Annals of Oncology* **2010,** *21*, v277-v282.

(27). Zagar, T. M.; Cardinale, D. M.; Marks, L. B., Breast cancer therapy-associated cardiovascular disease. *Nature Reviews Clinical Oncology* **2016,** *13*, 172-184.

(28). Vasudev, N. S.; Reynolds, A. R., Anti-angiogenic therapy for cancer: Current progress, unresolved questions and future directions. *Angiogenesis* **2014,** *17*, 471-494.

(29). Morgan, R. J.; Kauffmann, R. M., Toxicity of antineoplastic therapy and considerations for perioperative care. In *Surgical Emergencies in the Cancer Patient*, Fong, Y.; Kauffmann, R. M.; Marcinkowski, E.; Singh, G.; Schoellhammer, H. F., Eds. Springer International Publishing: 2017; pp 19-30.

(30). Oh, G.-S.; Kim, H.-J.; Shen, A.; Lee, S. B.; Khadka, D.; Pandit, A.; So, H.-S., Cisplatin-induced kidney dysfunction and perspectives on improving treatment strategies. *Electrolyte Blood Press* **2014,** *12*, 55-65.

(31). Deshaies, I.; Malka, D.; Soria, J.-C.; Massard, C.; Bahleda, R.; Elias, D., Antiangiogenic agents and late anastomotic complications. *Journal of Surgical Oncology* **2010,** *101*, 180-183.

(32). Gotink, K. J.; Verheul, H. M. W., Anti-angiogenic tyrosine kinase inhibitors: What is their mechanism of action? *Angiogenesis* **2010,** *13*, 1-14.

(33). Yadav, L.; Puri, N.; Rastogi, V.; Satpute, P.; Sharma, V., Tumour angiogenesis and angiogenic inhibitors: A review. *Journal of Clinical and Diagnostic Research* **2015,** *9*, 01-05.

(34). Mitscher, L. A.; Pillai, S. P.; Gentry, E. J.; Shankel, D. M., Multiple drug resistance. *Medicinal Research Reviews* **1999,** *19*, 477-496.

(35). Kane, S. E., Multidrug resistance of cancer cells. *Advances in Drug Research* **1996,** *28*, 181-252.

(36). Bosch, I.; Croop, J., P-glycoprotein multidrug resistance and cancer. *Biochimica et Biophysica Acta-Reviews on Cancer* **1996,** *1288*, 37-54.

(37). Amin, M. L., P-glycoprotein inhibition for optimal drug delivery. *Drug Target Insights* **2013,** *7*, 27-34.

(38). Hooijberg, J.; De Vries, N.; Kaspers, G.; Pieters, R.; Jansen, G.; Peters, G., Multidrug resistance proteins and folate supplementation: therapeutic implications for antifolates and other classes of drugs in cancer treatment. *Cancer Chemotherapy and Pharmacology* **2006,** *58*, 1-12.

(39). Avendaño, C.; Menéndez, J. C., Recent advances in multidrug resistance modulators. *Medicinal Chemistry Reviews-Online* **2004,** *1*, 419-444.

(40). Robert, J.; Jarry, C., Multidrug resistance reversal agents. *Journal of Medicinal Chemistry* **2003,** *46*, 4805-4817.

(41). Zamora, J. M.; Pearce, H.; Beck, W. T., Physical-chemical properties shared by compounds that modulate multidrug resistance in human leukemic cells. *Molecular Pharmacology* **1988,** *33*, 454-462.

(42). Das, U.; Molnár, J.; Baráth, Z.; Bata, Z.; Dimmock, J. R., 1-[4-(2-Aminoethoxy) phenylcarbonyl]-3, 5-bis-(benzylidene)-4-oxopiperidines: A novel series of highly potent revertants of P-glycoprotein associated multidrug resistance. *Bioorganic & Medicinal Chemistry Letters* **2008,** *18*, 3484-3487.

(43). Das, U.; Sharma, R.; Dimmock, J., 1, 5-Diaryl-3-oxo-1, 4-pentadienes: A case for antineoplastics with multiple targets. *Current Medicinal Chemistry* **2009,** *16*, 2001-2020.

(44). de Felício, R.; Pavão, G. B.; de Oliveira, A. L. L.; Erbert, C.; Conti, R.; Pupo, M. T.; Furtado, N. A. J. C.; Ferreira, E. G.; Costa-Lotufo, L. V.; Young, M. C. M.; Yokoya, N. S.; Debonsi, H. M., Antibacterial, antifungal and cytotoxic activities exhibited by endophytic fungi from the Brazilian marine red alga Bostrychia tenella (Ceramiales). *Revista Brasileira de Farmacognosia* **2015,** *25*, 641-650.

(45). Gomes, M.; Muratov, E.; Pereira, M.; Peixoto, J.; Rosseto, L.; Cravo, P.; Andrade, C.; Neves, B., Chalcone derivatives: Promising starting points for drug design. *Molecules* **2017,** *22*, 1210-1234.

(46). Xiang, D.-B.; Zhang, K.-Q.; Zeng, Y.-L.; Yan, Q.-Z.; Shi, Z.; Tuo, Q.-H.; Lin, L.-M.; Xia, B.-H.; Wu, P.; Liao, D.-F., Curcumin: From a controversial "panacea" to effective antineoplastic products. *Medicine* **2020,** *99*, 18467-18467.

(47). Mosley, C. A.; Liotta, D. C.; Snyder, J. P., Highly active anticancer curcumin analogues. In *The molecular targets and therapeutic uses of curcumin in health and disease*, Aggarwal, B. B.; Surh, Y.-J.; Shishodia, S., Eds. Springer US: Boston, MA, **2007**; pp 77-103.

(48). Dinkova-Kostova, A. T.; Abeygunawardana, C.; Talalay, P., Chemoprotective properties of phenylpropenoids, bis(benzylidene)cycloalkanones, and related Michael reaction acceptors: Correlation of potencies as phase 2 enzyme inducers and radical scavengers. *Journal of Medicinal Chemistry* **1998,** *41*, 5287-5296.

(49). Bennett, A., The production of prostanoids in human cancers, and their implications for tumor progression. *Progress in Lipid Research* **1986,** *25*, 539-542.

(50). Qiao, L.; Kozoni, V.; Tsioulias, G. J.; Koutsos, M. I.; Hanif, R.; Shiff, S. J.; Rigas, B., Selected eicosanoids increase the proliferation rate of human colon carcinoma cell lines and mouse colonocytes in vivo. *Biochimica et Biophysica Acta - Lipids and Lipid Metabolism* **1995,** *1258*, 215-223.

(51). Aggarwal, B. B.; Kumar, A.; Bharti, A. C., Anticancer potential of curcumin: preclinical and clinical studies. *Anticancer Research* **2003,** *23*, 363-398.

(52). Surh, Y. J.; Chun, K. S.; Cha, H. H.; Han, S. S.; Keum, Y. S.; Park, K. K.; Lee, S. S., Molecular mechanisms underlying chemopreventive activities of anti-inflammatory

phytochemicals: down-regulation of COX-2 and iNOS through suppression of NF-κB activation. *Mutation Research/Fundamental and Molecular Mechanisms of Mutagenesis* **2001,** *480*, 243-268.

(53). Jobin, C.; Bradham, C. A.; Russo, M. P.; Juma, B.; Narula, A. S.; Brenner, D. A.; Sartor, R. B., Curcumin blocks cytokine-mediated NF-κB activation and proinflammatory gene expression by inhibiting inhibitory factor I-κB kinase activity. *The Journal of Immunology* **1999,** *163*, 3474-3483.

(54). Huang, M.-T.; Lysz, T.; Ferraro, T.; Abidi, T. F.; Laskin, J. D.; Conney, A. H., Inhibitory effects of curcumin on in vitro lipoxygenase and cyclooxygenase activities in mouse epidermis. *Cancer Research* **1991,** *51*, 813-819.

(55). Cho, J.-W.; Lee, K.-S.; Kim, C.-W., Curcumin attenuates the expression of IL-1ß, IL-6, and TNF-α as well as cyclin E in TNF-α-treated HaCaT cells: NF-κB and MAPKs as potential upstream targets. *International Journal of Molecular Medicine* **2007,** *19*, 469-474.

(56). Karki, S. S.; Das, U.; Umemura, N.; Sakagami, H.; Iwamoto, S.; Kawase, M.; Balzarini, J.; De Clercq, E.; Dimmock, S. G.; Dimmock, J. R., 3,5-Bis(3-alkylaminomethyl-4-hydroxybenzylidene)-4-piperidones: A novel class of potent tumor-selective cytotoxins. *Journal of Medicinal Chemistry* **2016,** *59*, 763-769.

(57). Dimmock, J. R.; Arora, V. K.; Wonko, S. L.; Hamon, N. W.; Quail, J. W.; Jia, Z.; Warrington, R. C.; Fang, W. D.; Lee, J. S., 3,5-Bis-benzylidene-4-piperidones and related compounds with high activity towards P388 leukemia cells. *Drug Design and Delivery* **1990,** *6*, 183-194.

(58). Wike-Hooley, J. L.; van den Berg, A. P.; van der Zee, J.; Reinhold, H. S., Human tumour pH and its variation. *European Journal of Cancer and Clinical Oncology* **1985,** *21*, 785-791.

(59). Addala, E.; Rafiei, H.; Das, S.; Bandy, B.; Das, U.; Karki, S. S.; Dimmock, J. R., 3,5-Bis(3-dimethylaminomethyl-4-hydroxybenzylidene)-4-piperidone and related compounds induce glutathione oxidation and mitochondria-mediated cell death in HCT-116 colon cancer cells. *Bioorganic & Medicinal Chemistry Letters* **2017,** *27*, 3669-3673.

(60). Mutus, B.; Wagner, J. D.; Talpas, C. J.; Dimmock, J. R.; Phillips, O. A.; Reid, R. S., 1-*p*-Chlorophenyl-4, 4-dimethyl-5-diethylamino-1-penten-3-one hydrobromide, a sulfhydryl-specific compound which reacts irreversibly with protein thiols but reversibly with small molecular weight thiols. *Analytical Biochemistry* **1989,** *177*, 237-243.

(61). Mathews, S.; Rao, M., Interaction of curcumin with glutathione. *International Journal of Pharmaceutics* **1991,** *76*, 257-259.

(62). Awasthi, S.; Pandya, U.; Singhal, S. S.; Lin, J. T.; Thiviyanathan, V.; Seifert, W. E.; Awasthi, Y. C.; Ansari, G., Curcumin–glutathione interactions and the role of human glutathione S-transferase P1-1. *Chemico-Biological Interactions* **2000,** *128*, 19-38.

(63). Dimmock, J. R.; Kumar, P.; Nazarali, A. J.; Motaganahalli, N. L.; Kowalchuk, T. P.; Beazely, M. A.; Quail, J. W.; Oloo, E. O.; Allen, T. M.; Szydlowski, J., Cytotoxic 2, 6-bis

(arylidene) cyclohexanones and related compounds. *European Journal of Medicinal Chemistry* **2000,** *35*, 967-977.

(64). Dimmock, J. R.; Padmanilayam, M. P.; Zello, G. A.; Nienaber, K. H.; Allen, T. M.; Santos, C. L.; De Clercq, E.; Balzarini, J.; Manavathu, E. K.; Stables, J. P., Cytotoxic analogues of 2, 6-bis (arylidene) cyclohexanones. *European Journal of Medicinal Chemistry* **2003,** *38*, 169-177.

(65). Dimmock, J. R.; Padmanilayam, M. P.; Puthucode, R. N.; Nazarali, A. J.; Motaganahalli, N. L.; Zello, G. A.; Quail, J. W.; Oloo, E. O.; Kraatz, H.-B.; Prisciak, J. S., A conformational and structure− activity relationship study of cytotoxic 3, 5-bis (arylidene)-4-piperidones and related N-acryloyl analogues. *Journal of Medicinal Chemistry* **2001,** *44*, 586-593.

(66). Mutus, B.; Wagner, J. D.; Talpas, C. J.; Dimmock, J. R.; Phillips, O. A.; Reid, R. S., 1-p-Chlorophenyl-4,4-dimethyl-5-diethylamino-1-penten-3-one hydrobromide, a sulfhydryl-specific compound which reacts irreversibly with protein thiols but reversibly with small molecular weight thiols. *Analytical Biochemistry* **1989,** *177*, 237-243.

(67). Dimmock, J. R., Raghavan, S.K., Logan, B.M. and Bigam, G.E., Antileukemic Evaluation of Some Mannich Bases Derived from 2-Arylidene-1,3-diketones. *European Journal of Medicinal Chemistry* **1983,** *18*, 248-254.

(68). Ahmad, S.; Okine, L.; Wood, R.; Aljian, J.; Vistica, D. T., γ-glutamyl transpeptidase (γ-GT) and maintenance of thiol pools in tumor cells resistant to alkylating agents. *Journal of Cellular Physiology* **1987,** *131*, 240-246.

(69). Britten, R. A.; Green, J. A.; Warenius, H. M., Cellular glutathione (GSH) and glutathione S-transferase (GST) activity in human ovarian tumor biopsies following exposure to alkylating agents. *International Journal of Radiation Oncology-Biology-Physics* **1992,** *24*, 527-531.

(70). Schanenstein, E.; Nöhammer, G.; Rauch, H. J.; Kresbach, H., Significant decreases in the intensity of staining for proteins and protein thiols in basal-cell epitheliomas (basaliomas) as compared to normal skin. *Histochemistry* **1985,** *83*, 451-454.

(71). Pati, H. N.; Das, U.; Sharma, R. K.; Dimmock, J. R., Cytotoxic thiol alkylators. *Mini Reviews in Medicinal Chemistry* **2007,** *7*, 131-139.

(72). Das, S. Cytotoxic thiol alkylators containing the 1,5-diaryl-3-oxo-1,4-pentadienyl pharmacophore. University of Saskatchewan, Saskatoon, **2012**.

(73). Dimmock, J. R.; Sidhu, K. K.; Chen, M.; Reid, R. S.; Allen, T. M.; Kao, G. Y.; Truitt, G. A., Evaluation of some Mannich bases of cycloalkanones and related compounds for cytotoxic activity. *European Journal of Medicinal Chemistry* **1993,** *28*, 313-322.

(74). Hansson, J.; Berhane, K.; Castro, V. M.; Jungnelius, U.; Mannervik, B.; Ringborg, U., Sensitization of human melanoma cells to the cytotoxic effect of melphalan by the glutathione transferase inhibitor ethacrynic acid. *Cancer Research* **1991,** *51*, 94-98.

(75). Nagourney, R. A.; Messenger, J. C.; Kern, D. H.; Weisenthal, L. M., Enhancement of anthracycline and alkylator cytotoxicity by ethacrynic acid in primary cultures of human tissues. *Cancer Chemotherapy and Pharmacology* **1990,** *26*, 318-322.

(76). Bordoloi, D.; Kunnumakkara, A. B., Chapter 2 - The potential of curcumin: A multitargeting agent in cancer cell chemosensitization. In *Role of Nutraceuticals in Cancer Chemosensitization*, Bharti, A. C.; Aggarwal, B. B., Eds. Academic Press: **2018**; Vol. 2, pp 31-60.

(77). Dimmock, J. R.; Jha, A.; Zello, G. A.; Quail, J. W.; Oloo, E. O.; Nienaber, K. H.; Kowalczyk, E. S.; Allen, T. M.; Santos, C. L.; De Clercq, E., Cytotoxic N-[4-(3-aryl-3-oxo-1-propenyl) phenylcarbonyl]-3, 5-bis (phenylmethylene)-4-piperidones and related compounds. *European Journal of Medicinal Chemistry* **2002,** *37*, 961-972.

(78). Dimmock, J. R.; Padmanilyam, M. P.; Zello, G. A.; Quail, J. W.; Oloo, E. O.; Prisciak, J. S.; Kraatz, H.-B.; Cherkasov, A.; Lee, J. S.; Allen, T. M., Cytotoxic 1, 3-diarylidene-2-tetralones and related compounds. *European Journal of Medicinal Chemistry* **2002,** *37*, 813-824.

(79). Pati, H. N.; Das, U.; Quail, J. W.; Kawase, M.; Sakagami, H.; Dimmock, J. R., Cytotoxic 3,5-bis(benzylidene)piperidin-4-ones and N-acyl analogs displaying selective toxicity for malignant cells. *European Journal of Medicinal Chemistry* **2008,** *43*, 1-7.

(80). Dimmock, J. R.; Arora, V. K.; Duffy, M. J.; Reid, R. S.; Allen, T. M.; Kao, G. Y., Evaluation of some N-acyl analogues of 3, 5-bis (arylidene)-4-piperidones for cytotoxic activity. *Drug Design and Discovery* **1992,** *8*, 291-299.

(81). Das, U.; Alcorn, J.; Shrivastav, A.; Sharma, R. K.; De Clercq, E.; Balzarini, J.; Dimmock, J. R., Design, synthesis and cytotoxic properties of novel 1-[4-(2-alkylaminoethoxy) phenylcarbonyl]-3, 5-bis (arylidene)-4-piperidones and related compounds. *European Journal of Medicinal Chemistry* **2007,** *42*, 71-80.

(82). Das, U.; Sakagami, H.; Chu, Q.; Wang, Q.; Kawase, M.; Selvakumar, P.; Sharma, R. K.; Dimmock, J. R., 3,5-Bis(benzylidene)-1-[4-2-(morpholin-4-yl)ethoxyphenylcarbonyl]-4-piperidone hydrochloride: A lead tumor-specific cytotoxin which induces apoptosis and autophagy. *Bioorganic & Medicinal Chemistry Letters* **2010,** *20*, 912-917.

(83). Fong, W.-F.; Shen, X.-L.; Globisch, C.; Wiese, M.; Chen, G.-Y.; Zhu, G.-Y.; Yu, Z.-L.; Tse, A. K.-W.; Hu, Y.-J., Methoxylation of 3′,4′-aromatic side chains improves P-glycoprotein inhibitory and multidrug resistance reversal activities of 7,8-pyranocoumarin against cancer cells. *Bioorganic & Medicinal Chemistry* **2008,** *16*, 3694-3703.

(84). Sun, J.-f.; Hou, G.-g.; Zhao, F.; Cong, W.; Li, H.-j.; Liu, W.-s.; Wang, C., Synthesis, antiproliferative, and multidrug resistance reversal activities of heterocyclic α,β-unsaturated carbonyl compounds. *Chemical Biology & Drug Design* **2016,** *88*, 534-541.

(85). Jha, A.; Mukherjee, C.; Prasad, A. K.; Parmar, V. S.; Clercq, E. D.; Balzarini, J.; Stables, J. P.; Manavathu, E. K.; Shrivastav, A.; Sharma, R. K.; Nienaber, K. H.; Zello, G. A.; Dimmock, J.

R., E,E,E-1-(4-Arylamino-4-oxo-2-butenoyl)-3,5-bis(arylidene)-4-piperidones: A topographical study of some novel potent cytotoxins. *Bioorganic & Medicinal Chemistry* **2007,** *15*, 5854-5865.

(86). Yang, J. S.; Song, D.; Ko, W. J.; Kim, B.; Kim, B.-K.; Park, S.-K.; Won, M.; Lee, K.; Lee, K.; Kim, H. M.; Han, G., Synthesis and biological evaluation of novel aliphatic amido-quaternary ammonium salts for anticancer chemotherapy: Part II. *European Journal of Medicinal Chemistry* **2013,** *63*, 621-628.

(87). Wang, W.; Bai, Z.; Zhang, F.; Wang, C.; Yuan, Y.; Shao, J., Synthesis and biological activity evaluation of emodin quaternary ammonium salt derivatives as potential anticancer agents. *European Journal of Medicinal Chemistry* **2012,** *56*, 320-331.

(88). Song, D.; Yang, J. S.; Kim, S. J.; Kim, B.-K.; Park, S.-K.; Won, M.; Lee, K.; Kim, H. M.; Choi, K.-Y.; Lee, K.; Han, G., Design, synthesis and biological evaluation of novel aliphatic amido/sulfonamido-quaternary ammonium salts as antitumor agents. *Bioorganic & Medicinal Chemistry* **2013,** *21*, 788-794.

(89). Shao, J.; Zhang, F.; Bai, Z.; Wang, C.; Yuan, Y.; Wang, W., Synthesis and antitumor activity of emodin quaternary ammonium salt derivatives. *European Journal of Medicinal Chemistry* **2012,** *56*, 308-319.

(90). Das, S.; Das, U.; Selvakumar, P.; Sharma, R. K.; Balzarini, J.; De Clercq, E.; Molnár, J.; Serly, J.; Baráth, Z.; Schatte, G.; Bandy, B.; Gorecki, D. K. J.; Dimmock, J. R., 3,5-Bis(benzylidene)-4-oxo-1-phosphonopiperidines and related diethyl esters: Potent cytotoxins with multi-drug-resistance reverting properties. *ChemMedChem* **2009,** *4*, 1831-1840.

(91). Das, S.; Das, U.; Sakagami, H.; Hashimoto, K.; Kawase, M.; Gorecki, D. K. J.; Dimmock, J. R., Sequential cytotoxicity: A theory examined using a series of 3,5-bis(benzylidene)-1-diethylphosphono-4-oxopiperidines and related phosphonic acids. *Bioorganic & Medicinal Chemistry Letters* **2010,** *20*, 6464-6468.

(92). Singh, R. S. P.; Michel, D.; Das, U.; Dimmock, J. R.; Alcorn, J., Cytotoxic 1,5-diaryl-3-oxo-1,5-pentadienes: An assessment and comparison of membrane permeability using Caco-2 and MDCK monolayers. *Bioorganic & Medicinal Chemistry Letters* **2014,** *24*, 5199-5202.

(93). Makarov, M. V.; Rybalkina, E. Y.; Röschenthaler, G.-V.; Short, K. W.; Timofeeva, T. V.; Odinets, I. L., Design, cytotoxic and fluorescent properties of novel N-phosphorylalkyl substituted E,E-3,5-bis(arylidene)piperid-4-ones. *European Journal of Medicinal Chemistry* **2009,** *44*, 2135-2144.

(94). Makarov, M. V.; Leonova, E. S.; Rybalkina, E. Y.; Khrustalev, V. N.; Shepel, N. E.; Röschenthaler, G.-V.; Timofeeva, T. V.; Odinets, I. L., Methylenebisphosphonates with dienone pharmacophore: Synthesis, structure, antitumor and fluorescent properties. *Archiv der Pharmazie* **2012,** *345*, 349-359.

(95). Makarov, M. V.; Skvortsov, E. A.; Brel, V. K., Synthesis of diethyl (aryl)(4-oxopiperidin-1-yl)methylphosphonates. *Mendeleev Communications* **2015,** *25*, 232-233.

(96). Makarov, M. V.; Rybalkina, E. Y.; Anikina, L. V.; Pukhov, S. A.; Klochkov, S. G.; Mischenko, D. V.; Neganova, M. E.; Khrustalev, V. N.; Klemenkova, Z. S.; Brel, V. K., 1,5-Diaryl-3-oxo-1,4-pentadienes based on (4-oxopiperidin-1-yl)(aryl)methyl phosphonate scaffold: synthesis and antitumor properties. *Medicinal Chemistry Research* **2017,** *26*, 140-152.

(97). Sherr, C. J.; Bartek, J., Cell cycle–targeted cancer therapies. *Annual Review of Cancer Biology* **2017,** *1*, 41-57.

(98). Alberts B, J. A., Lewis J, et al Molecular Biology of the Cell. https://www.ncbi.nlm.nih.gov/books/NBK26894/ (accessed February 25, 2018).

(99). Gibbs, J. B., Mechanism-based target identification and drug discovery in cancer research. *Science* **2000,** *287*, 1969-1973.

(100). Kumar, S.; Ahmad, M.; Waseem, M.; Pandey, A., Drug targets for cancer treatment: An overview. *Medicinal Chemistry* **2015,** *5*, 115-123.

(101). Parakh, S.; King, D.; Gan, H. K.; Scott, A. M., Current Development of Monoclonal Antibodies in Cancer Therapy. In *Current Immunotherapeutic Strategies in Cancer*, Theobald, M., Ed. Springer International Publishing: Cham, **2020**; pp 1-70.

(102). Chen, R.; Hou, J.; Newman, E.; Kim, Y.; Donohue, C.; Liu, X.; Thomas, S. H.; Forman, S. J.; Kane, S. E., CD30 Downregulation, MMAE Resistance, and MDR1 Upregulation are all associated with resistance to Brentuximab Vedotin. *Molecular Cancer Therapeutics* **2015,** *14*, 1376-1384.

(103). Prince, H. M.; Newland, K. M., Denileukin diftitox for the treatment of cutaneous T-cell lymphoma. *Expert Opinion on Orphan Drugs* **2014,** *2*, 625-634.

(104). Abramson, R. G. Overview of Targeted Therapies for Cancer. https://www.mycancergenome.org/content/molecular-medicine/overview-of-targeted-therapies-for-cancer (accessed July 14, 2018).

(105). Jeswani, G.; Paul, S. D., Chapter 15 - Recent advances in the delivery of chemotherapeutic agents. In *Nano- and Microscale Drug Delivery Systems*, Grumezescu, A. M., Ed. Elsevier: 2017; pp 281-298.

(106). Engel, P.; Boumsell, L.; Balderas, R.; Bensussan, A.; Gattei, V.; Horejsi, V.; Jin, B.-Q.; Malavasi, F.; Mortari, F.; Schwartz-Albiez, R.; Stockinger, H.; van Zelm, M. C.; Zola, H.; Clark, G., CD Nomenclature 2015: Human leukocyte differentiation antigen workshops as a driving force in immunology. *The Journal of Immunology* **2015,** *195*, 4555-4563.

(107). Khalili, A.; Ahmad, M., A review of cell adhesion studies for biomedical and biological applications. *International Journal of Molecular Sciences* **2015,** *16*, 18149-18184.

(108). Girolamo, R.; Rosa, P.; Eustachio, R.; Severino, M.; Paolo, V.; Domenico, R., Vascular Endothelial Growth Factor (VEGF) as a target of Bevacizumab in cancer: From the biology to the clinic. *Current Medicinal Chemistry* **2006,** *13*, 1845-1857.

(109). Johnson, K. E.; Wilgus, T. A., Vascular endothelial growth factor and angiogenesis in the regulation of cutaneous wound repair. *Advances in Wound Care* **2014,** *3*, 647-661.

(110). Fadaka, A.; Ajiboye, B.; Ojo, O.; Adewale, O.; Olayide, I.; Emuowhochere, R., Biology of glucose metabolization in cancer cells. *Journal of Oncological Sciences* **2017,** *3*, 45-51.

(111). Abhinand, C. S.; Raju, R.; Soumya, S. J.; Arya, P. S.; Sudhakaran, P. R., VEGF-A/VEGFR2 signaling network in endothelial cells relevant to angiogenesis. *Journal of Cell Communication and Signaling* **2016,** *10*, 347-354.

(112). El-Kenawi, A. E.; El-Remessy, A. B., Angiogenesis inhibitors in cancer therapy: mechanistic perspective on classification and treatment rationales. *British Journal of Pharmacology* **2013,** *170*, 712-729.

(113). Lugano, R.; Ramachandran, M.; Dimberg, A., Tumor angiogenesis: causes, consequences, challenges and opportunities. *Cellular and Molecular Life Sciences* **2020,** *77*, 1745-1770.

(114). Hall, A., The cytoskeleton and cancer. *Cancer and Metastasis Reviews* **2009,** *28*, 5-14.

(115). Jordan, M. A.; Wilson, L., Microtubules as a target for anticancer drugs. *Nature Reviews Cancer* **2004,** *4*, 253-265.

(116). Dumontet, C.; Jordan, M. A., Microtubule-binding agents: a dynamic field of cancer therapeutics. *Nature Reviews Drug Discovery* **2010,** *9*, 790-803.

(117). AL-Sharif, M. M. Z., Studies on the genotoxic effects of anticancer drug Paclitaxel (Taxol) in mice. *World Applied Sciences Journal* **2012,** *16*, 989-997.

(118). Lopus, M., Mechanism of mitotic arrest induced by dolastatin 15 involves loss of tension across kinetochore pairs. *Molecular and Cellular Biochemistry* **2013,** *382*, 93-102.

(119). Ding, Z.; Li, F.; Zhong, C.; Li, F.; Liu, Y.; Wang, S.; Zhao, J.; Li, W., Structure-based design and synthesis of novel furan-diketopiperazine-type derivatives as potent microtubule inhibitors for treating cancer. *Bioorganic & Medicinal Chemistry* **2020,** *28*, 115435.

(120). Martinez, R.; Chacon-Garcia, L., The search of DNA-intercalators as antitumoral drugs: What it worked and what did not work. *Current Medicinal Chemistry* **2005,** *12*, 127-151.

(121). Kumar, S.; Ahmad, M.; Waseem, M.; Pandey, A., Drug targets for cancer treatment: An overview. *Medicinal Chemistry Reviews* **2015,** *5*, 115-123.

(122). Snyder, R. D., Assessment of atypical DNA intercalating agents in biological and in silico systems. *Mutation Research/Fundamental and Molecular Mechanisms of Mutagenesis* **2007,** *623*, 72-82.

(123). Bischoff, G. H., S., DNA-Binding of drugs used in medicinal therapies. *Current Medicinal Chemistry* **2002,** *9*, 321-348.

(124). Nazarov, A. A.; Meier, S. M.; Zava, O.; Nosova, Y. N.; Milaeva, E. R.; Hartinger, C. G.; Dyson, P. J., Protein ruthenation and DNA alkylation: chlorambucil-functionalized RAPTA complexes and their anticancer activity. *Dalton Transactions* **2015,** *44*, 3614–3623.

(125). Emadi, A.; Jones, R. J.; Brodsky, R. A., Cyclophosphamide and cancer: Golden anniversary. *Nature Reviews Clinical Oncology* **2009,** *6*, 638-647.

(126). Meister, A., Glutathione metabolism. *Methods in Enzymology* **1995,** *251*, 3-7.

(127). Ketterer, B., Protective role of glutathione and glutathione transferases in mutagenesis and carcinogenesis. *Mutation Research/Fundamental and Molecular Mechanisms of Mutagenesis* **1988,** *202*, 343-361.

(128). Jayawardana, S. A. S.; Samarasekera, J. K. R. R.; Hettiarachchi, G. H. C. M.; Gooneratne, M. J.; Choudhary, M. I.; Imad, R.; Naz, A., Glutathione S-Transferase and β-Glucuronidase enzymes inhibitory and cytotoxic activities of ethanolic and methanolic extracts of Sri Lankan finger millet (Eleusine coracana (L.) Gaertn.) varieties. *South Asian Research Journal of Natural Products* **2020,** *3*, 1-9.

(129). Calvert, P.; Yao, K.-S.; Hamilton, T. C.; O'Dwyer, P. J., Clinical studies of reversal of drug resistance based on glutathione. *Chemico-Biological Interactions* **1998,** *111*, 213-224.

(130). Estrela, J. M.; Ortega, A.; Obrador, E., Glutathione in cancer biology and therapy. *Critical Reviews in Clinical Laboratory Sciences* **2006,** *43*, 143-181.

(131). O'Brien, M.; Tew, K., Glutathione and related enzymes in multidrug resistance. *European Journal of Cancer* **1996,** *32*, 967-978.

(132). Dethmers, J. K.; Meister, A., Glutathione export by human lymphoid cells: depletion of glutathione by inhibition of its synthesis decreases export and increases sensitivity to irradiation. *Proceedings of the National Academy of Sciences* **1981,** *78*, 7492-7496.

(133). Anderson, M. E.; Powrie, F.; Puri, R. N.; Meister, A., Glutathione monoethyl ester: preparation, uptake by tissues, and conversion to glutathione. *Archives of Biochemistry and Biophysics* **1985,** *239*, 538-548.

(134). Ozols, R. F.; Louie, K. G.; Plowman, J.; Behrens, B. C.; Fine, R. L.; Dykes, D.; Hamilton, T. C., Enhanced melphalan cytotoxicity in human ovarian cancer in vitro and in tumor-bearing nude mice by buthionine sulfoximine depletion of glutathione. *Biochemical Pharmacology* **1987,** *36*, 147-153.

(135). Skapek, S. X.; Colvin, O. M.; Griffith, O. W.; Groothuis, D. R.; Colapinto, E. V.; Lee, Y.; Hilton, J.; Elion, G. B.; Bigner, D. D.; Friedman, H. S., Buthionine sulfoximine-mediated depletion of glutathione in intracranial human glioma-derived xenografts. *Biochemical Pharmacology* **1988,** *37*, 4313-4317.

(136). Mitchell, J. B.; Phillips, T. L.; Degraff, W.; Carmichael, J.; Rajpal, R. K.; Russo, A., The relationship of SR-2508 sensitizer enhancement ratio to cellular glutathione levels in human tumor cell lines. *International Journal of Radiation Oncology-Biology-Physics* **1986,** *12*, 1143-1146.

(137). Russo, A.; DeGraff, W.; Friedman, N.; Mitchell, J. B., Selective modulation of glutathione levels in human normal versus tumor cells and subsequent differential response to chemotherapy drugs. *Cancer Research* **1986,** *46*, 2845-2848.

(138). Russo, A.; Mitchell, J. B.; McPherson, S.; Friedman, N., Alteration of bleomycin cytotoxicity by glutathione depletion or elevation. *International Journal of Radiation Oncology-Biology-Physics* **1984,** *10*, 1675-1678.

(139). Meister, A., On the discovery of glutathione. *Trends in biochemical sciences* **1988,** *13*, 185-188.

(140). Messina, J. P.; Lawrence, D. A., Cell cycle progression of glutathione-depleted human peripheral blood mononuclear cells is inhibited at S phase. *The Journal of Immunology* **1989,** *143*, 1974-1981.

(141). Lu, S. C.; Ge, J., Loss of suppression of GSH synthesis at low cell density in primary cultures of rat hepatocytes. *American Journal of Physiology-Cell Physiology* **1992,** *263*, C1181-C1189.

(142). Benlloch, M.; Ortega, A.; Ferrer, P.; Segarra, R.; Obrador, E.; Asensi, M.; Carretero, J.; Estrela, J. M., Acceleration of glutathione efflux and inhibition of γ-glutamyltranspeptidase sensitize metastatic B16 melanoma cells to endothelium-induced cytotoxicity. *Journal of Biological Chemistry* **2005,** *280*, 6950-6959.

(143). Kuo, M. T.; Bao, J.-j.; Furuichi, M.; Yamane, Y.; Gomi, A.; Savaraj, N.; Masuzawa, T.; Ishikawa, T., Frequent coexpression of MRP/GS-X pump and γ-glutamylcysteine synthetase mRNA in drug-resistant cells, untreated tumor cells, and normal mouse tissues. *Biochemical Pharmacology* **1998,** *55*, 605-615.

(144). Oguri, T.; Fujiwara, Y.; Isobe, T.; Katoh, O.; Watanabe, H.; Yamakido, M., Expression of gamma-glutamylcysteine synthetase (gamma-GCS) and multidrug resistance-associated protein (MRP), but not human canalicular multispecific organic anion transporter (cMOAT), genes correlates with exposure of human lung cancers to platinum drugs. *British Journal of Cancer* **1998,** *77*, 1089-1096.

(145). Britten, R. A.; Green, J. A.; Warenius, H. M., Cellular glutathione (GSH) and glutathione S-transferase (GST) activity in human ovarian tumor biopsies following exposure to alkylating agents. *International Journal of Radiation Oncology Biology Physics* **1992,** *24*, 527-531.

(146). Ojeda, V. J.; Shilkin, K.; Walters, M.-I., Premalignant epithelial lesions of the gall bladder: a prospective study of 120 cholecystectomy specimens. *Pathology* **1985,** *17*, 451-454.

(147). Stern, H., Sulfhydryl groups and cell division. *Science* **1956,** *124*, 1292-1293.

(148). Roman, G., Mannich bases in medicinal chemistry and drug design. *European Journal of Medicinal Chemistry* **2015,** *89*, 743-816.

(149). Siedel, W.; Soder, A.; Lindner, F., Amino methylation of tetracyclines; chemistry of reverin. *Münchener medizinische Wochenschrift (1950)* **1958,** *100*, 661-663.

(150). Saab, A. N.; Sloan, K. B.; Beall, H. D.; Villanueva, R., Effect of aminomethyl (*N*-Mannich base) derivatization on the ability of S6 acetyloxymethyl-S-mercaptopurine prodrug to deliver 6-mercaptopurine through hairless mouse skin. *Journal of Pharmaceutical Sciences* **1990,** *79*, 1099-1104.

(151). Huttunen, K. M.; Rautio, J., Prodrugs - An efficient way to breach delivery and targeting barriers. *Current Topics in Medicinal Chemistry* **2011,** *11*, 2265-2287.

(152). Ahmad, A.; Mahal, K.; Padhye, S.; Sarkar, F. H.; Schobert, R.; Biersack, B., New ferrocene modified lawsone Mannich bases with anti-proliferative activity against tumor cells. *Journal of Saudi Chemical Society* **2017,** *21*, 105-110.

(153). Tandon, V. K.; Yadav, D. B.; Chaturvedi, A. K.; Shukla, P. K., Synthesis of (1,4)-naphthoquinono-[3,2-c]-1H-pyrazoles and their (1,4)-naphthohydroquinone derivatives as antifungal, antibacterial, and anticancer agents. *Bioorganic & Medicinal Chemistry Letters* **2005,** *15*, 3288-3291.

(154). Baiju, T. V.; Almeida, R. G.; Sivanandan, S. T.; de Simone, C. A.; Brito, L. M.; Cavalcanti, B. C.; Pessoa, C.; Namboothiri, I. N. N.; da Silva Júnior, E. N., Quinonoid compounds via reactions of lawsone and 2-aminonaphthoquinone with α-bromonitroalkenes and nitroallylic acetates: Structural diversity by C-ring modification and cytotoxic evaluation against cancer cells. *European Journal of Medicinal Chemistry* **2018,** *151*, 686-704.

(155). Al Nasr, I.; Jentzsch, J.; Winter, I.; Schobert, R.; Ersfeld, K.; Koko, W. S.; Mujawah, A. A. H.; Khan, T. A.; Biersack, B., Antiparasitic activities of new lawsone Mannich bases. *Archiv der Pharmazie* **2019,** *352*, 1900128.

(156). Nariya, P.; Shukla, F.; Vyas, H.; Devkar, R.; Thakore, S., Synthesis and characterization of Mannich bases of lawsone and their anticancer activity. *Synthetic Communications* **2020,** *50*, 1724-1735.

(157). Hossain, M.; Das, U.; Dimmock, J. R., Recent advances in α,β-unsaturated carbonyl compounds as mitochondrial toxins. *European Journal of Medicinal Chemistry* **2019,** *183*, 111687.

(158). Dimmock, J. R.; Elias, D. W.; Beazely, M. A.; Kandepu, N. M., Bioactivities of chalcones. *Current Medicinal Chemistry* **1999,** *6*, 1125-1149.

(159). Dimmock, J. R.; Kandepu, N. M.; Nazarali, A. J.; Motaganahalli, N. L.; Kowalchuk, T. P.; Pugazhenthi, U.; Prisciak, J. S.; Quail, J. W.; Allen, T. M.; LeClerc, R.; Santos, C. L.; De Clercq, E.; Balzarini, J., Sequential cytotoxicity: A theory evaluated using novel 2-[4-(3-aryl-2-

propenoyloxy)phenylmethylene]cyclohexanones and related compounds. *Journal of Medicinal Chemistry* **2000,** *43*, 3933-3940.

(160). Dimmock, J. R.; Vashishtha, S. C.; Patil, S. A.; Udupa, N.; Dinesh, S. B.; Devi, P. U.; Kamath, R., Cytotoxic and anticancer activities of some 1-aryl-2-dimethylaminomethyl- 2-propen-1-one hydrochlorides. *Pharmazie* **1998,** *53*, 702-706.

(161). Dimmock, J. R.; Kandepu, N. M.; Hetherington, M.; Quail, J. W.; Pugazhenthi, U.; Sudom, A. M.; Chamankhah, M.; Rose, P.; Pass, E.; Allen, T. M.; Halleran, S.; Szydlowski, J.; Mutus, B.; Tannous, M.; Manavathu, E. K.; Myers, T. G.; De Clercq, E.; Balzarini, J., Cytotoxic activities of Mannich bases of chalcones and related compounds. *Journal of Medicinal Chemistry* **1998,** *41*, 1014-1026.

(162). Dimmock, J. R., Kumar, P., Anticancer and cytotoxic properties of Mannich bases. *Current Medicinal Chemistry* **1997,** *4*, 1-22.

(163). Haudecoeur, R.; Boumendjel, A., Recent advances in the medicinal chemistry of aurones. *Current Medicinal Chemistry* **2012,** *19*, 2861-2875.

(164). Sim, H. M.; Loh, K. Y.; Yeo, W. K.; Lee, C. Y.; Go, M. L., Aurones as modulators of ABCG2 and ABCB1: Synthesis and Structure-Activity Relationships. *ChemMedChem* **2011,** *6*, 713-724.

(165). Popova, A. V.; Frasinyuk, M. S.; Bondarenko, S. P.; Zhang, W.; Xie, Y.; Martin, Z. M.; Cai, X.; Fiandalo, M. V.; Mohler, J. L.; Liu, C.; Watt, D. S.; Sviripa, V. M., Efficient synthesis of aurone Mannich bases and evaluation of their antineoplastic activity in PC-3 prostate cancer cells. *Chemical Papers* **2018,** *72*, 2443-2456.

(166). Tugrak, M.; Gul, H. I.; Sakagami, H.; Mete, E., Synthesis and anticancer properties of mono Mannich bases containing vanillin moiety. *Medicinal Chemistry Research* **2017,** *26*, 1528-1534.

(167). Das, S.; Das, U.; Michel, D.; Gorecki, D. K. J.; Dimmock, J. R., Novel 3,5-bis(arylidene)-4-piperidone dimers: Potent cytotoxins against colon cancer cells. *European Journal of Medicinal Chemistry* **2013,** *64*, 321-328.

(168). G.M., C., The Cell: A Molecular Approach. In *Mitochondria* [Online] Sinauer Associates: Sunderland (MA), 2000. https://www.ncbi.nlm.nih.gov/books/NBK9896/ (accessed February 26, 2018).

(169). D, M. W. Mitochondria. https://micro.magnet.fsu.edu/cells/mitochondria/mitochondria.html (accessed February 26, 2018).

(170). Rogers, K. Mitochondrion. https://www.britannica.com/science/mitochondrion (accessed June 26, 2018).

(171). Scitable: Nature Education. https://www.nature.com/scitable/topicpage/mitochondria-14053590 (accessed May 18, 2018).

(172). Sakamuru, S.; Attene-Ramos, M. S.; Xia, M., Mitochondrial membrane potential assay. *Methods in Molecular Biology* **2016,** *1473*, 17-22.

(173). Mitchell, P., Coupling of phosphorylation to electron and hydrogen transfer by a chemi-osmotic type of mechanism. *Nature* **1961,** *191*, 144-8.

(174). Perry, S. W.; Norman, J. P.; Barbieri, J.; Brown, E. B.; Gelbard, H. A., Mitochondrial membrane potential probes and the proton gradient: a practical usage guide. *BioTechniques* **2011,** *50*, 98-115.

(175). Pieczenik, S. R.; Neustadt, J., Mitochondrial dysfunction and molecular pathways of disease. *Experimental and Molecular Pathology* **2007,** *83*, 84-92.

(176). Lemasters, J. J.; Qian, T.; He, L.; Kim, J.-S.; Elmore, S. P.; Cascio, W. E.; Brenner, D. A., Role of mitochondrial inner membrane permeabilization in necrotic cell death, apoptosis, and autophagy. *Antioxidants & Redox Signaling* **2002,** *4*, 769-781.

(177). Springett, R., Novel methods for measuring the mitochondrial membrane potential. In *Mitochondrial Medicine: Volume I, Probing Mitochondrial Function*, Weissig, V.; Edeas, M., Eds. Springer New York: New York, NY, **2015**; pp 195-202.

(178). Fantin, V. R.; Berardi, M. J.; Scorrano, L.; Korsmeyer, S. J.; Leder, P., A novel mitochondriotoxic small molecule that selectively inhibits tumor cell growth. *Cancer Cell* **2002,** *2*, 29-42.

(179). Modica-Napolitano, J. S.; Aprille, J. R., Delocalized lipophilic cations selectively target the mitochondria of carcinoma cells. *Advanced Drug Delivery Reviews* **2001,** *49*, 63-70.

(180). Bagkos, G.; Koufopoulos, K.; Piperi, C., A new model for mitochondrial membrane potential production and storage. *Medical Hypotheses* **2014,** *83*, 175-181.

(181). Georgios, B.; Kostas, K.; Christina, P., ATP synthesis revisited: New avenues for the management of mitochondrial diseases. *Current Pharmaceutical Design* **2014,** *20*, 4570-4579.

(182). Heerdt, B. G.; Houston, M. A.; Augenlicht, L. H., The intrinsic mitochondrial membrane potential of colonic carcinoma cells is linked to the probability of tumor progression. *Cancer Research* **2005,** *65*, 9861-9867.

(183). Heerdt, B. G.; Houston, M. A.; Augenlicht, L. H., Growth properties of colonic tumor cells are a function of the intrinsic mitochondrial membrane potential. *Cancer Research* **2006,** *66*, 1591-1596.

(184). Houston, M. A.; Augenlicht, L. H.; Heerdt, B. G., Stable differences in intrinsic mitochondrial membrane potential of tumor cell subpopulations reflect phenotypic heterogeneity. *International Journal of Cell Biology* **2011,** *2011*, 1-11.

(185). Fantin, V. R.; St-Pierre, J.; Leder, P., Attenuation of LDH-A expression uncovers a link between glycolysis, mitochondrial physiology, and tumor maintenance. *Cancer Cell* **2006,** *9*, 425-434.

(186). Bonnet, S.; Archer, S. L.; Allalunis-Turner, J.; Haromy, A.; Beaulieu, C.; Thompson, R.; Lee, C. T.; Lopaschuk, G. D.; Puttagunta, L.; Bonnet, S.; Harry, G.; Hashimoto, K.; Porter, C. J.; Andrade, M. A.; Thebaud, B.; Michelakis, E. D., A Mitochondria-K+ Channel axis is suppressed in cancer and its normalization promotes apoptosis and inhibits cancer growth. *Cancer Cell* **2007,** *11*, 37-51.

(187). Ross, Meredith F.; Da Ros, T.; Blaikie, Frances H.; Prime, Tracy A.; Porteous, Carolyn M.; Severina, Inna I.; Skulachev, Vladimir P.; Kjaergaard, Henrik G.; Smith, Robin A J.; Murphy, Michael P., Accumulation of lipophilic dications by mitochondria and cells. *Biochemical Journal* **2006,** *400*, 199-208.

(188). Koya, K.; Li, Y.; Wang, H.; Ukai, T.; Tatsuta, N.; Kawakami, M.; Shishido, T.; Chen, L. B., MKT-077, a novel rhodacyanine dye in clinical trials, exhibits anticarcinoma activity in preclinical studies based on selective mitochondrial accumulation. *Cancer Research* **1996,** *56*, 538-543.

(189). Britten, C. D.; Rowinsky, E. K.; Baker, S. D.; Weiss, G. R.; Smith, L.; Stephenson, J.; Rothenberg, M.; Smetzer, L.; Cramer, J.; Collins, W.; Von Hoff, D. D.; Eckhardt, S. G., A phase I and pharmacokinetic study of the mitochondrial-specific rhodacyanine dye analog MKT 077. *Clinical Cancer Research* **2000,** *6*, 42-49.

(190). Zielonka, J.; Joseph, J.; Sikora, A.; Hardy, M.; Ouari, O.; Vasquez-Vivar, J.; Cheng, G.; Lopez, M.; Kalyanaraman, B., Mitochondria-targeted triphenylphosphonium based compounds: Syntheses, mechanisms of action, and therapeutic and diagnostic applications. *Chemical Reviews* **2017,** *117*, 10043-10120.

(191). Lin, M. T.; Beal, M. F., Mitochondrial dysfunction and oxidative stress in neurodegenerative diseases. *Nature* **2006,** *443*, 787-795.

(192). Cadonic, C.; Sabbir, M. G.; Albensi, B. C., Mechanisms of mitochondrial dysfunction in Alzheimer's disease. *Molecular Neurobiology* **2016,** *53*, 6078-6090.

(193). Cheng, G.; Zielonka, J.; McAllister, D.; Hardy, M.; Ouari, O.; Joseph, J.; Dwinell, M. B.; Kalyanaraman, B., Antiproliferative effects of mitochondria-targeted cationic antioxidants and analogs: Role of mitochondrial bioenergetics and energy-sensing mechanism. *Cancer Letters* **2015,** *365*, 96-106.

(194). Sassi, N.; Mattarei, A.; Azzolini, M.; Szabo, I.; Paradisi, C.; Zoratti, M.; Biasutto, L., Cytotoxicity of mitochondria-targeted resveratrol derivatives: Interactions with respiratory chain complexes and ATP synthase. *Biochimica et Biophysica Acta (BBA)-Bioenergetics* **2014,** *1837*, 1781-1789.

(195). Rao, V. A.; Klein, S. R.; Bonar, S. J.; Zielonka, J.; Mizuno, N.; Dickey, J. S.; Keller, P. W.; Joseph, J.; Kalyanaraman, B.; Shacter, E., The antioxidant transcription factor Nrf2 negatively regulates autophagy and growth arrest induced by the anticancer redox agent mitoquinone. *The Journal of Biological Chemistry* **2010,** *285*, 34447-34459.

(196). Hiller, R.; Schaefer, A.; Zibirre, R.; Kaback, H. R.; Koch, G., Factors influencing the accumulation of tetraphenylphosphonium cation in HeLa cells. *Molecular and Cellular Biology* **1984,** *4*, 199-202.

(197). Rottenberg, H., Membrane potential and surface potential in mitochondria: Uptake and binding of lipophilic cations. *The Journal of Membrane Biology* **1984,** *81*, 127-138.

(198). Flewelling, R. F.; Hubbell, W. L., Hydrophobic ion interactions with membranes. Thermodynamic analysis of tetraphenylphosphonium binding to vesicles. *Biophysical Journal* **1986,** *49*, 531-540.

(199). Ono, A.; Miyauchi, S.; Demura, M.; Asakura, T.; Kamo, N., Activation energy for permeation of phosphonium cations through phospholipid bilayer membrane. *Biochemistry* **1994,** *33*, 4312-4318.

(200). Wu, J.; Zhang, Y.; Cai, Y.; Wang, J.; Weng, B.; Tang, Q.; Chen, X.; Pan, Z.; Liang, G.; Yang, S., Discovery and evaluation of piperid-4-one-containing mono-carbonyl analogs of curcumin as anti-inflammatory agents. *Bioorganic & Medicinal Chemistry* **2013,** *21*, 3058-3065.

(201). Motohashi, N.; Wakabayashi, H.; Kurihara, T.; Takada, Y.; Maruyama, S.; Sakagami, H.; Nakashima, H.; Tani, S.; Shirataki, Y.; Kawase, M.; Wolfard, K.; Molnár, J., Cytotoxic and multidrug resistance reversal activity of a vegetable, 'Anastasia Red', a variety of sweet pepper. *Phytotherapy Research* **2003,** *17*, 348-52.

(202). Lema, C.; Varela-Ramirez, A.; Aguilera, R. J., Differential nuclear staining assay for high-throughput screening to identify cytotoxic compounds. *Current cellular biochemistry* **2011,** *1*, 1-14.

(203). Santiago-Vázquez, Y.; Das, U.; Varela-Ramirez, A.; Baca, S. T.; Ayala-Marin, Y.; Lema, C.; Das, S.; Baryyan, A.; Dimmock, J. R.; Aguilera, R. J., Tumor-selective cytotoxicity of a novel pentadiene analogue on human leukemia/ lymphoma cells. *Clinical cancer drugs* **2016,** *3*, 138-146.

(204). Varela-Ramirez, A.; Costanzo, M.; Carrasco, Y. P.; Pannell, K. H.; Aguilera, R. J., Cytotoxic effects of two organotin compounds and their mode of inflicting cell death on four mammalian cancer cells. *Cell biology and toxicology* **2011,** *27*, 159-168.

(205). Hansch, C.; Leo, A. J., *Substituent constants for correlation analysis in chemistry and biology*. John Wiley and Sons: New York, **1979**, p. 49.

(206). Taft, R. W. Jr., *Separation of polar, steric and resonance effects in reactivity, In : Steric effects in organic chemistry*. Newman, M. S. Ed., John Wiley and Sons: New York, **1956**, p. 591.

(207). Blankson, G.; Parhi, A. K.; Kaul, M.; Pilch, D. S.; LaVoie, E. J., Structure-activity relationships of potentiators of the antibiotic activity of clarithromycin against Escherichia coli. *European Journal of Medicinal Chemistry* **2019,** *178*, 30-38.

(208). Lema, C.; Varela-Ramirez, A.; Aguilera, R. J., Differential nuclear staining assay for high-throughput screening to identify cytotoxic compounds. *Current Celularl Biochemistry* **2011,** *1*, 1-14.

(209). Hassner, A.; Mead, T. C., The stereochemistry of 2-benzalcyclohexanones and 2-benzalcyclopentanones. *Tetrahedron* **1964,** *20*, 2201-2210.

(210). Lu, Y.; Chen, J.; Xiao, M.; Li, W.; Miller, D. D., An overview of tubulin inhibitors that interact with the colchicine binding site. *Pharmaceutical Research* **2012,** *29*, 2943-71.

(211). Xu, Y.; Sheng, C.; Wang, W.; Che, X.; Cao, Y.; Dong, G.; Wang, S.; Ji, H.; Miao, Z.; Yao, J.; Zhang, W., Structure-based rational design, synthesis and antifungal activity of oxime-containing azole derivatives. *Bioorganic & Medicinal Chemistry Letters* **2010,** *20*, 2942-2945.

(212). Sivandzade, F.; Bhalerao, A.; Cucullo, L., Analysis of the mitochondrial membrane potential using the cationic JC-1 dye as a sensitive fluorescent probe. *Bio-protocol* **2019,** *9*, 3128.

(213). Chabner, B. A., NCI-60 cell line screening: A radical departure in its time. *JNCI: Journal of the National Cancer Institute* **2016,** *108*.

(214). Amslinger, S., The tunable functionality of alpha,beta-unsaturated carbonyl compounds enables their differential application in biological systems. *ChemMedChem* **2010,** *5*, 351-6.

(215). Boyd, M. R.; Paull, K. D., Some practical considerations and applications of the national cancer institute in vitro anticancer drug discovery screen. *Drug Development Research* **1995,** *34*, 91-109.

(216). Grever, M. R.; Schepartz, S. A.; Chabner, B. A., The National Cancer Institute: Cancer drug discovery and development program. *Seminars in Oncology* **1992,** *19*, 622-38.

(217). Santiago-Vazquez, Y.; Das, S.; Das, U.; Robles-Escajeda, E.; Ortega, N. M.; Lema, C.; Varela-Ramírez, A.; Aguilera, R. J.; Balzarini, J.; De Clercq, E.; Dimmock, S. G.; Gorecki, D. K. J.; Dimmock, J. R., Novel 3,5-bis(arylidene)-4-oxo-1-piperidinyl dimers: Structure–activity relationships and potent antileukemic and antilymphoma cytotoxicity. *European Journal of Medicinal Chemistry* **2014,** *77*, 315-322.

(218). Lipinski, C. A.; Lombardo, F.; Dominy, B. W.; Feeney, P. J., Experimental and computational approaches to estimate solubility and permeability in drug discovery and development settings. *Advanced Drug Delivery Reviews* **1997,** *23*, 3-25.

(219). Veber, D. F.; Johnson, S. R.; Cheng, H. Y.; Smith, B. R.; Ward, K. W.; Kopple, K. D., Molecular properties that influence the oral bioavailability of drug candidates. *Journal of Medicinal Chemistry* **2002,** *45*, 2615-23.

(220). Khan, A.; Andrews, D.; Blackburn, A. C., Long-term stabilization of stage 4 colon cancer using sodium dichloroacetate therapy. *World Journal of Clinical Cases* **2016,** *4*, 336-343.